Quantum Information & Computation: a primer

Frank Verstraete
Universiteit Gent

Central mantra:

quantum superposition principle can be used to
process information differently and more efficiently

Overview

- Quantum Mechanics: from postulates to quantum bits
- Quantum Entanglement
- Quantum Computing
  - Complexity theory
  - Quantum Algorithms
- Quantum Error Correction
  - Topological quantum order

Quantum Mechanics: postulates

- Galindo & Pascual, Quantum Mechanics I:

Postulate I. The description of a physical system in QM is accomplished in terms of the elements of a separable complex Hilbert space associated with the physical system. At a given instant of time t, a pure state for the physical system is represented by a unit ray $|\Psi(t)\rangle_{\mathrm{R}}$ in the corresponding Hilbert space. An element $|\Psi(t)\rangle$ of the ray $|\Psi(t)\rangle_{\mathrm{R}}$ is called a *state vector* or *ket*.

Postulate II. Every observable of a physical system is represented in the mathematical formalism of QM by a linear self-adjoint operator which acts in the Hilbert space (specified in Postulate I) associated with the physical system being considered.

Postulate III. If a physical system is in a pure state described by a normalized vector $|\psi\rangle$, the probability of obtaining a value λ from a Borel set $\Delta \subseteq \mathbb{R}$ when measuring the observable A is given by

$$P_{A,\psi}(\Delta) = \|E_A(\Delta)\psi\|^2 .$$

Postulate IV. If a physical system is in the state ϱ, the state resulting after an ideal measurement of an observable A which acts as a filter for the values in the set Δ is described by the density matrix $\varrho_{A,\Delta}$:

$$\varrho_{A,\Delta} = \frac{1}{\mathrm{Tr}\{\varrho E_A(\Delta)\}} \sum_{\alpha\in\Delta} E_{M_\alpha} \varrho E_{M_\alpha} . \qquad (2.107)$$

Postulate V. In the time interval between two consecutive measurements, pure states of a physical system continue to be pure, and there exists in every unit ray $|\Psi(t)\rangle_{\mathrm{R}}$ some representative state vector $|\Psi(t)\rangle$ such that the evolution is given by the Schrödinger equation

$$\boxed{i\hbar\frac{d}{dt}|\Psi(t)\rangle = H(t)|\Psi(t)\rangle} , \qquad (2.119)$$

where $H(t)$ is an observable called the *Hamiltonian* of the system. The observables of the system are represented by operators that are constant in time, unless the devices which measure those observables explicitly change in time, in which case the representative operators should also contain the change.

Postulate VI. For a physical system in which the cartesian coordinates are $q_1, q_2 \ldots, q_N$, with corresponding conjugate momenta $p_1, p_2, \ldots, p_N$, the operators X_r and P_s, which represent these observables in QM, must satisfy the commutation relations

$$\boxed{[X_r, X_s] = 0 , \quad [P_r, P_s] = 0 , \quad [X_r, P_s] = i\hbar\delta_{rs} I} . \qquad (2.165)$$

If the system has an observable whose classical expression is $A(q_1, \ldots, q_N, p_1, \ldots p_N; t)$, in usual applications of QM the corresponding operator is obtained from this expression, conveniently written, by substituting the operators X_r and P_s for the variables q_r and p_s, respectively.

Hydrogen atom

- Stationary Schrodinger equation: $$-\frac{\hbar^2}{2m}\nabla^2\psi - \frac{e^2}{4\pi\varepsilon_0 r}\psi = E\psi$$

- Eigenvalues are quantized; corresponding eigenvectors:

$$|\psi_n\rangle = |n\rangle$$

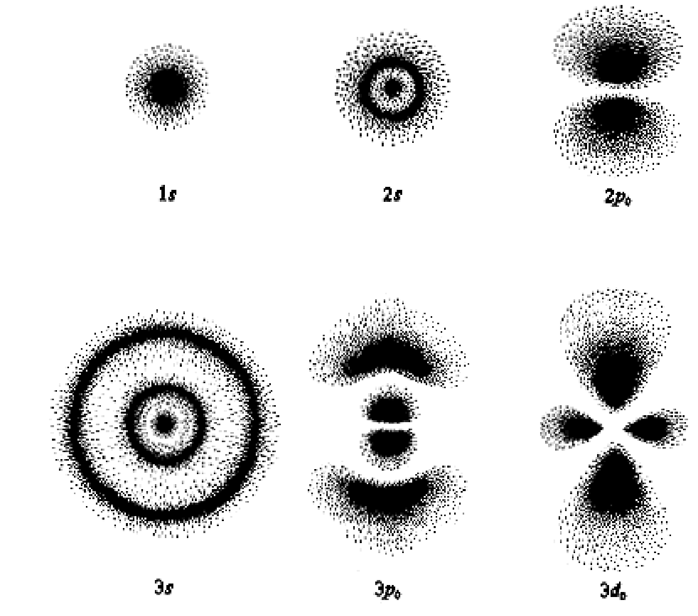

- In the sequel, we will consider 2 eigenstates $|0\rangle, |1\rangle$ and call this system a "*qubit*"

Different Architectures for building a quantum computer:

- Superconducting quantum computing[3][4] (qubit implemented by the state of nonlinear resonant superconducting circuits containing Josephson junctions)
- Trapped ion quantum computer (qubit implemented by the internal state of trapped ions)
- Neutral atom quantum computer (qubit implemented by internal states of neutral atoms trapped in an optical lattice or an array of dipole traps, i.e. optical tweezers)[5][6][7]
- Quantum dot computer, spin-based (e.g. the Loss-DiVincenzo quantum computer[8]) (qubit given by the spin states of trapped electrons)
- Quantum dot computer, spatial-based (qubit given by electron position in double quantum dot)[9]
- Quantum computing using engineered quantum wells, which could in principle enable the construction of a quantum computer that operates at room temperature[10][11]
- Coupled quantum wire (qubit implemented by a pair of quantum wires coupled by a quantum point contact)[12][13][14]
- Nuclear magnetic resonance quantum computer (NMRQC) implemented with the nuclear magnetic resonance of molecules in solution, where qubits are provided by nuclear spins within the dissolved molecule and probed with radio waves
- Solid-state NMR Kane quantum computer (qubit realized by the nuclear spin state of phosphorus donors in silicon)
- Vibrational quantum computer (qubits realized by vibrational superpositions in cold molecules)[15]
- Electrons-on-helium quantum computer (qubit is the electron spin)
- Cavity quantum electrodynamics (CQED) (qubit provided by the internal state of trapped atoms coupled to high-finesse cavities)
- Molecular magnet[16] (qubit given by spin states)
- Fullerene-based ESR quantum computer (qubit based on the electronic spin of atoms or molecules encased in fullerenes)[17]
- Nonlinear optical quantum computer (qubits realized by processing states of different modes of light through both linear and nonlinear elements)[18][19]
- Linear optical quantum computer (LOQC) (qubits realized by processing states of different modes of light through linear elements e.g. mirrors, beam splitters and phase shifters).[20] Quantum microprocessor based on laser photonics at room temperature made possible.[21][22]
- Diamond-based quantum computer[23][24][25][26] (qubit realized by the electronic or nuclear spin of nitrogen-vacancy centers in diamond)
- Bose–Einstein condensate-based quantum computer[27][28]
- Transistor-based quantum computer (string quantum computers with entrainment of positive holes using an electrostatic trap)
- Rare-earth-metal-ion-doped inorganic crystal based quantum computer[29][30] (qubit realized by the internal electronic state of dopants in optical fibers)
- Metallic-like carbon nanospheres-based quantum computer[31]

Quantum Superposition Principle:

$$|\psi\rangle = \alpha|0\rangle + \beta|1\rangle \qquad \langle\psi|\psi\rangle = |\alpha|^2 + |\beta|^2 = 1$$

- Any complex linear combination yields a valid quantum state, as long as normalized (in L_2) to 1

- Asterisk:
  - Quantum States are rays, it is we have to identify two states which only differ by a global phase (projective space)

$$|\psi\rangle \equiv e^{i\theta}|\psi\rangle$$

  - This has a nontrivial consequence: physical symmetries (such as rotation) can be represented using *projective representations*. This is precisely the reason that spin ½ systems are allowed, and also fermions (spin-statistics theorem) which are crucial for establishing the stability of matter

  - Another consequence is that superselection rules emerge for which kind of superpositions are allowed: we cannot make superpositions of two quantum states with different mass, as the mass is the "central charge" for Galilei transformations

Many-body systems: tensor product

- When considering wavefunctions of several spins / particles / modes /…, the Hilbert space is obtained by taking tensor products:
  - n qubits: $$\left(\mathcal{C}^2\right)^{\otimes n} = \mathcal{C}^{2^n}$$
  - This is the so-called "exponential wall" in quantum physics:
    - It makes it impossible to simulate the Schrodinger equation exactly for many-body systems; most big breakthroughs in quantum physics are effectively good ways of turning this exponential problem into an approximate polynomial one.
    - This is one of the big motivations for building a quantum computer: simulate many-body systems (relevant for e.g. high energy physics, superconductors, …)

- Asterisk: the exponential wall is already there for "classical" spin systems: n Ising spins can also be in 2^n configurations. What is of special to QM is the fact that any superposition is also allowed, giving rise to an effective double exponential scaling:

$$\left(\frac{1}{\epsilon}\right)^{2^n}$$

The illusion of Hilbert space

- A main additional ingredient: locality of quantum Hamiltonians

$$\mathcal{H} = \sum_{ij} h_{ij} \hat{O}_i \otimes \hat{O}_j \otimes \hat{I}_{\{1..n\}-\{i,j\}}$$

  - Question: Starting from a given fiducial state, and allowing for any time-dependent Hamiltonian of the above form, how long does it typically take to get e-close to a random state in Hilbert space?

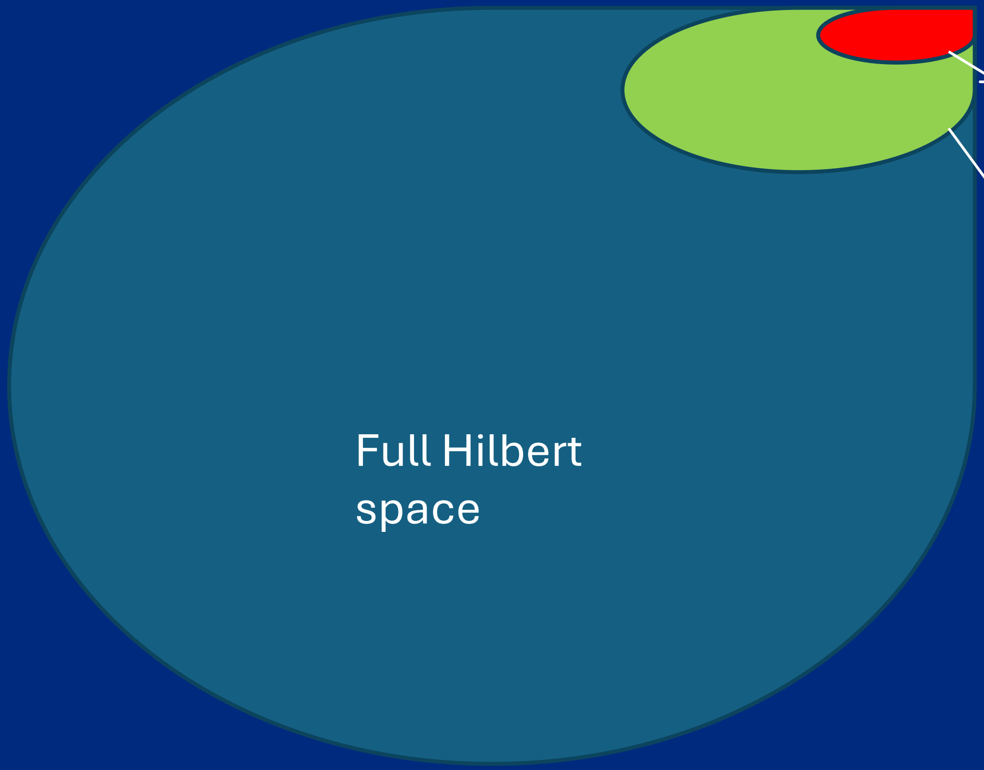

Ground and thermal states of local n-body quantum Hamiltonians

Manifold of States reachable in polynomial time with time dependent evolution with 2-body Hamiltonians starting from fully polarized state

$$\left(\frac{1}{\epsilon}\right)^{2^N} \gg N^{N^\alpha} \gg N^2$$

Overview

- Quantum Mechanics: from postulates to quantum bits
- Quantum Entanglement
- Quantum Computing
  - Complexity theory
  - Quantum Algorithms
- Quantum Error Correction
  - Topological quantum order

Quantum Entanglement

- Superposition principle for two qubits implies the existence of *entangled* states: $|\psi_{AB}\rangle \neq |\psi_A\rangle \otimes |\psi_B\rangle$
    - Example: Bell states: $\frac{1}{\sqrt{2}}\left(|0\rangle|0\rangle \pm |1\rangle|1\rangle\right)$
- Schrodinger: essence of entanglement is that “the whole is more than the sum of its parts
    - Local measurements cannot reveal the sign:

$$\rho_A = \mathrm{Tr}_B|\psi_{AB}\rangle\langle\psi_{AB}| = \frac{1}{2}\left(|0\rangle\langle 0| + |1\rangle\langle 1|\right)$$

- Entanglement entropy: $S(|\psi_{AB}\rangle) = -\mathrm{Tr}\rho_A \log \rho_A$
- Large part of quantum information: resource theory of entanglement (interconversion, distillation, capacities of quantum channels, …)

Quantum Physics in the 21st century

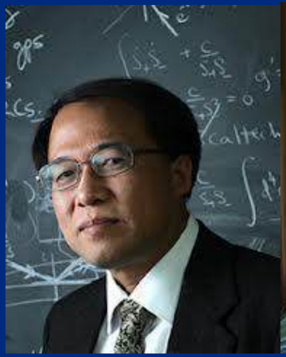



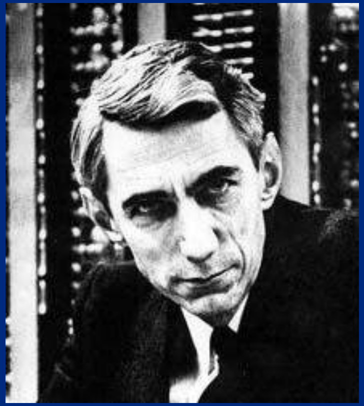

Entanglement

Quantum Statistics

- Entanglement as a resource: use entanglement for constructing better sensors

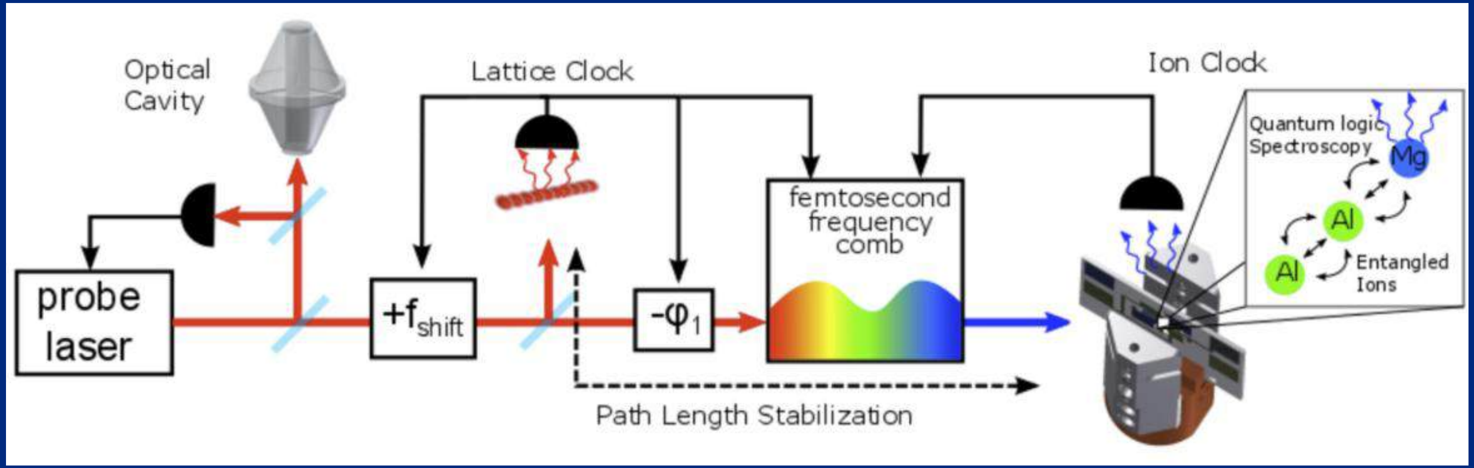

- This leads to interesting mathematical problems in the field of quantum statistics, generalizing the normal statistics to the non-commutative setting
  - Quantum hypothesis testing
  - Quantum Tomography, quantum Fisher information, …
    - Eg: optimal ways of measuring spectrum of a density matrix via Young tableaux (Keyl & Werner)
  - Quantum de Finetti theorems for quantum cryptography

Bell inequalities

- Although entanglement cannot be used to send information superluminally (cfr. Einstein-Podolsky-Rosen), it allows to violate Bell inequalities / win quantum games:

payoff: $p(a, b|s, t)$

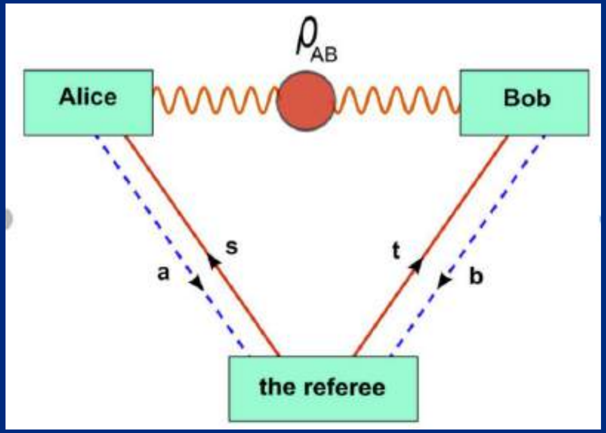

- Combined with the concept of entanglement monogamy, this forms the foundation of Quantum Cryptography

Entanglement and new foundations for quantum many-body physics

- Area law for quantum entanglement entropy of ground states of quantum spin systems:

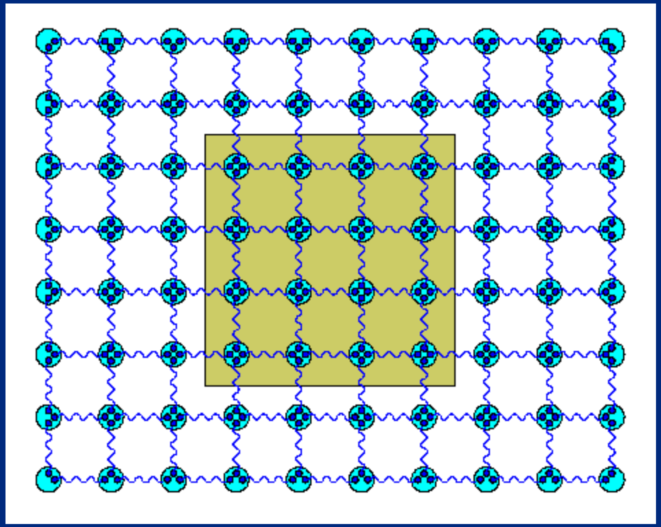

$$S(\rho_A) \leq c.\partial A$$

Proof of area laws by M.B. Hastings ('07) using Lieb-Robinson bounds and tensor networks

- Tensor networks / Matrix Product States / Projected Entangled Pair States span "physical corner of Hilbert space" and provide a new framework for real-space renormalization group methods
- Entangled pairs form the syntax, large worldwide effort to reveal the semantics of entanglement
  - "shadow world", holographic principle, "it from bit", …
  - Those tensor networks provide explicit realizations of systems exhibiting topological quantum order; Condensed matter theory people all over the world are now studying group cohomology, fusion categories, …

Overview

- Quantum Mechanics: from postulates to quantum bits
- Quantum Entanglement
- Quantum Computing
  - Complexity theory
  - Quantum Algorithms
- Quantum Error Correction
  - Topological quantum order

Quantum Circuit Model

- Basic premise: any physical realization of a quantum computer will consist of acting with a set of local unitary transformations on some fiducial input state, followed by a measurement

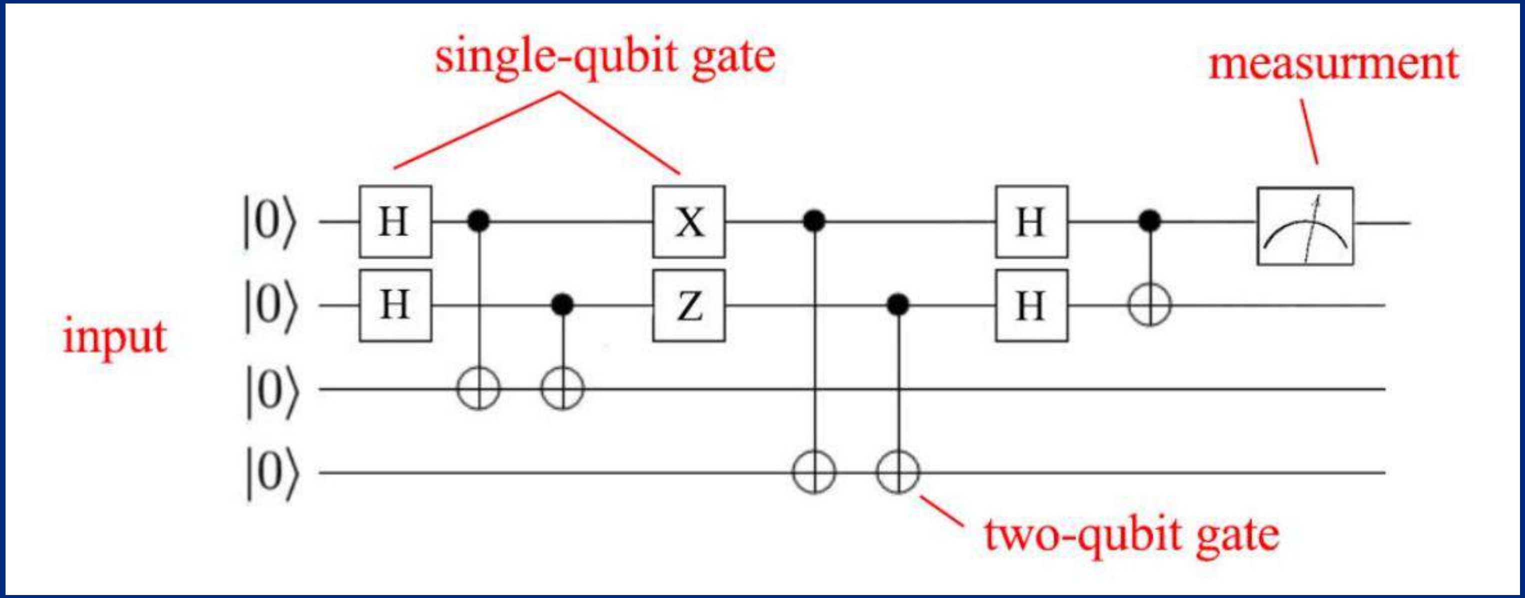

$$H = \frac{1}{\sqrt{2}}\begin{bmatrix} 1 & 1 \\ 1 & -1 \end{bmatrix}$$

$$-\boxed{R_\theta}- = \begin{bmatrix} 1 & 0 \\ 0 & e^{i\theta} \end{bmatrix}$$

$$X = \begin{bmatrix} 0 & 1 \\ 1 & 0 \end{bmatrix}, \quad Y = \begin{bmatrix} 0 & -i \\ i & 0 \end{bmatrix}, \quad Z = \begin{bmatrix} 1 & 0 \\ 0 & -1 \end{bmatrix}$$

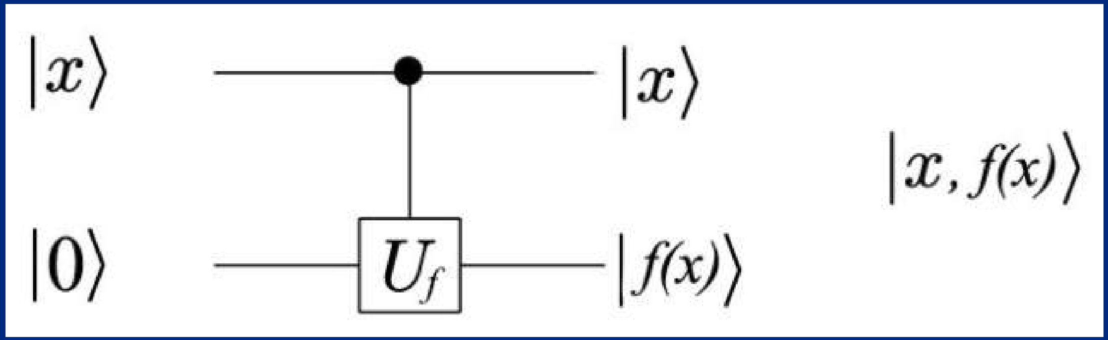

Universal Gate Set

- Universal gate set: is a finite set of unitaries from which any other unitary can be made by multiplying them
  - Example: single qubit Pauli + R(p/8) gates, CNOT on any pair of qubits

$$\mathrm{CNOT} = \begin{bmatrix} 1 & 0 & 0 & 0 \\ 0 & 1 & 0 & 0 \\ 0 & 0 & 0 & 1 \\ 0 & 0 & 1 & 0 \end{bmatrix}$$

- How many gates are needed to get an e-dense net?

  Solovay-Kitaev:

Let $\mathcal{G}$ be a finite set of elements in SU(2) containing its own inverses (so $g \in \mathcal{G}$ implies $g^{-1} \in \mathcal{G}$) and such that the group $\langle \mathcal{G} \rangle$ they generate is dense in SU(2). Consider some $\varepsilon > 0$. Then there is a constant c such that for any $U \in \mathrm{SU}(2)$, there is a sequence S of gates from $\mathcal{G}$ of length $O(\log^c(1/\varepsilon))$ such that $\|S - U\| \leq \varepsilon$. That is, S approximates U to operator norm error.

- For general unitary on n-qubits: we obviously need exponentially many gates

BQP

- BQP: Bounded error quantum polynomial time
- Colloquially speaking: class of decision problems solvable by a (uniform) quantum circuit with a polynomial number of gates as a function of input length of the problem
- Formally:

A language L is in **BQP** if and only if there exists a polynomial-time uniform family of quantum circuits $\{Q_n : n \in \mathbb{N}\}$, such that

- For all $n \in \mathbb{N}$, Q_n takes n qubits as input and outputs 1 bit
- For all x in L, $\mathrm{Pr}(Q_{|x|}(x) = 1) \geq \frac{2}{3}$
- For all x not in L, $\mathrm{Pr}(Q_{|x|}(x) = 0) \geq \frac{2}{3}$

- Alternative defenitions in terms of quantum Turing machines are possible.

Problems in BQP

- All problems in complexity classes P and BPP
- Integer factorization (Shor's algorithm '94) / discrete logarithm

$$O\left((\log N)^2 (\log\log N)(\log\log\log N)\right)$$ versus classical $$O\left(e^{1.9(\log N)^{1/3}(\log\log N)^{2/3}}\right)$$

- Approximating Jones polynomial at some roots of unity:
  - Contracting a unitary "tensor network" constructed using Temperley-Lieb algebra

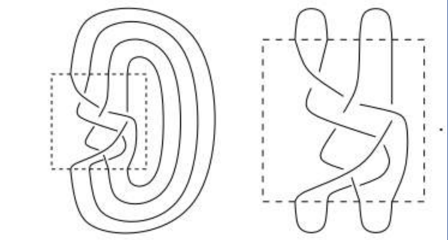

- Quantum simulation: given a many-body quantum system, a local Hamiltonian, and an initial state, evolve that state as a function of time
  - This problem was motivation of Feynman ('82) to look into quantum computers
  - Technical tool: Suzuki-Trotter approximations $e^{\delta(A+B)} = \lim_{\delta\to 0}[e^{\delta A}e^{\delta B}] + O(\delta^2)$
- Quantum algorithm for linear system of equations in runtime $O(\log(N)\kappa^2)$ (Harrow, Hassidim, Lloyd '09)

Central building block: Quantum Fourier Transform

Discrete Fourier transform of a vector $x_j \in \mathcal{C}^N$: $y_k = \frac{1}{\sqrt{N}} \sum_{j=0}^{N-1} e^{2\pi i \frac{j.k}{N}} x_j$.

Quantum Fourier transform:
given a basis state for n qubits $|j\rangle \in \mathcal{C}^{2^n}$ (e.g. $|01101...\rangle$), implement the unitary transform

$$|j\rangle \rightarrow \frac{1}{\sqrt{2^n}} \sum_{j=0}^{2^n} e^{2\pi i \frac{j.k}{2^n}} |j\rangle$$

- QFT = DFT
- QFT can be implemented with $O(n \log n)$ gates which is exponentially smaller than DFT $\mathcal{O}(n.2^n)$:

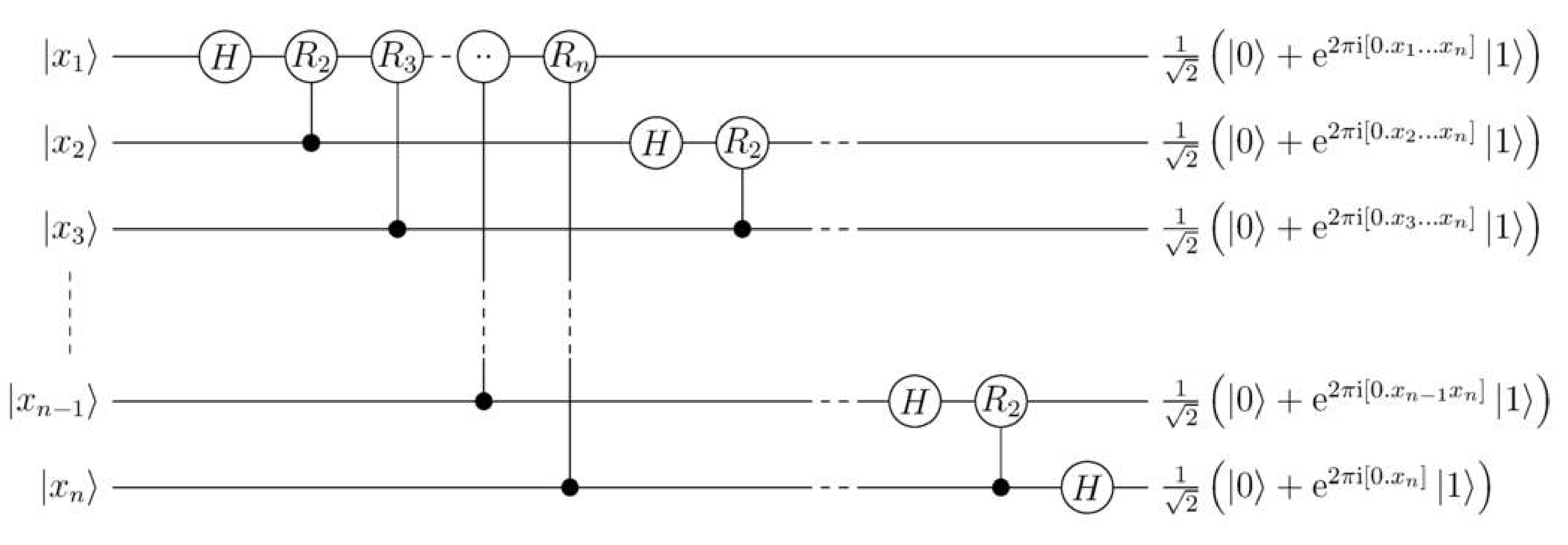

Designing quantum algorithms

- Central issue: problem at hand must have some structure, such that interference pattern emerges with very few “peaks”
  - Eg: factoring problem can be reduced to period finding
  - Stated differently: highly entangled states do not reveal any information when doing a final measurement: at the end of the computation, we need a simple state
- NP-complete problems do not seem to have such a structure
  - Candidate problems seem to lie in intersection of P and co-NP
- Most obvious application of quantum computers: simulating quantum many-body systems
  - It is however not obvious to find ground states (in worst case QMA-hard)
  - Currently large effort in designing quantum algorithms for ground state problems:
    - Quantum adiabatic algorithms
    - Quantum Metropolis sampling
    - Mimicking imaginary time evolution
    - …
    - Quantum approach is also inspiring state of the art classical methods: quantum tensor networks

Complexity Classes & Church-Turing thesis

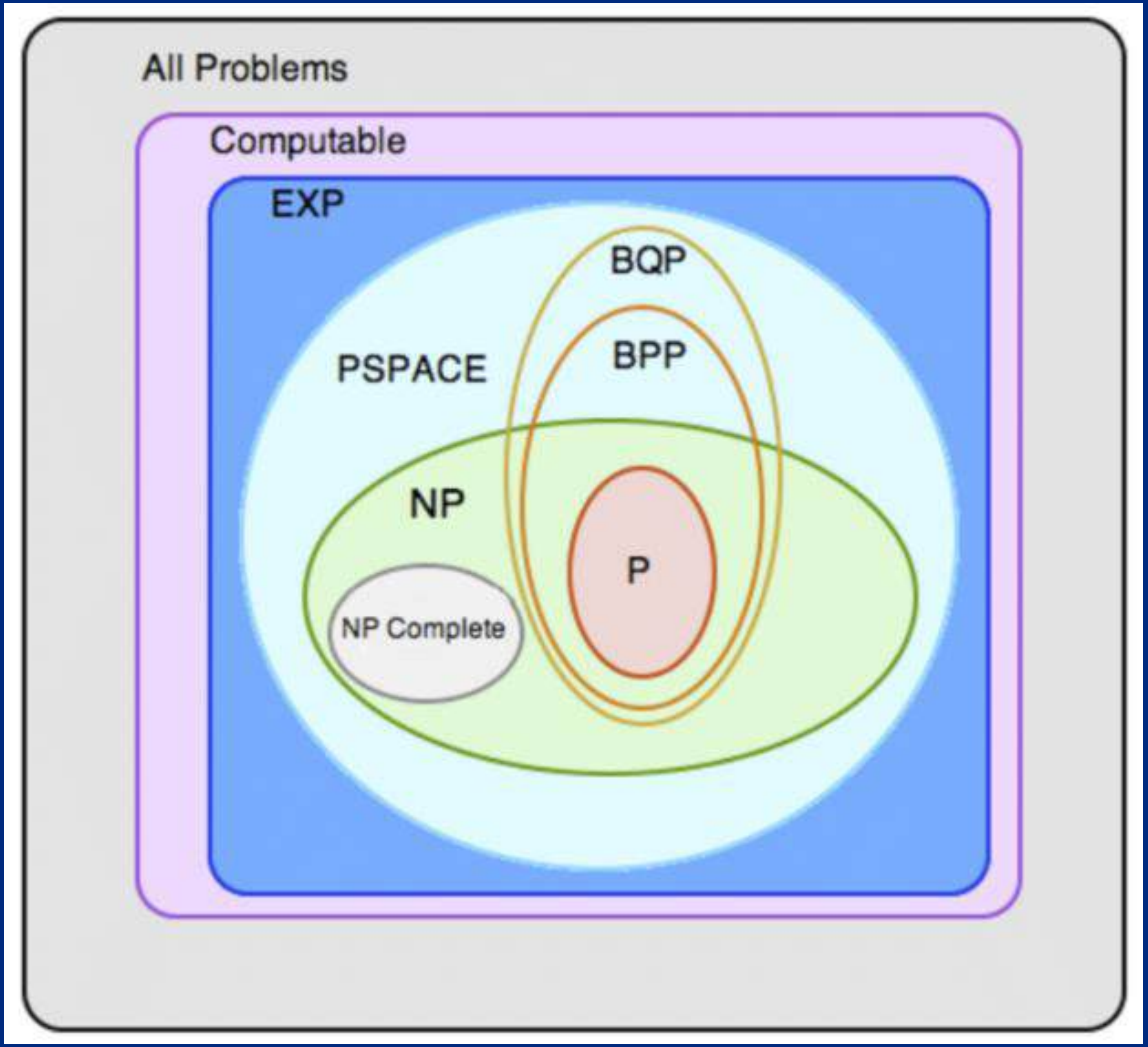

Noisy Intermediate-Scale Quantum computers

Quantum Computing in the NISQ era and beyond

John Preskill

Institute for Quantum Information and Matter and Walter Burke Institute for Theoretical Physics, California Institute of Technology, Pasadena CA 91125, USA

30 July 2018

Noisy Intermediate-Scale Quantum (NISQ) technology will be available in the near future. Quantum computers with 50-100 qubits may be able to perform tasks which surpass the capabilities of today's classical digital computers, but noise in quantum gates will limit the size of quantum circuits that can be executed reliably. NISQ devices will be useful tools for exploring many-body quantum physics, and may have other useful applications, but the 100-qubit quantum computer will not change the world right away — we should regard it as a significant step toward the more powerful quantum technologies of the future. Quantum technologists should continue to strive for more accurate quantum gates and, eventually, fully fault-tolerant quantum computing.

Article | Published: 23 October 2019

Quantum supremacy using a programmable superconducting processor

Frank Arute, Kunal Arya, Ryan Babbush, Dave Bacon, Joseph C. Bardin, Rami Barends, Rupak Biswas, Sergio Boixo, Fernando G. S. L. Brandao, David A. Buell, Brian Burkett, Yu Chen, Zijun Chen, Ben Chiaro, Roberto Collins, William Courtney, Andrew Dunsworth, Edward Farhi, Brooks Foxen, Austin Fowler, Craig Gidney, Marissa Giustina, Rob Graff, Keith Guerin, ... John M. Martinis + Show authors

Nature **574**, 505–510 (2019) | Cite this article

Abstract

The promise of quantum computers is that certain computational tasks might be executed exponentially faster on a quantum processor than on a classical processor[1]. A fundamental challenge is to build a high-fidelity processor capable of running quantum algorithms in an exponentially large computational space. Here we report the use of a processor with programmable superconducting qubits[2,3,4,5,6,7] to create quantum states on 53 qubits, corresponding to a computational state-space of dimension 2^{53} (about 10^{16}). Measurements from repeated experiments sample the resulting probability distribution, which we verify using classical simulations. Our Sycamore processor takes about 200 seconds to sample one instance of a quantum circuit a million times—our benchmarks currently indicate that the equivalent task for a state-of-the-art classical supercomputer would take approximately 10,000 years. This dramatic increase in speed compared to all known classical algorithms is an experimental realization of quantum supremacy[8,9,10,11,12,13,14] for this specific computational task, heralding a much-anticipated computing paradigm.

Review Article | Open access | Published: 12 January 2016

Quantum algorithms: an overview

Ashley Montanaro

npj Quantum Information **2**, Article number: 15023 (2016) | Cite this article

Abstract

Quantum computers are designed to outperform standard computers by running quantum algorithms. Areas in which quantum algorithms can be applied include cryptography, search and optimisation, simulation of quantum systems and solving large systems of linear equations. Here we briefly survey some known quantum algorithms, with an emphasis on a broad overview of their applications rather than their technical details. We include a discussion of recent developments and near-term applications of quantum algorithms.

Review Article | Published: 12 August 2021

Variational quantum algorithms

M. Cerezo, Andrew Arrasmith, Ryan Babbush, Simon C. Benjamin, Suguru Endo, Keisuke Fujii, Jarrod R. McClean, Kosuke Mitarai, Xiao Yuan, Lukasz Cincio & Patrick J. Coles

Nature Reviews Physics **3**, 625–644 (2021) | Cite this article

Abstract

Applications such as simulating complicated quantum systems or solving large-scale linear algebra problems are very challenging for classical computers, owing to the extremely high computational cost. Quantum computers promise a solution, although fault-tolerant quantum computers will probably not be available in the near future. Current quantum devices have serious constraints, including limited numbers of qubits and noise processes that limit circuit depth. Variational quantum algorithms (VQAs), which use a classical optimizer to train a parameterized quantum circuit, have emerged as a leading strategy to address these constraints. VQAs have now been proposed for essentially all applications that researchers have envisaged for quantum computers, and they appear to be the best hope for obtaining quantum advantage. Nevertheless, challenges remain, including the trainability, accuracy and efficiency of VQAs. Here we overview the field of VQAs, discuss strategies to overcome their challenges and highlight the exciting prospects for using them to obtain quantum advantage.

arXiv > quant-ph > arXiv:2510.26300

Search...

Help | Adv

Quantum Physics

[Submitted on 30 Oct 2025]

Fermionic dynamics on a trapped-ion quantum computer beyond exact classical simulation

Faisal Alam, Jan Lukas Bosse, Ieva Čepaitė, Adrian Chapman, Laura Clinton, Marcos Crichigno, Elizabeth Crosson, Toby Cubitt, Charles Derby, Oliver Dowinton, Paul K. Faehrmann, Steve Flammia, Brian Flynn, Filippo Maria Gambetta, Raúl García-Patrón, Max Hunter-Gordon, Glenn Jones, Abhishek Khedkar, Joel Klassen, Michael Kreshchuk, Edward Harry McMullan, Lana Mineh, Ashley Montanaro, Caterina Mora, John J. L. Morton, Dhrumil Patel, Pete Rolph, Raul A. Santos, James R. Seddon, Evan Sheridan, Wilfrid Somogyi, Marika Svensson, Niam Vaishnav, Sabrina Yue Wang, Gethin Wright

Simulation of the time-dynamics of fermionic many-body systems has long been predicted to be one of the key applications of quantum computers. Such simulations -- for which classical methods are often inaccurate -- are critical to advancing our knowledge and understanding of quantum chemistry and materials, underpinning a wide range of fields, from biochemistry to clean-energy technologies and chemical synthesis. However, the performance of all previous digital quantum simulations has been matched by classical methods, and it has thus far remained unclear whether near-term, intermediate-scale quantum hardware could offer any computational advantage in this area. Here, we implement an efficient quantum simulation algorithm on Quantinuum's System Model H2 trapped-ion quantum computer for the time dynamics of a 56-qubit system that is too complex for exact classical simulation. We focus on the periodic spinful 2D Fermi-Hubbard model and present evidence of spin-charge separation, where the elementary electron's charge and spin decouple. In the limited cases where ground truth is available through exact classical simulation, we find that it agrees with the results we obtain from the quantum device. Employing long-range Wilson operators to study deconfinement of the effective gauge field between spinons and the effective potential between charge carriers, we find behaviour that differs from predictions made by classical tensor network methods. Our results herald the use of quantum computing for simulating strongly correlated electronic systems beyond the capacity of classical computing.

Comments: 54 pages, 43 figures

Subjects: **Quantum Physics (quant-ph)**; Materials Science (cond-mat.mtrl-sci)

Cite as: arXiv:2510.26300 **[quant-ph]**

(or arXiv:2510.26300v1 **[quant-ph]** for this version)

https://doi.org/10.48550/arXiv.2510.26300

Search...

Help | Adv

antum computer beyond exact classical simulation

Laura
Gambe
eh, As
ika Sv

ng bee
owledg
ever, th
ale qua
ed-ion
nd pres
al simu
eld betw
d the u

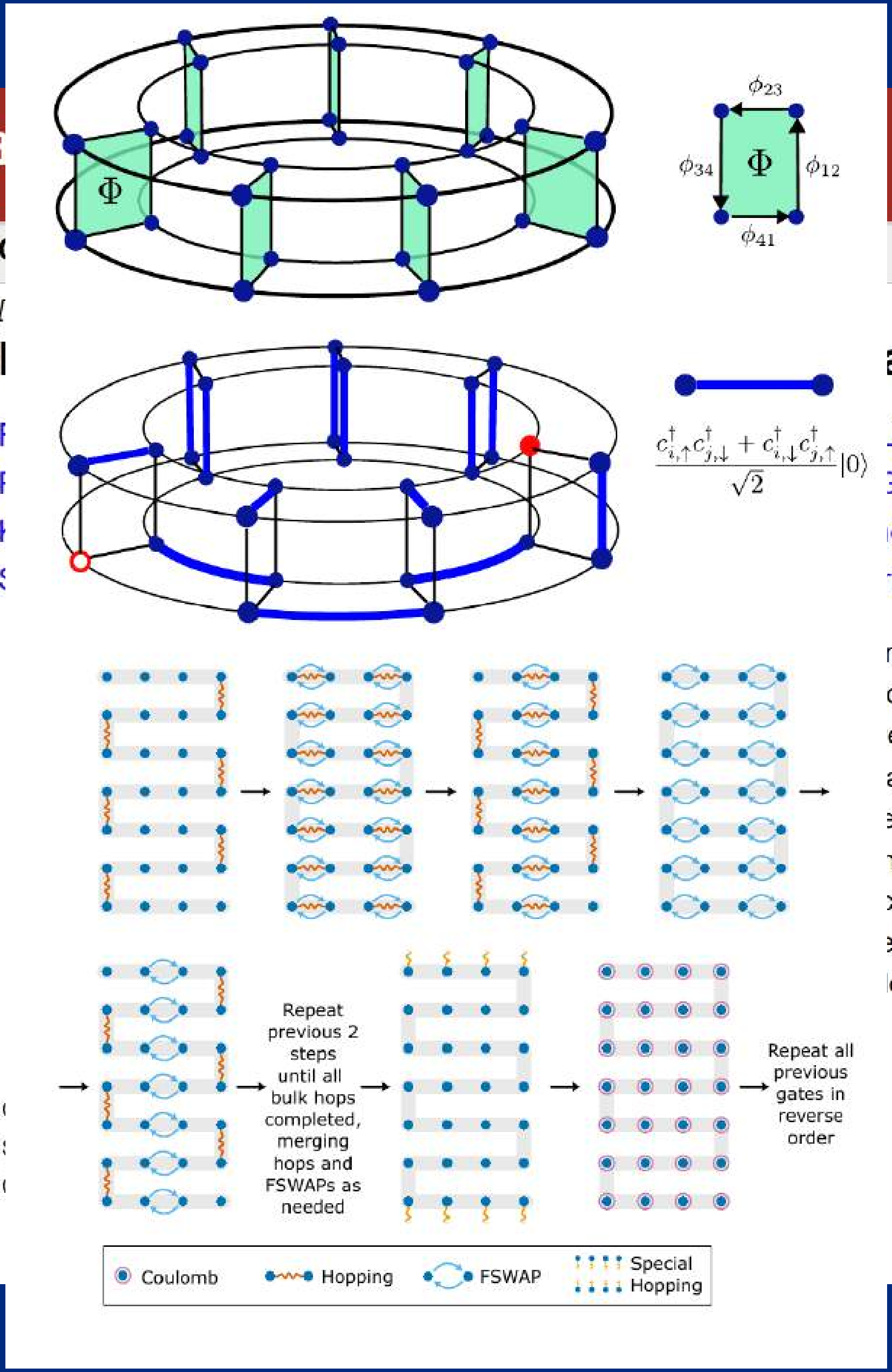

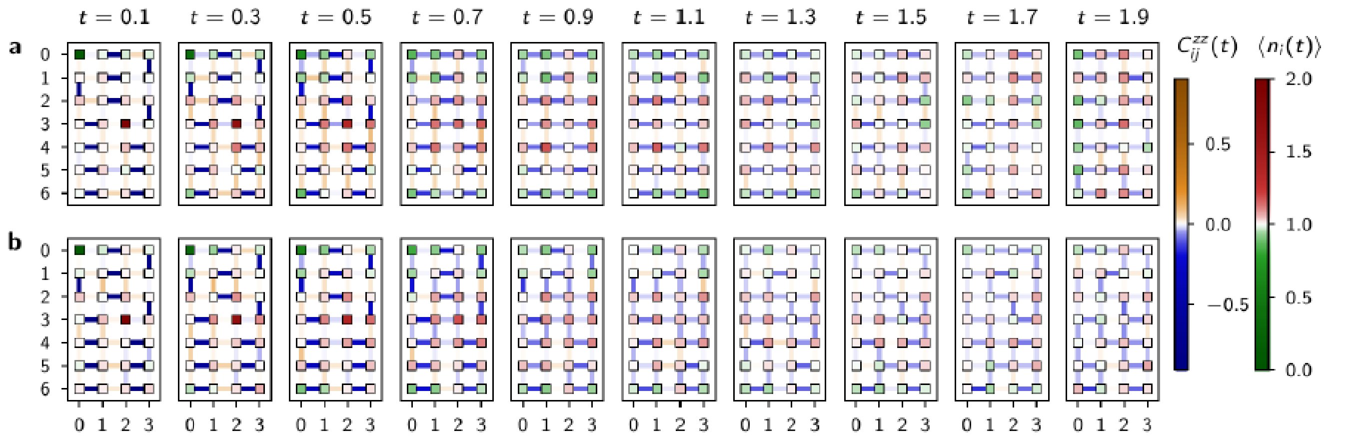

FIG. 2. **Evolution of local charge, and spin correlations.** Local charge density $\langle n_i(t)\rangle$ (squares as sites) and spin (connected) correlation function $C^{zz}_{ij}(t)$ between nearest-neighbours (represented by links) as a function of time for **a,** $U = 0.0$ and **b,** $U = 4.0$ for the error mitigated (TFLO + GPR) experimental data. In the charge sector, we see diffusion from the initial holon-doublon configuration towards the uniform state. In the free case **(a)**, the charges develop a charge-density profile oscillating in the y direction, while in the interacting case **(b)**, the charge profile is more disordered. In the spin sector, the initial triplet configuration takes $\sim t = 0.7$ to melt, leaving behind a residual antiferromagnetic correlation, greater for the interacting case (see also Figure 3).

Quantum Physics

[Submitted on 30 Oct 2025]

Programmable digital quantum simulation of 2D Fermi-Hubbard dynamics using 72 superconducting qubits

Faisal Alam, Jan Lukas Bosse, Ieva Čepaitė, Adrian Chapman, Laura Clinton, Marcos Crichigno, Elizabeth Crosson, Toby Cubitt, Charles Derby, Oliver Dowinton, Paul K. Faehrmann, Steve Flammia, Brian Flynn, Filippo Maria Gambetta, Raúl García-Patrón, Max Hunter-Gordon, Glenn Jones, Abhishek Khedkar, Joel Klassen, Michael Kreshchuk, Edward Harry McMullan, Lana Mineh, Ashley Montanaro, Caterina Mora, John J. L. Morton, Dhrumil Patel, Pete Rolph, Raul A. Santos, James R. Seddon, Evan Sheridan, Wilfrid Somogyi, Marika Svensson, Niam Vaishnav, Sabrina Yue Wang, Gethin Wright

Simulating the time-dynamics of quantum many-body systems was the original use of quantum computers proposed by Feynman, motivated by the critical role of quantum interactions between electrons in the properties of materials and molecules. Accurately simulating such systems remains one of the most promising applications of general-purpose digital quantum computers, in which all the parameters of the model can be programmed and any desired physical quantity output. However, performing such simulations on today's quantum computers at a scale beyond the reach of classical methods requires advances in the efficiency of simulation algorithms and error mitigation techniques. Here we demonstrate programmable digital quantum simulation of the dynamics of the 2D Fermi-Hubbard model -- one of the best-known simplified models of electrons in crystalline solids -- at a scale beyond exact classical simulation. We implement simulations of this model on lattice sizes up to 6×6 using 72 qubits on Google's Willow quantum processor, across a range of physical parameters, including on-site electron-electron interaction strength and magnetic flux, and study phenomena including formation of magnetic polarons, i.e. charge carriers surrounded by local magnetic polarisation, dynamical symmetry breaking in stripe-ordered states, attraction of charge carriers on an entangled state known as a valence bond solid, and the approach to equilibrium through thermalisation. We validate our results against exact calculations in parameter regimes where these are feasible, and compare them to approximate classical simulations performed using tensor network and operator propagation methods. Our results demonstrate that programmable digital quantum simulation of many-body interacting electron models is now competitive on state-of-the-art quantum hardware.

Comments: 98 pages, 75 figures
Subjects: **Quantum Physics (quant-ph)**; Materials Science (cond-mat.mtrl-sci)
Cite as: arXiv:2510.26845 **[quant-ph]**
(or arXiv:2510.26845v1 **[quant-ph]** for this version)
https://doi.org/10.48550/arXiv.2510.26845

Quantum Physics

[Submitted on 30 Oct 2025]

Programmable digital quantum simulation of 2D Fermi-Hubbard dynamics using 72 superconducting qubits

Faisal Alam, Jan Luk
Paul K. Faehrmann,
Klassen, Michael Kr
Santos, James R. S
n,

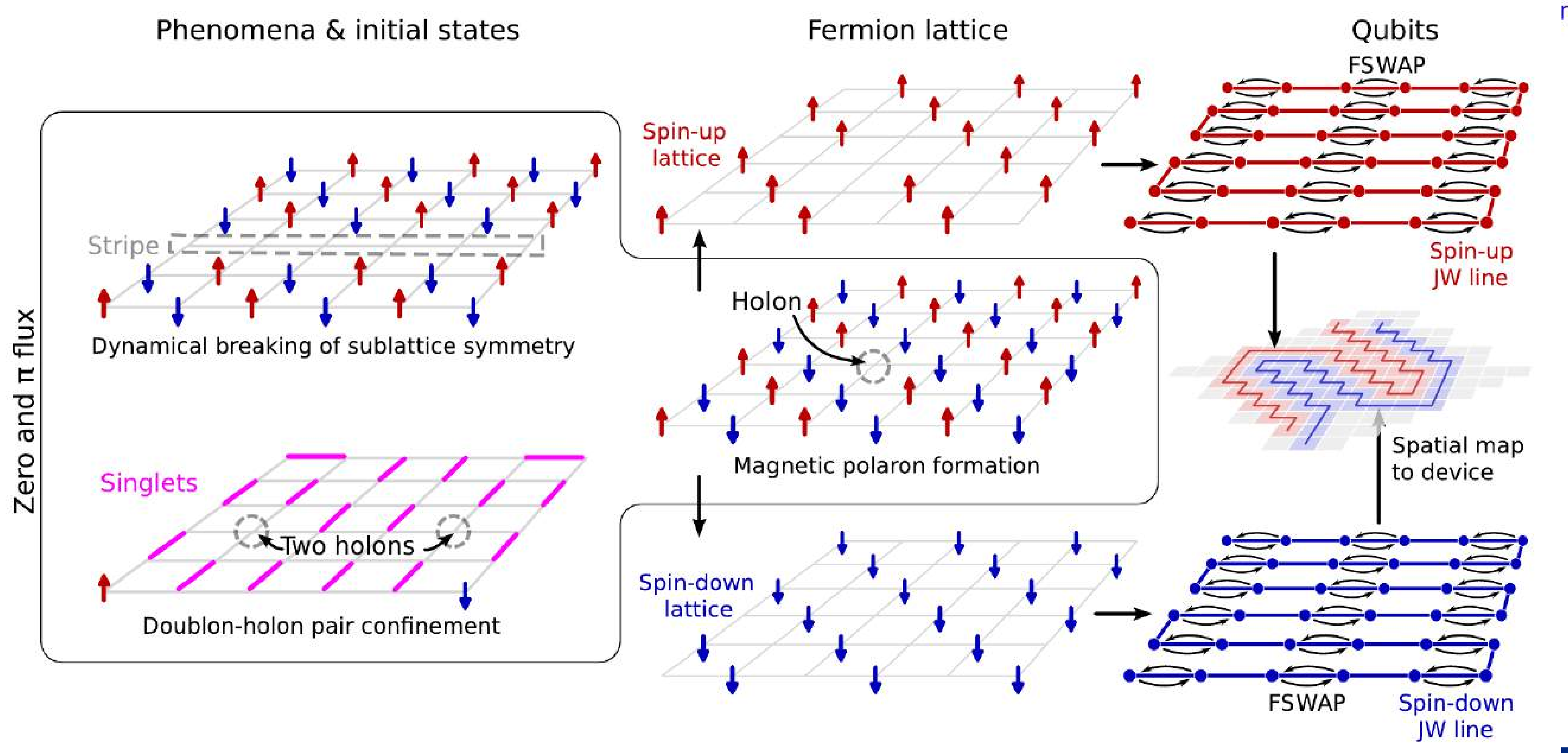

Simulating the time-
interactions between
digital quantum com
quantum computers
demonstrate progran
at a scale beyond ex
range of physical pa
carriers surrounded
bond solid, and the a
them to approximate
simulation of many-b

Comments: 98 pages, 75 f
Subjects: **Quantum Phy**
Cite as: arXiv:2510.26
(or arXiv:2510
https://doi.org/

Overview

- Quantum Mechanics: from postulates to quantum bits
- Quantum Entanglement
- Quantum Computing
  - Complexity theory
  - Quantum Algorithms
- Quantum Error Correction
  - Topological quantum order

Quantum Error Correction

- Biggest technological hurdle to build a quantum computer: Quantum Decoherence:

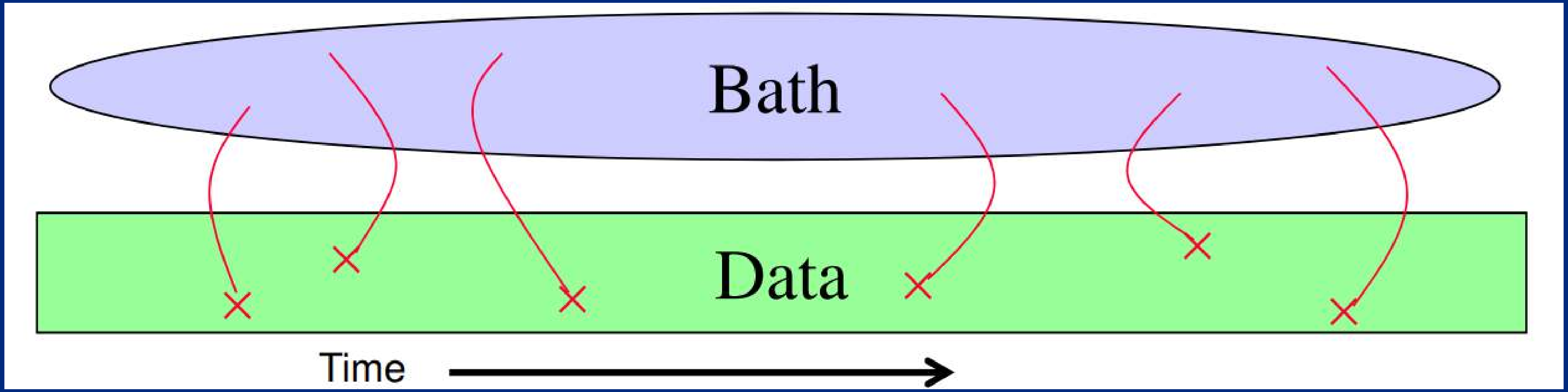

- It is very difficult to isolate a quantum system of its environment, certainly if you want to interact with is by quantum gates
  - Interaction of system – environment entangles them, and this leads to decoherence
  - There are much more ways for qubits to incur errors than classical bits

- Classical error correction: variants on the scheme of repetition codes: 0->000, 1->111
  - von Neumann: fault tolerant computers can be build

Quantum error correction

- At first sight, it looks impossible to devise a similar repetition code for quantum systems:
  - State-space / errors are continuous as opposed to discrete
  - Quantum no-cloning theorem: an unknown quantum state cannot be cloned (as this would violate unitarity) $|\psi\rangle \not\to |\psi\rangle|\psi\rangle$
  - Measurements to decrease the entropy destroy the quantum information: measurement / disturbance

- Peter Shor demonstrated how those issues can be overcome
  - Use entanglement to fight entanglement: delocalize the quantum information in the system such that local measurements / decoherence do not reveal any information about the logical quantum bits

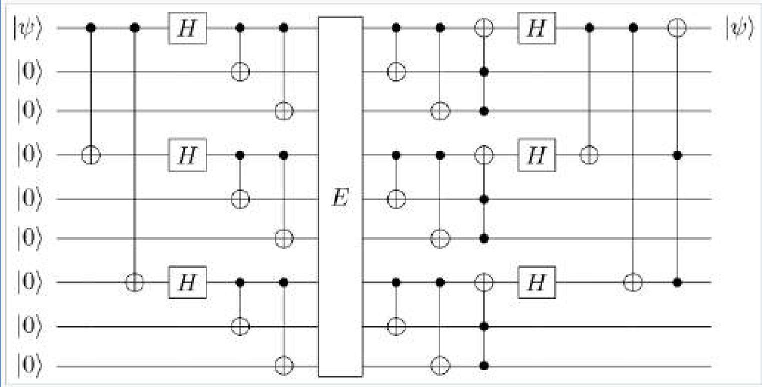

  - Quantum threshold theorem: a quantum computer with a physical error rate below a certain threshold can, through application of quantum error correction schemes, suppress the logical error rate to arbitrarily low levels
    - Overhead: $O(\log^c(p(n)/\varepsilon)p(n))$

Article | Open Access | Published: 14 July 2021

Exponential suppression of bit or phase errors with cyclic error correction

Google Quantum AI

Nature **595**, 383–387 (2021) | Cite this article

Abstract

Realizing the potential of quantum computing requires sufficiently low logical error rates[1]. Many applications call for error rates as low as 10^{-15} (refs. [2,3,4,5,6,7,8,9]), but state-of-the-art quantum platforms typically have physical error rates near 10^{-3} (refs. [10,11,12,13,14]). Quantum error correction[15,16,17] promises to bridge this divide by distributing quantum logical information across many physical qubits in such a way that errors can be detected and corrected. Errors on the encoded logical qubit state can be exponentially suppressed as the number of physical qubits grows, provided that the physical error rates are below a certain threshold and stable over the course of a computation. Here we implement one-dimensional repetition codes embedded in a two-dimensional grid of superconducting qubits that demonstrate exponential suppression of bit-flip or phase-flip errors, reducing logical error per round more than 100-fold when increasing the number of qubits from 5 to 21. Crucially, this error suppression is stable over 50 rounds of error correction. We also introduce a method for analysing error correlations with high precision, allowing us to characterize error locality while performing quantum error correction. Finally, we perform error detection with a small logical qubit using the 2D surface code on the same device[18,19] and show that the results from both one- and two-dimensional codes agree with numerical simulations that use a simple depolarizing error model. These experimental demonstrations provide a foundation for building a scalable fault-tolerant quantum computer with superconducting qubits.

Article | Published: 04 October 2021

Fault-tolerant control of an error-corrected qubit

Laird Egan, Dripto M. Debroy, Crystal Noel, Andrew Risinger, Daiwei Zhu, Debopriyo Biswas, Michael Newman, Muyuan Li, Kenneth R. Brown, Marko Cetina & Christopher Monroe

Nature **598**, 281–286 (2021) | Cite this article

Abstract

Quantum error correction protects fragile quantum information by encoding it into a larger quantum system[1,2]. These extra degrees of freedom enable the detection and correction of errors, but also increase the control complexity of the encoded logical qubit. Fault-tolerant circuits contain the spread of errors while controlling the logical qubit, and are essential for realizing error suppression in practice[3,4,5,6]. Although fault-tolerant design works in principle, it has not previously been demonstrated in an error-corrected physical system with native noise characteristics. Here we experimentally demonstrate fault-tolerant circuits for the preparation, measurement, rotation and stabilizer measurement of a Bacon–Shor logical qubit using 13 trapped ion qubits. When we compare these fault-tolerant protocols to non-fault-tolerant protocols, we see significant reductions in the error rates of the logical primitives in the presence of noise. The result of fault-tolerant design is an average state preparation and measurement error of 0.6 per cent and a Clifford gate error of 0.3 per cent after offline error correction. In addition, we prepare magic states with fidelities that exceed the distillation threshold[7], demonstrating all of the key single-qubit ingredients required for universal fault-tolerant control. These results demonstrate that fault-tolerant circuits enable highly accurate logical primitives in current quantum systems. With improved two-qubit gates and the use of intermediate measurements, a stabilized logical qubit can be achieved.

Quantum error correction

- A. Kitaev: theory of quantum error correcting codes == theory of topological field theory (TFT)
  - Use normal physical qubits to mimic strongly correlated systems with anyon excitations: artificially engineer TFTs
  - Encode quantum information into topological sectors / anyons of lattice versions of TFTs

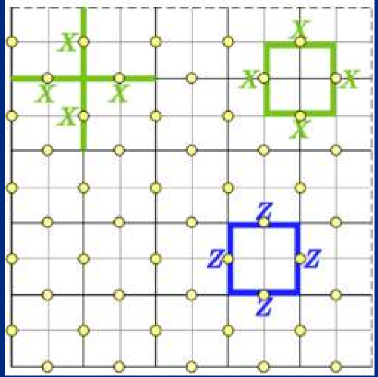

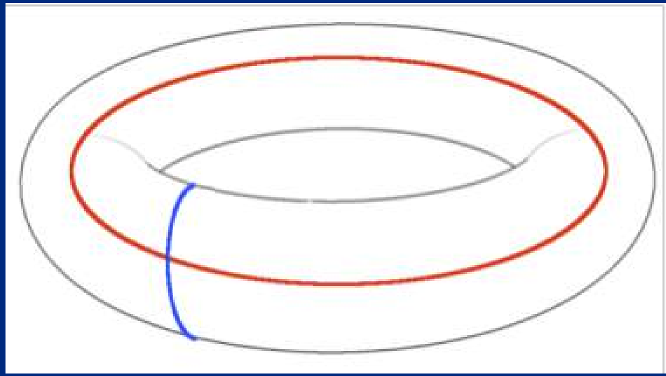

Anyons: elementary excitations in the system with nontrivial braiding

- Apply quantum gates to those logical qubits by braiding:

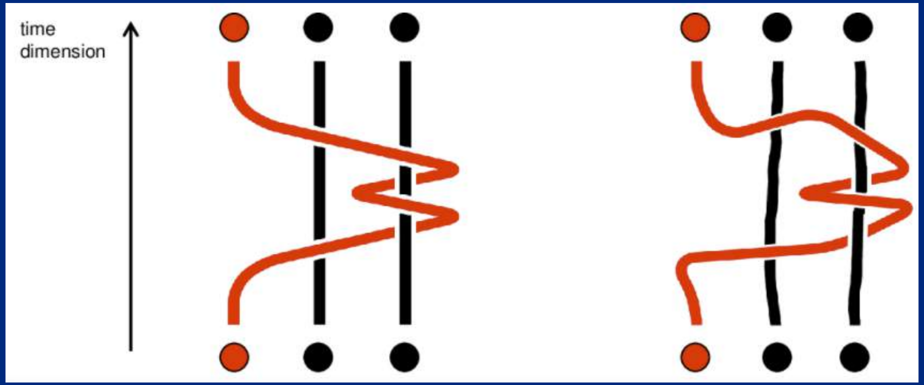

- Non-Abelian anyons needed for universal quantum computation

- Mathematics needed to describe TFTs: tensor categories / bimodule categories. Anyons and boundary excitations are then be described by theit centers

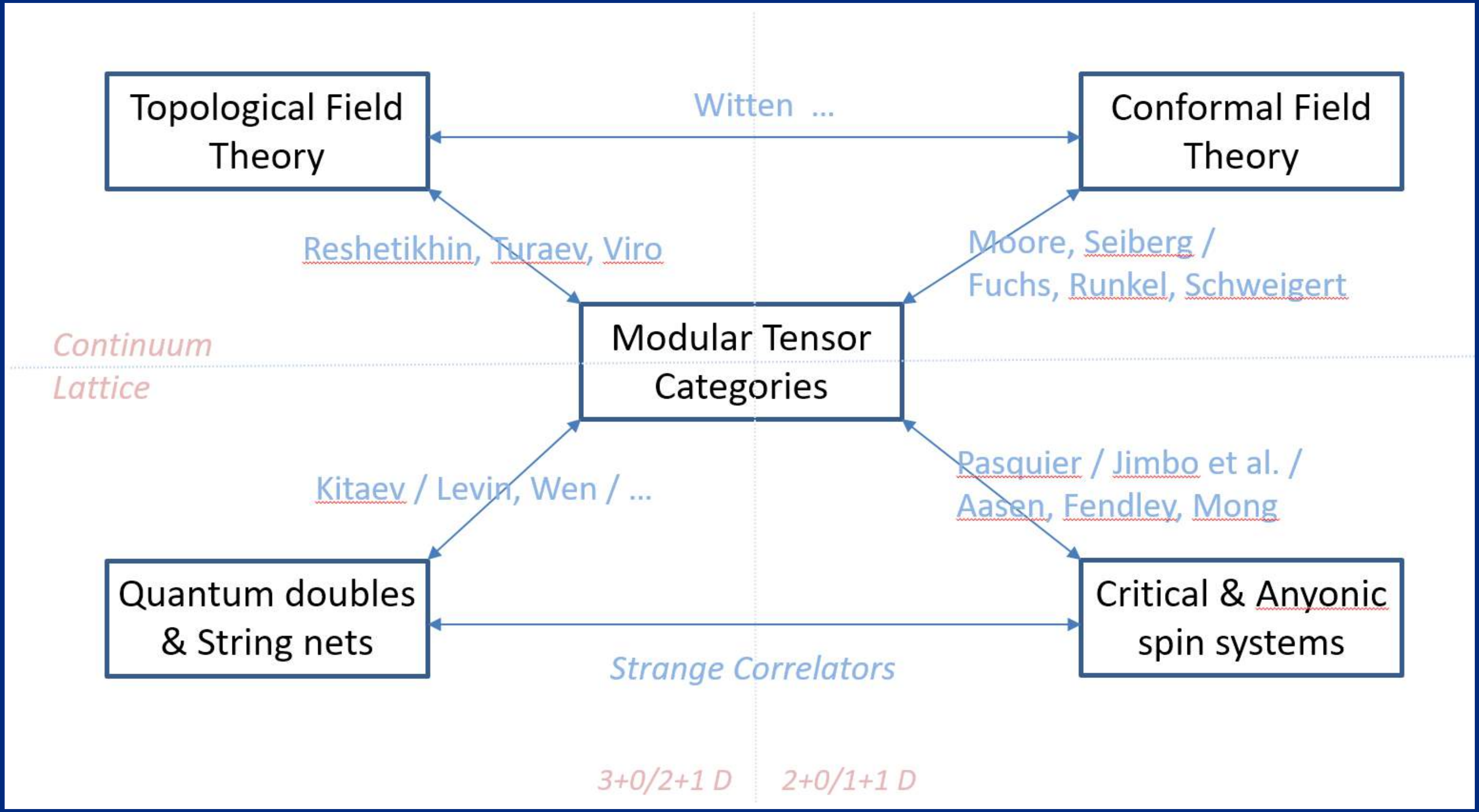

- Group of M. Lukin (2025):

  physical implementation of toric code + transversal gates using neutral (Rydberg) atoms

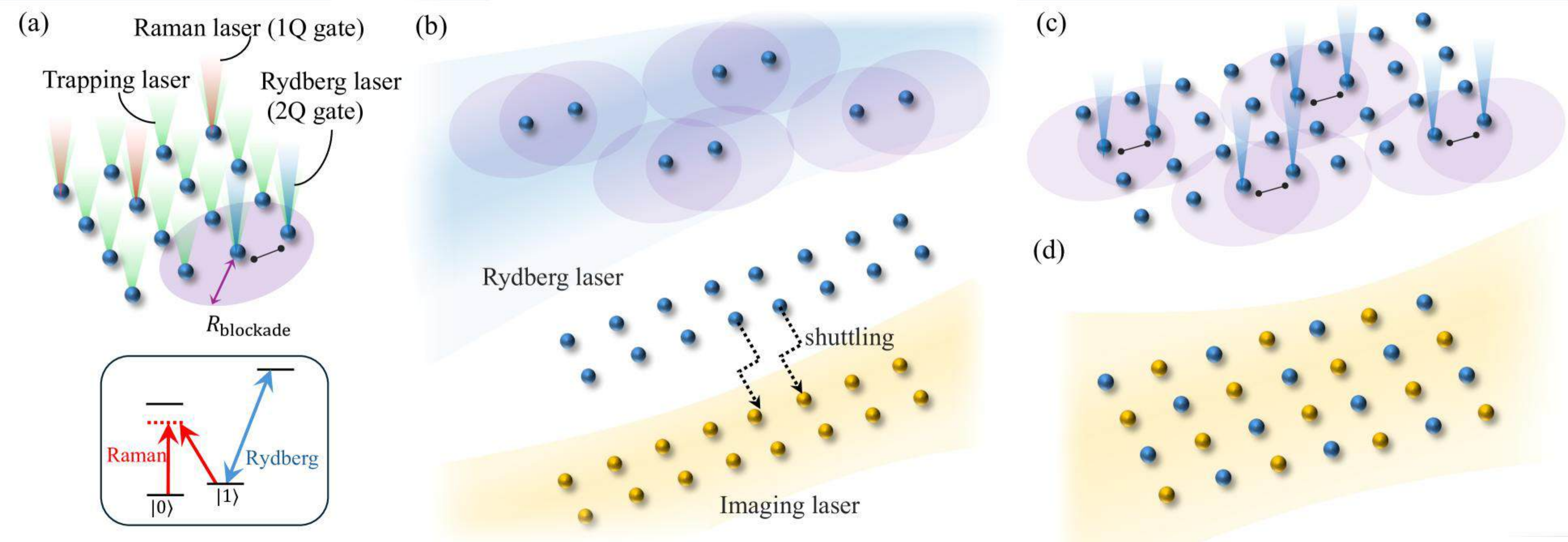

Conclusion

- Quantum Computation is still very much in a stage of fundamental science, but huge strides are being made to make a full scale quantum computer

- Biggest bottlenecks:

  - Quantum fault tolerance leads to huge overheads
  - Where are the quantum algorithms?

Central open problems in field of quantum computation

- Central problem: which experimental platform is best suited to scale, and how to fight decoherence?
  - Ion traps, superconducting qubits, optical lattices, photonic, Josephson junctions, …
- Algorithms: what mathematical problems (such as factoring) have a structure amenable to quantum interference patterns?
- Construction of better and simpler quantum error correcting codes
  - (Higher) fusion categories for describing topologically ordered states of matter
- Post-quantum cryptography: which one-way functions cannot be broken with quantum computers (e.g. lattice problems such as shortest vector problem)
- Quantum Statistics: optimal tomography, quantum hypothesis testing, …

Theory of Quantum Key Distribution: protocols and security

Thomas Van Himbeeck

Postdoctoral researcher
Inria Paris, France

BeQCI workshop
IMEC – Leuven, Belgium
November 5, 2025

Based on: TVH, P. Brown, A general and tight finite-size security proof of quantum key distribution

Outline

1. Introduction to security proofs

2. Finite-size security

3. Device-Independent QKD

What is Quantum Key Distribution ?

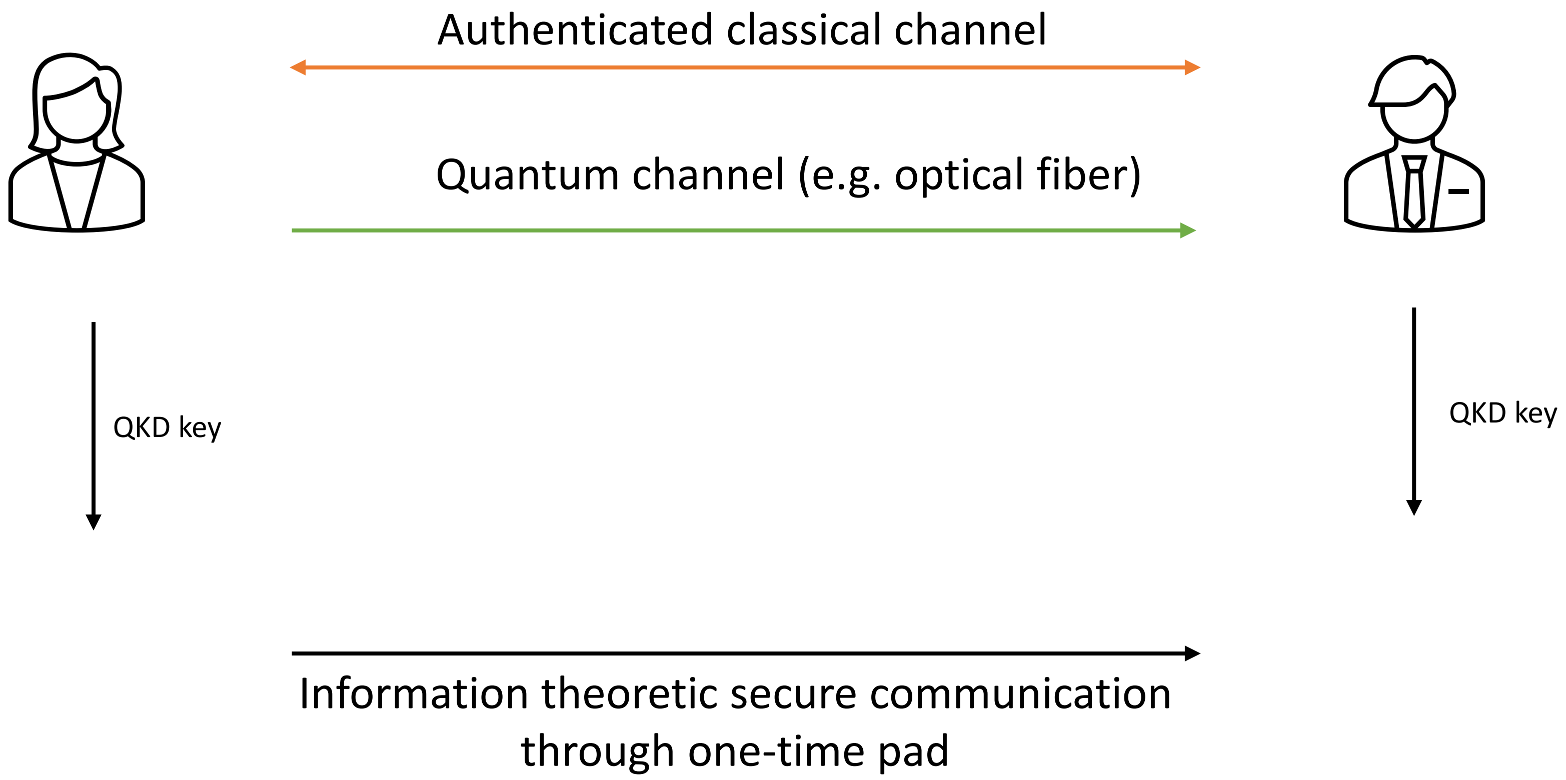

Simplest protocol: Bennett-Brassard '84

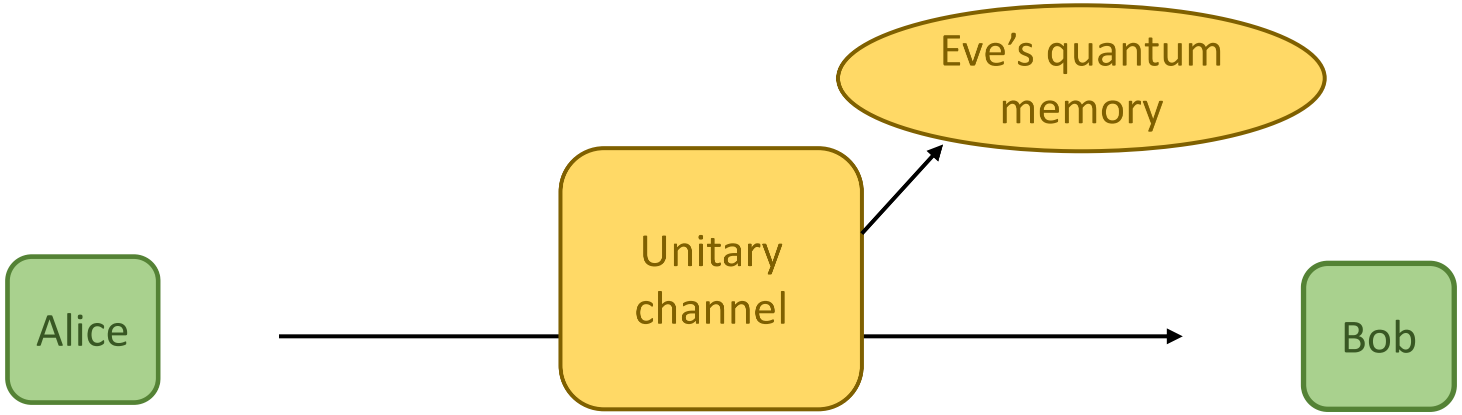

Prepares 4 "BB84" states:

$|0\rangle, |1\rangle, |+\rangle, |-\rangle$

Measures in the σ_X, σ_Z basis

Simple security proof (noiseless case)

If the Z and X basis are perfectly correlated,
Eve didn't eavesdrop on the channel -> the key is secure

Entanglement-based version: Eckert '91

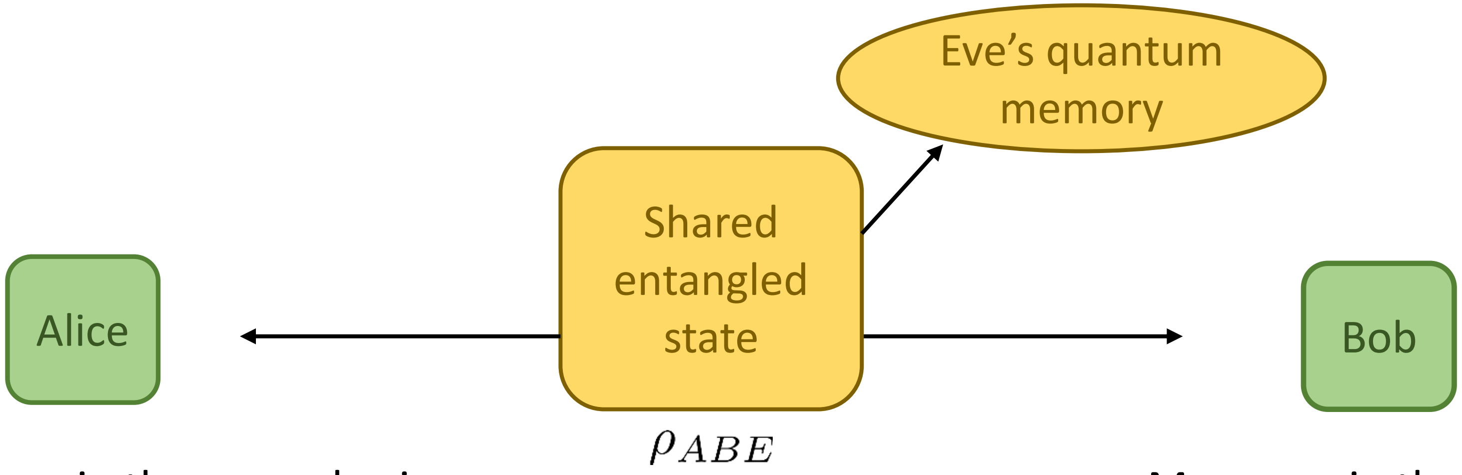

Measures in the σ_X, σ_Z basis

Measures in the σ_X, σ_Z basis

Simple security proof (noiseless case)

If the Z and X basis are perfectly correlated at Alice and Bob,

$$\langle \sigma_X^a \sigma_X^b \rangle = \langle \sigma_Z^a \sigma_Z^b \rangle = 1$$

then they shared a maximally entangled state (Eve is decoupled)

$$\rho_{ABE} = |\phi^+\rangle\langle\phi^+|_{AB} \otimes \rho_E$$

Missing in this security proof

What about noise resistance ?

What about other protocols ?

What about finite-size effects and coherent attacks?

What about untrusted devices ?

How to handle noise:
One-way key distillation (Devetak-Winter)

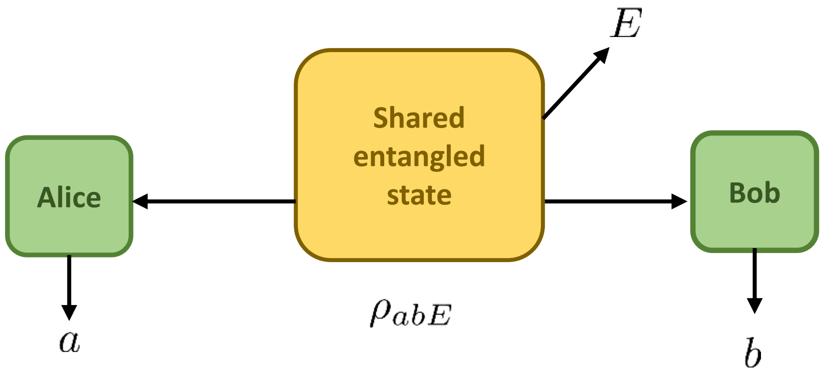

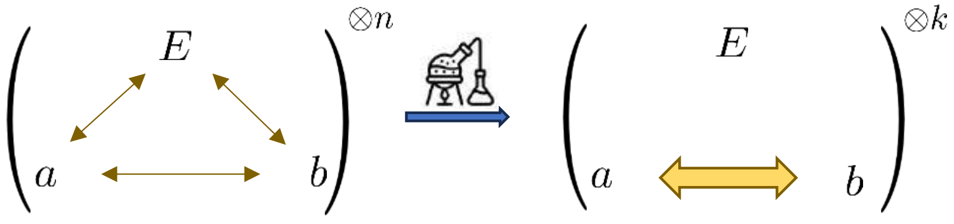

Unsecure key   Perfect key

One-way distillation protocol

Step 1: error correction

Alice sends $n\,H(a|b) + o(n)$ bits of error correction information to Bob

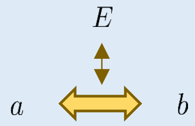

Step 2: privacy amplification

Alice and Bob hash their (identical) n bit keys into an $n[H(a|E) - H(a|b)] + o(n)$-bit fully secure key

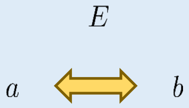

Devetak Winter key-rate: $\mathrm{r}_{DW} = H(a|E) - H(a|b) = I(a{:}b) - I(a{:}E)$

Note 1: DW key rate is not symmetric (reverse reconcilliation in continuous variable QKD)
Note 2: Keyrate can be « boosted » with tricks such noisy preprocessing and advantage distillation
Note 3: We don't know the optimal 2-way reconcilliation scheme

$^*H(a|E) = S(\rho_{aE}) - S(\rho_E)$

Asymptotic key rate:
Find the worst-case attack compatible with observations

Computing asymptotic key rates

minimize $\quad H(a|E) - H(a|b)$

subject to $\quad \mathrm{p}(\mathrm{a}, b) = \mathrm{Tr}[\rho_{AB} M_a \otimes M_b]$

$\quad Tr_{EB}[\rho] = \sigma_A$

$variables$: ρ_{ABE}

Numerical QKD
[Winnick et al. 2018]

Change of variables

Efficiently solvable
convex optimization problem

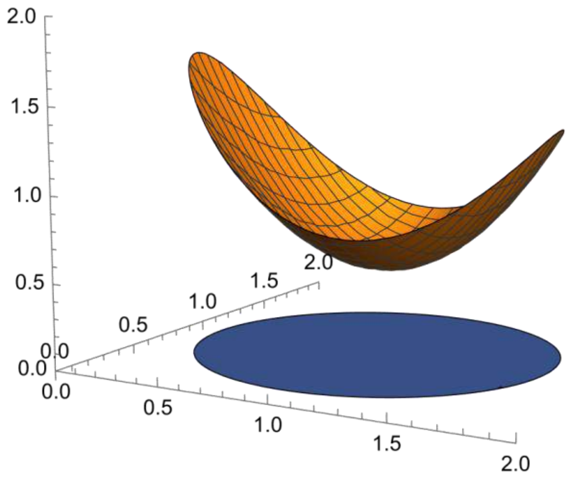

$variables$: ρ_{AB}
(assuming Eve holds a purification)

Asymptotic key rate: application to BB84/E91

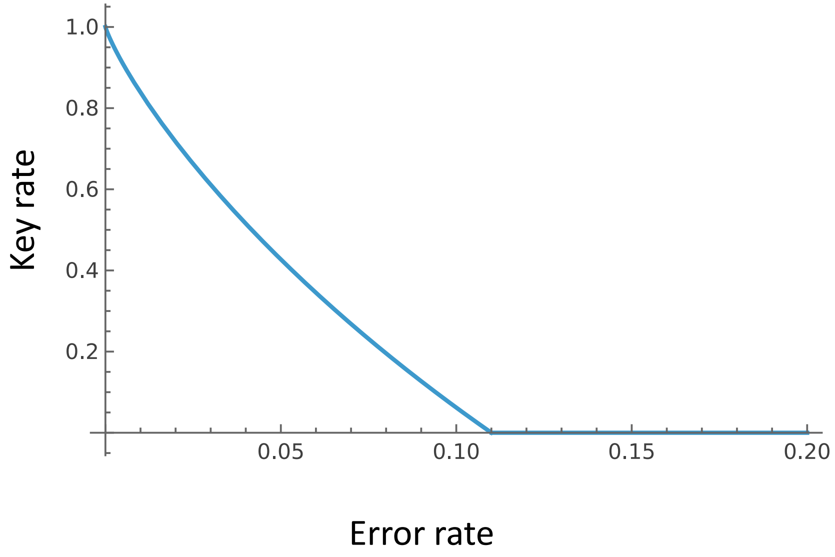

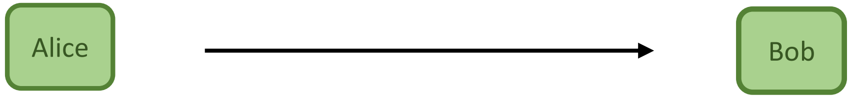

Prepares 4 “BB84” states:
$|0\rangle, |1\rangle, |+\rangle, |-\rangle$

Measures in the σ_X, σ_Z basis

Error rate: probability of an error in a given basis (X or Z)

BB84 key rate formula (Shor-Preskill)
« bit and phase error rate »

$$r_{DW} = 1 - h(e_X) - h(e_Z)$$

$$h(e) = -e \log_2 e - (1-e) \log_2 (1-e)$$

BB84 protocol: the fine print

BB84 Protocol

1. Alice sends n random BB84 states
2. Bob measure in a random X or Z basis
3. (sifting) discard rounds with different basis ($\approx$ 50% of the rounds)
4. (post-selection) postselect on rounds with a detection
5. (noisy preprocessing) add small random noise to Alice's outcome
4. (parameter estimation) estimate bit and phase error rate in test rounds (e.g. 10% of the rounds)
5. (key distillation) perform error correction and privacy amplification in remaining rounds
6. (test final key) verify if Alice and Bob's final key match

Outline

1. Introduction to security proofs

2. Finite-size security

3. Device-Independent QKD and outlook

Two important properties for a security proof

Efficiency

Get highest possible key rate

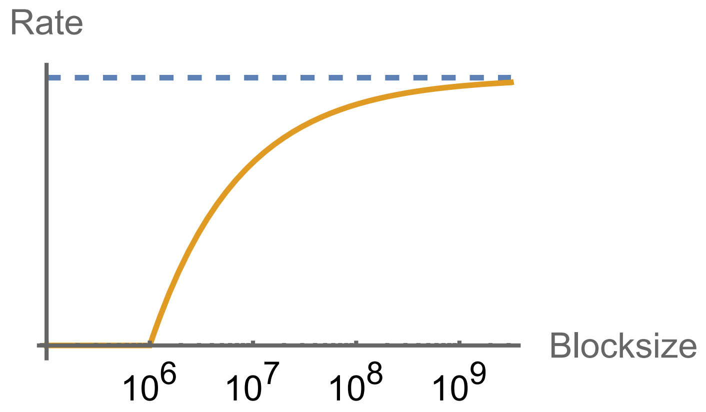

Generality

Apply to many QKD protocols

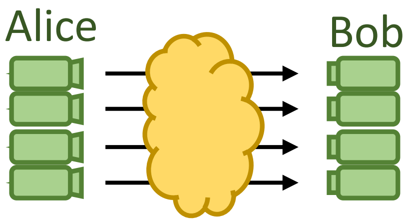

This work:

- Tight asymptotic and leading order $O\left(\frac{1}{\sqrt{n}}\right)$ finite-size corrections

- Applies to *device-dependent round-based protocols* (including CV and DV)

TVH, P. Brown, A general and tight finite-size security proof of quantum key distribution

Efficiency: Finite-size expansion of the key rate

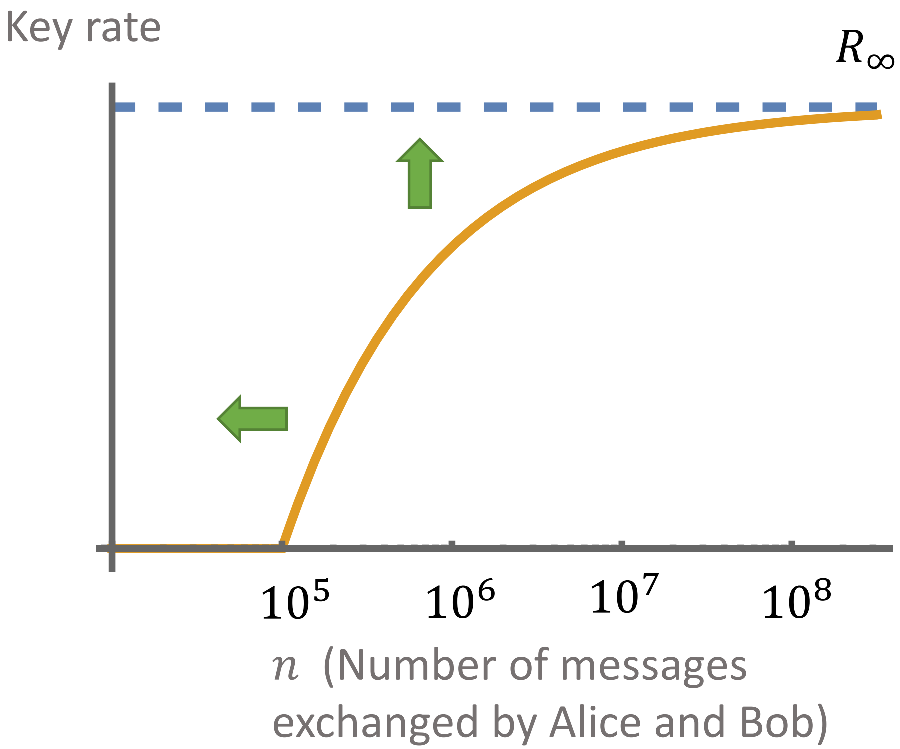

$$rate = R_{DW} - \frac{v}{\sqrt{n}} + O\left(\frac{1}{n}\right)$$

We achieve an optimal R_∞ and v parameters in the key rate expansion

Why we want small blocksizes…

Evolution of QKD: from structured to generic protocols

1/ Early QKD research
(Tight, protocol dependent)

2/ Follow-up research
(suboptimal, protocol dependent)

3/ Modern approach
(Tight, protocol independent)

More structure

Less structure

Elementary protocols
(Qubit BB84, Gaussian CV…)

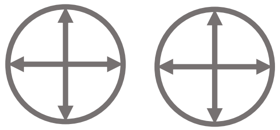

Realistic implementations
(Decoy state, Discrete-modulated CV…)

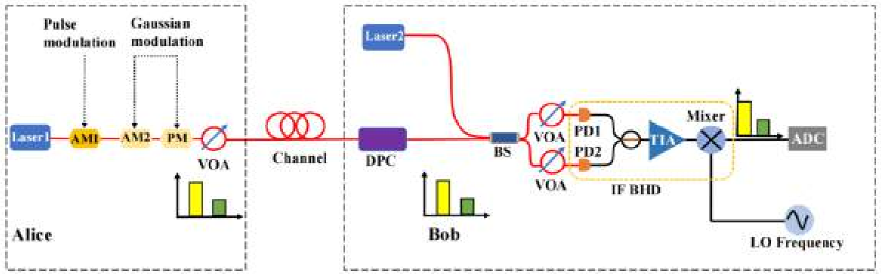

Generic protocol

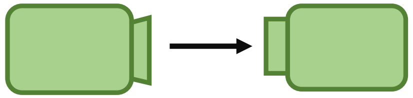

Usual approach vs modern approach

	Applicability		Efficiency (key rate)		
Usual approach *(protocol dependent)*	Entanglement- Based	Prepare-and-Measure	Asymptotic	Finite-size	Succesfully applied in practice, but limited…
[Shor-Preskill ‘00, Koashi ‘09]	Binary only	Binary only	Effective	Effective	
Modern approach *(protocol independent)*					
Renner’s early work [Renner et al. ‘07-’08]	All	All	Devetak-Winter (how to apply ?)	Large correction	More ambitious program but unfinished…
Numerical QKD [Winnick ‘18]	All	All	Devetak-Winter*	Large correction	

*May require numerical optimisation

Generalised EAT has practical limitations

Prepare-and-measure protocol over 100km of optical fiber
(= 5 msec latency)

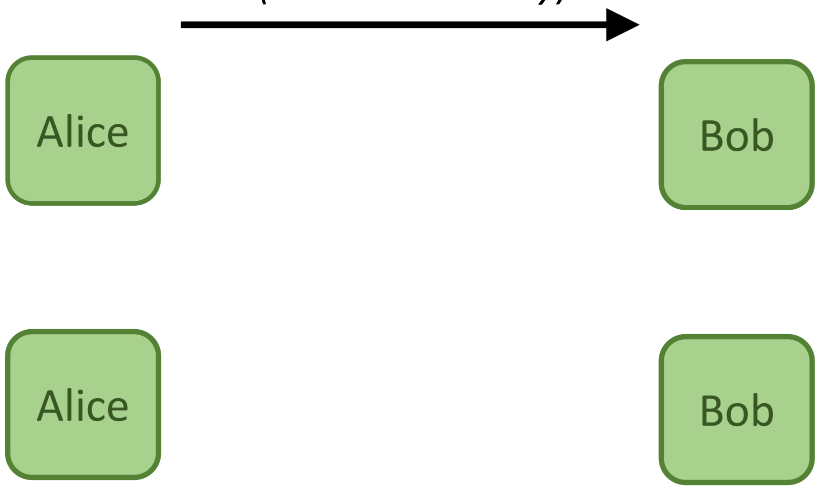

	Repetition rate @100km	Key rate @100km
Generalised EAT	Limited max. 0.2 kHz	Limited max. 2 Hz
Current work	Unlimited ex. 1 GHz	Unlimited ex. 10 MHz

We can send all pulses in parallel:
Rate increased by 6 orders of magnitude !

Assuming: $loss\ =\ 0.2\ dB/km$, *speed of light in fiber* $=\ 200\ 000\ km/s$, *and 1 bit of key/detected pulse*

Generic QKD protocol structure considered here

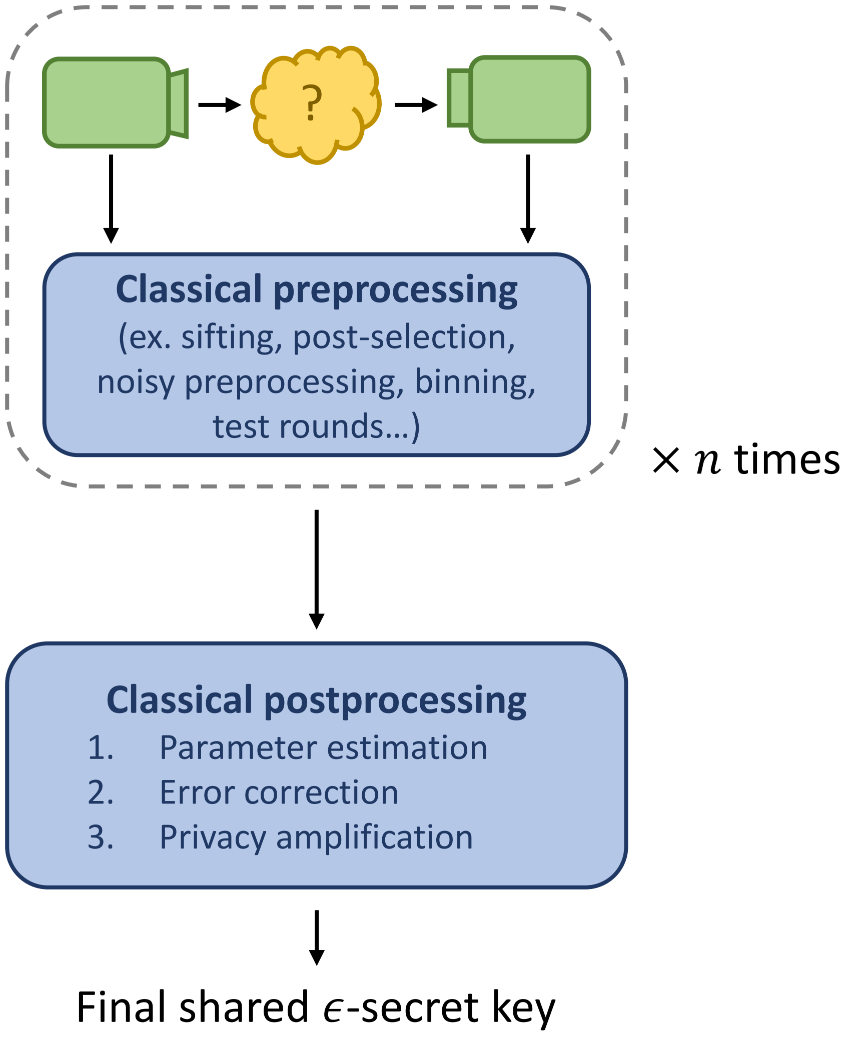

This generic structure fits all device-dependent, round-based QKD protocols.

NB: this excludes Device-Independent, DPS and COW protocols

Key idea (1/3): the abstract protocol framework

Abstract protocol map
$N: Q_i \to K_i P_i Z_i$

$\times\, n$ times

Protocol specific information is hidden

$K_i\ P_i\ Z_i$

Only variables that matter

K_i	Raw key of Alice
P_i	Public announcements of Alice and Bob
Z_i	Test information
E	Eve's quantum memory

Classical postprocessing

1. Parameter estimation
2. Error correction
3. Privacy amplification

Final shared ϵ-secret key

Proof sketch:

" Lower-bound randomness in K^n, when given information P^n and E and conditioned on a test on Z^n "

Our assumptions on the protocol map

Abstract protocol map
$N: Q_i \rightarrow K_i P_i Z_i$

$\times\, n$ times

$K_i\ P_i\ Z_i$

Classical postprocessing

1. Parameter estimation
2. Error correction
3. Privacy amplification

Final shared ϵ-secret key

Assumptions

1. Trusted devices
2. Identical rounds,
   applying in tensor product
3. Finite dimensions
4. Test information is public

Key idea (2/3): linearly adaptive protocols

Final key rate as a function of the observed statistics

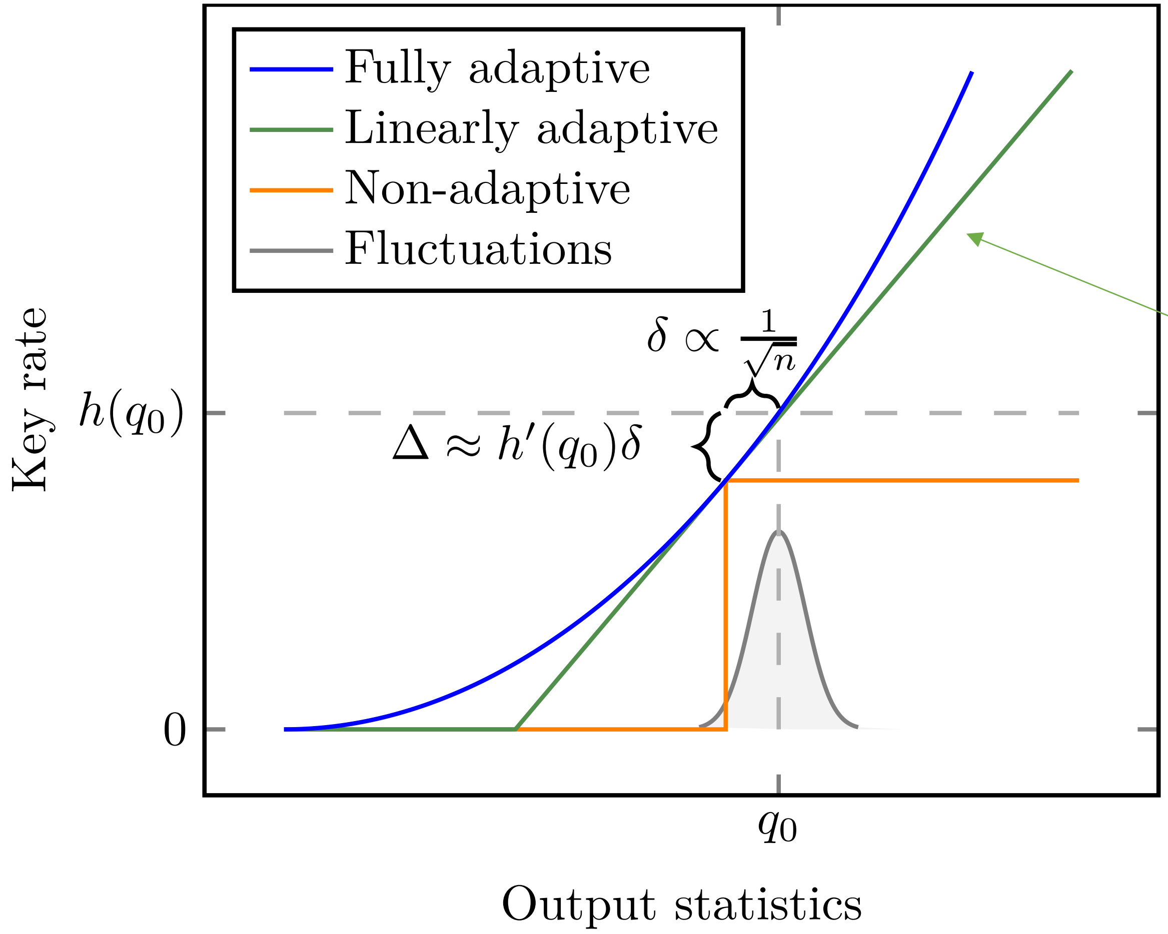

Non-adaptive: Suboptimal of order $O\left(\frac{1}{\sqrt{n}}\right)$

Linearly adaptive: No penalty

Tradeoff function

Linear lower-bound on $H(K|PE)$

$$E[f(Z)] \leq H(K|PE)$$

Fully adaptive protocol: (Future work)

Key idea (3/3): weighted Renyi entropy to control finite-size fluctuations

Fluctuations in parameter estimation

Fluctuations in privacy amplification

$$H_\alpha^{\uparrow,f}(K|PE) \quad = \max_{\sigma_x} -\frac{1}{\beta}\log\sum_{kp}\exp(\beta f(p))\mathcal{R}_\alpha(\rho_{kp}||\sigma_p)$$

Defined for any ccq state $\rho_{KPE} = \sum_{kp}|kp\rangle\langle kp| \otimes \rho_{kp}$

Depends on additional $\beta > 0$ parameter to be optimized

Similar to probability estimation factors [Y. Zhang et al. 2018] but with additional maximization over σ_p

$$\mathcal{R}_\alpha(\rho||\sigma) \quad = \mathrm{Tr}\left[\left(\sigma^{-\frac{\beta}{2\alpha}}\rho\sigma^{-\frac{\beta}{2\alpha}}\right)^\alpha\right], \alpha = 1+\beta$$

Key step in the proof (1/2): a new exact IID reduction

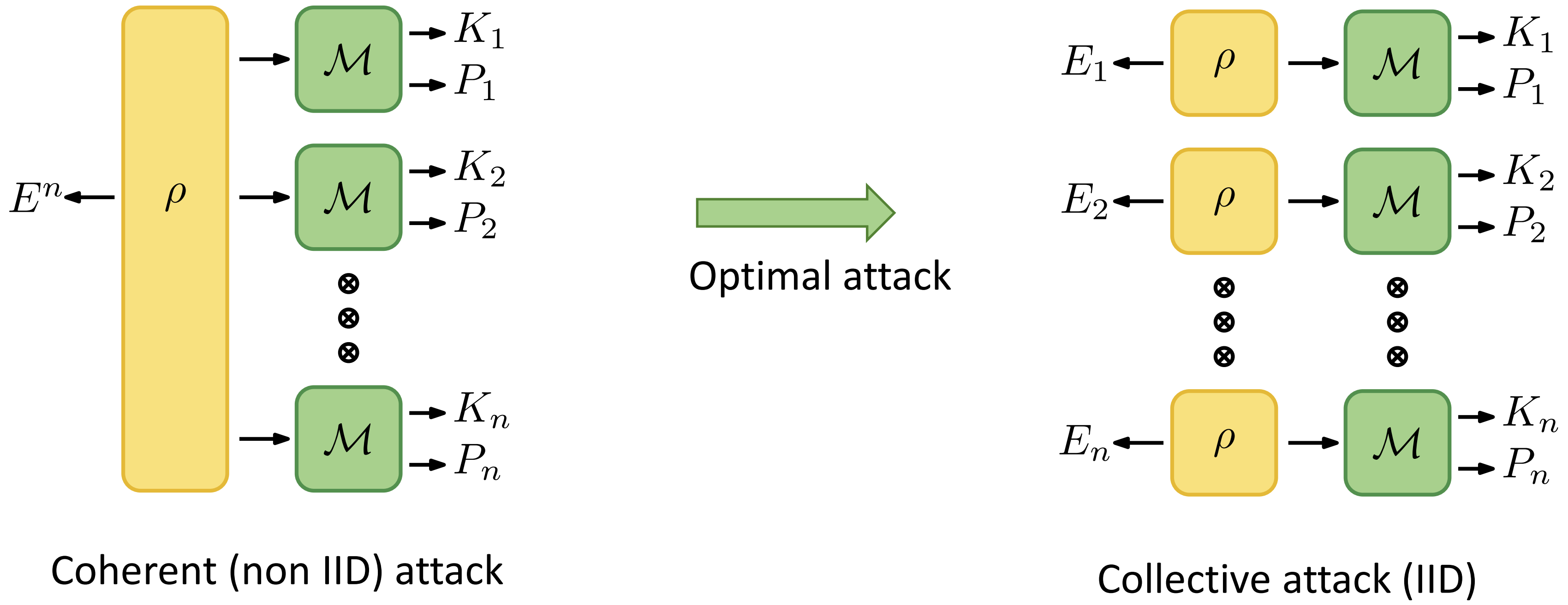

New result: Collective attacks (IID states) minimize the new entropy

$$\min H_\alpha^{\uparrow,f}(K^n|P^nE) = n\min H_\alpha^{\uparrow,f}(K|PE)$$

(also holds under partial trace constraints $Tr_{EB^n}[\rho] = \sigma_A \otimes \cdots \otimes \sigma_A$)

Key steps proof (2/2):
Using convex optimization for computing single round attacks

Computing asymptotic key rates

minimize $H(K|PE)$

subject to $\mathrm{p}(\mathrm{a}, b) = \mathrm{Tr}[\rho_{AB} M_a \otimes M_b]$

$Tr_{EB}[\rho] = \sigma_A$

Numerical QKD
[Winnick et al. 2018]

Change of variables

Computing finite-size key rates

minimize $H_{\alpha}^{\uparrow, f}(K|PE)$

subject to $Tr_{EB}[\rho] = \tau_A$

This work

Efficiently solvable
convex optimization problem

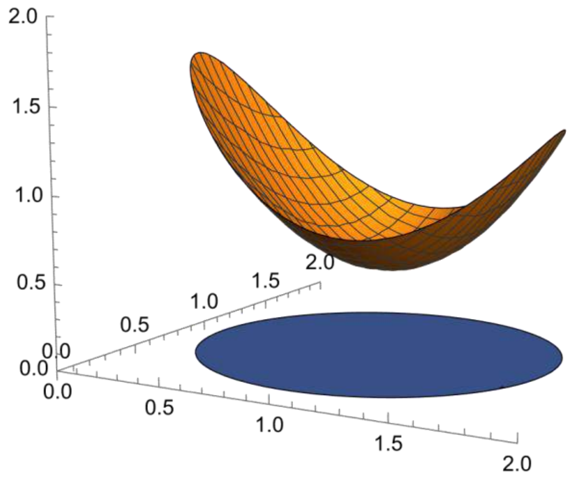

Final result: Key rate with optimal finite-size expansion

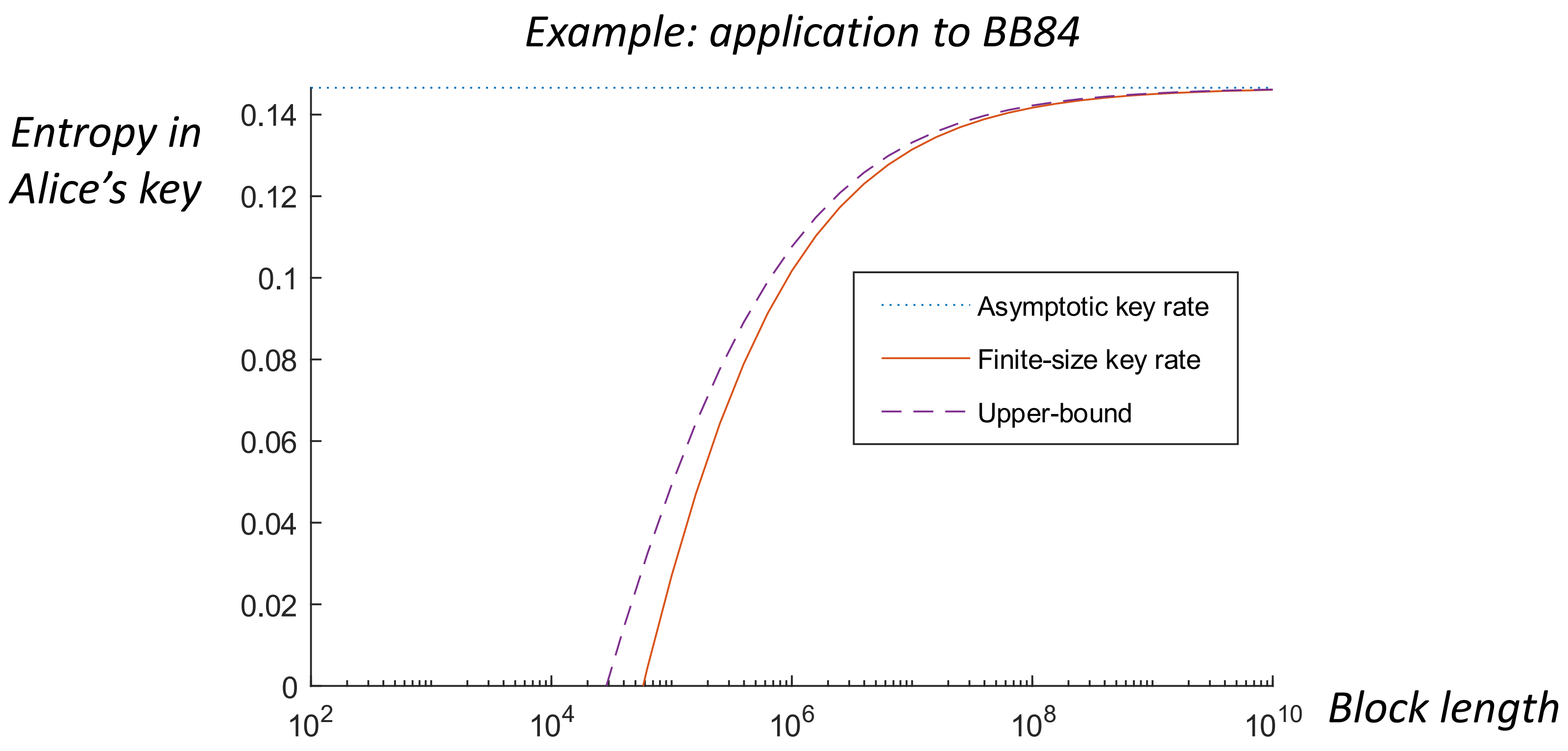

$$key\ rate\ = R_\infty - \sqrt{(1-\gamma)V(K|PE) + \gamma Var(f)}\frac{\sqrt{2\log\epsilon^{-1}}}{\sqrt{n}} + O\left(\frac{1}{n}\right)$$

$$upper - bound\ = R_\infty - \sqrt{(1-\gamma)V(K|PE) + \gamma Var(f)}\frac{\sqrt{2\log\epsilon^{-1}}}{\sqrt{n}}\left(1 + O\left(\frac{1}{\log(\epsilon^{-1})}\right)\right) + O\left(\frac{1}{n}\right)$$

Future extensions of this work

Infinite dimensions

Applications to Discrete-Modulated CV QKD

Numerical software suite

Collaborations with experimental groups

Keymaker
QKD key rate toolbox (Matlab)

nonlinSDP
Nonlinear SDP solver (Matlab)

Generalized IID reductions

Adaptive protocols for satellite QKD [Kochanovsky, Fawzi, Rouzé, TVH, 2024]

Outline

1. Introduction to security proofs

2. Finite-size security

3. Device-Independent QKD and outlook

Device-Independent QKD

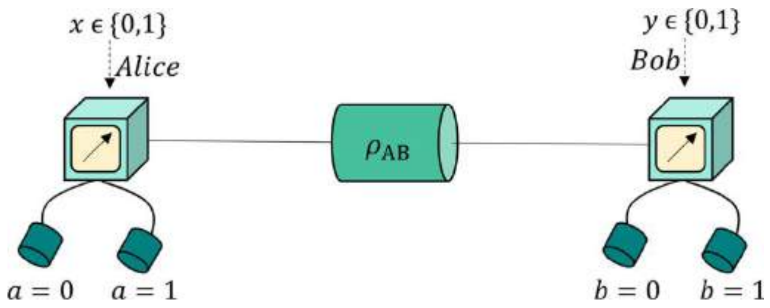

Based on Bell inequalities
eg. $CHSH = \langle A_0 B_0 \rangle + \langle A_1 B_0 \rangle + \langle A_0 B_1 \rangle - \langle A_1 B_1 \rangle$

$CHSH \leq 2$ (local deterministic stategy, no key)

$CHSH \geq 2.43$ (positive key)
$CHSH = 2\sqrt{2} \approx 2.83$ (self-tests the maximaly entangled state)

$CHSH \leq 2\sqrt{2} \approx 2.83$ (quantum stategies)
$CHSH \leq 4$ (no-signalling)

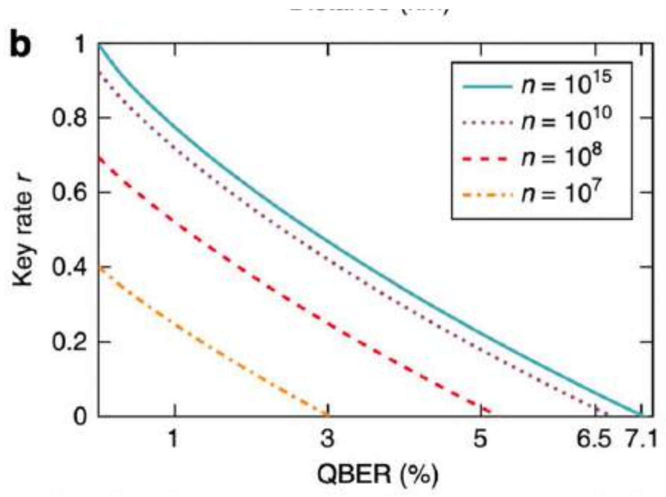

Pironio et al. Device-independent quantum key distribution secure against collective attacks (2009)
Zapatero et al. Advances in device-independent quantum key distribution (2023)

Keyrate scaling with distance/loss

« Device-dependent QKD »

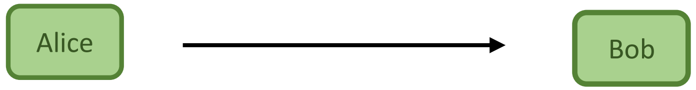

Prepares 4 "BB84" states:
$|0\rangle, |1\rangle, |+\rangle, |-\rangle$

Measures in the σ_X, σ_Z basis

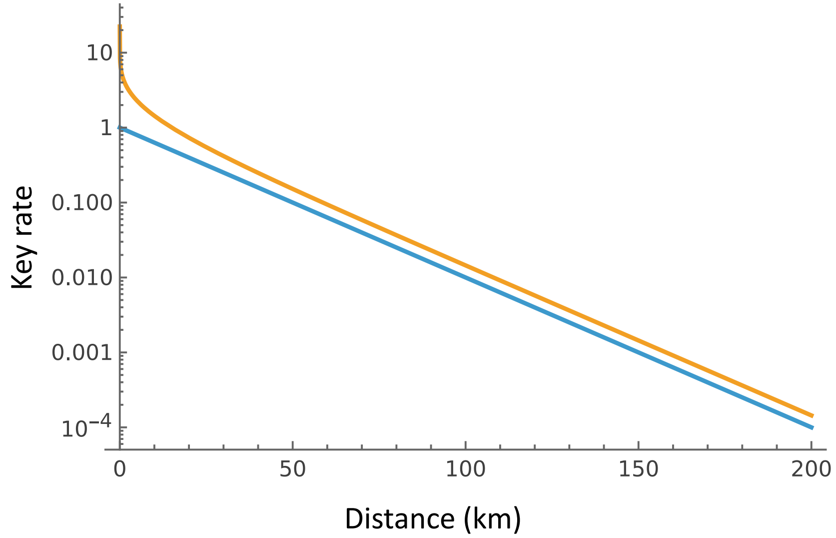

Device-independent QKD

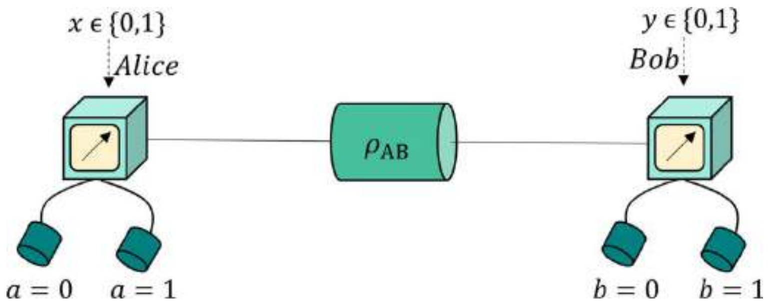

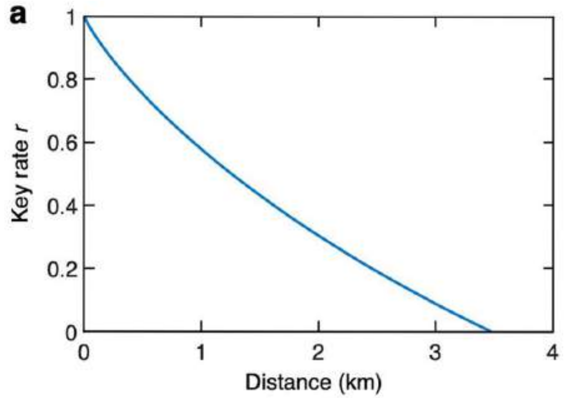

Assuming transmission over optical fiber with 0.2 dB/km loss, no excess noise

QKD as a technology: Main open questions

1. Efficiency: keyrate scaling with loss

What is the market ?
Do we need repeaters/quantum satellites ?

2. Security:
Decide on a security model Device-dependent vs. Device-independent (or intermediate)

- Assesse security vulnerabilities of real life implementations though prototyping and hacking
- Standardization (ETSI)

Theory of Quantum Key Distribution: protocols and security

Thomas Van Himbeeck

Postdoctoral researcher
Inria Paris, France

BeQCI workshop
IMEC – Leuven, Belgium
November 5, 2025

Based on: TVH, P. Brown, A general and tight finite-size security proof of quantum key distribution

Annexes

New entropy is used to define β-tradeoff function

(Usual) Tradeoff Functions

Function $f(z)$ such that for all states

$$E[f(Z)] \leq H(K|PE),$$

Generalisation

Limit $\beta \to 0$

(New) strong $\boldsymbol{\beta}$-tradeoff function $(\beta > 0)$

Function $f(z)$ such that for all states

$$H_{\alpha}^{\uparrow,f}(K|PE) \geq 0$$

Key idea II: linearly adaptive key rate

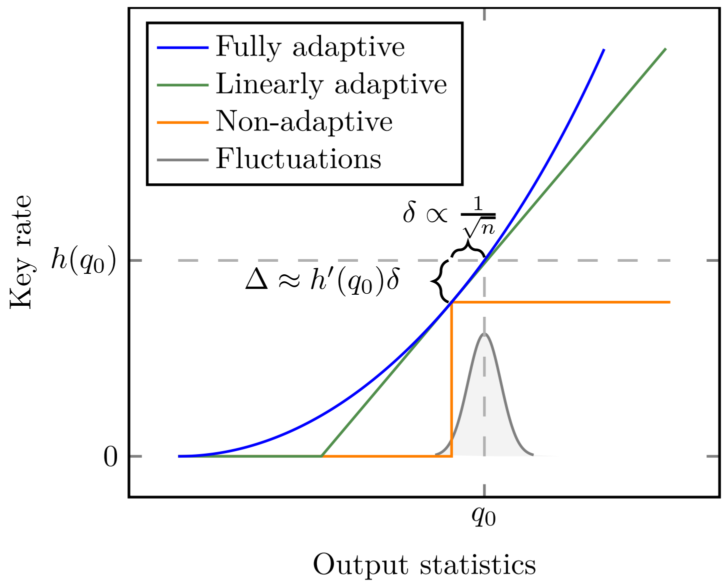

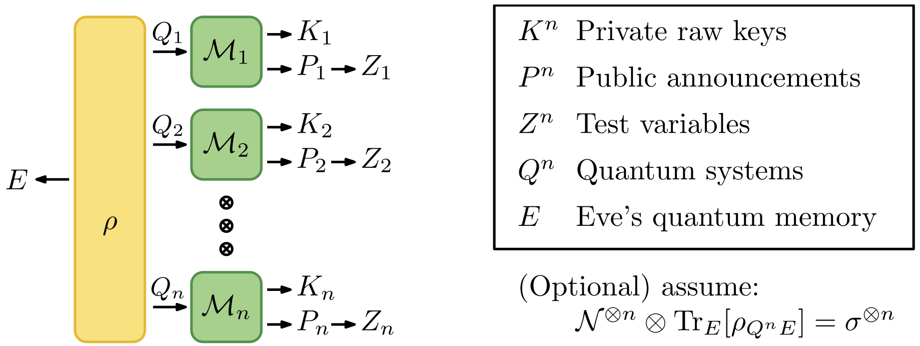

Tradeoff function

- Linear lower-bound on $H(K|PE)$
- Parametrized by function $f(z)$ such that

$$E[f(Z)] \leq H(K|PE)$$

Protocol sketch (asymptotic version)

1. Run protocol, announcing P^n
2. Evaluate $\langle f \rangle = \frac{1}{n} \sum_i f(Z_i)$
3. Apply extractor $F\colon K^n \times S \to \{0,1\}^l$ of output length $l = \langle f \rangle$ with seed S

Result final key $F(K^n)$ is ϵ-secure wrt $P^n ES$

Protocol structure: finite-size case

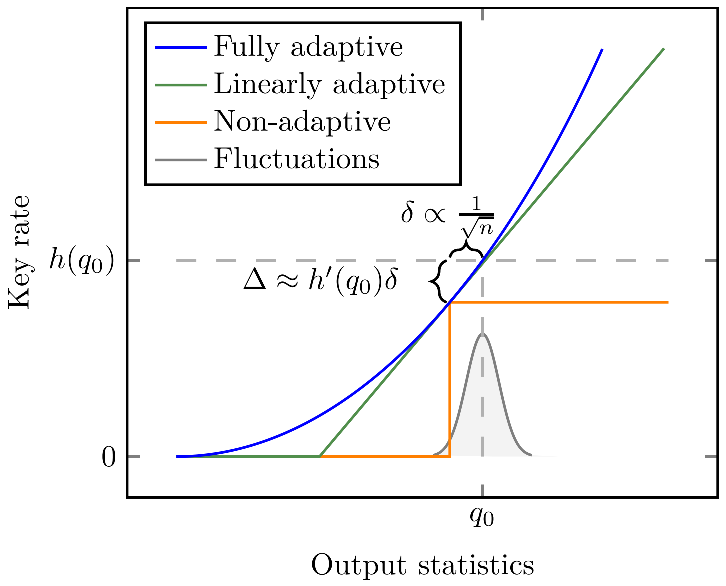

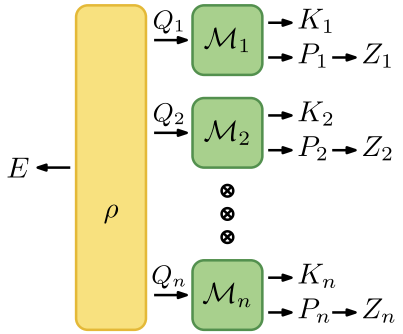

K^n	Private raw keys
P^n	Public announcements
Z^n	Test variables
Q^n	Quantum systems
E	Eve's quantum memory

(Optional) assume:
$$\mathcal{N}^{\otimes n} \otimes \mathrm{Tr}_E[\rho_{Q^n E}] = \sigma^{\otimes n}$$

Protocol sketch (finite-size version)

1. Run protocol n times
2. Evaluate β-strong tradeoff function $\langle f_\beta \rangle = \frac{1}{\mathrm{n}} \sum_i f(Z_i)$
3. Apply 2-universal extractor

$$F: K^n \times S \rightarrow \{0,1\}^l$$

with output length

$$l = \langle f_\beta \rangle - \frac{1 + \beta}{\beta} \frac{\log(\epsilon^{-1})}{n}$$

Result: Final key $F(K^n)$ is ϵ-secure with respect to $P^n E S$

TECHNOLOGIES FOR QKD

QKD: A TECHNOLOGY RICH APPLICATION

Stéphane Clemmen

OPERA-LIQ (ULB)

Photonics Research Group (UGent - imec)

OUTLINE

Introduction

- Typical building blocks
- Features, light's degrees of freedom and QKD protocols

Various protocols ➔ different hardware

~~Various quantum channels ➔ different hardware~~

Outlook

Typical building blocks: First setup

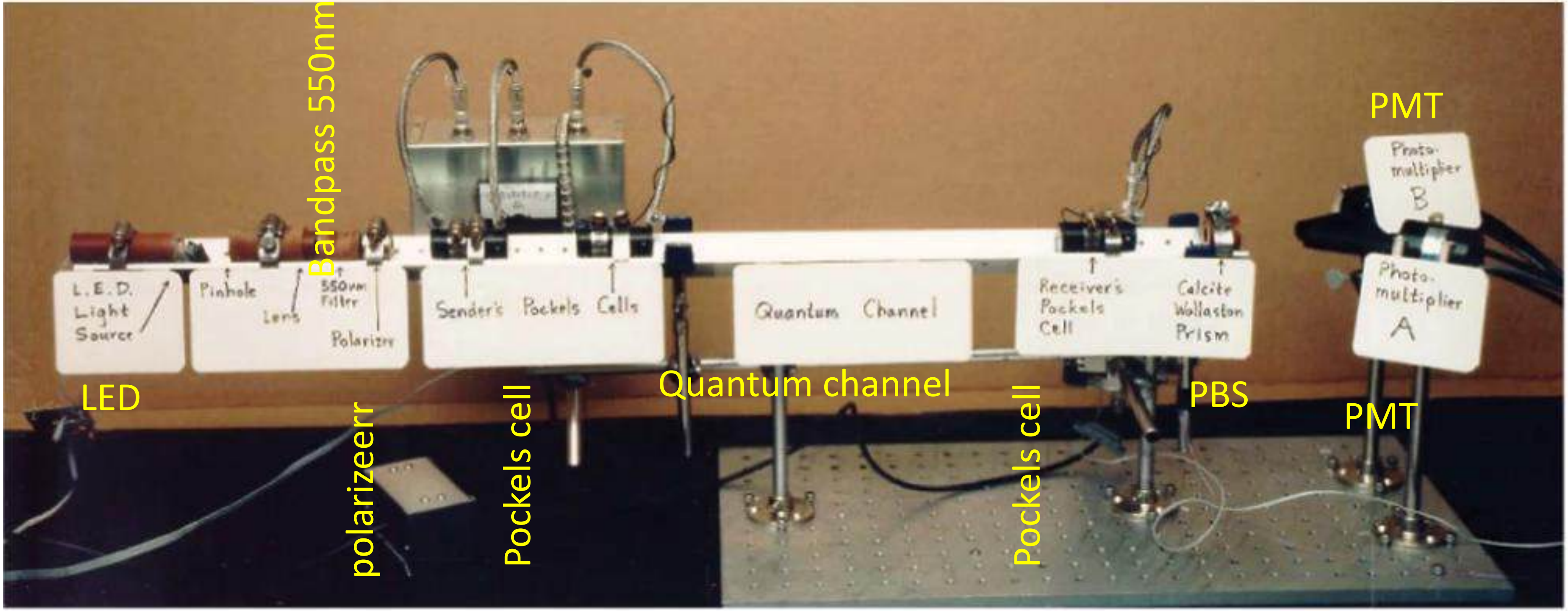

[Bennett 1992]

TYPICAL BUILDING BLOCKS: FIRST SETUP

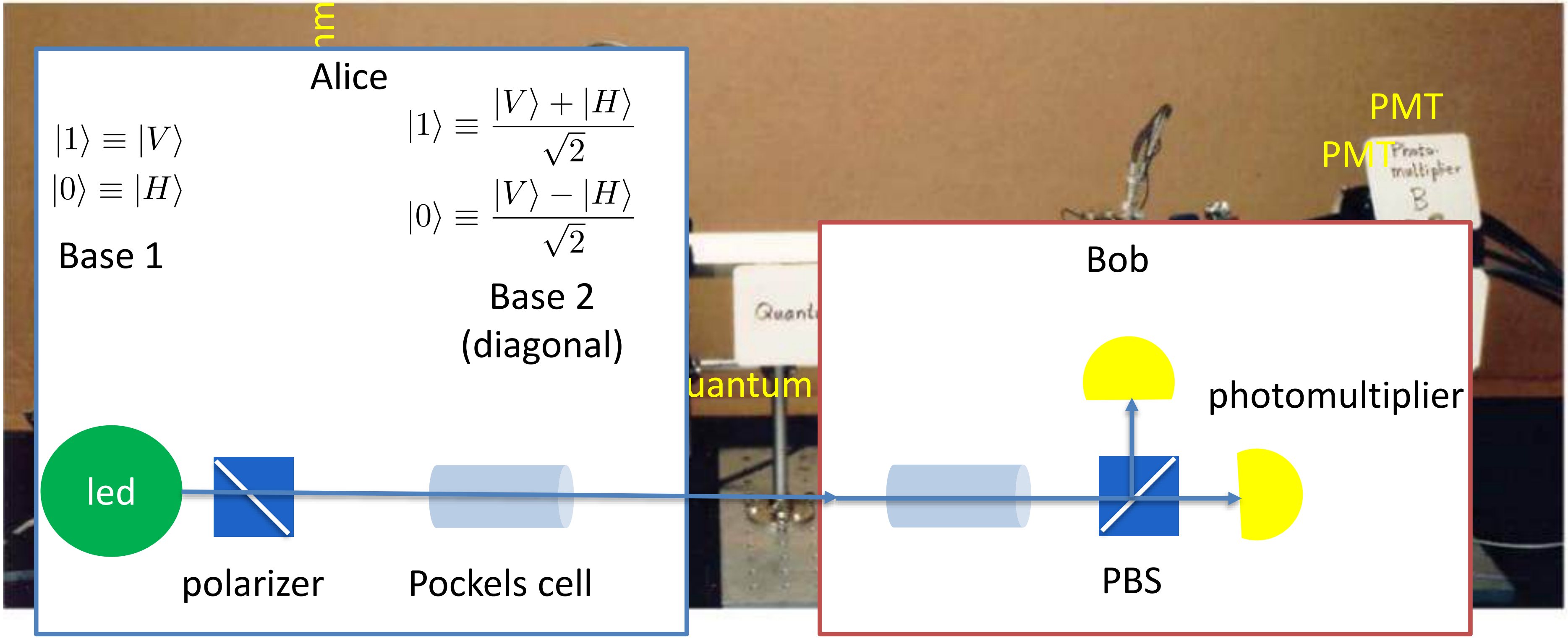

[Bennett 1992]

TYPICAL BUILDING BLOCKS AND TECHNOLOGIES

More complicated/expensive →

- Light source: LED, attenuated pulsed laser, photon pair source, photon pair source
- Encoder: Pockels cell, phaseshifter, optical switch, RF modulator
- Random number generator: pseudorandom, optical, electronics
- Quantum channel: optical fiber (SMF, multicore, HCF), terrestrial free space, satellite
- Receiver/decoder: same as encoder, beam splitter, …
- Light measurement: PMT, coherent receiver, single photon APD, SnSPD

Technologies depend on protocol, desired features/contraints, …

Introduction

- Typical building blocks
- Features, light's degrees of freedom and QKD protocols

Various protocols ➔ different hardware

Outlook

OUTLINE

ULB

Desirable features of QKD systems

GHENT UNIVERSITY

- Secure (no vulnerability to attack on the receiver/transmitter)
- Long range
- Easy to deploy (both for operator and end user)
    - No need for intermediate **secure** nodes
    - No need for dedicated fibers
- Cheap to build and to operate
- Operation in common environment
    - No excessive noise, size, temperature constraints
- High key rate; Low error rate
- Compact

DEGREEES OF FREEDOM FOR ENCODING/DECODING

Light polarization: $\{|H\rangle, |V\rangle\}, \{|D\rangle, |A\rangle\}, \{|L\rangle, |R\rangle\}$

Timing: $\{|early\rangle, |late\rangle\}, \left\{\frac{|early\rangle \pm |late\rangle}{\sqrt{2}}\right\}$

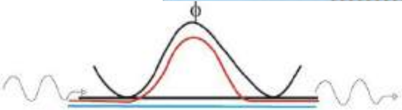

Path: $\{|left\rangle, |right\rangle\}, \{\frac{|left\rangle \pm |right\rangle}{\sqrt{2}}\}$

Color: $\{|red\rangle, |blue\rangle\}, \{\frac{|red\rangle \pm |blue\rangle}{\sqrt{2}}\}$

Phase: $\left\{\mu \left|e^{i\varphi}\right\rangle \; ; \varphi \in [0, 2\pi)\right\}$

Intensity: $\left\{\mu \left|e^{i\varphi}\right\rangle \; ; \mu \in [0, \mu_{max})\right\}$

Continuous variables

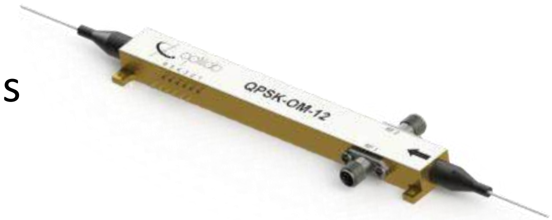

Today: $|\pm\rangle \equiv \frac{|0\rangle + e^{in\pi}|1\rangle}{\sqrt{2}}$; $\{|H\rangle, |V\rangle; |\pm\rangle\}$ and $\{|E\rangle, |L\rangle; |\pm\rangle\}$

Protocols

Coherent one way (COW)

BB84

CV-QKD

Eckert91

MDI-QKD (time-reverse Eckert91)

Twin-field QKD

DI-QKD

Repeaters

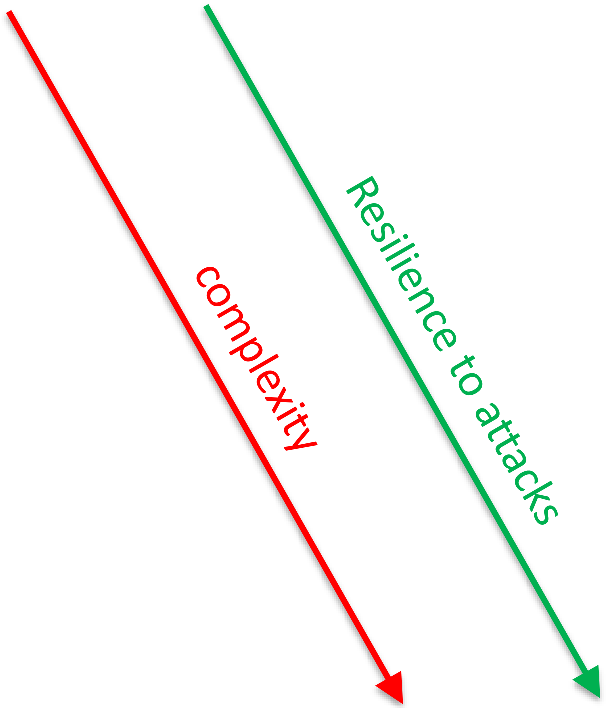

Introduction

Various protocols ➔ different hardware

- COW & BB84 in a world without good single photon sources
- BB84 with single photon sources
- CV-QKD
- Ekert91 & MDI-QKD
- Twin-field QKD
- Quantum repeaters

Outlook

OUTLINE

BB84 & COW: TYPICAL LIMITATIONS

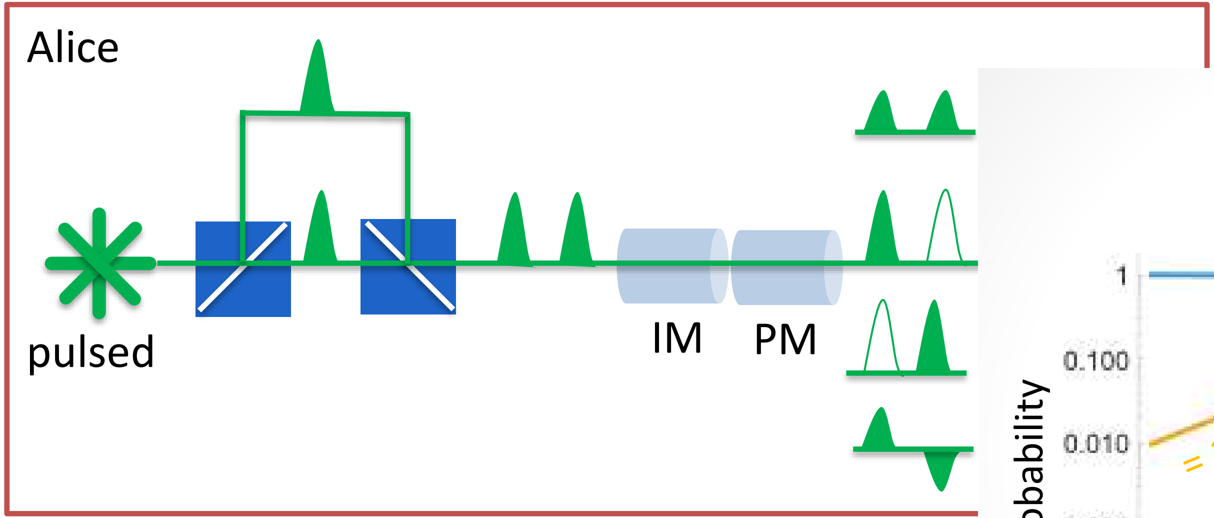

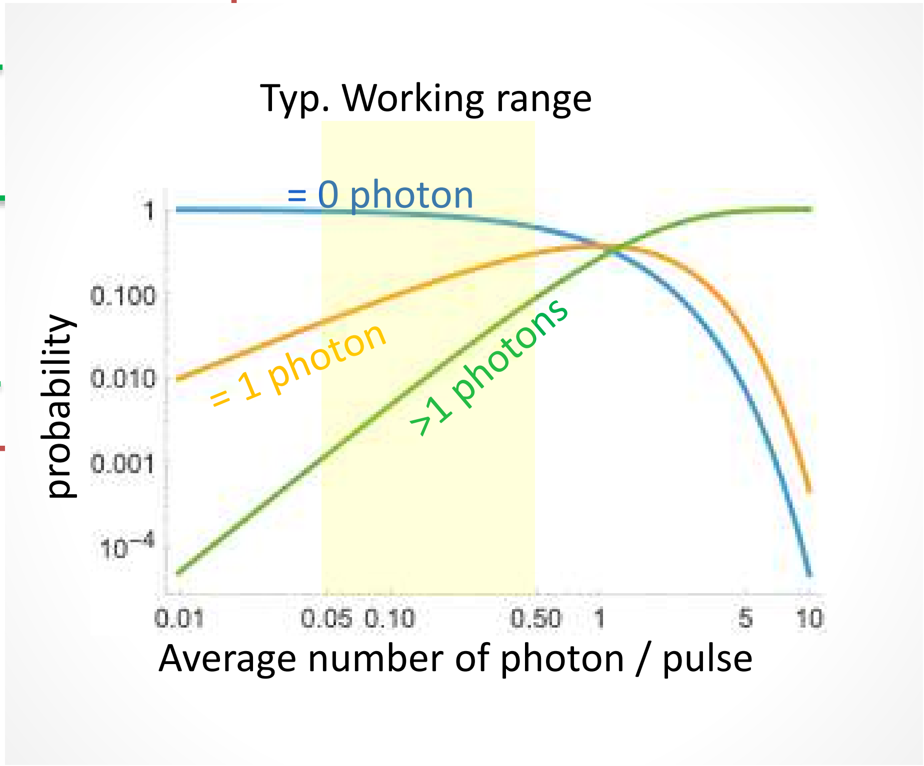

Light source:

- attenuated pulses (Poisson statistic)

→ most pulses are empty on departure

BB84 & COW: TYPICAL LIMITATIONS

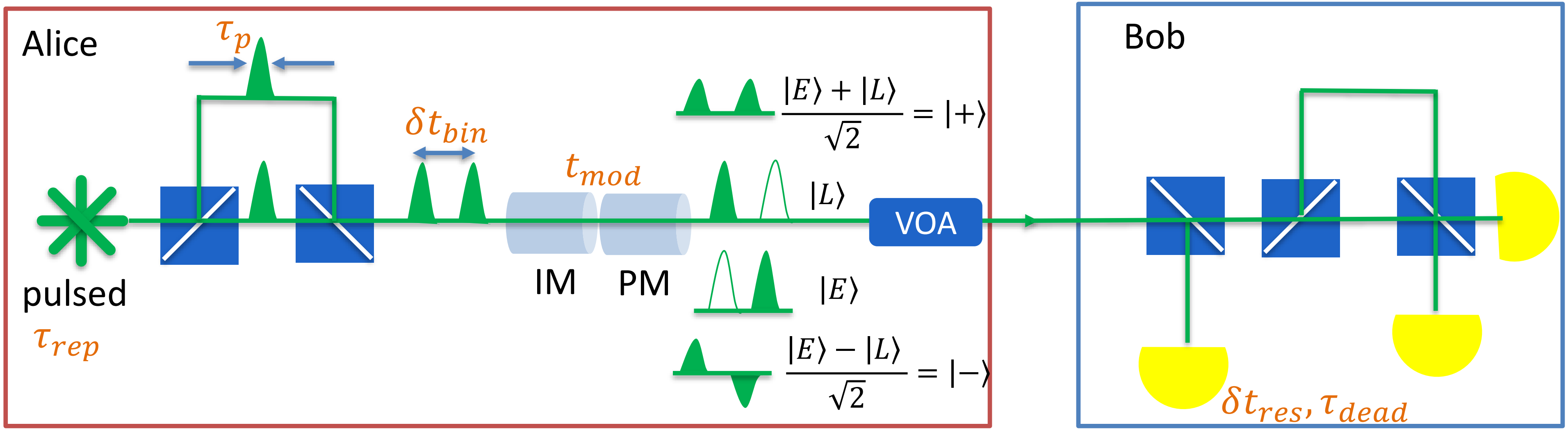

We want : $\tau_{rep} \approx \delta t_{res} \approx t_{mod} < \delta t_{bin} < \tau_{dead} \approx \tau_{rep}$

Channel loss : 0.2dB/km
(150km ⇔ 30dB)

Detector and measurement electronics (InGaAS spad, SnSPD)
- often operated at $\tau_{dead} \geq 1\text{ns}$ (limited by deadtime & afterpulse)
- time jitter δt_{res} : 200ps (spad) to 50ps (SnSPD)

Encoder switching speed t_{mod} (typ. standalone EOMs < 1ns, polar encoding slower)

BB84 & COW: TYPICAL LIMITATIONS

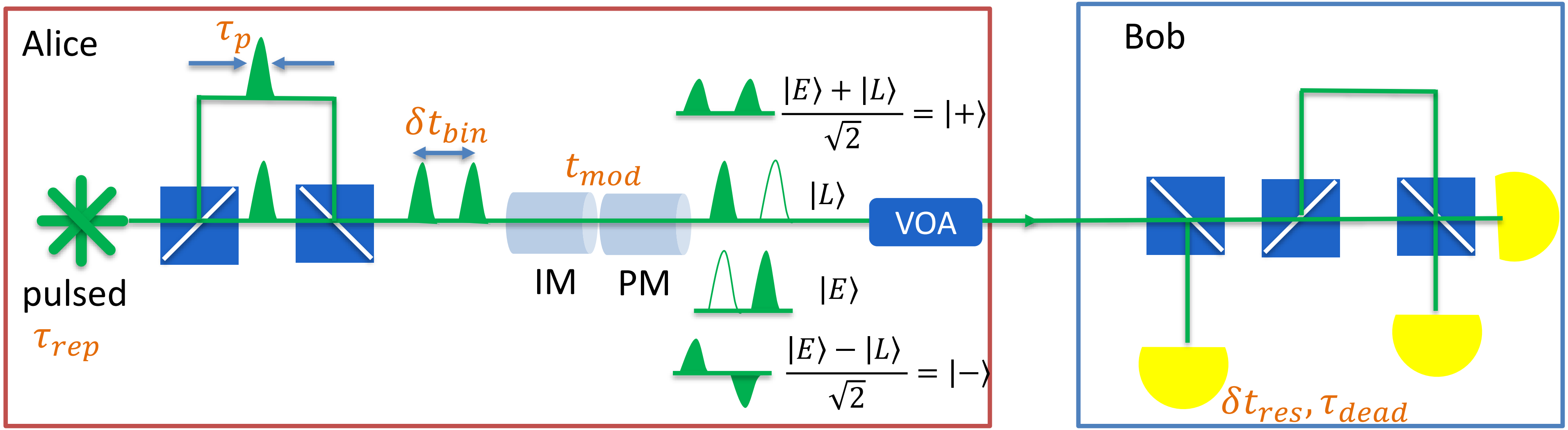

BB84

both basis $\{|early\rangle, |late\rangle\}$ & $\{|+\rangle, |-\rangle\}$

Decoys optional (only acting against photon number splitting attacks)

Coherent One-Way (COW)

$\{|early\rangle, |late\rangle\}$ for encoding; $\{|+\rangle, |-\rangle\}$ for decoys

Security is based on **monitoring coherence** between pulses (decoys necessary)

COMMERCIAL PRODUCTS: BB84-LIKE

1 Mb/s key over 50 km (10dB)
(lower rate operation up to 20dB loss)
→ allows the one-time pad to be implemented

Key technologies:

- self-differencing circuit on InGaAs spad (2GHz operation, 50ps pulse)
- BB84 protocol with decoy states
- Phase encoding
- Coexistence with telecom 32 × 10 Gbit/s

1 kb/s key over 120 km (24dB)
→ allows the one-time pad to be implemented
Key technologies:

- BB84 protocol with 2 decoy states
- O-band version: Coexistence wdm

ULB

Chip scale QKD transmitters: silicon PIC

GHENT UNIVERSITY

Promisses : cheaper, mechanically stable (ideal for phase based implementation)

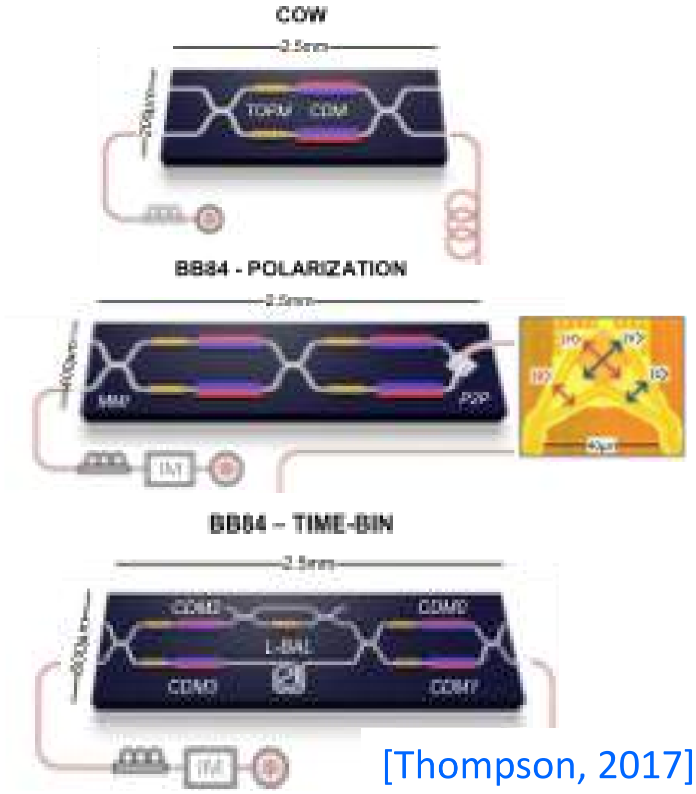

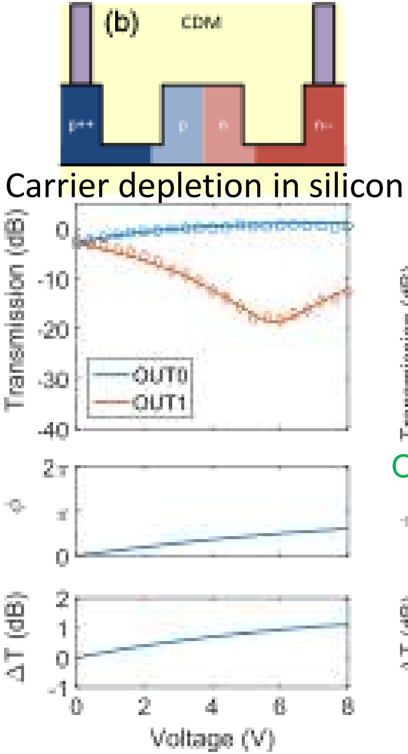

Thermal + CDM → high contrast

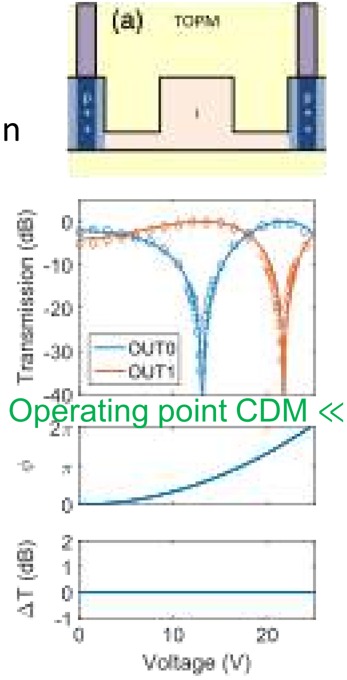

Results:

- Mod 175ps of CW
- 25 dB extinction
- 0.86Ghz clock rate
- QBER 1.1% @20km

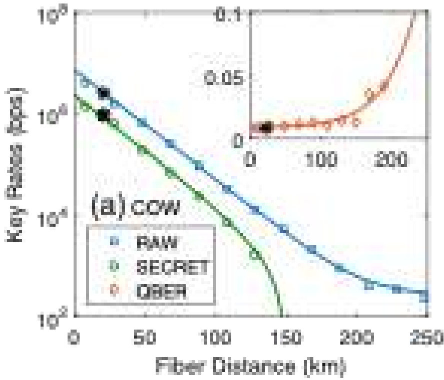

[Thompson, 2017]

CHIP SCALE QKD TRANSMITTERS: MORE INTEGRATION

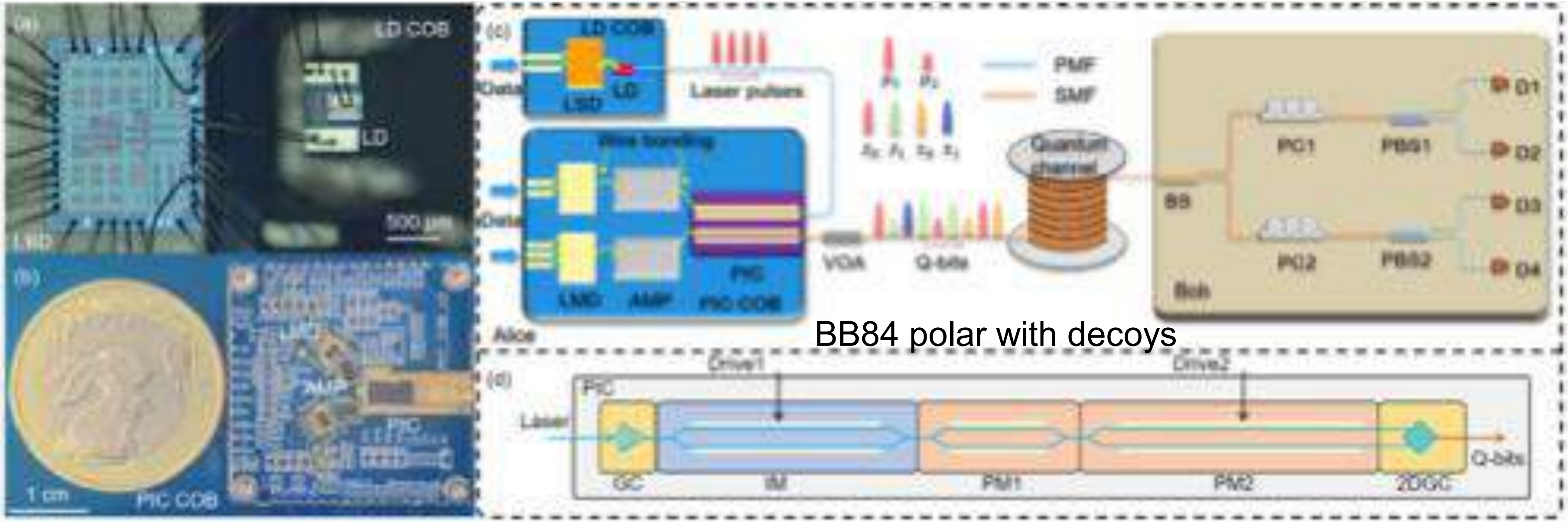

BB84 polar with decoys

[Peng, 2022]

Results:

- pulses 50ps
- 3.3 Ghz clock rate
- QBER 1.4% @100km
- Secret key rate 2.8Mbps

BB84 References

[Thompson, 2017] Sibson, P., Kennard, J. E., Stanisic, S., Erven, C., O'Brien, J. L., & Thompson, M. G. (2017). Integrated silicon photonics for high-speed quantum key distribution. *Optica*, *4*(2), 172-177.

[Bennett 1992] Bennett, C. H., Bessette, F., Brassard, G., Salvail, L. & Smolin, J. Experimental quantum cryptography. *J. Cryptol.* **5**, 3–28 (1992).

[Peng, 2022] Chen, Z. Y., Wang, X. Z., Li, Y., Wang, Y. A., Wang, C. Z., Zhang, L. K., ... & Peng, C. Z. (2025). Integrated Photonics and Electronics for High-Speed Quantum Key Distribution. *Laser & Photonics Reviews*, e01080.

Introduction

Various protocols → different hardware

- COW & BB84 in a world without good single photon sources
- BB84 with single photon sources
- CV-QKD
- Ekert91 & MDI-QKD
- Twin-field QKD
- Quantum repeaters

Outlook

OUTLINE

BB84 WITH TRUE SINGLE PHOTONS

[Midolo 2024]

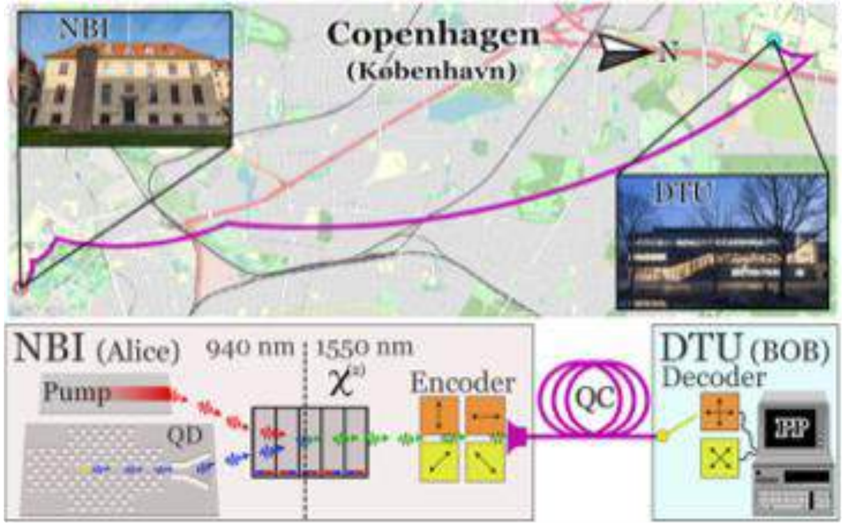

BB84 WITH TRUE SINGLE PHOTONS: HERO EXP.

[Midolo 2024]

$SKR \approx 2.5\ kb/s;\ QBER \approx 4\%$

Rep rate 72.6 MHz → 12 MHz count rate ($\eta_s = 16.5\%$)

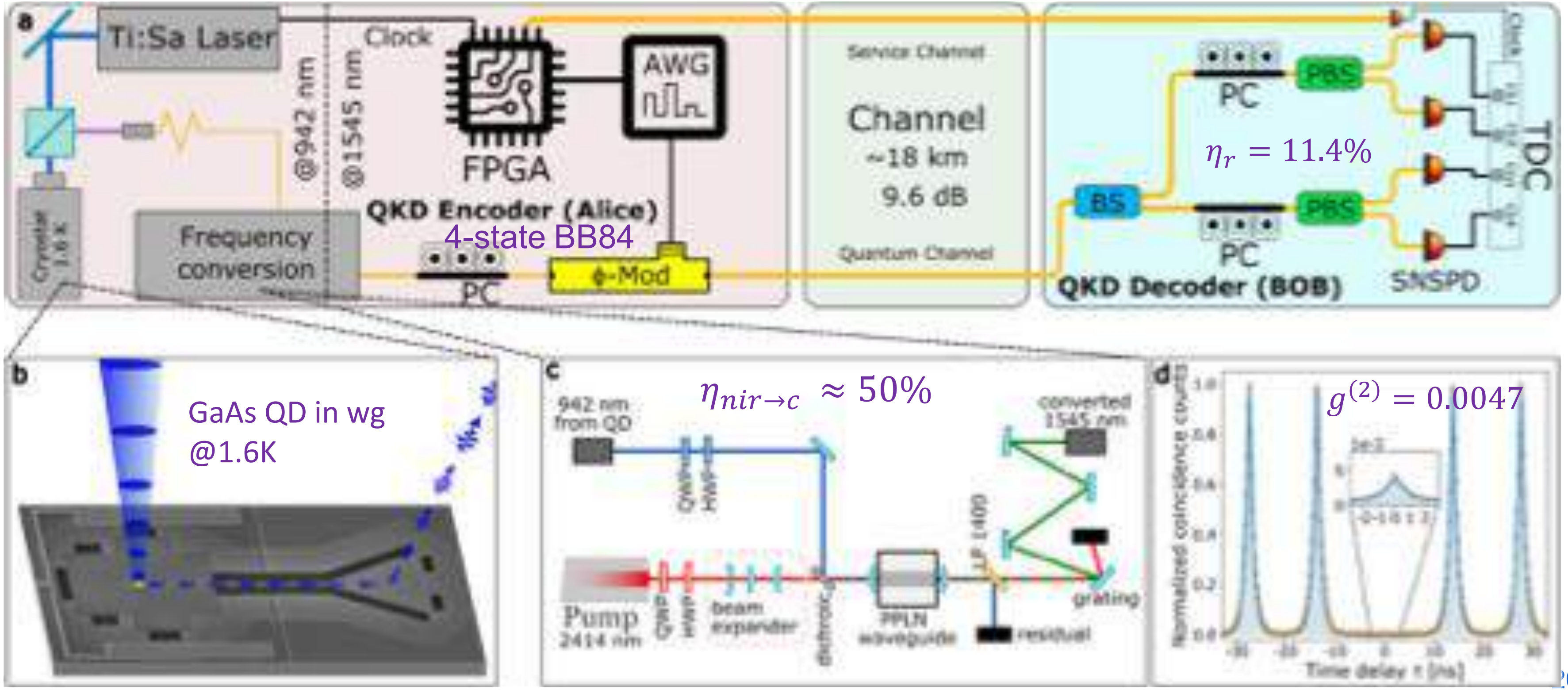

BB84 WITH TRUE SINGLE PHOTONS: HERO EXP.

[Midolo 2024]

Rep rate 72.6 MHz →

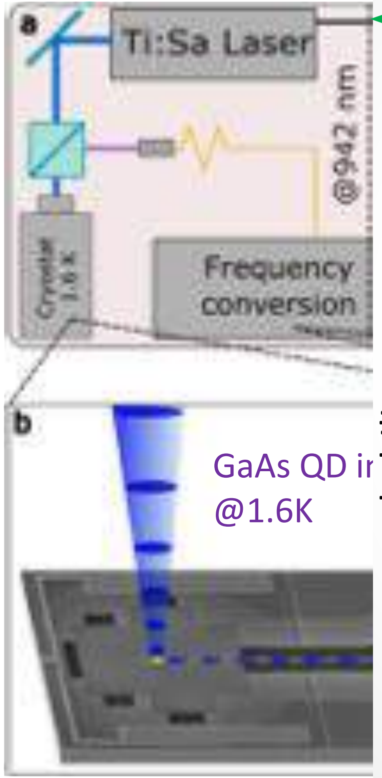

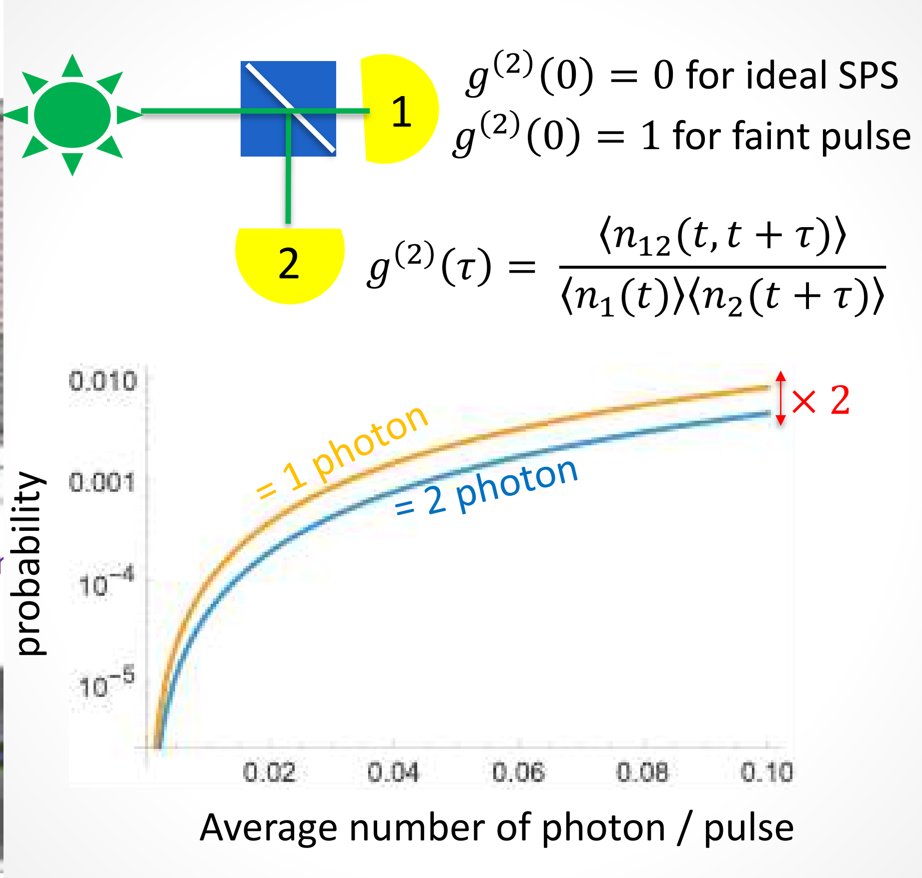

4%

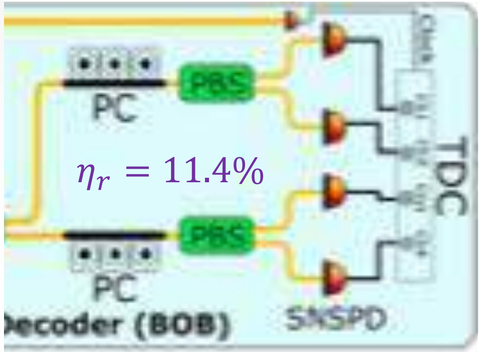

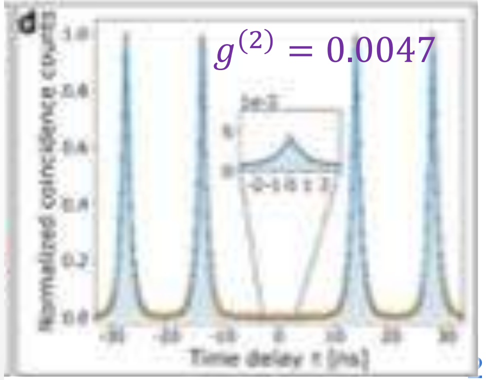

BB84 WITH TRUE SINGLE PHOTONS: HIGHER SKR

Comparison between BB84 with infinite decoy (for faint pulses) and BB84 without decoy (for SP-source)

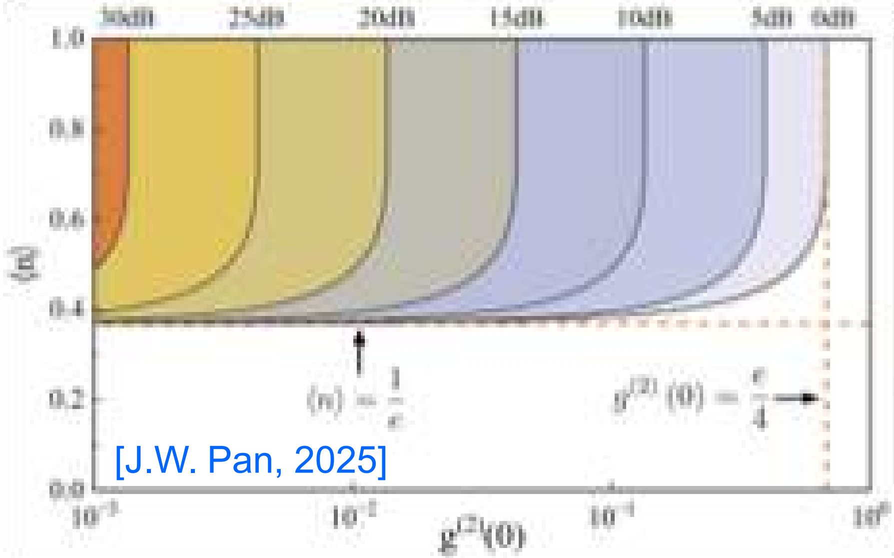

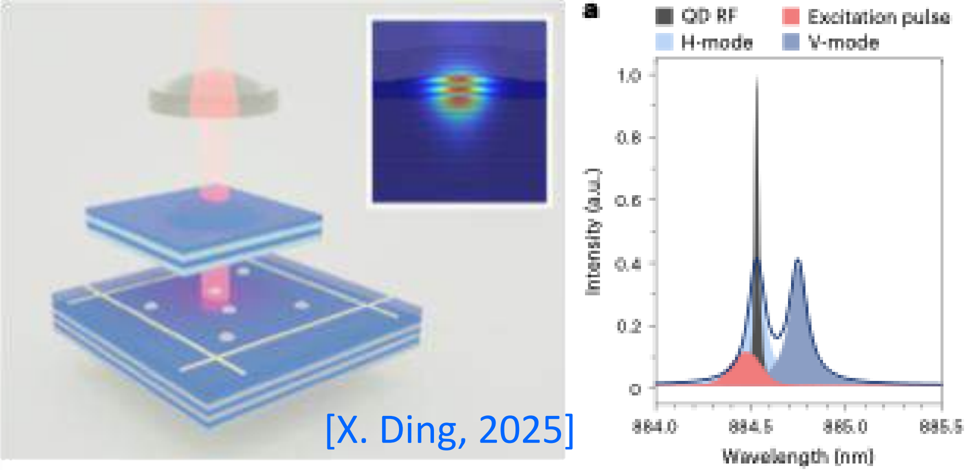

More loss means $\langle n \rangle$ must grow to keep an advantage

InAs/GaAs quantum dot plane-concave Fabry-Perot cavity
Collection efficiency of 0.71(2) and $g^{(2)} = 0.02$
Collection rate up to 54 MHz

Experiment: 3 state BB84 protocol, free space QKD (on the field)

Settings: $\langle n \rangle = 0.29$; $g^{(2)} = 0.007$ and polar encoding error of 2.54%.

→ Rep rate QKD transmitter 76.13 MHz → SKRs 4.30 Mcps (82.4 kcps) for channel losses of 0.18 (15 dB)

BET ON NEXT: QD @ 1550NM

A quantum-coherent photon–emitter interface in the original telecom band

Marcus Albrechtsen[1*†], Severin Krüger[2†], Juan Loredo[3], Lucio Stefan[3], Zhe Liu[1], Yu Meng[1], Lukas L. Niekamp[4], Bianca F. Seyschab[4], Nikolai Spitzer[2], Richard J. Warburton[4], Peter Lodahl[1,3], Arne Ludwig[2], Leonardo Midolo[1*]

[1] *Center for Hybrid Quantum Networks (Hy-Q), Niels Bohr Institute, University of Copenhagen, Jagtvej 155A, DK-2200 Copenhagen, Denmark.*
[2] *Lehrstuhl für Angewandte Festkörperphysik, Ruhr-Universität Bochum, Universitätsstraße 150, 44801 Bochum, Germany.*
[3] *Sparrow Quantum ApS, Nordre Fasanvej 215, DK-2000 Frederiksberg, Copenhagen, Denmark.*
[4] *Department of Physics, University of Basel, Klingelbergstrasse 82, CH-4056 Basel, Switzerland.*
*Corresponding authors. E-mails: m.albrechtsen@nbi.ku.dk, midolo@nbi.ku.dk
†These authors contributed equally.

(Dated: October 13, 2025)

Quantum dots stand out as the most advanced and versatile light-matter interface available today. Their ability to deliver high-quality, high-rate, and pure photons has set benchmarks that far surpass other emitters. Yet, a critical frontier has remained elusive: achieving these exceptional capabilities at telecom wavelengths, bridging the gap to fiber-optic infrastructure and scalable silicon photonics. Overcoming this challenge demands high-quality quantum materials and devices which, despite extensive efforts, have not been realized yet. Here, we demonstrate waveguide-integrated quantum dots and realize a fully quantum-coherent photon-emitter interface operating in the original telecommunication band. The quality is assessed by recording transform-limited linewidths only 8 % broader than the inverse lifetime and bright 41.7 MHz emission rate under 80 MHz π-pulse excitation, unlocking the full potential of quantum dots for scalable quantum networks.

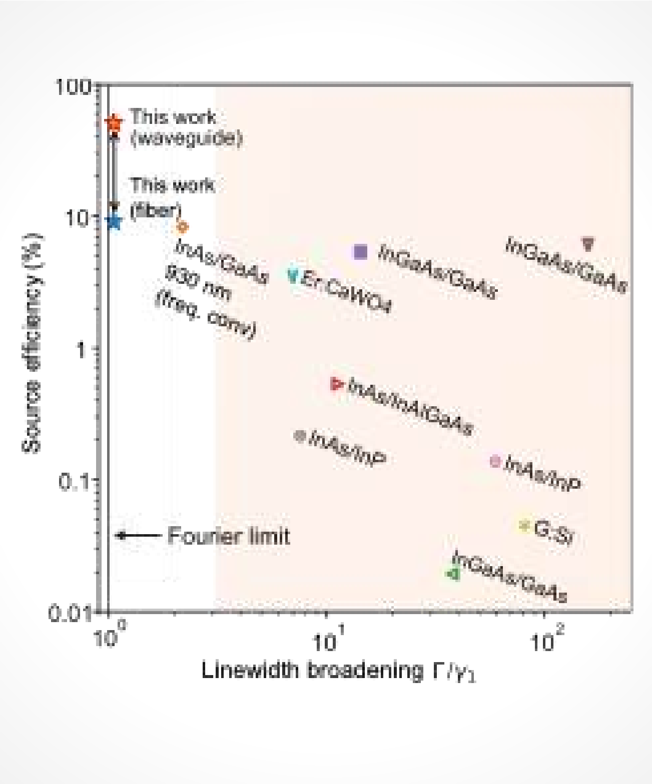

10 oct 2025 https://arxiv.org/abs/2510.09251

BB84 single photon References

[Midolo 2024] Zahidy, M., Mikkelsen, M. T., Müller, R., Da Lio, B., Krehbiel, M., Wang, Y., ... & Midolo, L. (2024). Quantum key distribution using deterministic single-photon sources over a field-installed fibre link. npj Quantum Information, 10(1), 2.

[J.W. Pan, 2025] Zhang, Y., Ding, X., Li, Y., Zhang, L., Guo, Y. P., Wang, G. Q., ... & Pan, J. W. (2025). Experimental Single-Photon Quantum Key Distribution Surpassing the Fundamental Weak Coherent-State Rate Limit. Physical Review Letters, 134(21), 210801.

[X. Ding, 2025] Ding, X., Guo, Y. P., Xu, M. C., Liu, R. Z., Zou, G. Y., Zhao, J. Y., ... & Pan, J. W. (2025). High-efficiency single-photon source above the loss-tolerant threshold for efficient linear optical quantum computing. Nature Photonics, 1-5.

Introduction

Various protocols → different hardware

- COW & BB84 in a world without good single photon sources
- BB84 with single photon sources
- CV-QKD
- Ekert91 & MDI-QKD
- Twin-field QKD
- Quantum repeaters

Outlook

OUTLINE

CV-QKD: TYPICAL SETUP

Promiss : QKD with standard telecommunication technology. [Grosshans & Grangier, 2002]

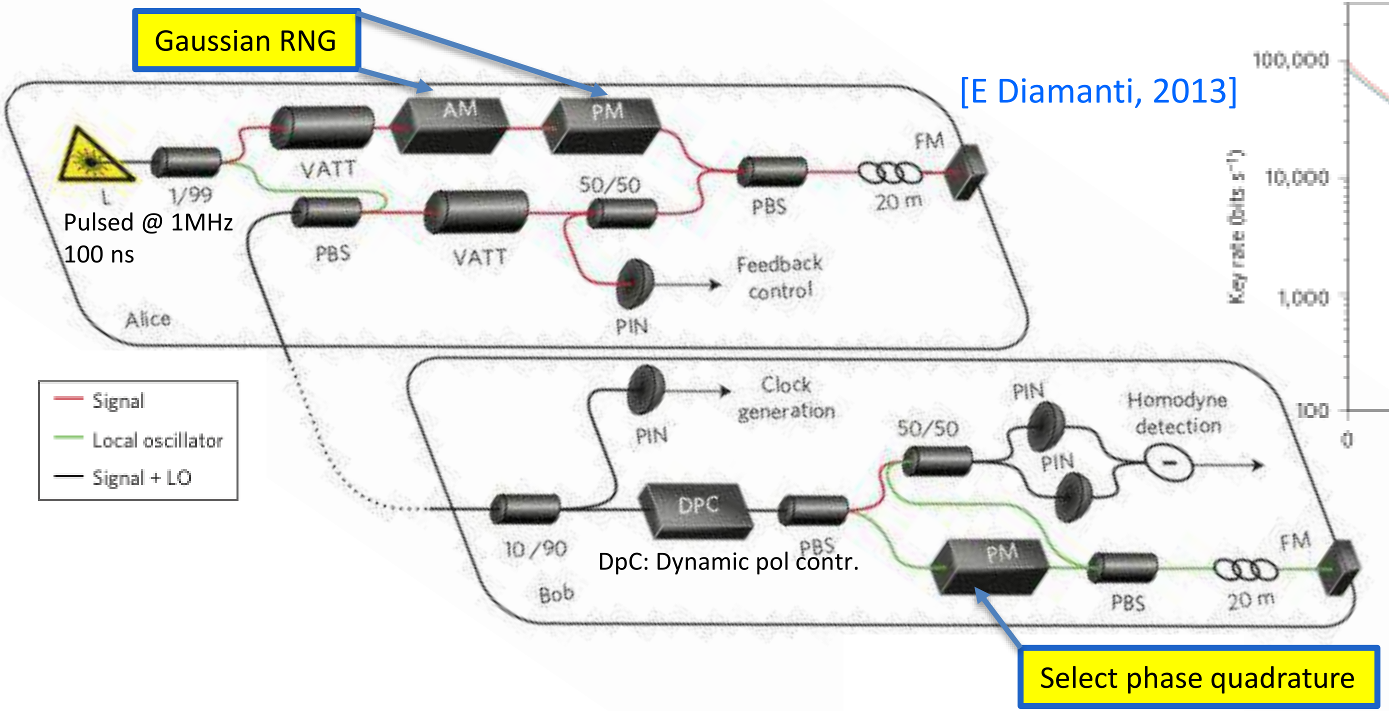

[E Diamanti, 2013]

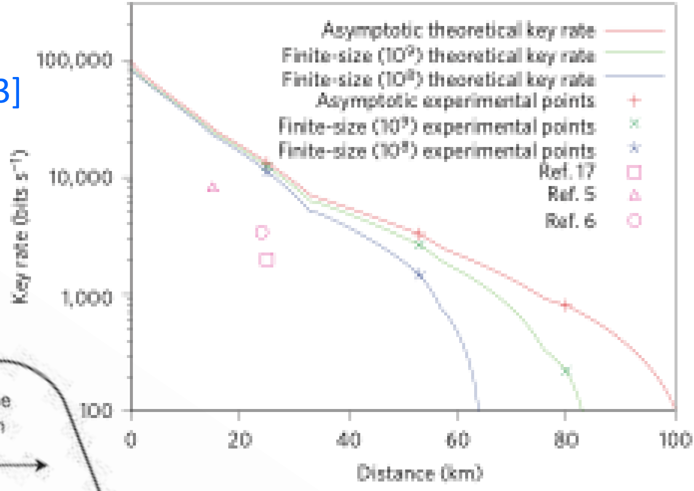

Specific hardware components: balanced detectors & electronics for Gaussian mod. (high resolution DAC)

COMMERCIAL PRODUCTS: CV-QKD

KEEQuant

Typ. Skr: 10kb/s
Up to 40km

CUbIQ Technologie

Quintessence labs

Skr: 4.3 kb/s @ 40km

CV-QKD: IMPROVED RECEIVER

space separated TIAs for limited crosstalk between 2 channels

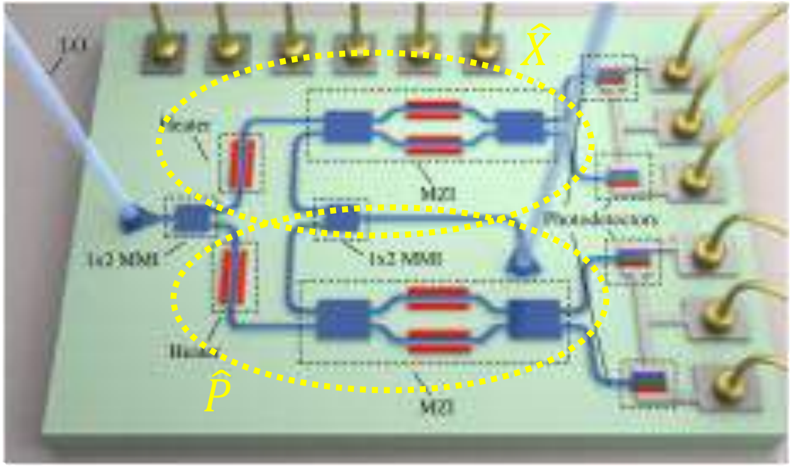

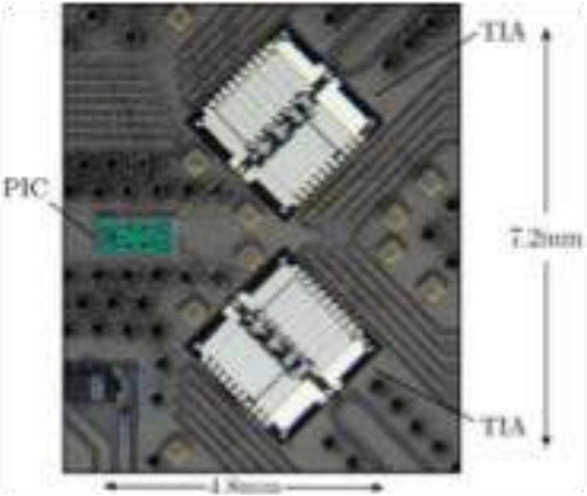

[T. Gehring, 2024]

- Ge PD from iSiPP50G silicon photonics platforms
- Dedicated TIA → shot-noise-limited bandwidth > 20 GHz.
- Discrete-modulated → 10 Gbaud operation

M	ν, a.u.	Rep. Rates, GBaud	Distance, km	SKR_{finite}, Gb/s
16	0.215	10	10	0.351
16	0.215	8	5	0.171
32	0.162	10	5	0.194
64	0.129	8	5	0.746

Reconciliation efficiency $\beta = 0.95$, detector efficien

+ many other tricks on the transmitter

CV-QKD References

[Grosshans & Grangier, 2002] Grosshans, F., & Grangier, P. (2002). Continuous variable quantum cryptography using coherent states. *Physical review letters*, *88*(5), 057902.

[E Diamanti, 2013] Jouguet, P., Kunz-Jacques, S., Leverrier, A., Grangier, P., & Diamanti, E. (2013). Experimental demonstration of long-distance continuous-variable quantum key distribution. *Nature photonics*, *7*(5), 378-381

[T. Gehring, 2024] Hajomer, A. A., Bruynsteen, C., Derkach, I., Jain, N., Bomhals, A., Bastiaens, S., ... & Gehring, T. (2024). Continuous-variable quantum key distribution at 10 gbaud using an integrated photonic-electronic receiver. Optica, 11(9), 1197-1204.

Other references:

[Poppe 2018] Karinou, F., Brunner, H. H., Fung, C. H. F., Comandar, L. C., Bettelli, S., Hillerkuss, D., ... & Poppe, A. (2018). Toward the integration of CV quantum key distribution in deployed optical networks. IEEE Photonics Technology Letters, 30(7), 650-653.

[Pirandola 2025] Fletcher, A., Harney, C., Ghalaii, M., Papanastasiou, P., Mountogiannakis, A. G., Spedalieri, G., ... & Pirandola, S. (2025). An Overview of CV-MDI-QKD. Reports on Progress in Physics.

[Andersen 2024] Hajomer, A. A., Derkach, I., Jain, N., Chin, H. M., Andersen, U. L., & Gehring, T. (2024). Long-distance continuous-variable quantum key distribution over 100-km fiber with local local oscillator. Science Advances, 10(1), eadi9474.

[Guo, 2020] Zhang, Y., Chen, Z., Pirandola, S., Wang, X., Zhou, C., Chu, B., ... & Guo, H. (2020). Long-distance continuous-variable quantum key distribution over 202.81 km of fiber. Physical review letters, 125(1), 010502.

[H. Guo, 2024] Zhang, Y., Bian, Y., Li, Z., Yu, S., & Guo, H. (2024). Continuous-variable quantum key distribution system: Past, present, and future. Applied Physics Reviews, 11(1).

[A.Q. Liu, 2019] Zhang, G., Haw, J. Y., Cai, H., Xu, F., Assad, S. M., Fitzsimons, J. F., ... & Liu, A. Q. (2019). An integrated silicon photonic chip platform for continuous-variable quantum key distribution. Nature Photonics, 13(12), 839-842.

Introduction

Various protocols → different hardware

- COW & BB84 in a world without good single photon sources
- BB84 with single photon sources
- CV-QKD
- Ekert91 & MDI-QKD
- Twin-field QKD
- Quantum repeaters

Outlook

OUTLINE

EKERT 91 = TRANSMITTER DEVICE INDEP. QKD

U $\{|H\rangle, |V\rangle, |+\rangle, |-\rangle\}$ U

U $\{|H\rangle, |V\rangle, |+\rangle, |-\rangle\}$ U

$$|\phi^+\rangle = \frac{|H\rangle_R|H\rangle_L + |V\rangle_R|V\rangle_L}{\sqrt{2}} = \frac{|+\rangle_R|+\rangle_L + |-\rangle_R|-\rangle_L}{\sqrt{2}}$$

$$|\phi^-\rangle = \frac{|H\rangle_R|H\rangle_L - |V\rangle_R|V\rangle_L}{\sqrt{2}} = \frac{|+\rangle_R|-\rangle_L + |-\rangle_R|+\rangle_L}{\sqrt{2}}$$

$$|\psi^+\rangle = \frac{|H\rangle_R|V\rangle_L + |V\rangle_R|H\rangle_L}{\sqrt{2}} = \frac{|+\rangle_R|+\rangle_L - |-\rangle_R|-\rangle_L}{\sqrt{2}}$$

$$|\psi^-\rangle = \frac{|H\rangle_R|V\rangle_L - |V\rangle_R|H\rangle_L}{\sqrt{2}} = \frac{|+\rangle_R|-\rangle_L - |-\rangle_R|+\rangle_L}{\sqrt{2}}$$

Parties encode in the same basis → information is shared between Alice & Bob

Added Benefits: by tuning their measurement apparatus differently (yet another basis), Alice & Bob can make a *Bell test* (violation of CSHC inequality = proof of security)

→ See also Device-Independent QKD

DI-QKD References

[H. Weinfurter, 2022] Zhang, W., van Leent, T., Redeker, K., Garthoff, R., Schwonnek, R., Fertig, F., ... & Weinfurter, H. (2022). A device-independent quantum key distribution system for distant users. Nature, 607(7920), 687-691

[J.D. Bancal, 2022] Nadlinger, D. P., Drmota, P., Nichol, B. C., Araneda, G., Main, D., Srinivas, R., ... & Bancal, J. D. (2022). Experimental quantum key distribution certified by Bell's theorem. Nature, 607(7920), 682-686..

[Y.B. Sheng, 2023] Zhou, L., Xu, B. W., Zhong, W., & Sheng, Y. B. (2023). Device-independent quantum secure direct communication with single-photon sources. Physical Review Applied, 19(1), 014036.

Time reversal of Ekert91: MDI-QKD

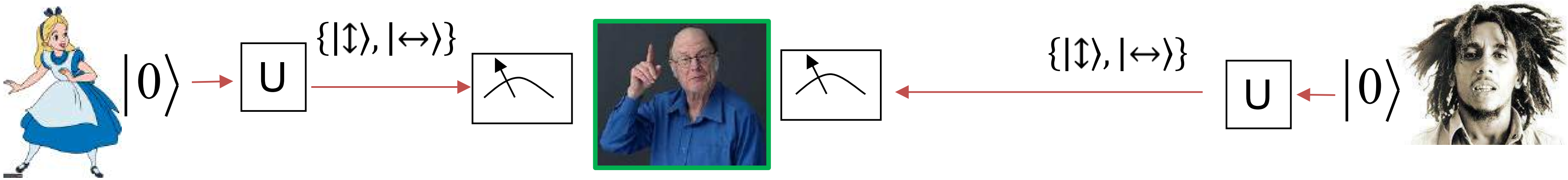

Relies on photon bunching (HOM)

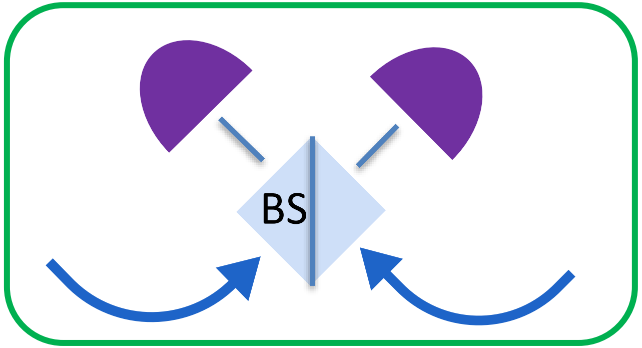

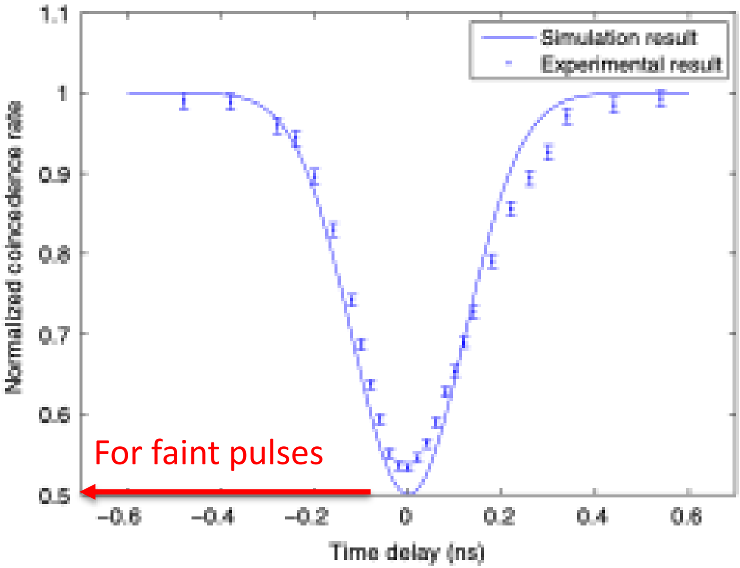

[B Qi, 2012]

TIME REVERSAL OF EKERT91: MDI-QKD

$|0\rangle \rightarrow$ U $\xrightarrow{\{|\updownarrow\rangle, |\leftrightarrow\rangle\}}$

$\xleftarrow{\{|\updownarrow\rangle, |\leftrightarrow\rangle\}}$ U $\leftarrow |0\rangle$

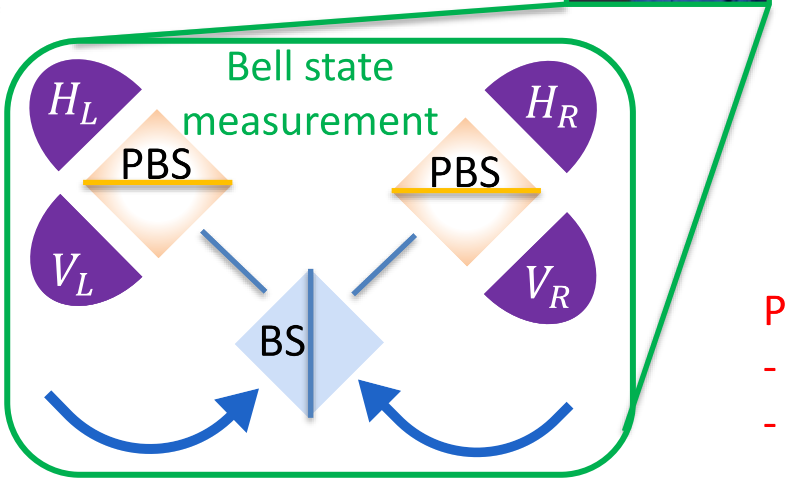

If detection on each side (left, right)

One know the state is $|\psi^{\pm}\rangle$

→ Alice & Bob know $|?\rangle_{bob} \neq |?\rangle_{alice}$

But Charlie does NOT know

PRO

- Improvement to security: MDI
- Well suited to star topology

[B Qi, 2012]

Alice\Bob	$\lvert H\rangle$	$\lvert V\rangle$
$\lvert H\rangle$	$\lvert H\rangle_L \lvert H\rangle_L$ *or* $\lvert H\rangle_R \lvert H\rangle_R$	$(\lvert H\rangle_L$or $\lvert H\rangle_R) \otimes (\lvert V\rangle_L$or $\lvert V\rangle_R)$
$\lvert V\rangle$	$(\lvert H\rangle_L$or $\lvert H\rangle_R) \otimes (\lvert V\rangle_L$or $\lvert V\rangle_R)$	$\lvert V\rangle_L \lvert V\rangle_L$ *or* $\lvert V\rangle_R \lvert V\rangle_R$

MDI-QKD IMPLEMENTATION

Require **synchronized identical** photon sources (HOM)

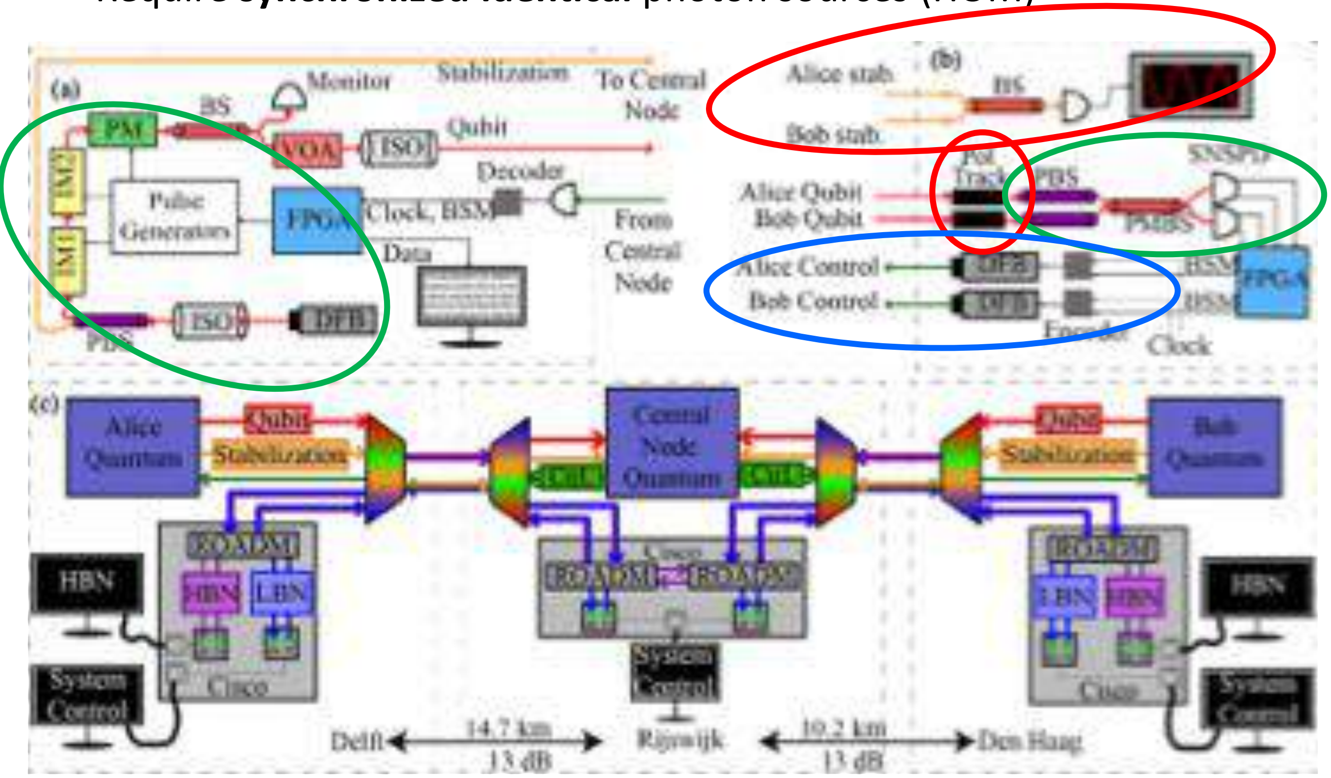

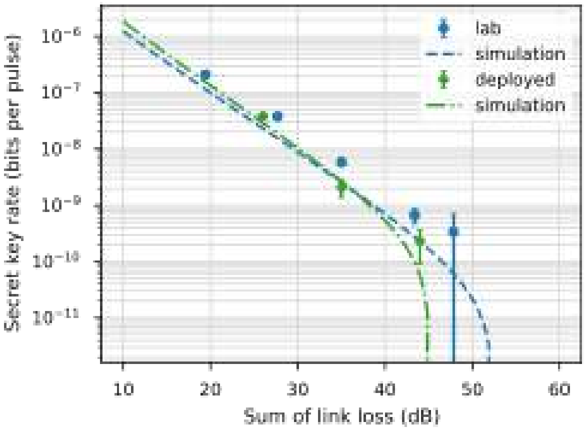

Commercial product

PLUG & PLAY MDI-QKD (TIME-BIN)

[S. Moon, 2018]

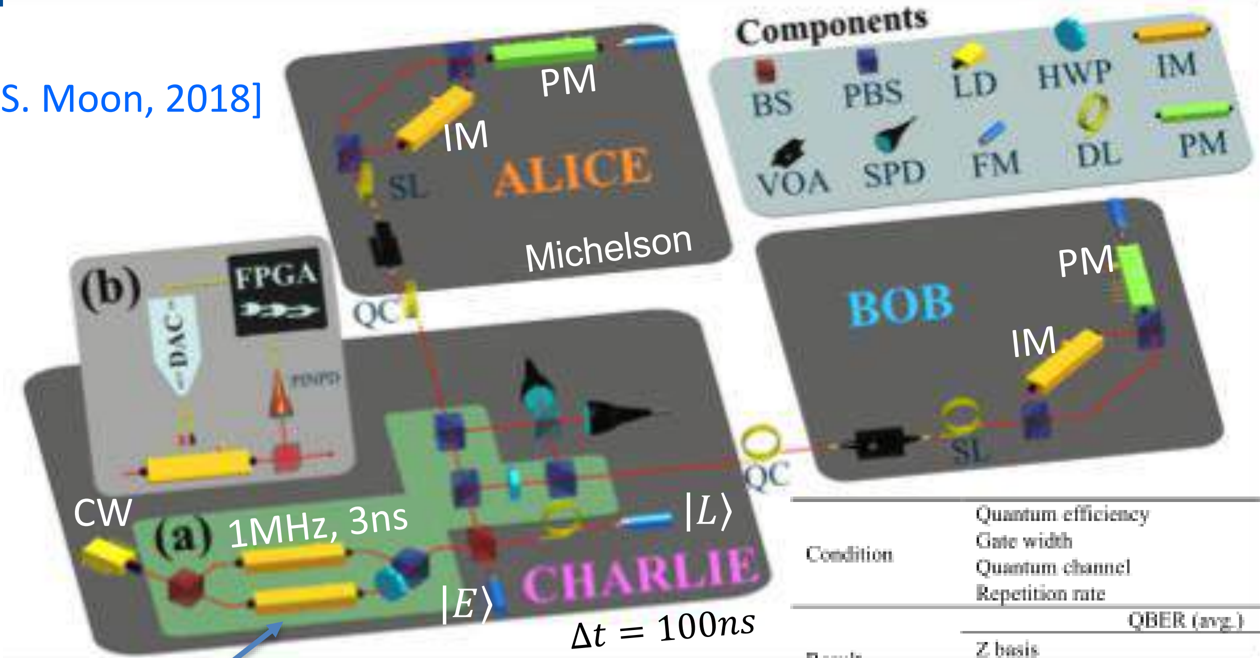

Condition	Quantum efficiency	10%	Dead time	1 μs
	Gate width	3 ns	Laser width	3 ns
	Quantum channel	25 km	Storage line	15 km
	Repetition rate	1 MHz	Wavelength	1550 nm
Result	QBER (avg.)		Key rate	
	Z basis	2.4%	$6.25\times10^{-[illegible]}$ bits per pulse	
	X basis	28%		

Sends light to either Bob or Alice (depending on polar)
(allows sync – compensates temperature induced delay)
(b)Takes care of drift in IM

MDI-QKD References

[J. Slater, 2022] Berrevoets, R. C., Middelburg, T., Vermeulen, R. F., Chiesa, L. D., Broggi, F., Piciaccia, S., ... & Slater, J. A. (2022). Deployed measurement-device independent quantum key distribution and Bell-state measurements coexisting with standard internet data and networking equipment. Communications Physics, 5(1), 186.

[Tittel 2013] Rubenok, A., Slater, J. A., Chan, P., Lucio-Martinez, I., & Tittel, W. (2013). Real-World Two-Photon Interference and Proof-of-Principle Quantum Key Distribution Immune to Detector Attacks. Physical review letters, 111(13), 130501.

[B Qi, 2012] Lo, H. K., Curty, M., & Qi, B. (2012). Measurement-device-independent quantum key distribution. Physical review letters, 108(13), 130503.

[S. Moon, 2016] Choi, Y., Kwon, O., Woo, M., Oh, K., Han, S. W., Kim, Y. S., & Moon, S. (2016). Plug-and-play measurement-device-independent quantum key distribution. Physical Review A, 93(3), 032319.

Other ref.

[J.W. Pan, 2013] Liu, Y., Chen, T. Y., Wang, L. J., Liang, H., Shentu, G. L., Wang, J., ... & Pan, J. W. (2013). Experimental measurement-device-independent quantum key distribution. Physical review letters, 111(13), 130502.

[S. Moon, 2018] Park, C. H., Woo, M. K., Park, B. K., Lee, M. S., Kim, Y. S., Cho, Y. W., ... & Moon, S. (2018). Practical plug-and-play measurement-device-independent quantum key distribution with polarization division multiplexing. IEEE Access, 6, 58587-58593.

Introduction

Various protocols → different hardware

- COW & BB84 in a world without good single photon sources
- BB84 with single photon sources
- CV-QKD
- Ekert91 & MDI-QKD
- Twin-field QKD
- Quantum repeaters

Outlook

OUTLINE

TWIN-FIELD QKD / SENDING-OR-NOT-SENDING (SNS)

Base choice + bit choice

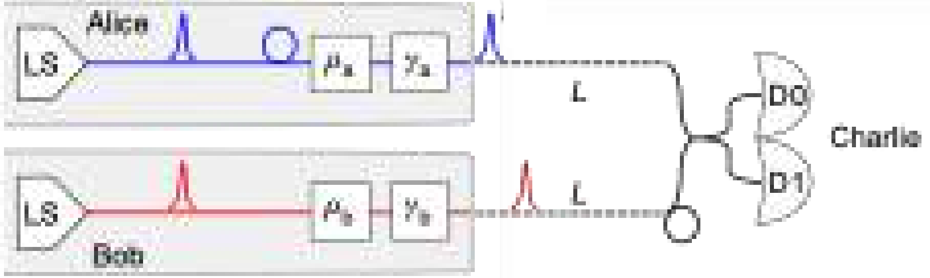

[A. Shields, 2018; H. X. Hu, 2018; H. Zhou, 2018]

$SKR \propto \sqrt{\eta}$

$$\delta_{ba} = \frac{2\pi}{s}(\Delta\nu L + \nu\Delta L)$$

Requires
-frequency stabilization
-Phase tracking

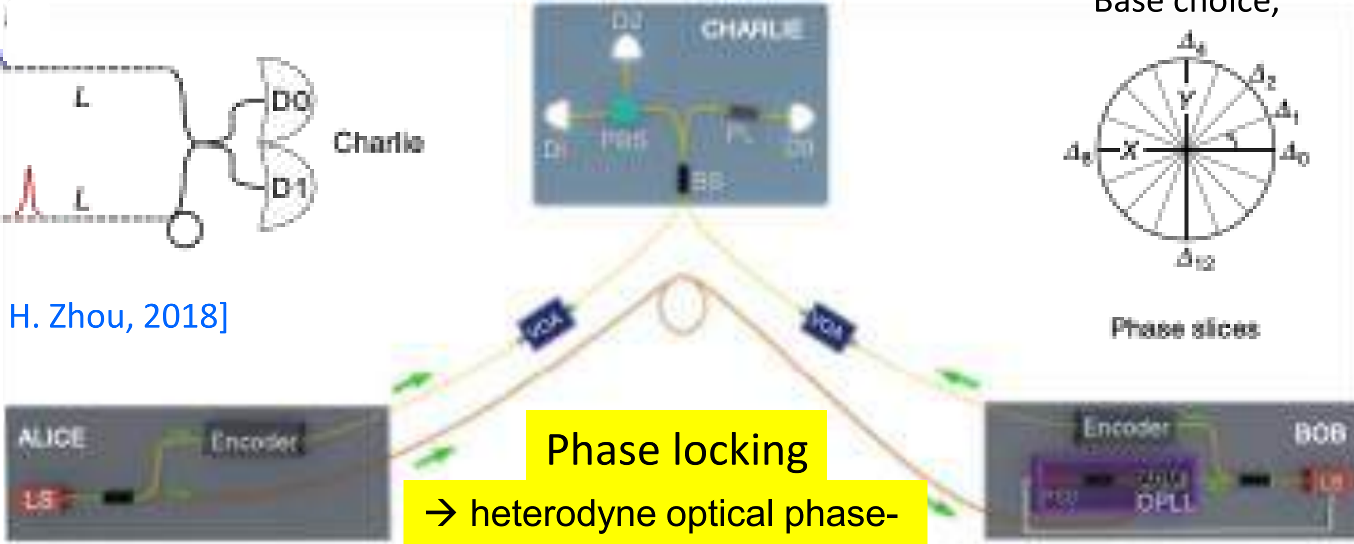

[A. Shields, 2019]

Phase locking

→ heterodyne optical phase-locked loop
Note: no locking of quantum channel (short)

Base choice,

Phase slices

b

Twin-field QKD / Sending-or-Not-Sending (SNS)

[A. Shields, 2019]

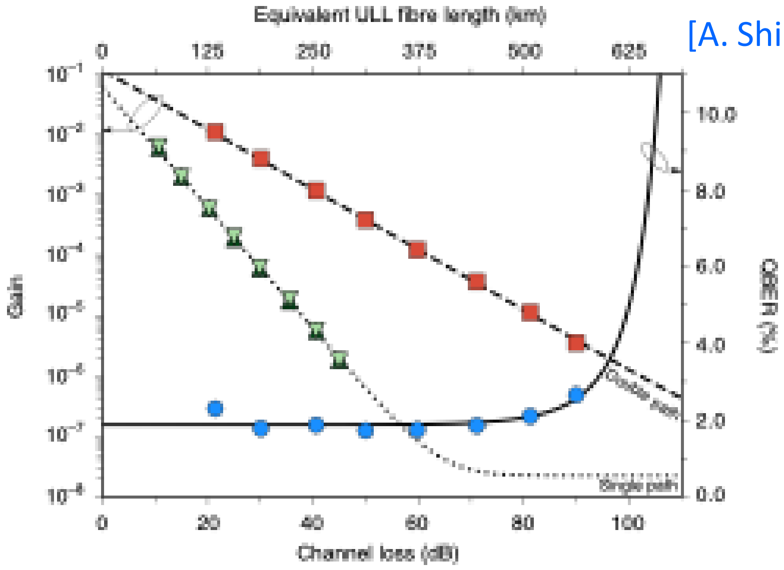

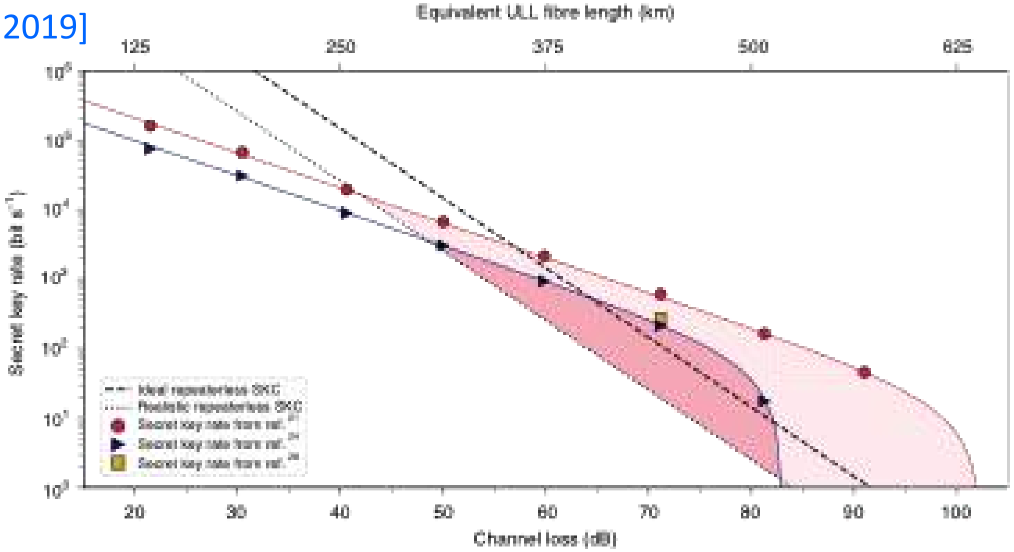

TWIN-FIELD QKD / SENDING-OR-NOT-SENDING (SNS)

[J.W. Pan, 2020]

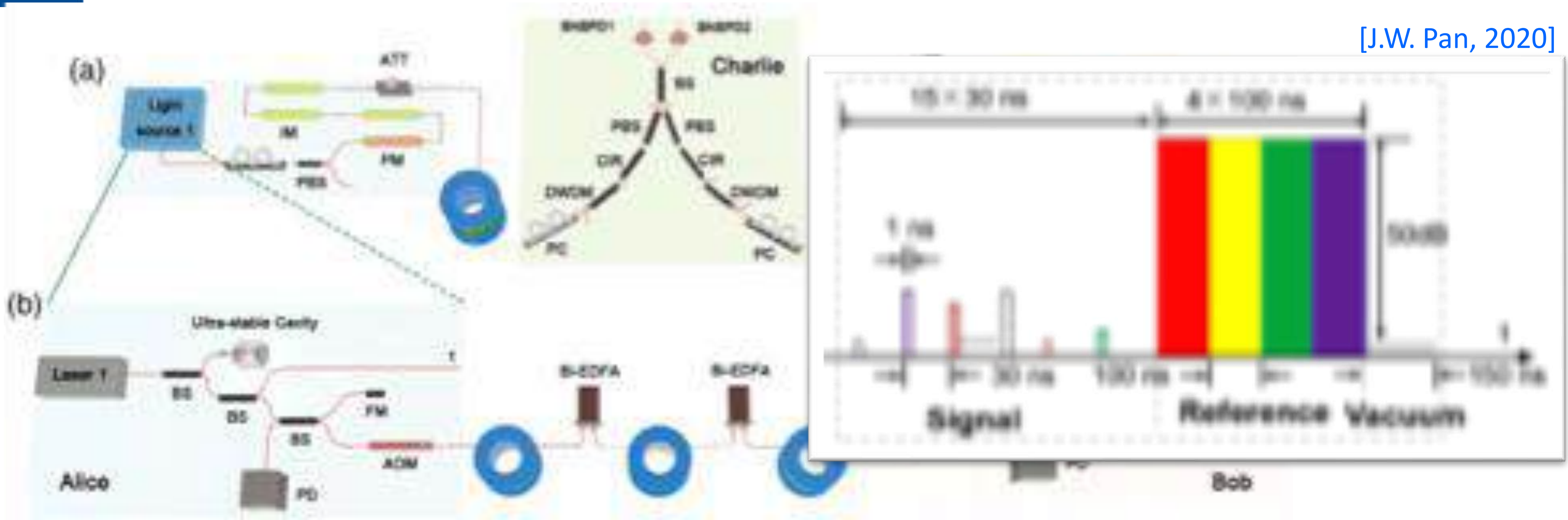

Laser line locking with cavity : 1Hz; 2 lasers locked at frequency difference of 112MHz.
Bidirectional EDFA for frequency stabilization, distributed gain avoids SBS.

Fiber phase drift estimated with reference pulses time multiplexed with qubit transmission (no actual stabilization)

Brillouin, Rayleight scattering removed by time filtering, Raman scatterings mitigated spectrally, reflexions + backward Rayleigh rejected using circulator.

Twin-field QKD / Sending-or-Not-Sending (SNS)

[J.W. Pan, 2020]

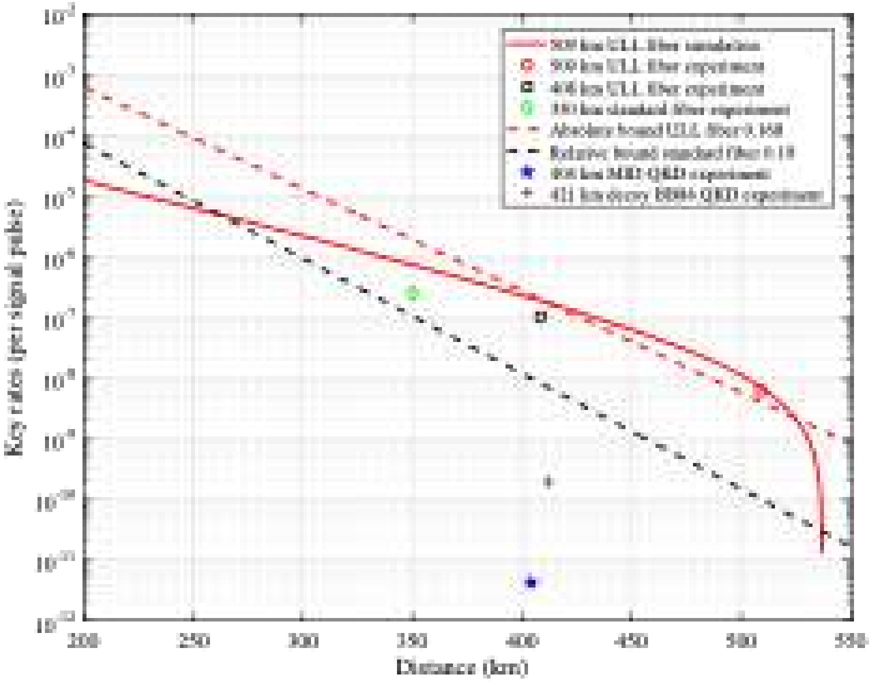

Exceed Pirandola-Laurenza-Ottaviani-Bianchi (PLOB) bound (repeaterless bound) in realistic scenario
Total length : 509 km (later: also deployed on field)

Results improved further :

- Distance over **1000 km** [J.W. Pan 2023]
  - super low dk detection : 0.02Hz
  - dual band phase estimation
- TF-QKD without frequency dissemination [Z. Yuan, 2023]
  - Frequency comb + nominally identical ν_{MW}

References

[A. Shields, 2018] Lucamarini, M., Yuan, Z. L., Dynes, J. F., & Shields, A. J. (2018). Overcoming the rate–distance limit of quantum key distribution without quantum repeaters. *Nature*, *557*(7705), 400-403

[H. X. Hu, 2018] Wang, X. B., Yu, Z. W., & Hu, X. L. (2018). Twin-field quantum key distribution with large misalignment error. *Physical Review A*, *98*(6), 062323.

[A. Shields, 2019] Minder, M., Pittaluga, M., Roberts, G. L., Lucamarini, M., Dynes, J. F., Yuan, Z. L., & Shields, A. J. (2019). Experimental quantum key distribution beyond the repeaterless secret key capacity. *Nature Photonics*, *13*(5), 334-338.

[J. W. Pan, 2020] Chen, J. P., Zhang, C., Liu, Y., Jiang, C., Zhang, W., Hu, X. L., ... & Pan, J. W. (2020). Sending-or-not-sending with independent lasers: Secure twin-field quantum key distribution over 509 km. *Physical review letters*, *124*(7), 070501.

[J.W. Pan, 2023] Liu, Y., Zhang, W. J., Jiang, C., Chen, J. P., Zhang, C., Pan, W. X., ... & Pan, J. W. (2023). Experimental twin-field quantum key distribution over 1000 km fiber distance. *Physical Review Letters*, *130*(21), 210801.

[Yuan, 2023] Zhou, L., Lin, J., Jing, Y., & Yuan, Z. (2023). Twin-field quantum key distribution without optical frequency dissemination. *nature communications*, *14*(1), 928.

[H. Zhou, 2018] Ma, X., Zeng, P., & Zhou, H. (2018). Phase-matching quantum key distribution. Physical Review X, 8(3), 031043.

Introduction

Various protocols → different hardware

- COW & BB84 in a world without good single photon sources
- BB84 with single photon sources
- CV-QKD
- Ekert91 & MDI-QKD
- Twin-field QKD
- Quantum repeaters

OUTLINE

Entanglement swapping + quantum memory

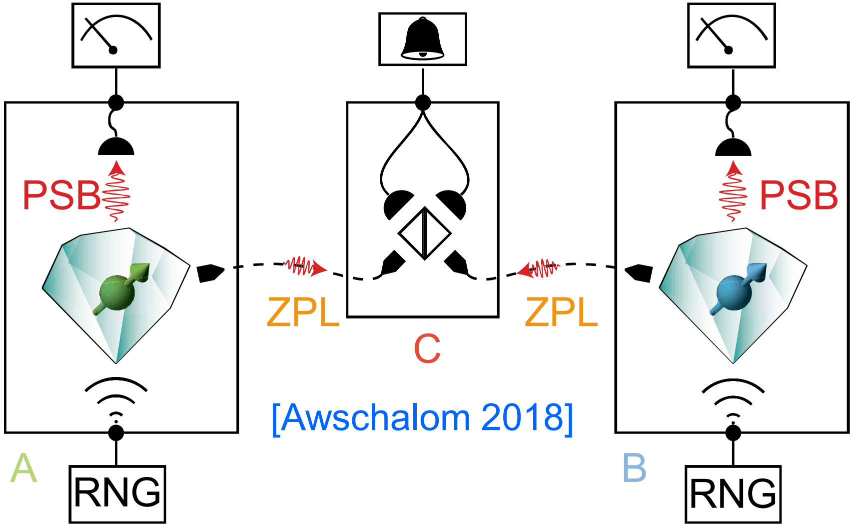

[Awschalom 2018]

Spin-spin entanglement via BSM

GENERATING SPIN-PHOTON ENTANGLEMENT

- Decay based

Protocol for entanglement generation

- Initialization to the ground (green CW)
- Π-pulse to $|+1\rangle$
- Π-pulse to $|A_2\rangle$
- PL ↔ entanglement $|\Psi\rangle = |+1\rangle\,|\sigma_-\rangle + |-1\rangle\,|\sigma_+\rangle$

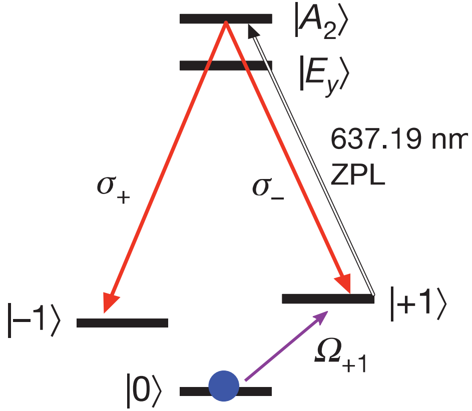

[Togan2010]

- NL interaction

[Bhaskar 2020]

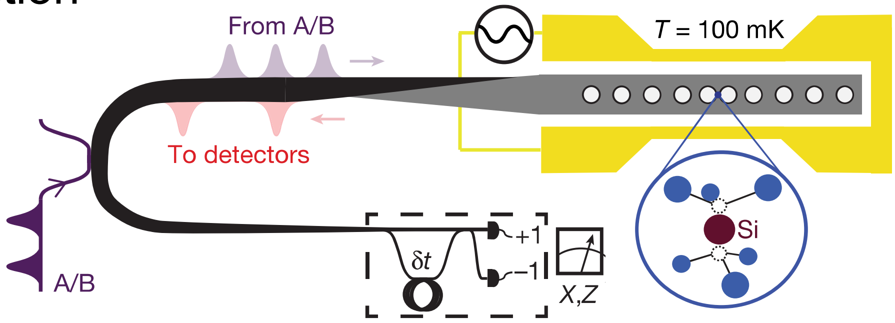

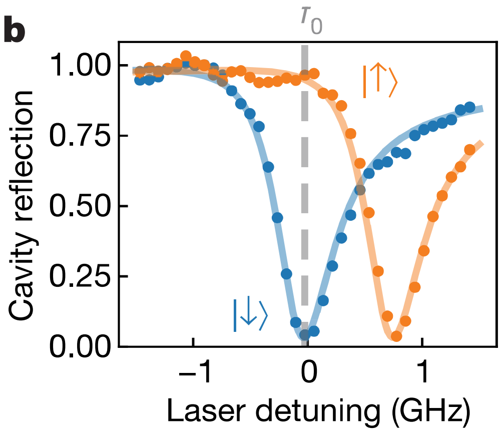

Note: also a way to read the spin

QUANTUM MEMORY NODE

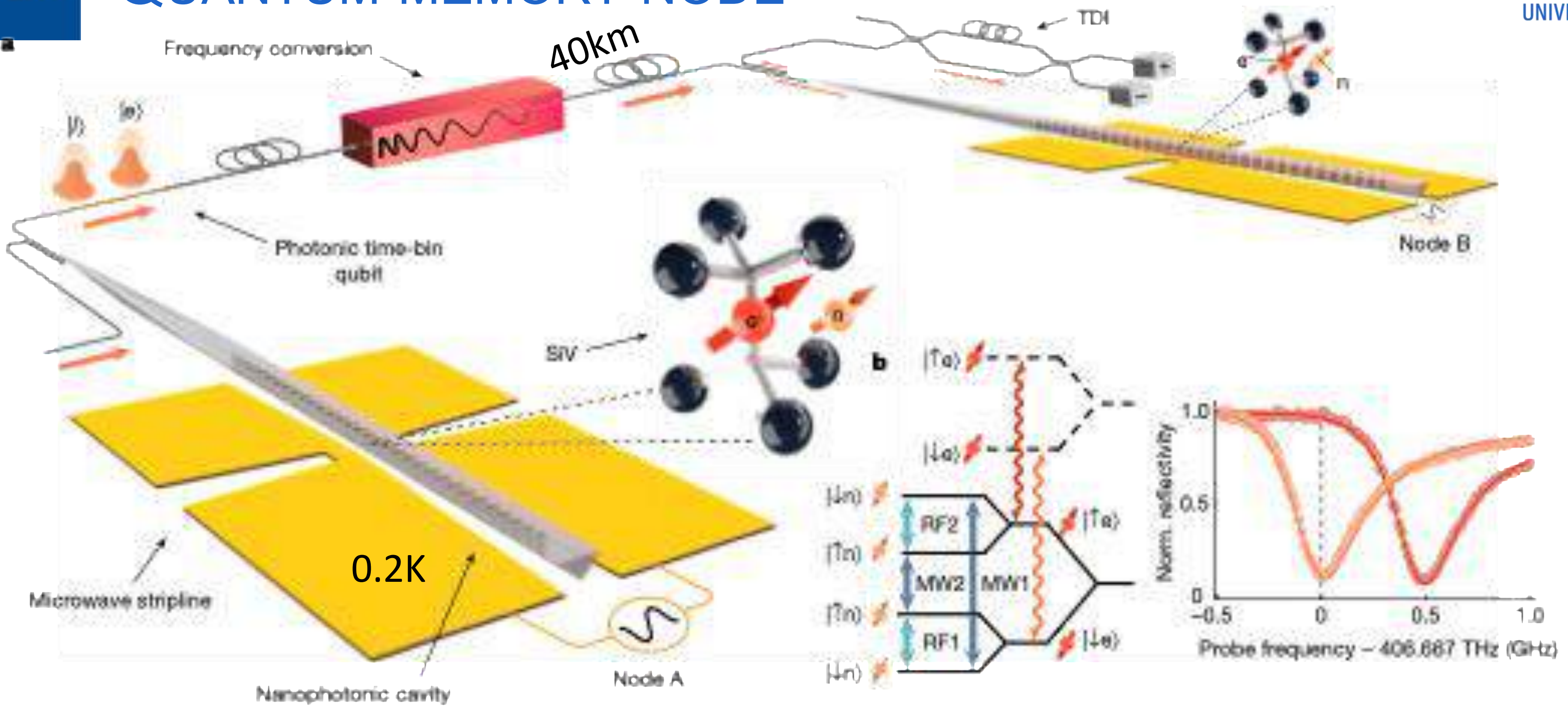

[M.D. Lukin, 2024]

Memory in nuclear spin (^{29}Si)
Light interface thru electronics spin

success rate: 1Hz

Metro range spin entanglement

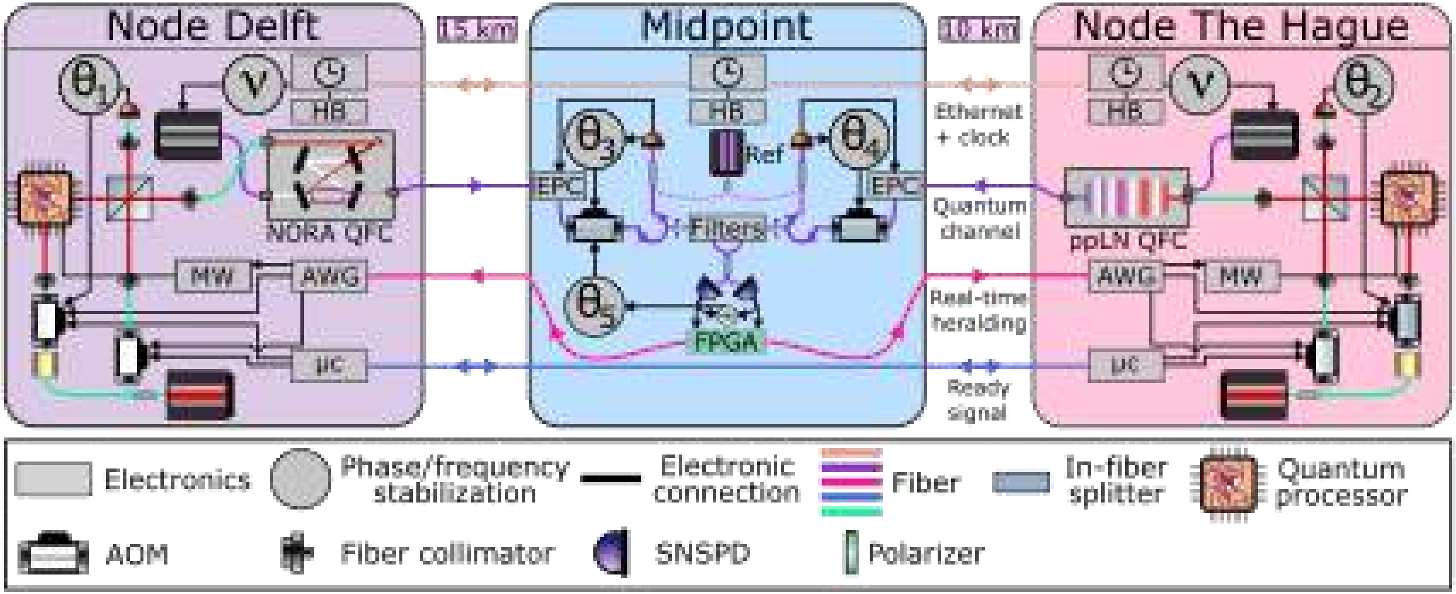

[R. Hanson 2024]

References

[Bhaskar 2020] Bhaskar, Mihir K., et al. "Experimental demonstration of memory-enhanced quantum communication." *Nature*580.7801 (2020): 60-64.

[Togan2010] Togan, E., Chu, Y., Trifonov, A. S., Jiang, L., Maze, J., Childress, L., ... & Lukin, M. D. (2010). Quantum entanglement between an optical photon and a solid-state spin qubit. *Nature*, *466*(7307), 730-734.

[M.D. Lukin, 2024] Knaut, C. M., Suleymanzade, A., Wei, Y. C., Assumpcao, D. R., Stas, P. J., Huan, Y. Q., ... & Lukin, M. D. (2024). Entanglement of nanophotonic quantum memory nodes in a telecom network. Nature, 629(8012), 573-578.

[R. Hanson, 2022] Hermans, S. L. N., Pompili, M., Beukers, H. K. C., Baier, S., Borregaard, J., & Hanson, R. (2022). Qubit teleportation between non-neighbouring nodes in a quantum network. Nature, 605(7911), 663-668

[R. Hanson 2024] Stolk, A. J., van der Enden, K. L., Slater, M. C., te Raa-Derckx, I., Botma, P., Van Rantwijk, J., ... & Hanson, R. (2024). Metropolitan-scale heralded entanglement of solid-state qubits. Science advances, 10(44), eadp6442.

[R. Hanson 2021] Pompili, M., Hermans, S. L., Baier, S., Beukers, H. K., Humphreys, P. C., Schouten, R. N., ... & Hanson, R. (2021). Realization of a multinode quantum network of remote solid-state qubits. Science, 372(6539), 259-264.

Introduction

Various protocols → different hardware

Outlook

OUTLOOK / RECENT TRENDS

- Phase stabilization & laser locking
- Matter qubit finding their way in networks
- Photonic integrated circuits to the rescue
- Tight integration between electronics and optics
- QKD technologies diverse and driven by new protocols
- Some technologies close to OPERA’s expertise: ν −comb, phase locking, ..

Thank you for listening

Stephane.clemmen@ulb.be

IEEE Photonics Benelux Annual Symposium 2025

20-Nov-2025 – 21-Nov-2025

Université Libre de Bruxelles, Brussels, Belgium

Register now

Full program available

Registration deadline : 6 November at noon

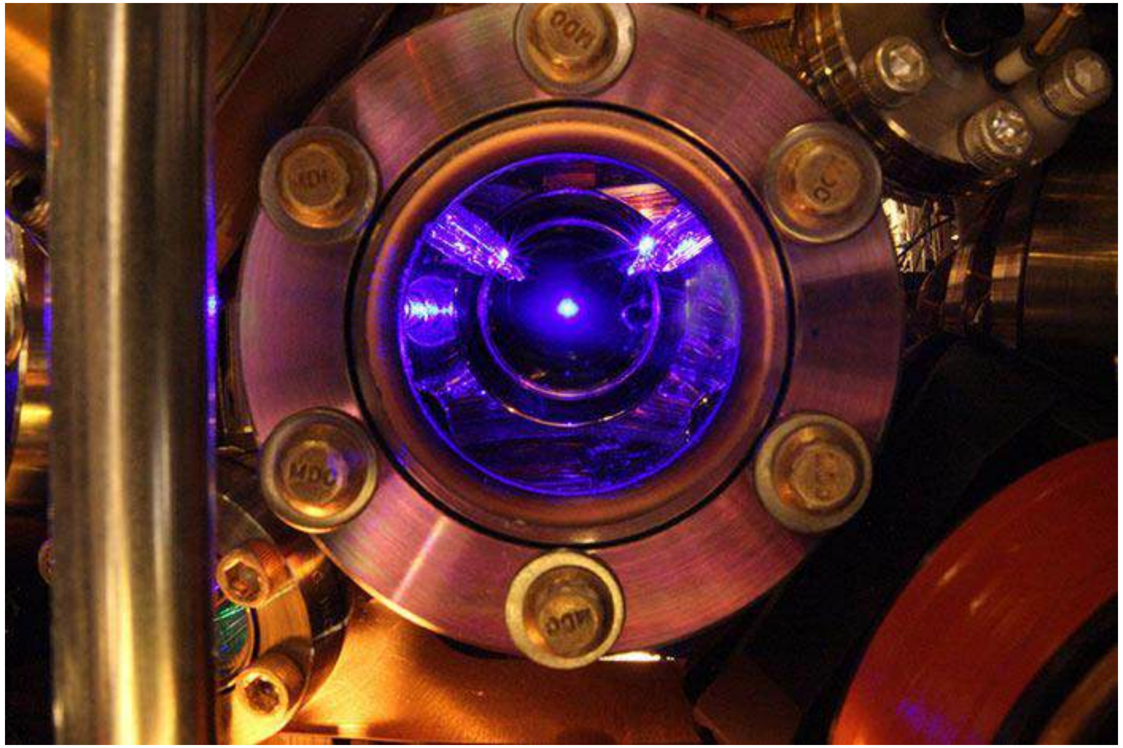

Atomic clocks:
from current trends to photonic integration

K. Van Gasse

5th of November 2025 – BeQCI workshop

GHENT UNIVERSITY

imec

Photonics Research Group of Ghent University and imec

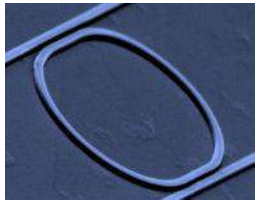
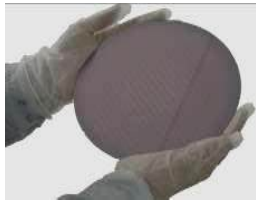

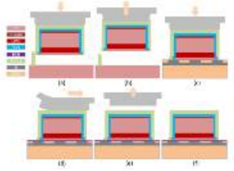
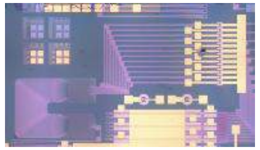

Located at Ghent University

- Faculty of Engineering and Architecture
- Associated laboratory of IMEC
- Member of the Center for Nano- & Biophotonics (NB photonics)

Technology Research

- Photonic Integration of Systems on a chip
- Advanced Silicon Photonics
- Enhanced with new materials:
  III-V, ferro-electrics, graphene, …

Applications

- High-speed telecom and datacom
- Sensing for life sciences
- Optical information processing
- Quantum information

GHENT UNIVERSITY

imec

12 Professors
27 postdocs
64 PhD students
15 support staff

20+ nationalities
9 ERC grantees
6 spin-off companies
50 journal papers/year
Class 100 clean rooms
M.Sc. Photonics program

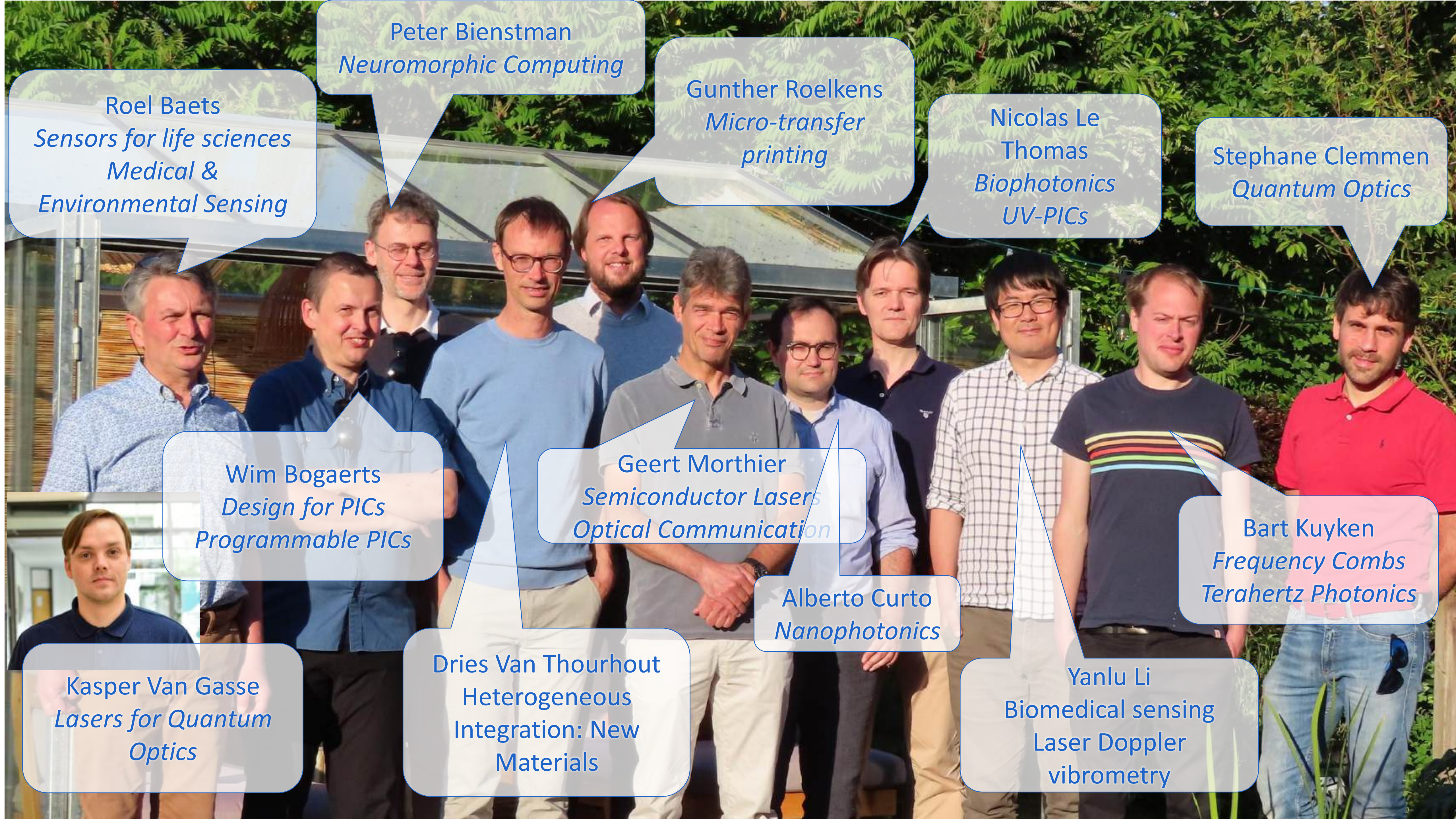

Roel Baets
Sensors for life sciences
Medical &
Environmental Sensing
Peter Bienstman
Neuromorphic Computing
Gunther Roelkens
Micro-transfer
printing
Nicolas Le
Thomas
Biophotonics
UV-PICs
Stephane Clemmen
Quantum Optics
Wim Bogaerts
Design for PICs
Programmable PICs
Geert Morthier
Semiconductor Lasers
Optical Communication
Alberto Curto
Nanophotonics
Bart Kuyken
Frequency Combs
Terahertz Photonics
Kasper Van Gasse
Lasers for Quantum
Optics
Dries Van Thourhout
Heterogeneous
Integration: New
Materials
Yanlu Li
Biomedical sensing
Laser Doppler
vibrometry

Overview

- What is an (atomic) clock?
- Why do we need atomic clocks?
- How does an optical atomic clock work?
- Chip-scale optical atomic clocks
- Activities at UGent – imec: photonic integrated circuits
- Conclusion and summary

GHENT UNIVERSITY

imec

What is a clock?

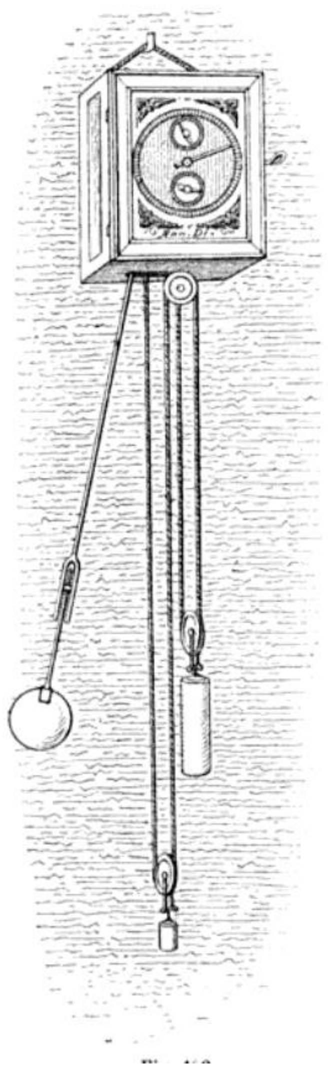

Christiaan Huygens - pendulum clock (1656)
Drift: 15 seconds per day

A clock is a device that measures the passing of time.

We need a device that can:

- Generate a stable oscillation
- Count these oscillations
- Convert a number of oscillations to a unit of time (the second)

Example: pendulum clock

Perfect clock: oscillation period never changes

Reality: oscillation period drifts due to temperature, vibrations, wear, …

Clock evolution

Technology has helped advance the performance of clocks significantly.

Even the best oscillators drift over time, is there a way to stabilize them?

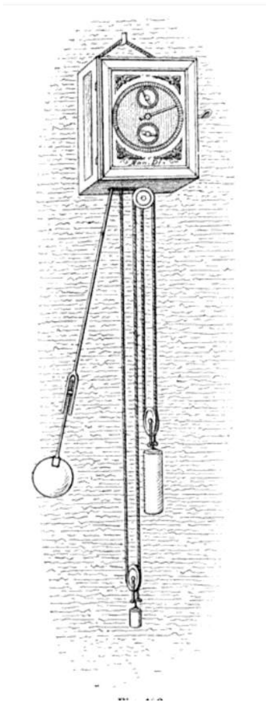

Christiaan Huygens - pendulum clock
(1656)
Drift: 15 seconds per day

Harrison – H4 Chronometer
(1762)
Drift: 0.2 seconds per day

Quartz crystal oscillator
(1927)
Drift: 0.004 seconds per day

What is an atomic clock?

Standard atomic clock used today is the cesium microwave clock

10 MHz referenced signal to the user

Quartz oscillator

Microwave interrogation

Feedback

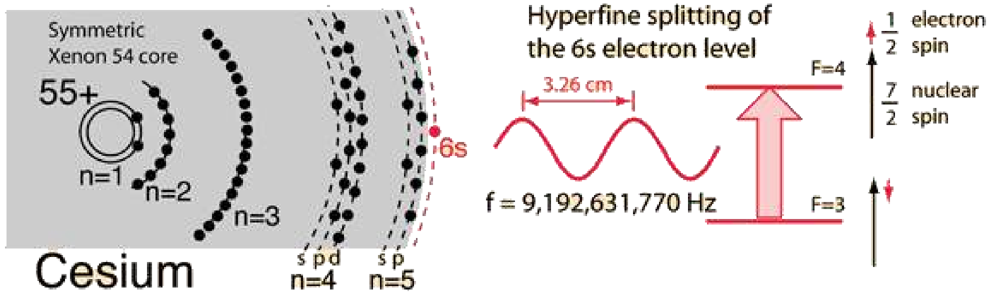

Definition in SI system

The second is the duration of 9 192 631 770 periods of the radiation corresponding to the transition between the two hyperfine levels of the ground state of cesium-133 (1967).

Cesium clocks all over the world help define International Atomic Time (TAI)
Which is used to define Coordinated Universal Time (UTC)

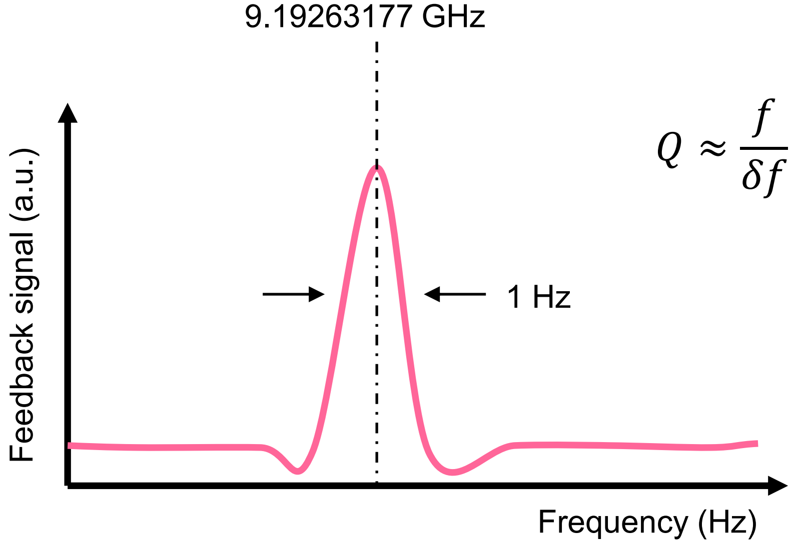

$$Q \approx \frac{f}{\delta f} \approx 10^{10}$$

Drift: 10 ps a day

Atomic clocks used for UTC

Cesium fountain clocks

Cesium beam clock

Ytterbium trapped ion clock

PTB – Physikalisch-Technische Bundesanstalt National Metrology Institute of Germany - Braunschweig

NIST Cesium fountain

NPL Cesium fountain

METAS FoCS-2

…

Atomic clocks enable navigation and distribute accurate time

Global navigation satellite system (GNSS): GPS, GLONASS, BDS, Galileo, …

Galileo rubidium clock

Galileo hydrogen maser

How are atomic clocks connected to our daily life?

All navigation:

- Google maps, …
- Ships
- Airplanes
- Modern agriculture

All modern timing depends on syncing with GNSS:

- Mobile networks
- IT infrastructure
- Power grid
- Financial institutions

GNSS outage would cost UK an estimated 1.6 billion EUR a day.

London Economics, The Economic Impact on the UK of a Disruption to GNSS: Issue 4, 2021 Update – Final Report, London Economics, Aug. 2023

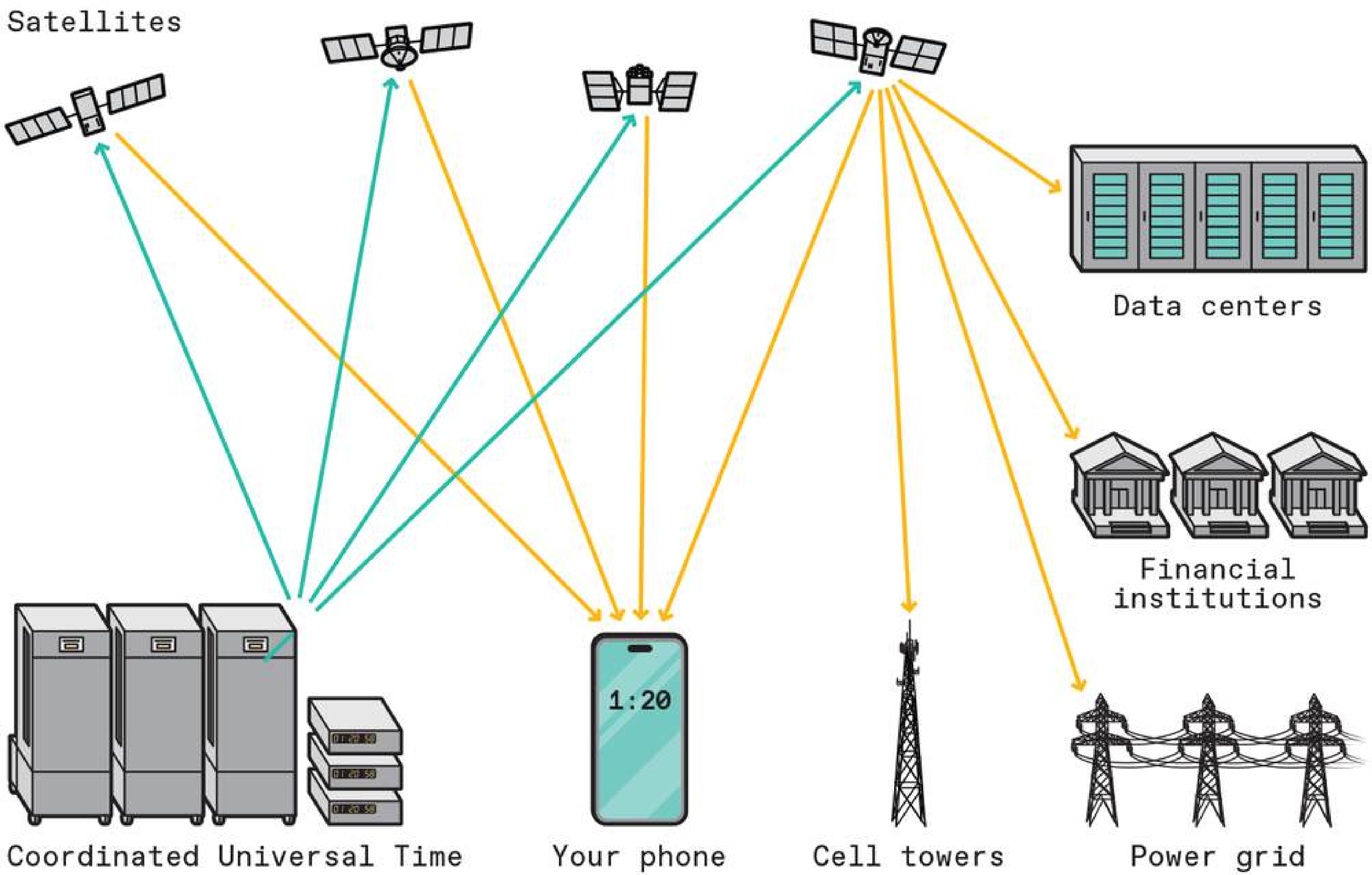

https://spectrum.ieee.org/optical-atomic-clocks Nov 2024

Next generation of atomic clocks: the optical atomic clock

Until now we only discussed microwave atomic clocks.

Stability still limited by the "Q-factor" of the resonance.

Further improvement can be achieved by increasing the carrier frequency,

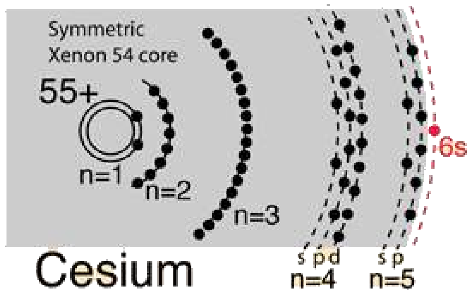

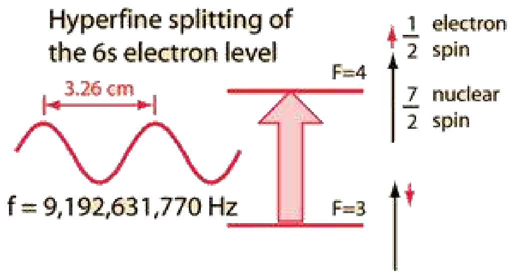

9.19263177 GHz

$$Q \approx \frac{f}{\delta f} \approx 10^{10}$$

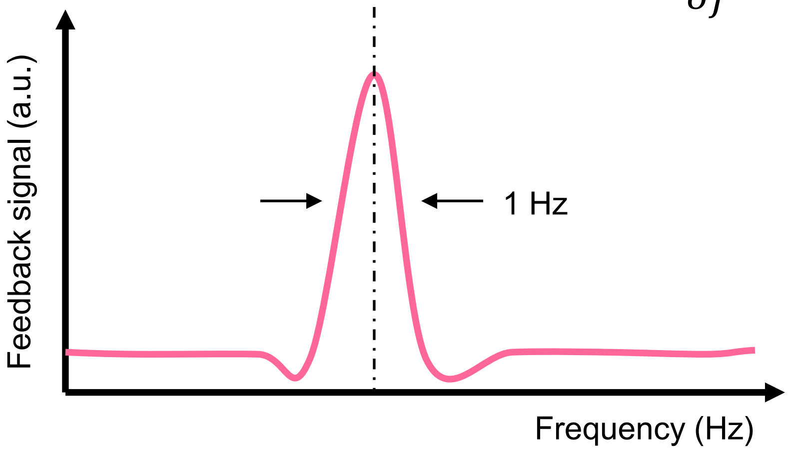

Further increase stability by orders of magnitude by going to optical clocks

Resonance of the Al+ clock transition using quantum logic spectroscopy (Chou et al., 2010b).

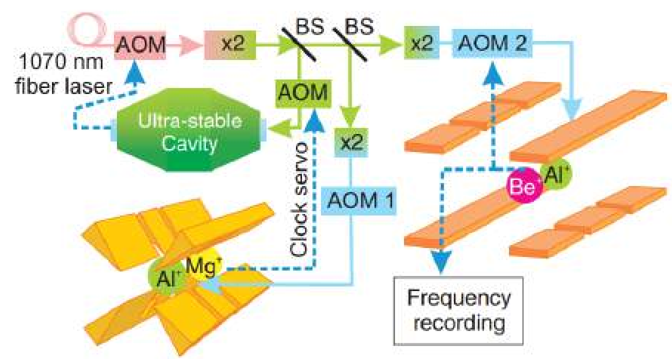

1 121 015.393 GHz (267 nm)

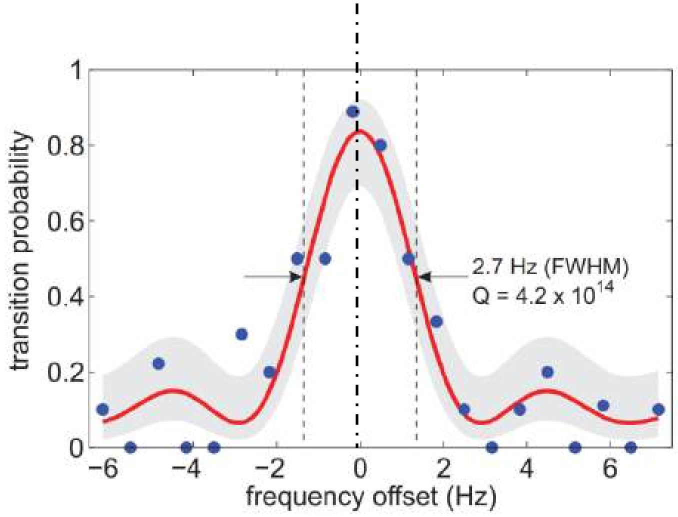

What is an optical atomic clock?

Same principle as a microwave atomic clock

Laser interrogates the atomic transition

Highly improved performance at the cost of greatly increased complexity

Main challenge: how to measure frequency of light?

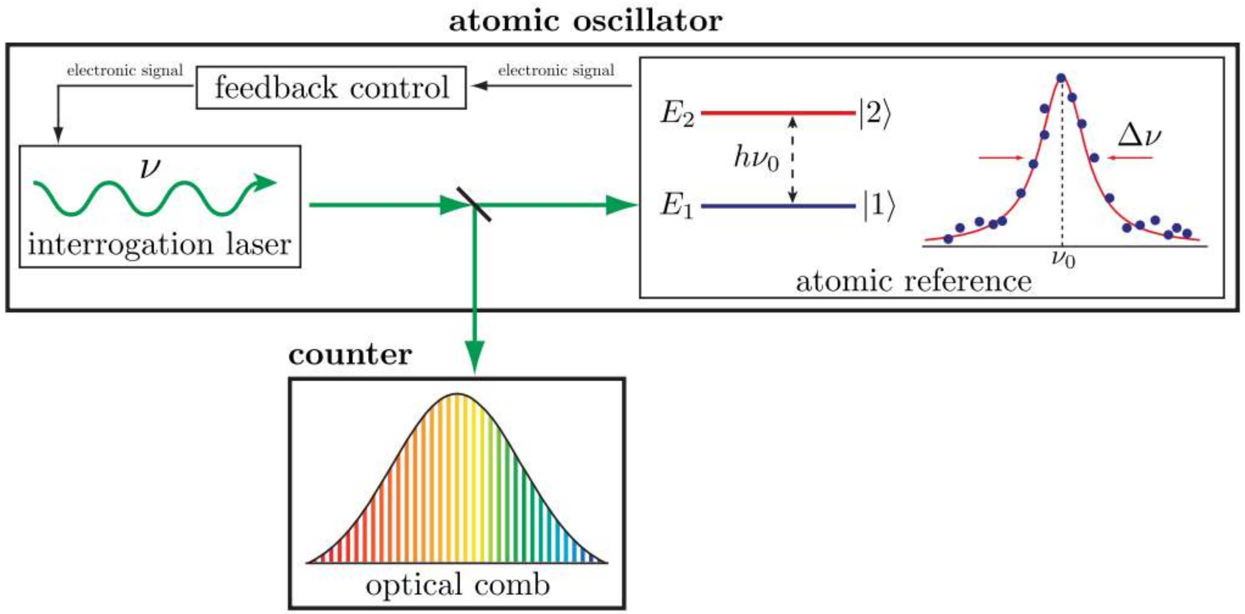

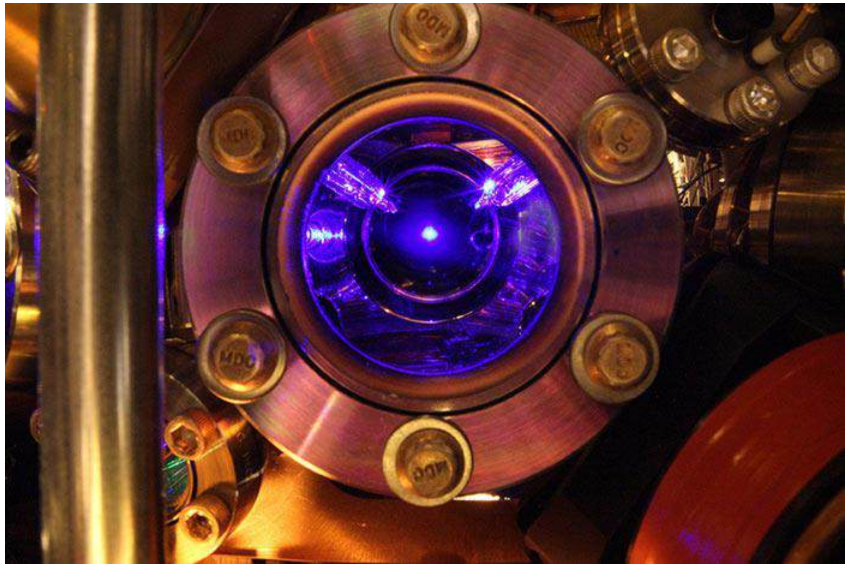

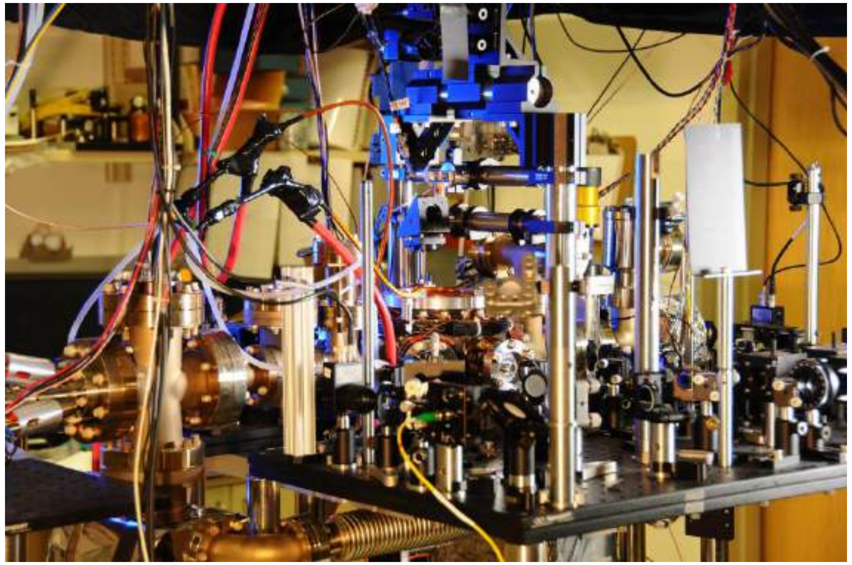

Strontium lattice optical atomic clock at JILA

Optical frequency comb: measuring the frequency of light

How can we convert an optical frequency to the microwave domain?

We need an optical frequency comb:

- Mode-locked pulsed laser:
  - train of short optical pulses
  - comb of laser lines in the frequency domain
- Measurement of the repetition rate (50 MHz – 1 GHz)
- Stabilize the 2 degrees of freedom

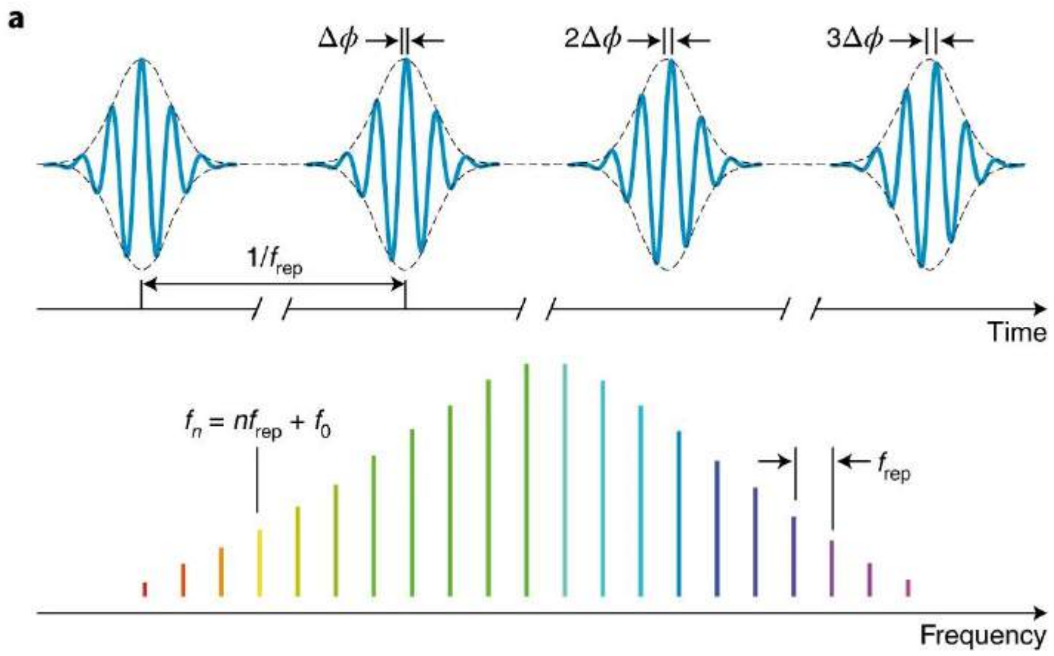

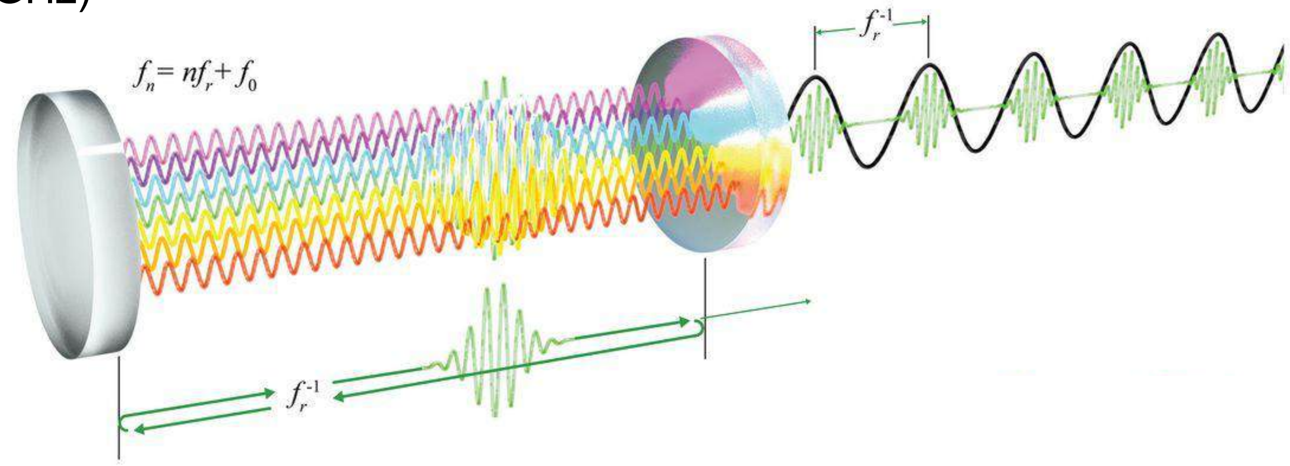

Scott A. Diddams et al. ,Optical frequency combs: Coherently uniting the electromagnetic spectrum. Science 369, eaay3676 (2020).

Optical frequency comb: measuring the repetition rate

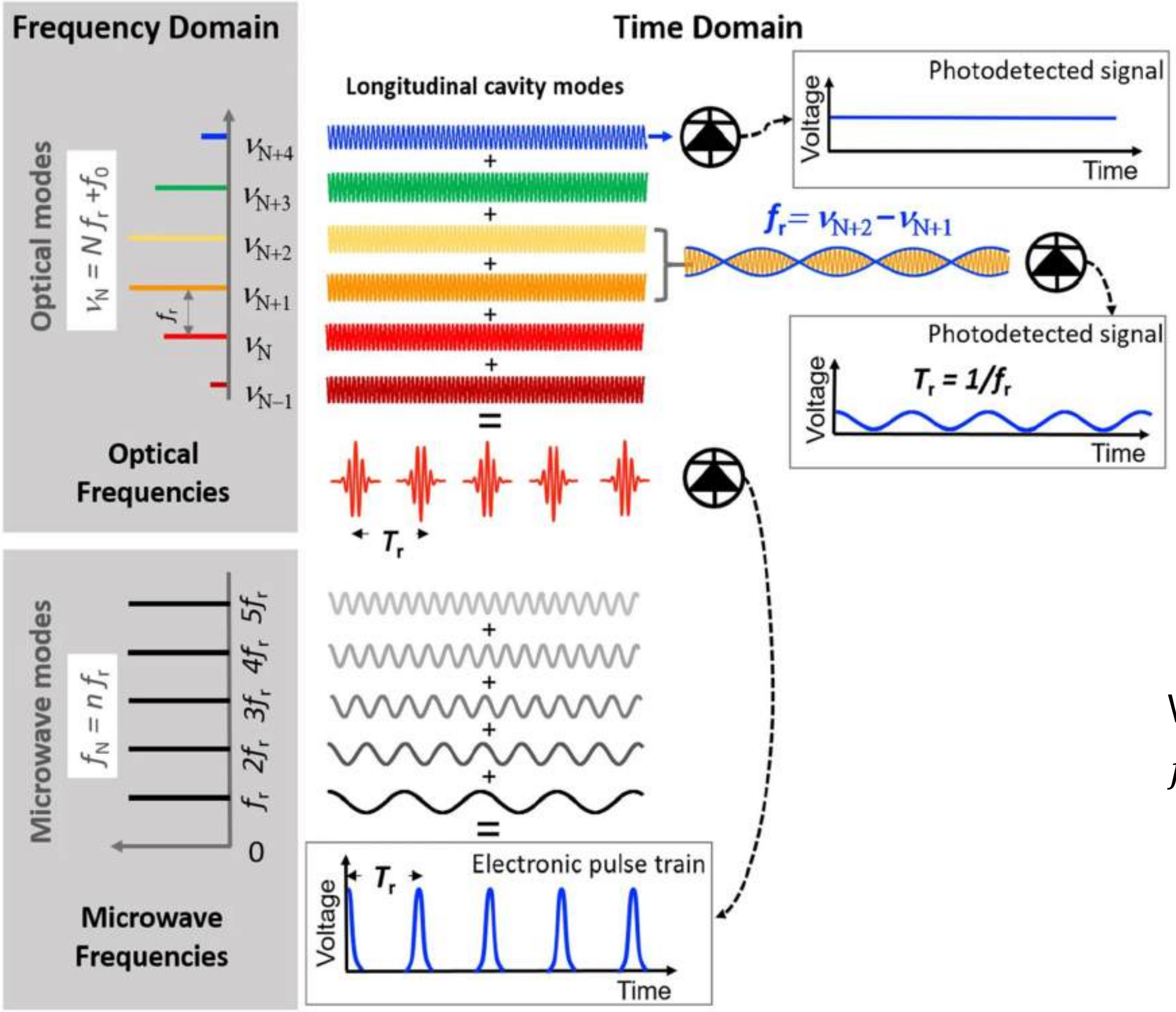

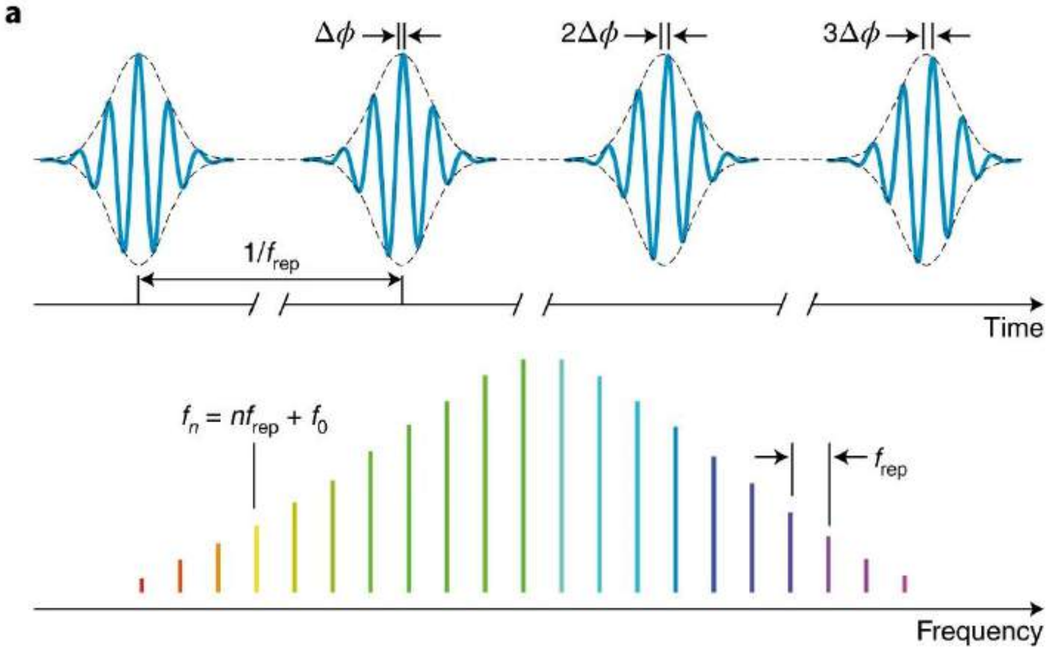

We can directly measure the comb line spacing f_{rep} in the microwave domain.

Fortier, T., Baumann, E. 20 years of developments in optical frequency comb technology and applications. Commun Phys 2, 153 (2019).

Optical frequency comb: measuring the offset frequency

The offset frequency is not directly measurable.

Optical frequency doubling is needed

Use periodically poled lithium niobate crystals (PPLN)

Beating a frequency doubled comb line with a regular comb lines allows to measure f_0 in the microwave domain

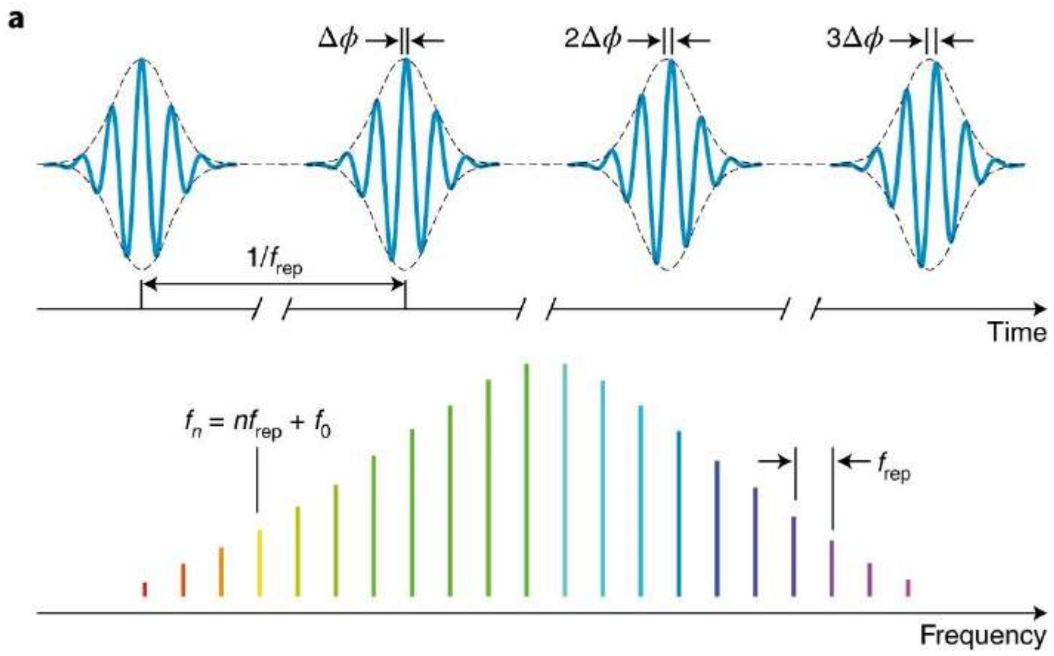

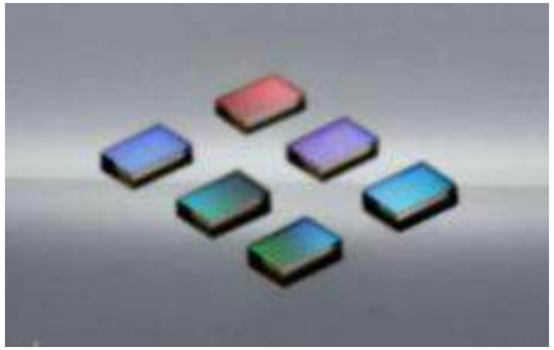

PPLN crystal

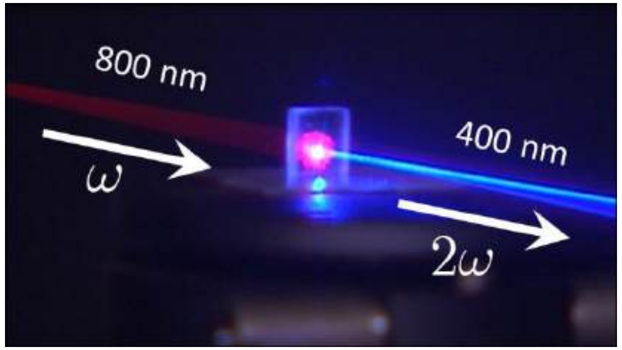

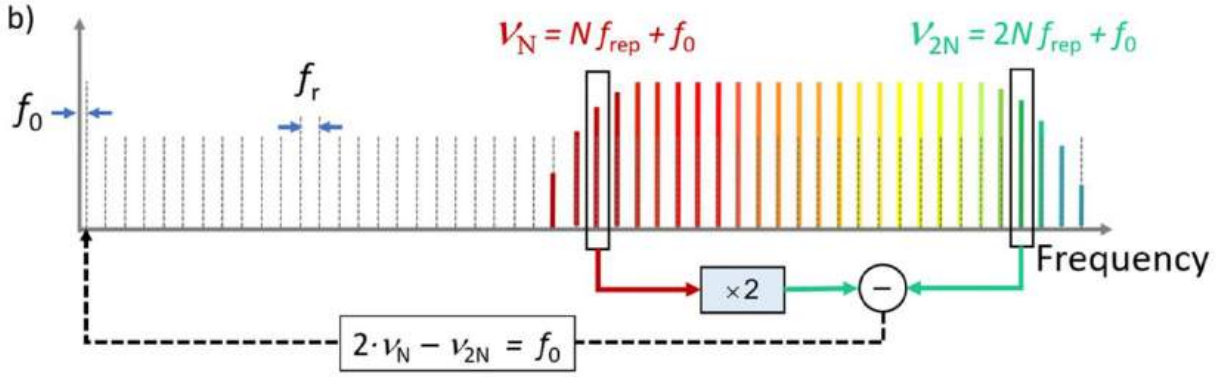

Fortier, T., Baumann, E. 20 years of developments in optical frequency comb technology and applications. Commun Phys 2, 153 (2019).

Optical frequency comb: creating optical clock output

This allows us to down convert the laser locked to the atom:

- Pin f_0 to zero
- Lock a comb teeth to CW laser
- Detect f_{rep} with a photodetector
- The detected microwave signal is the output clock signal

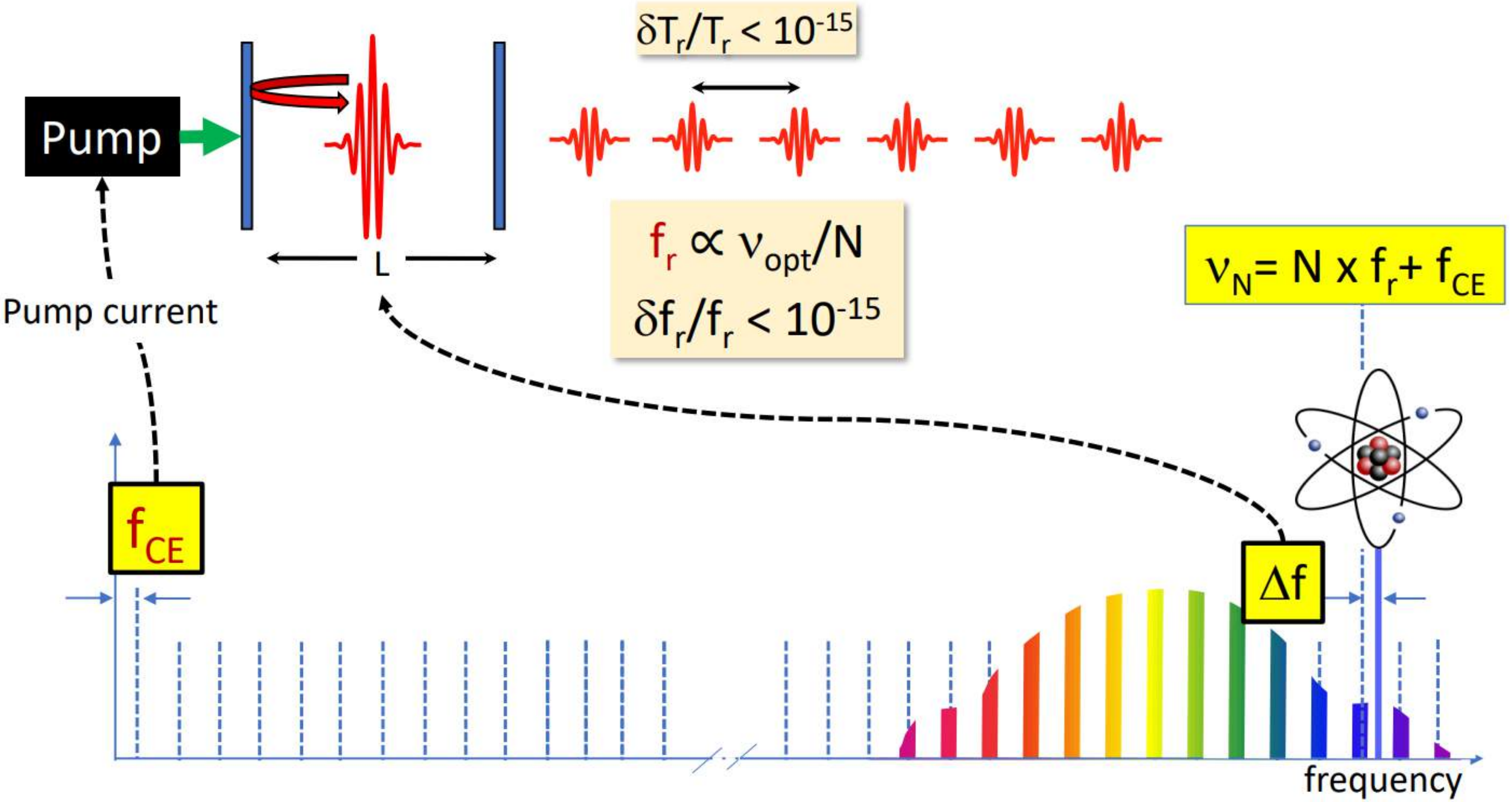

Anatomy of an optical clock

Laser and nonlinear components

Mode-locked laser (fiber or solid state)

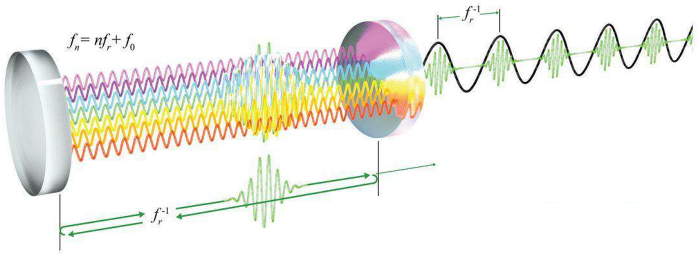

Non-linear crystal (PPLN)

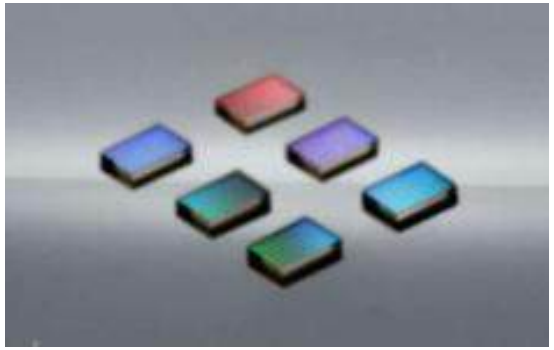

Narrow linewidth CW laser

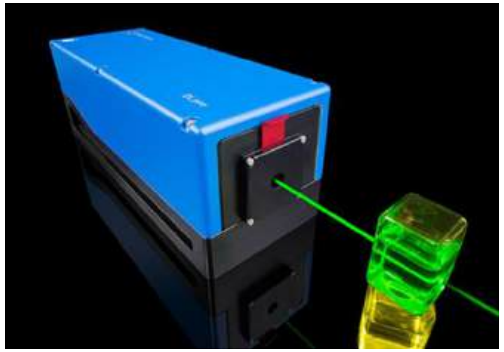

Atomic frequency reference

Medium drift

"Hot" atomic or molecular vapor such as Rb, Cs, iodine.
Can be fabricated with MEMS process in mm-sized package.

Very low drift

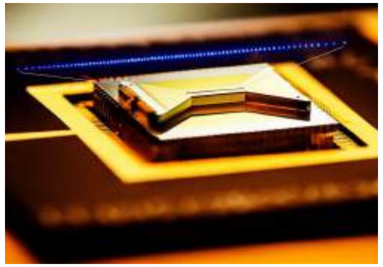

Single or multiple trapped ions. Need for large ultra-high vacuum setup and cooling lasers.

Very low drift

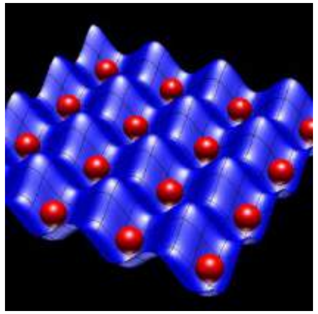

Single or multiple optically trapped neutral atoms. Need for large ultra-high vacuum setup and cooling lasers.

Cold atom optical clocks state of the art: measuring gravity at millimeter scale

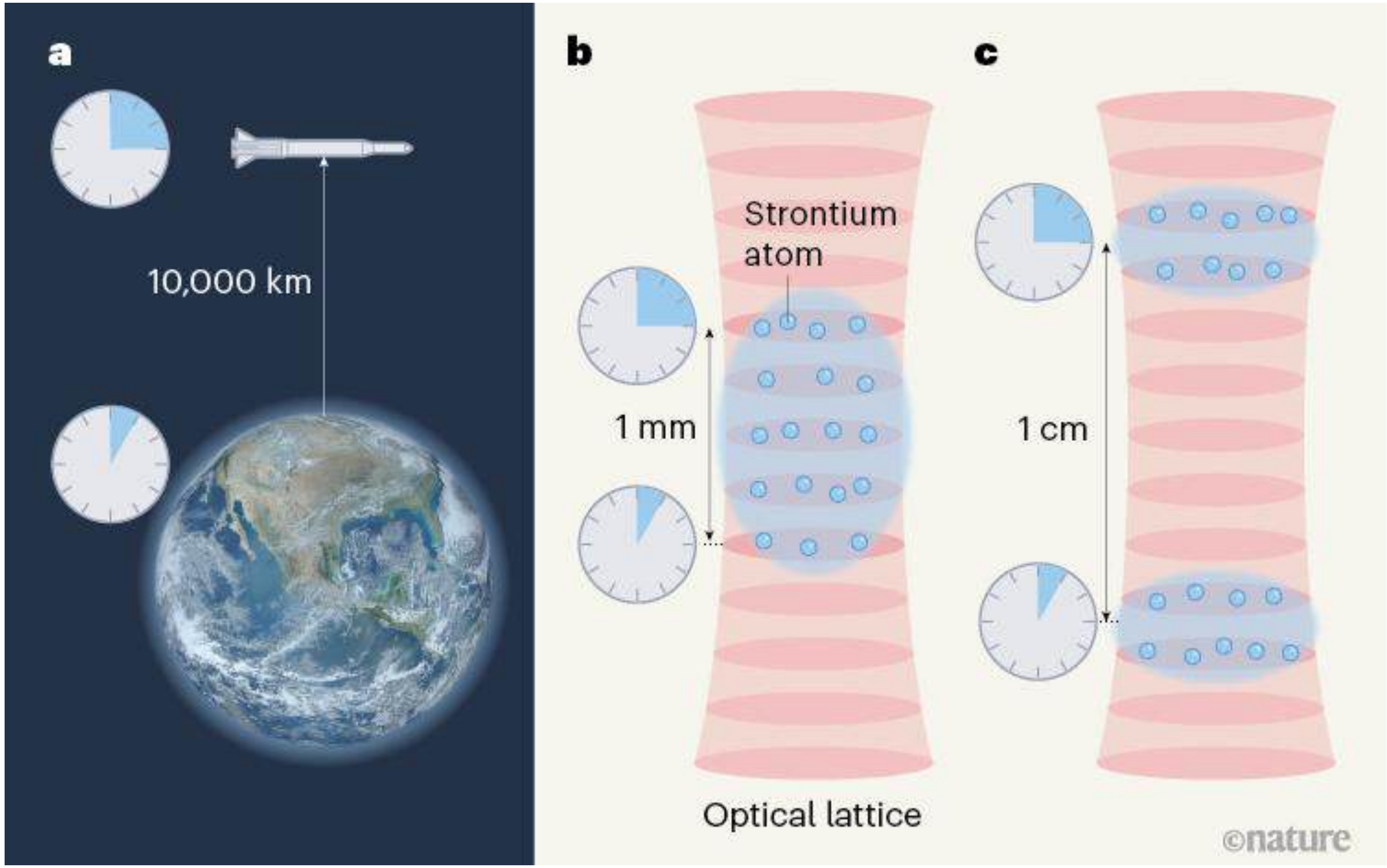

Bothwell, T., Kennedy, C.J., Aeppli, A. et al. Resolving the gravitational redshift across a millimetre-scale atomic sample. Nature 602, 420–424 (2022).
Zheng, X., Dolde, J., Lochab, V. et al. Differential clock comparisons with a multiplexed optical lattice clock. Nature 602, 425–430 (2022).

Optical clocks current trends: towards a nuclear clock

Article | Published: 24 May 2023

Observation of the radiative decay of the ^{229}Th nuclear clock isomer

Sandro Kraemer, Janni Moens, Michail Athanasakis-Kaklamanakis, Silvia Bara, Kjeld Beeks, Premaditya Chhetri, Katerina Chrysalidis, Arno Claessens, Thomas E. Cocolios, João G. M. Correia, Hilde De Witte, Rafael Ferrer, Sarina Geldhof, Reinhard Heinke, Niyusha Hosseini, Mark Huyse, Ulli Köster, Yuri Kudryavtsev, Mustapha Laatiaoui, Razvan Lica, Goele Magchiels, Vladimir Manea, Clement Merckling, Lino M. C. Pereira, ... Ulrich Wahl + Show authors

Nature **617**, 706–710 (2023) | Cite this article

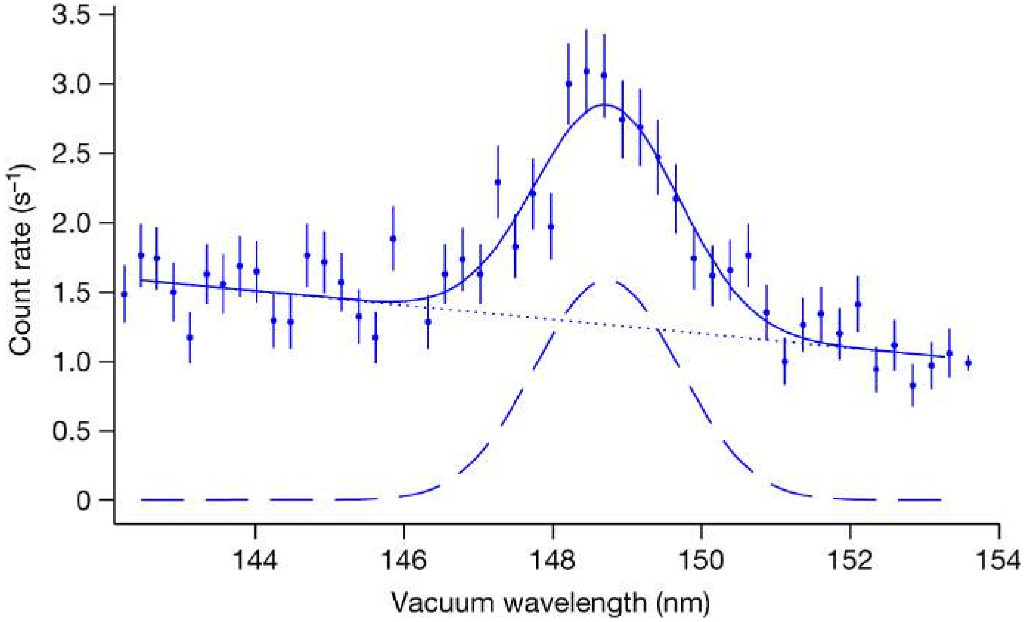

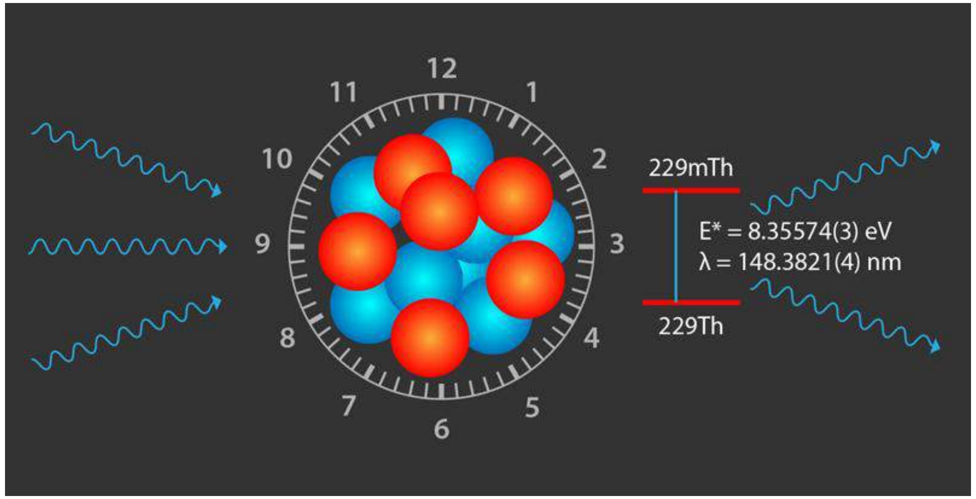

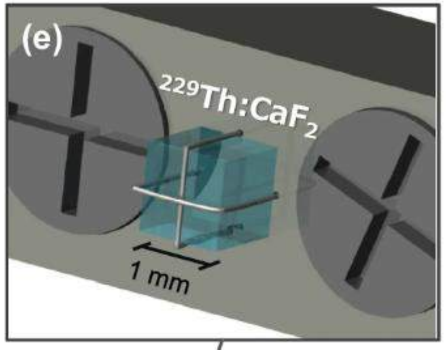

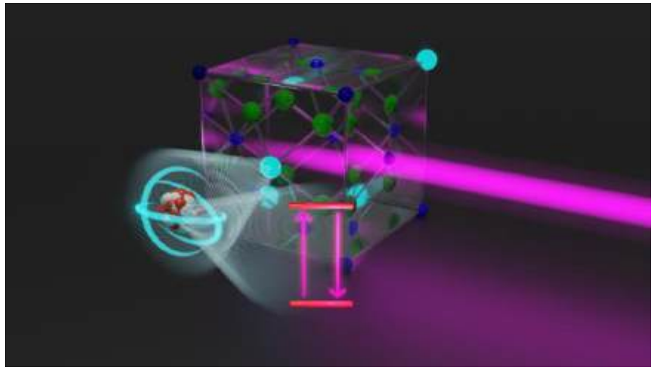

KULeuven and imec contributions

Optical clocks current trends: towards a nuclear clock

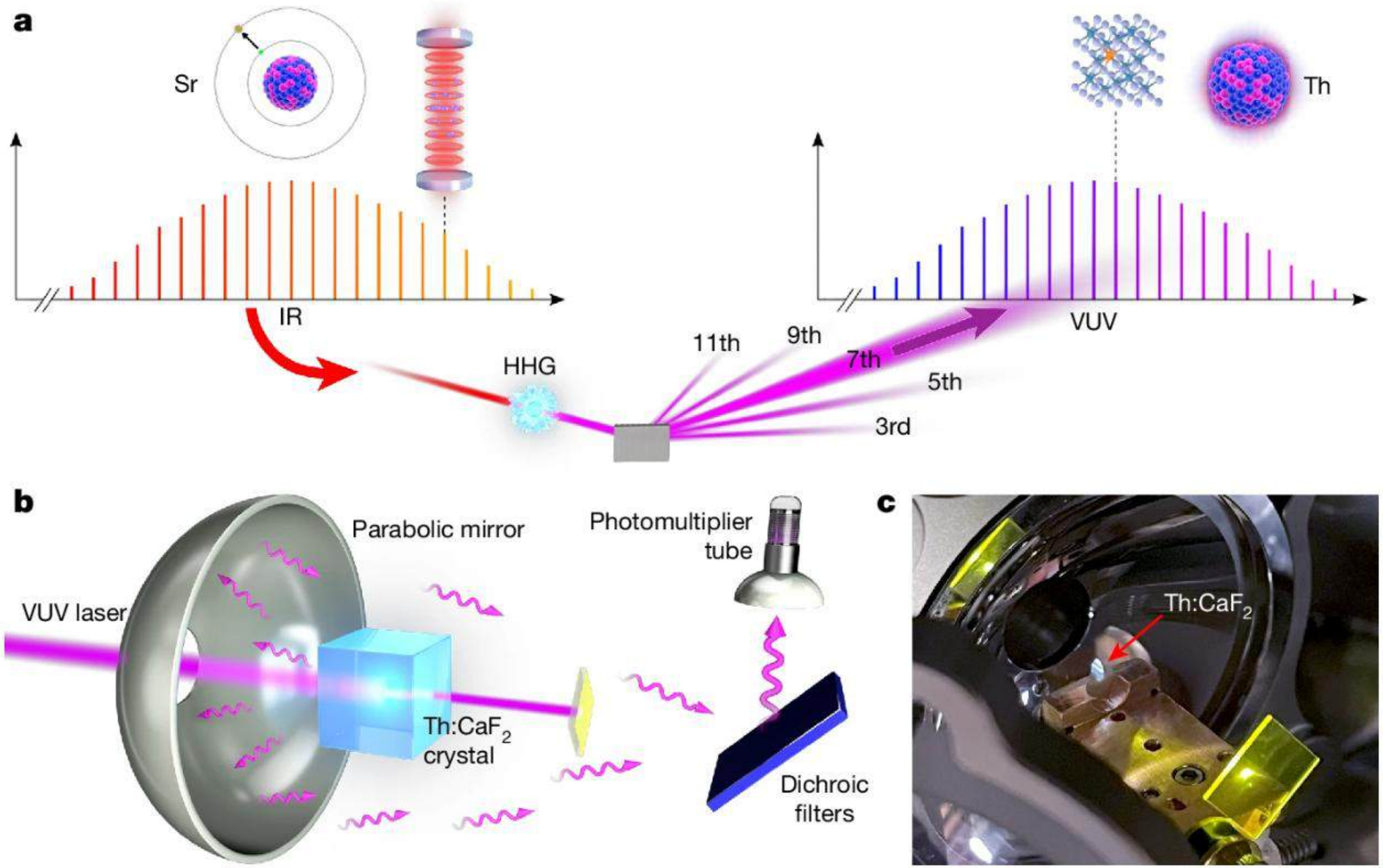

Zhang, C., Ooi, T., Higgins, J.S. et al. Frequency ratio of the 229mTh nuclear isomeric transition and the 87Sr atomic clock. Nature 633, 63–70 (2024).

Optical clocks current trends: towards practical applications

Making optical atomic clocks affordable and ruggedized allows for accurate navigation and timing in GNSS denied environments.

Cannot provide the same performance as lab scale systems but outperforms alternative compact atomic clocks. (rubidium, hydrogen maser)

Example: Vector Atomic rack mounted optical clock

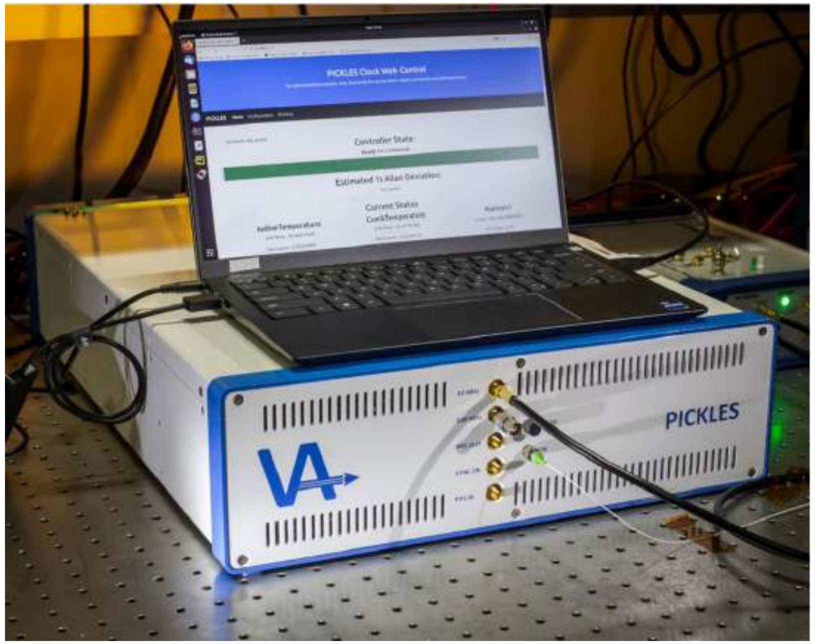

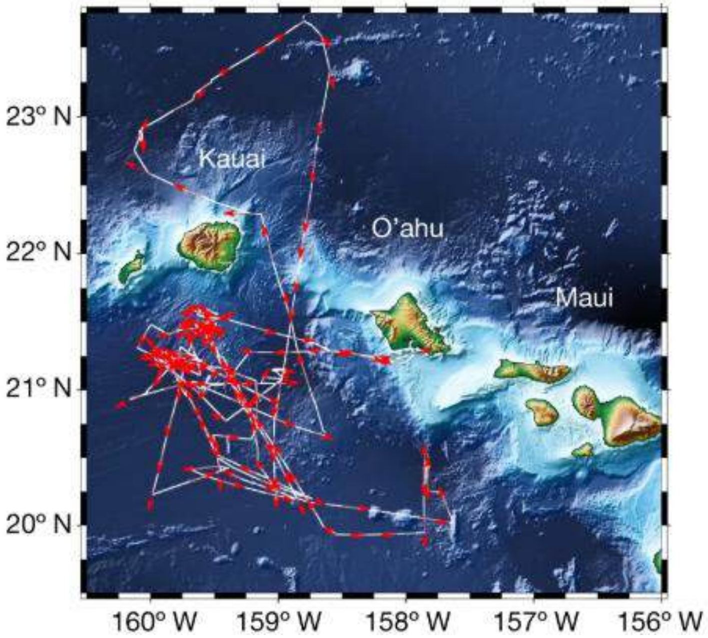

Roslund, J.D., Cingöz, A., Lunden, W.D. et al. Optical clocks at sea. Nature 628, 736–740 (2024).

Vector Atomic Acquired by IONQ

Optical clocks current trends: towards practical applications (2)

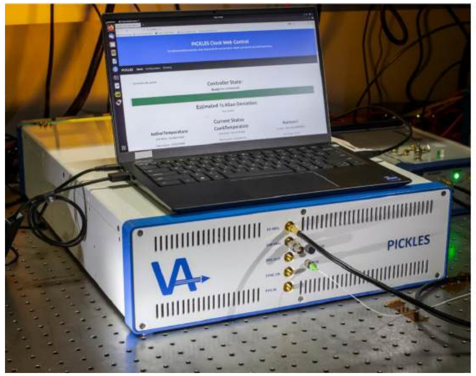

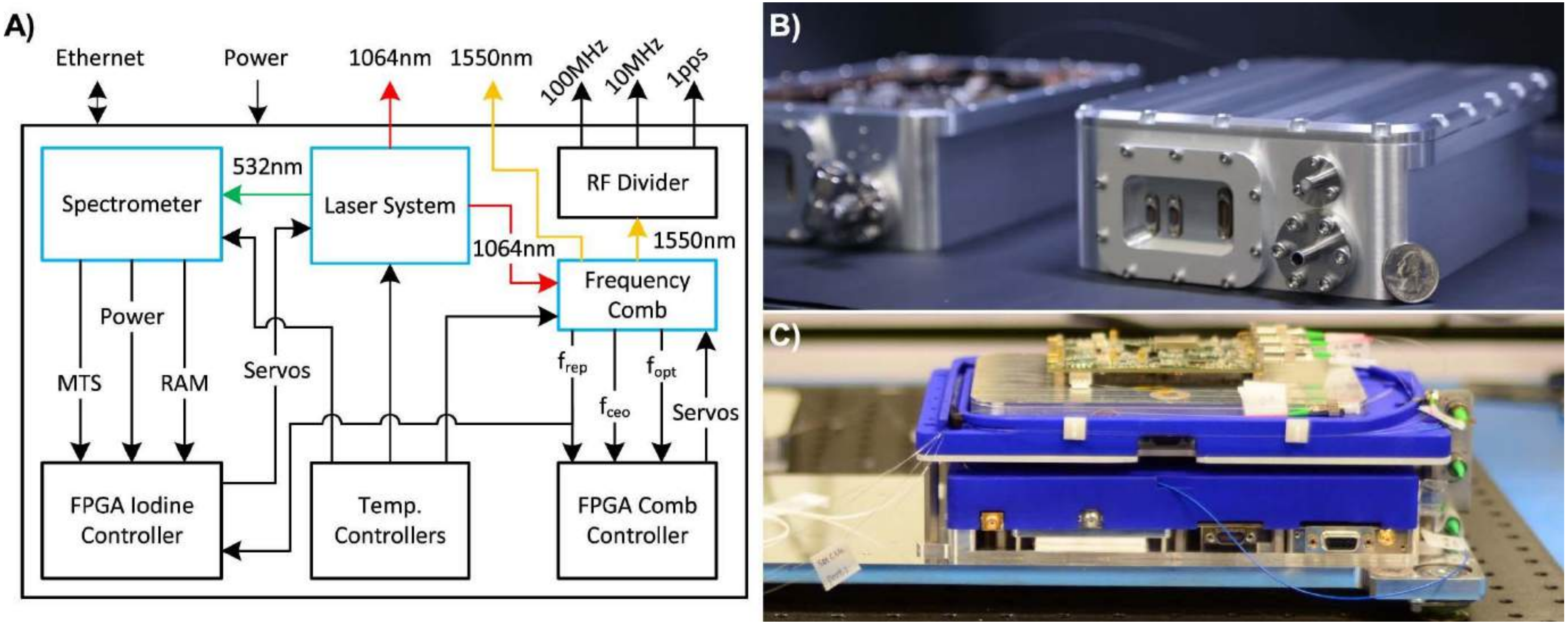

Roslund, J.D., Cingöz, A., Lunden, W.D. et al. Optical clocks at sea. Nature 628, 736–740 (2024).

Optical clocks current trends: towards practical applications (3)

Making optical atomic clocks affordable and ruggedized allows for accurate navigation and timing in GNSS denied environments.

Cannot provide the same performance as lab scale systems but outperform alternative compact atomic clocks.

Example: Infleqtion rack mounted optical clock

Tiqker

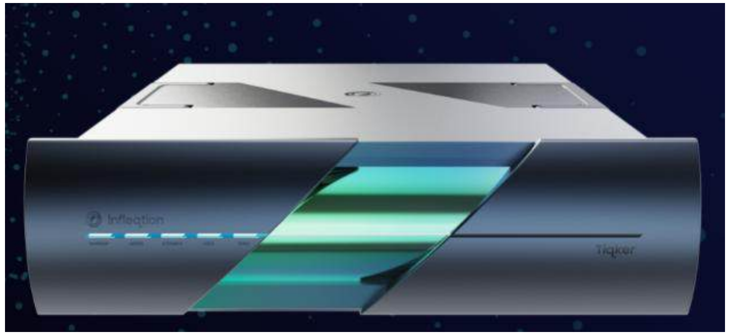

Infleqtion and Royal Navy Demonstrate World's First Quantum Optical Clock on Underwater Autonomous Submarine to advance GPS-Free Navigation

October 28, 2025

Need for further miniaturization of optical atomic clocks

Modern society has become heavily reliant on GNSS for positioning and time dissemination.

GNSS outage has large economical impact. (spoofing, jamming, satellite defect, …)

Need for affordable, compact and mass-manufacturable atomic clocks as GNSS backup.


Three Finnish airports mitigate Russian GPS interference with radio navigation

By Anne Kauranen

November 7, 2024 2:33 PM GMT+1 · Updated November 7, 2024


UN aviation assembly closes with rebuke of Russia over satellite navigation jamming

By Reuters

October 3, 2025 5:56 PM GMT+2 · Updated October 3, 2025

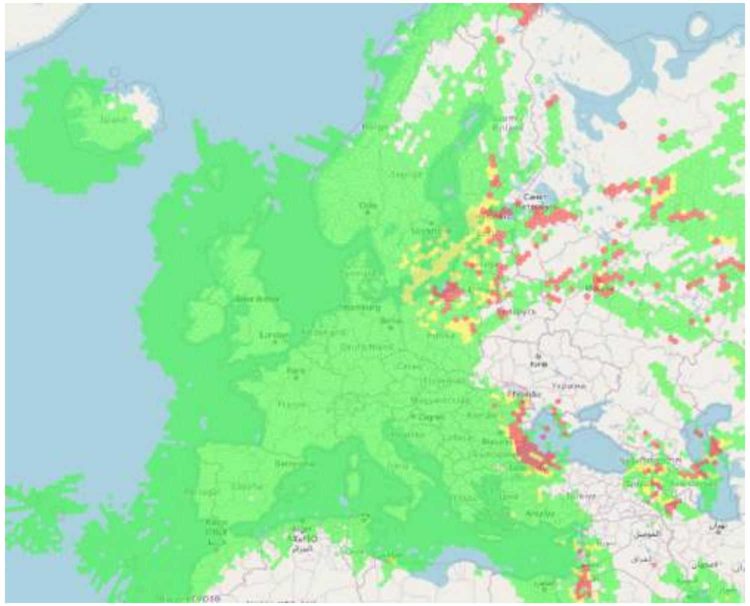

gpsjam.org

Towards chip-scale integration of optical atomic clocks

Further miniaturization and reduction in cost can be achieved by using photonic integrated components.

First demonstration with separate chip-scale components by NIST.

New goal: create a single chip that has all necessary laser and nonlinear components.

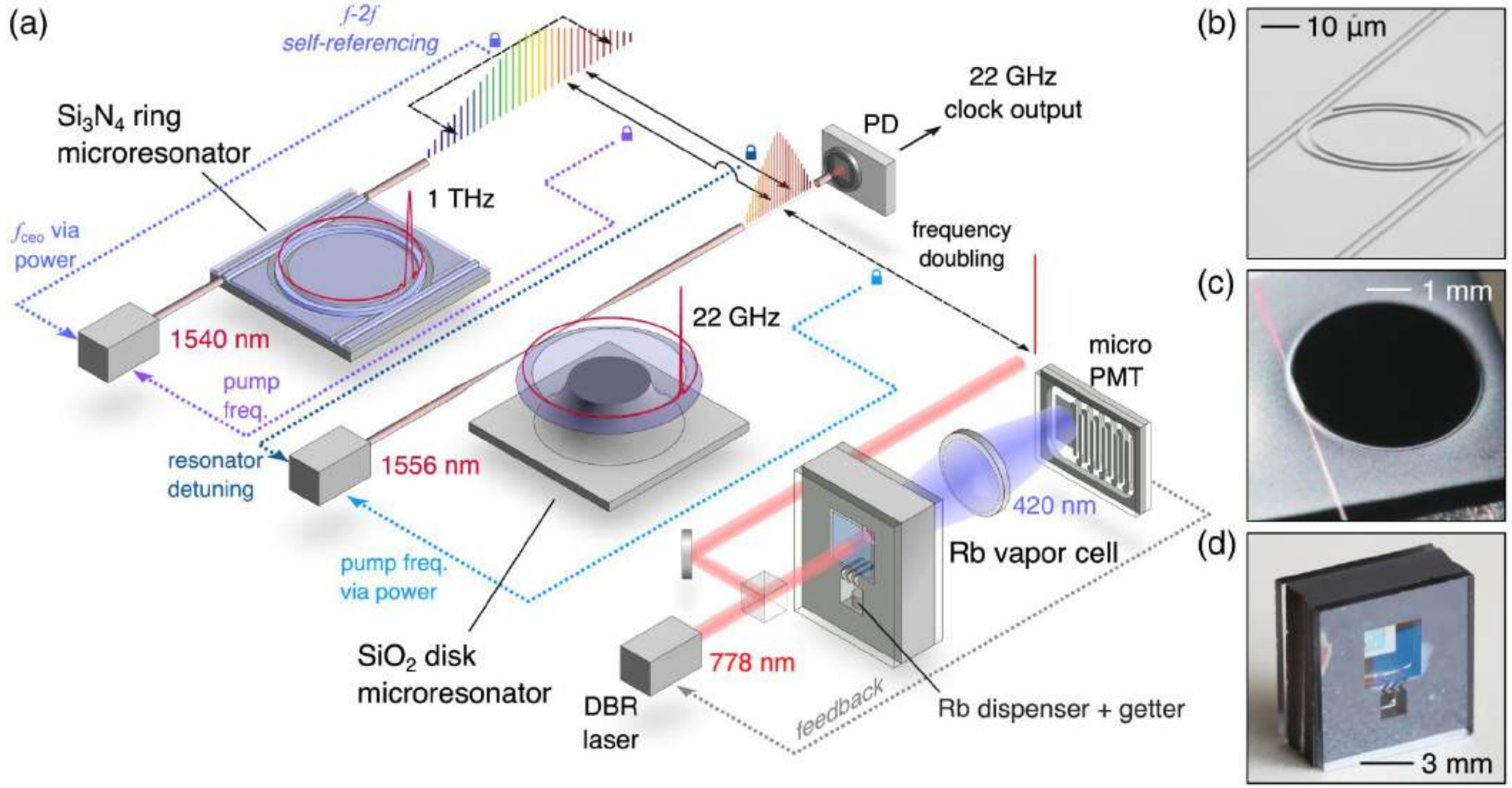

Z. L. Newman et al., "Architecture for the photonic integration of an optical atomic clock," Optica, vol. 6, pp. 680–685, 2019.

Work at UGent – imec: towards chip-scale optical atomic clocks

Micro-transfer printing allows to integrate a wide variety of optical components on a single photonic integrated circuit.

Goal: integration of narrow linewidth CW lasers, mode-locked lasers, frequency doubling components, detectors

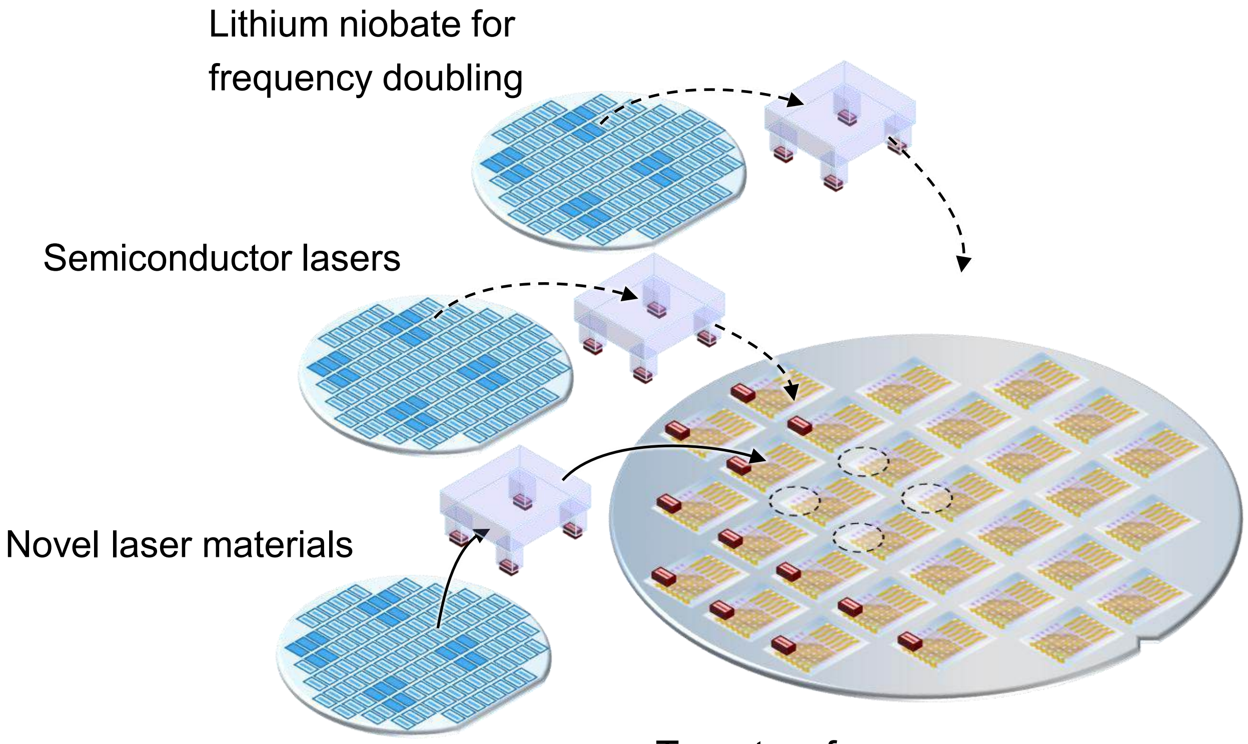

Target wafer:
Low loss SiN-waveguides

Prof. Bart Kuyken

Prof. Kasper Van Gasse

GHENT UNIVERSITY

imec

Recent work at UGent – imec: on-chip lasers at rubidium wavelength

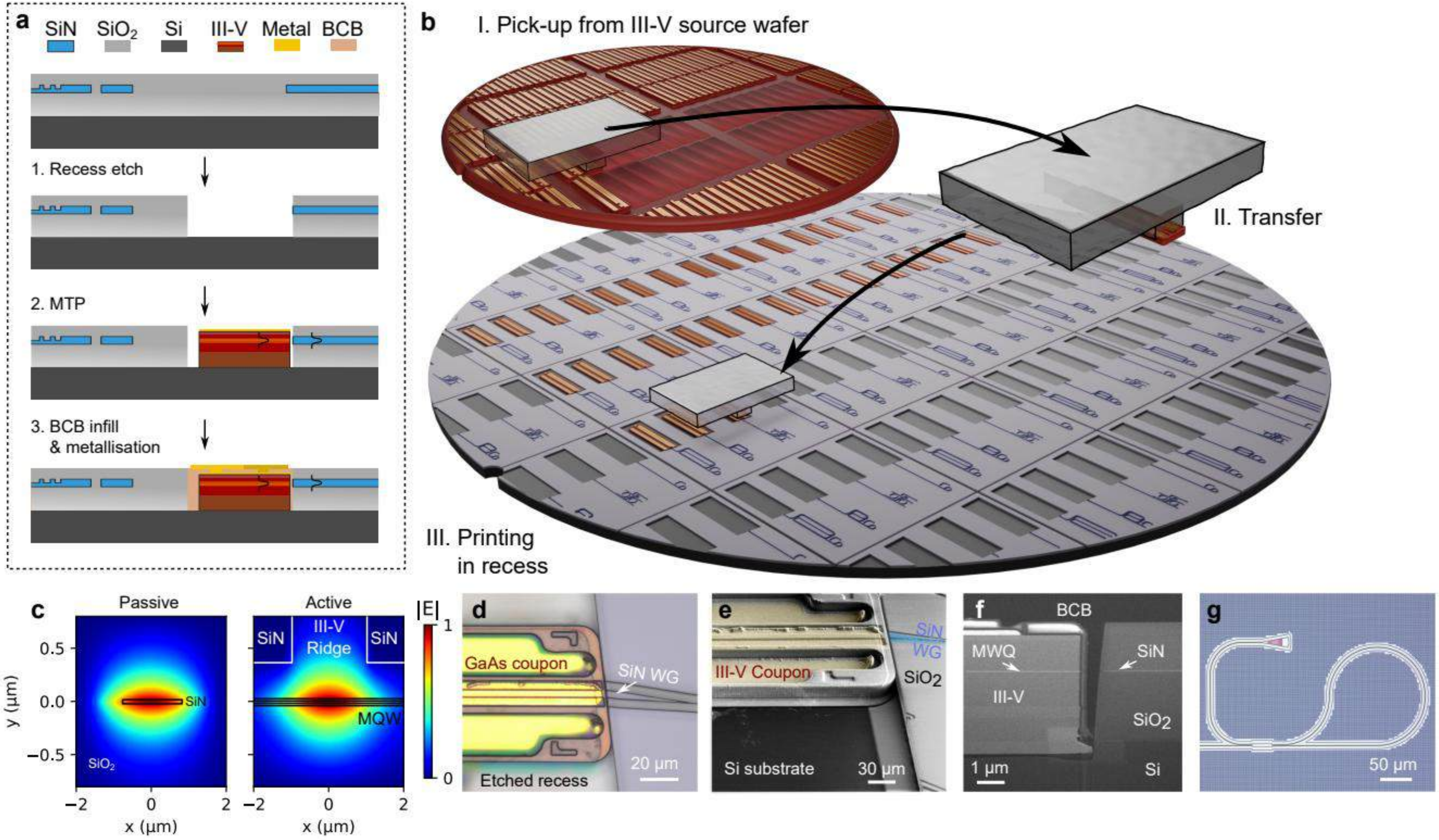

Max Kiewiet, Stijn Cuyvers, Maximilien Billet, Konstantinos Akritidis, Valeria Bonito Oliva, Gaudhaman Jeevanandam, Sandeep Saseendran, Manuel Reza, Pol Van Dorpe, Roelof Jansen, Joost Brouckaert, Günther Roelkens, Kasper Van Gasse, Bart Kuyken, "Micro-Transfer Printed Continuous-Wave and Mode-Locked Laser Integration at 800 nm on a Silicon Nitride Platform," arXiv:2504.16993, 2025.

Recent work at UGent – imec: on-chip lasers at rubidium wavelength

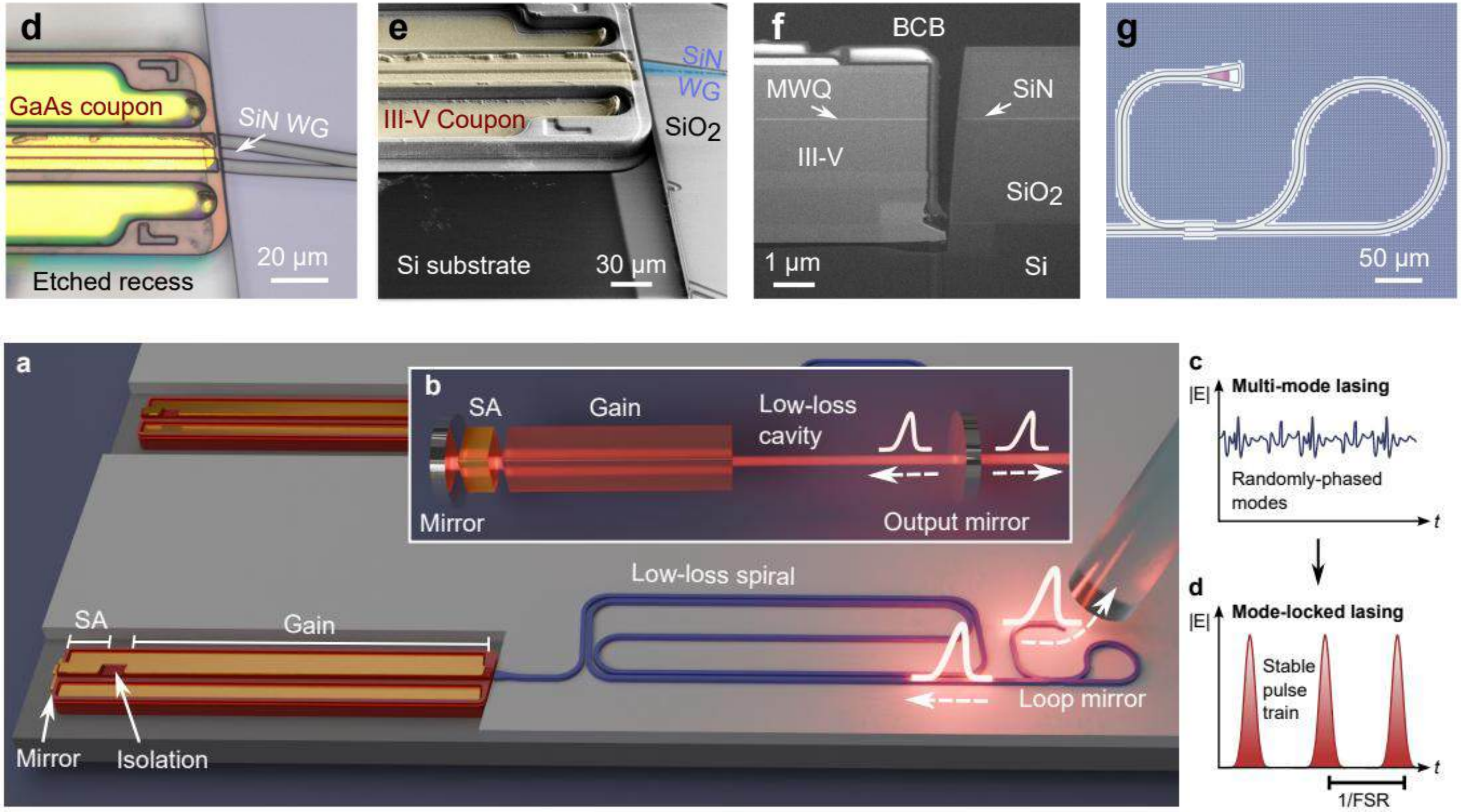

Max Kiewiet, Stijn Cuyvers, Maximilien Billet, Konstantinos Akritidis, Valeria Bonito Oliva, Gaudhaman Jeevanandam, Sandeep Saseendran, Manuel Reza, Pol Van Dorpe, Roelof Jansen, Joost Brouckaert, Günther Roelkens, Kasper Van Gasse, Bart Kuyken, “Micro-Transfer Printed Continuous-Wave and Mode-Locked Laser Integration at 800 nm on a Silicon Nitride Platform,” arXiv:2504.16993, 2025.

Recent work at UGent – imec: on-chip frequency doubling

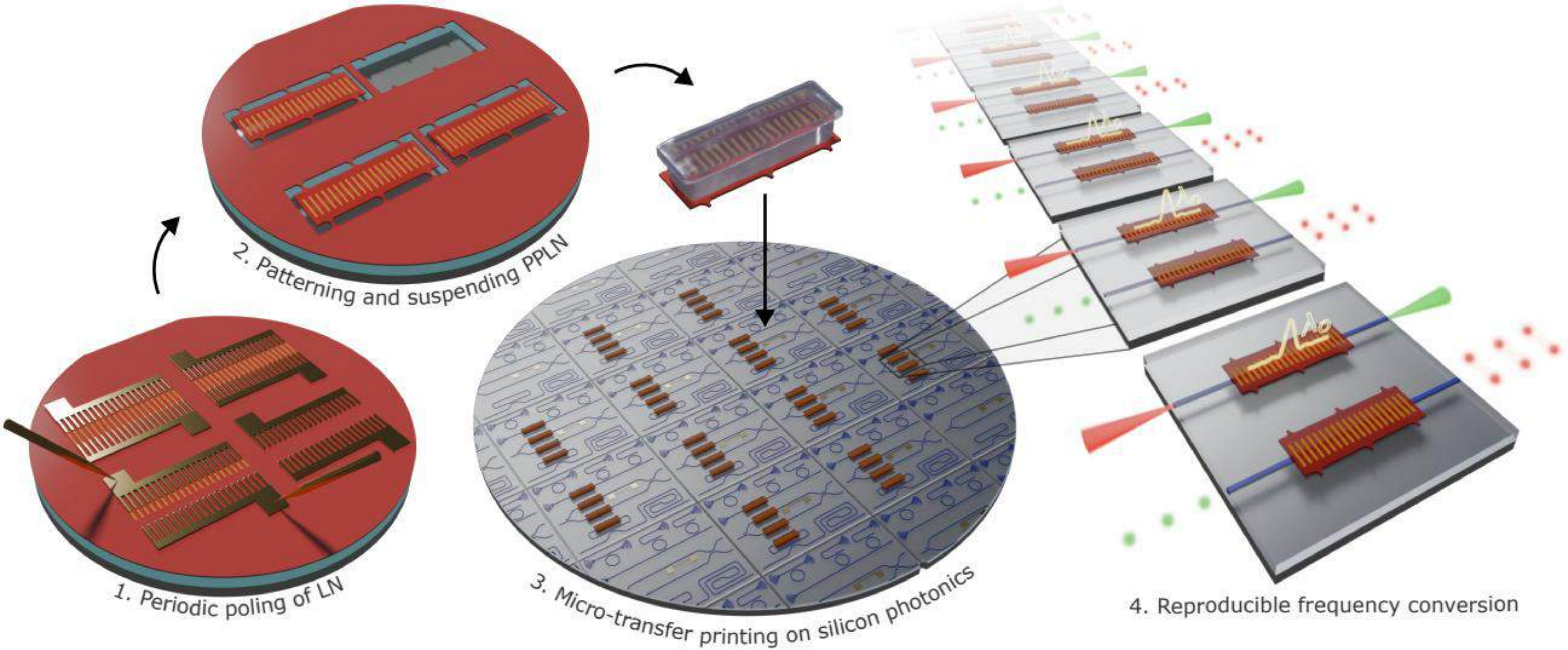

T. Vandekerckhove, J. De Witte, L. De Jaeger, E. Vissers, S. Janssen, P. Verheyen, N. Singh, D. Bode, M. Davi, F. Ferraro, P. Absil, S. Balakrishnan, J. Van Campenhout, D. Van Thourhout, G. Roelkens, S. Clemmens, and B. Kuyken, "A scalable quadratic nonlinear silicon photonics platform with printable entangled photon-pair sources," arXiv:2503.08783, 2025.

Recent work at UGent – imec: on-chip frequency doubling (2)

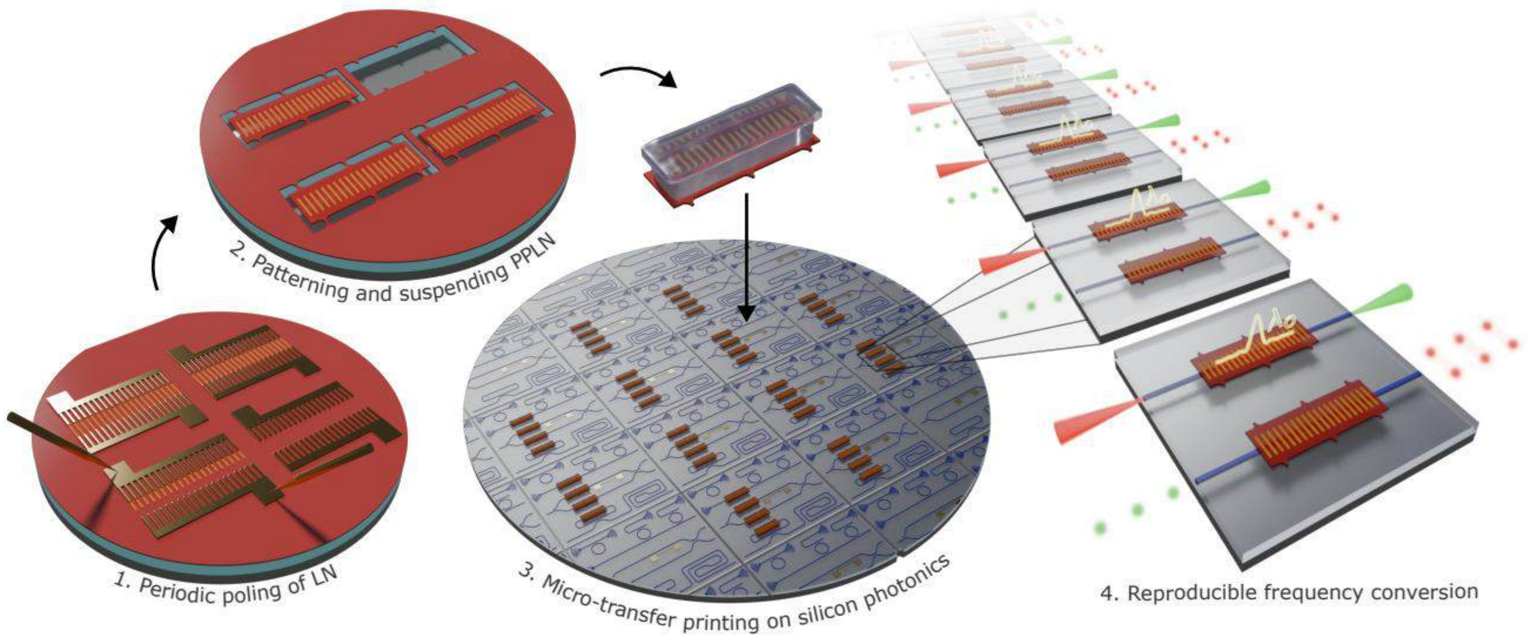

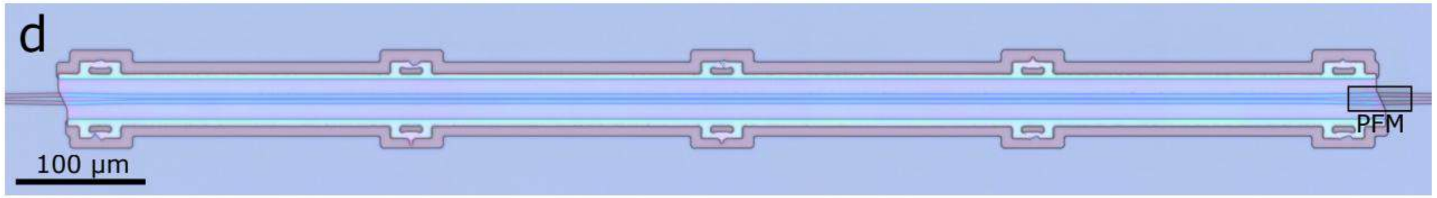

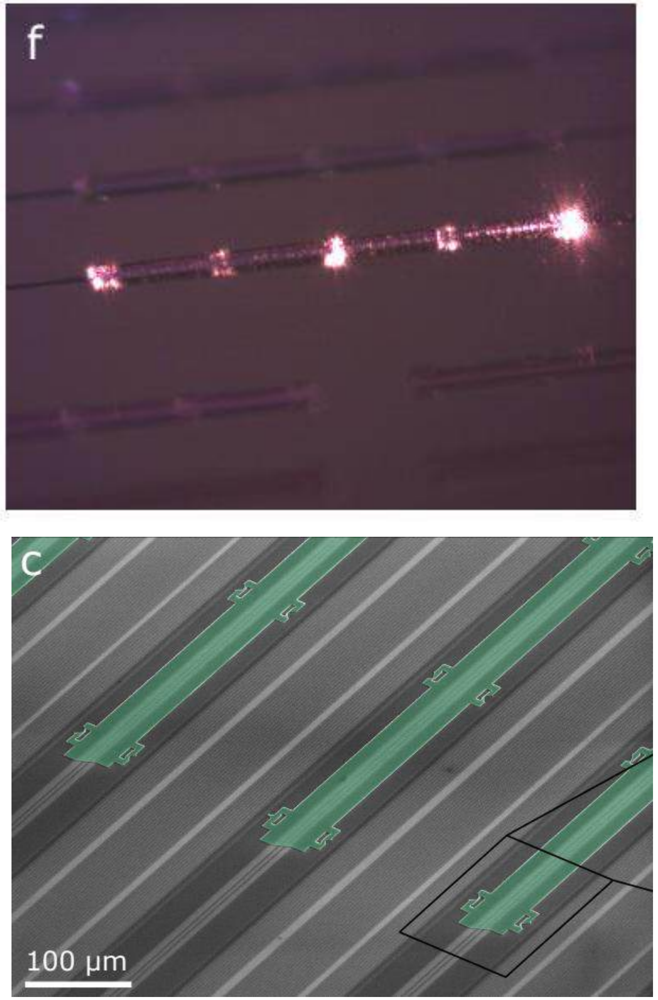

T. Vandekerckhove, J. De Witte, L. De Jaeger, E. Vissers, S. Janssen, P. Verheyen, N. Singh, D. Bode, M. Davi, F. Ferraro, P. Absil, S. Balakrishnan, J. Van Campenhout, D. Van Thourhout, G. Roelkens, S. Clemmens, and B. Kuyken, “A scalable quadratic nonlinear silicon photonics platform with printable entangled photon-pair sources,” arXiv:2503.08783, 2025.

Novel laser materials

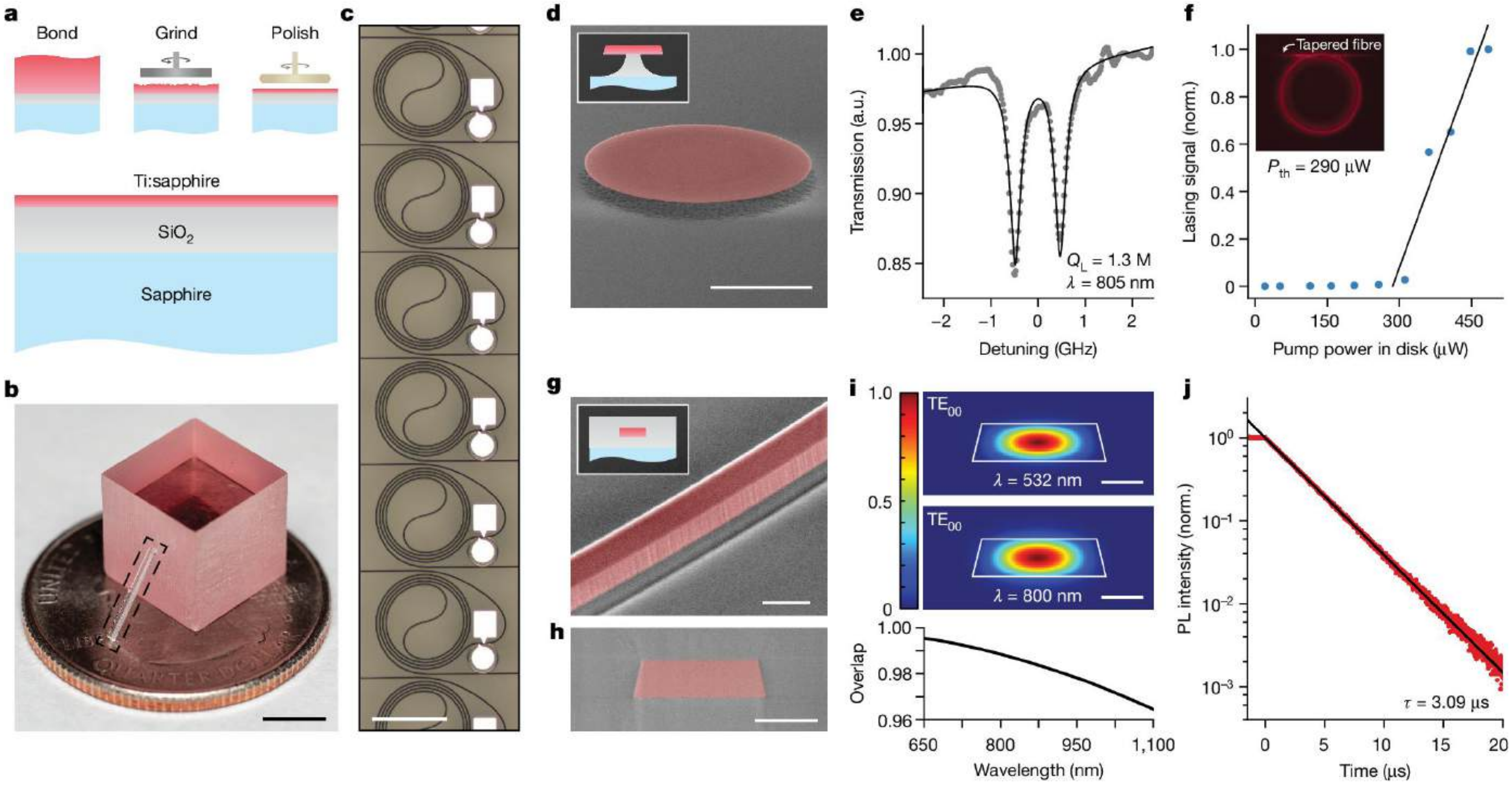

Yang, J., Van Gasse, K., Lukin, D.M. *et al.* Titanium:sapphire-on-insulator integrated lasers and amplifiers. *Nature* **630**, 853–859 (2024).

UGent – imec: Towards laser integration of novel laser materials

TiSaOI previously demonstrated to be ideally suited for control of quantum system.

Now looking towards wafer scale integration at UGent.

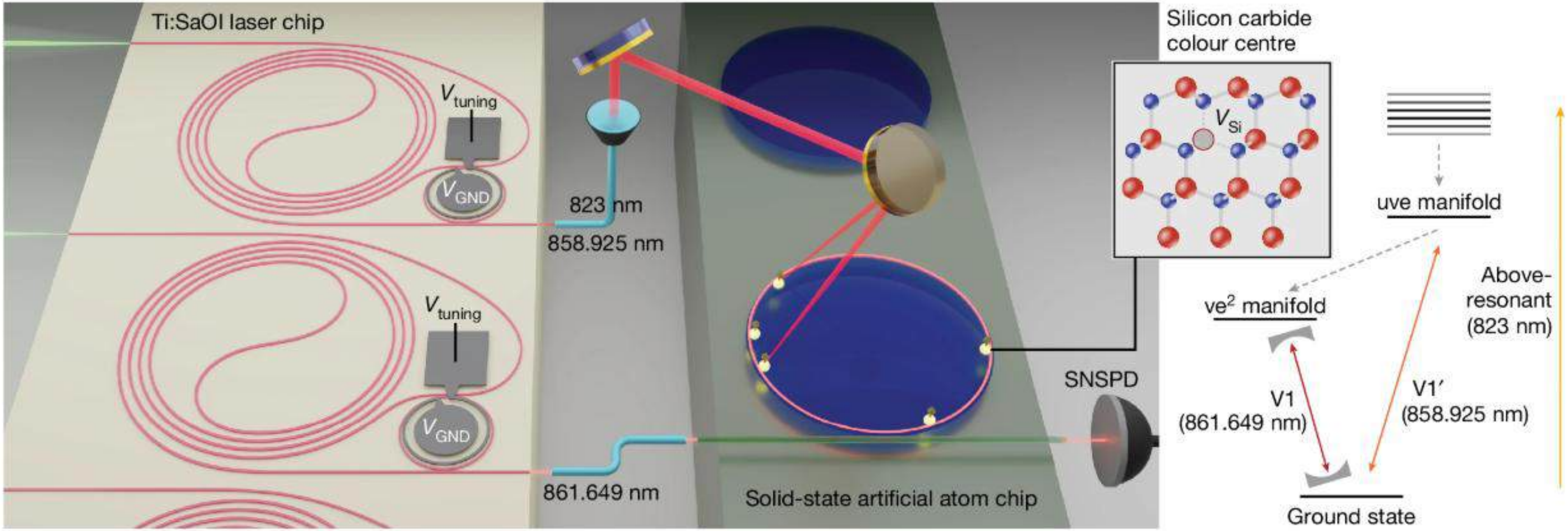

Yang, J., Van Gasse, K., Lukin, D.M. *et al.* Titanium:sapphire-on-insulator integrated lasers and amplifiers. *Nature* **630**, 853–859 (2024).

Summary and conclusion

- Atomic (optical) clocks are fundamental for navigation, communication, and precise timekeeping in modern society.

- Laboratory-scale optical clocks continue to push the limits of metrology, opening new frontiers in fundamental physics.

- Commercial optical atomic clocks are now being deployed by IonQ and Infleqtion, signaling a transition from research to real-world applications.

- Strong global efforts are underway toward the miniaturization and integration of optical atomic clocks.

- The field is entering a new era where quantum precision meets practical implementation.

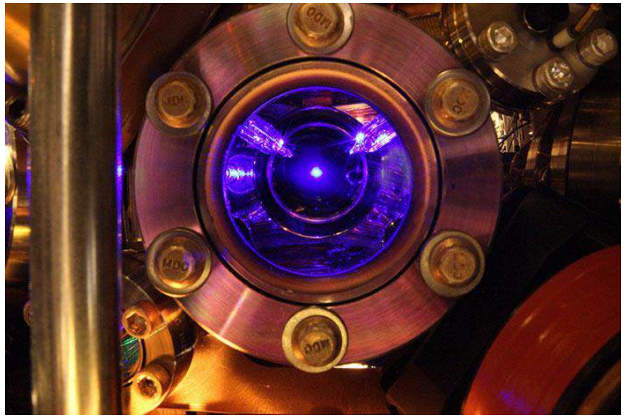

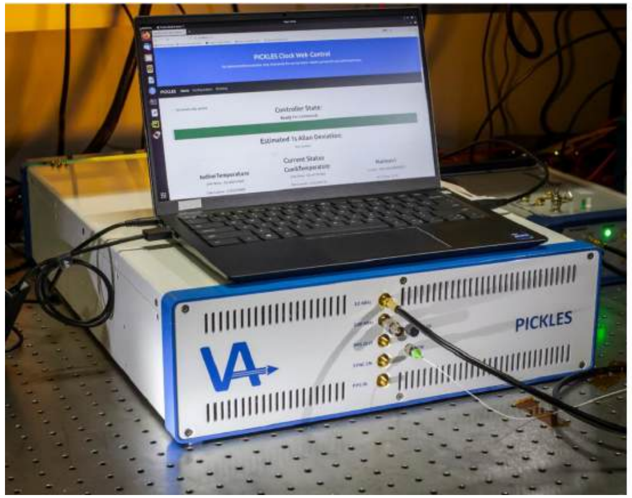

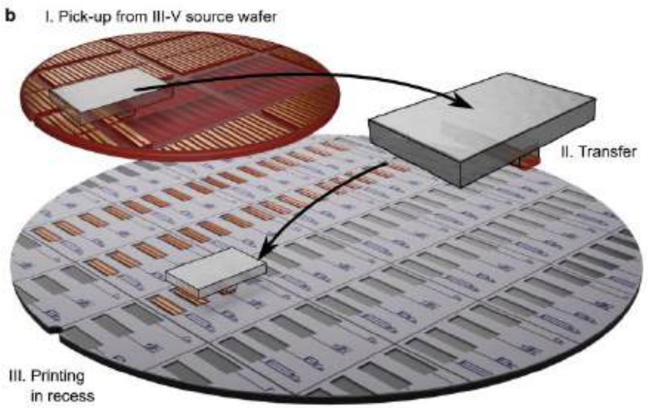

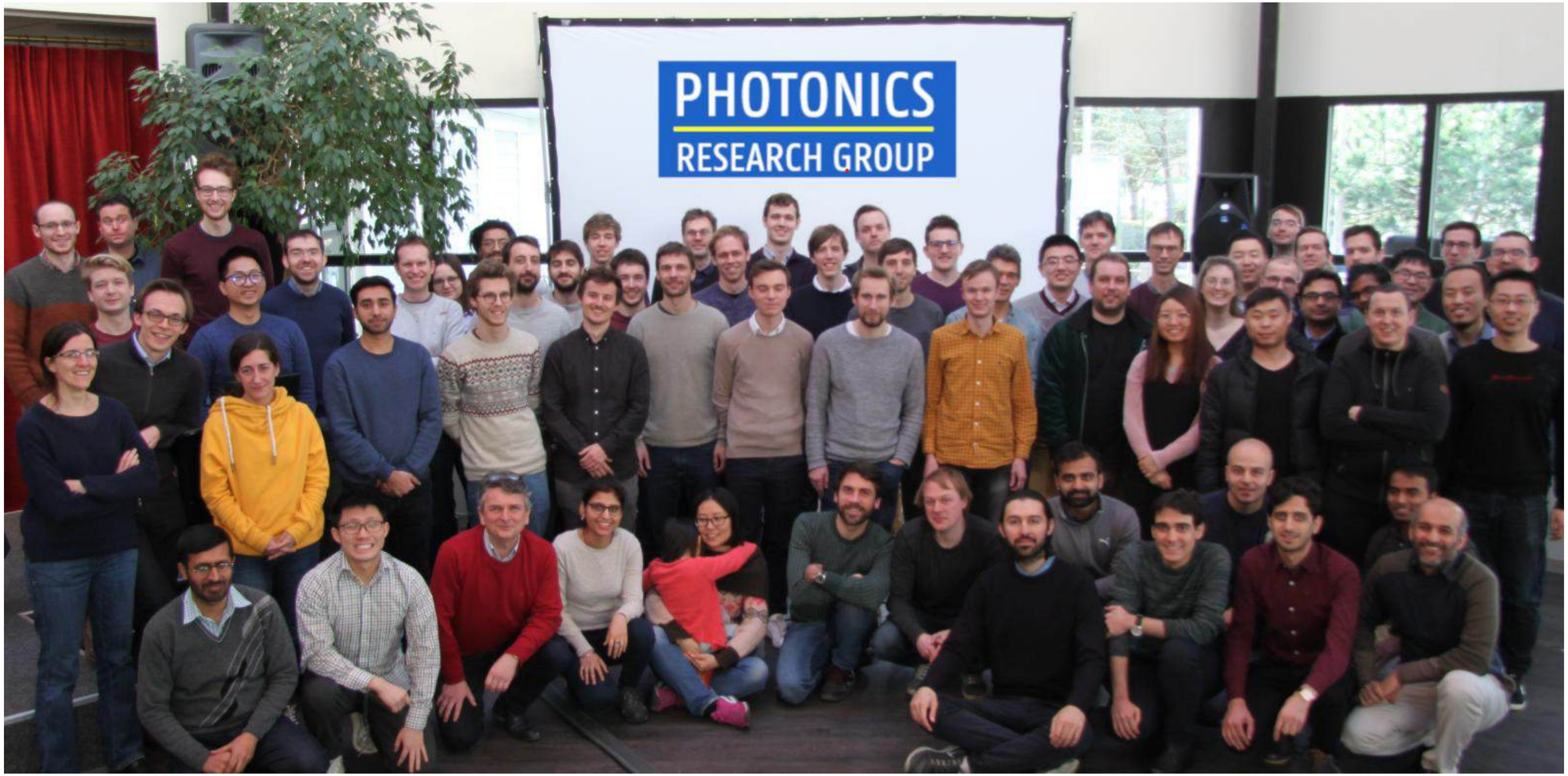

Thank you for your attention!

GHENT UNIVERSITY

imec

GHENT UNIVERSITY

imec

Anatomy of chip-scale atomic clock

(a)

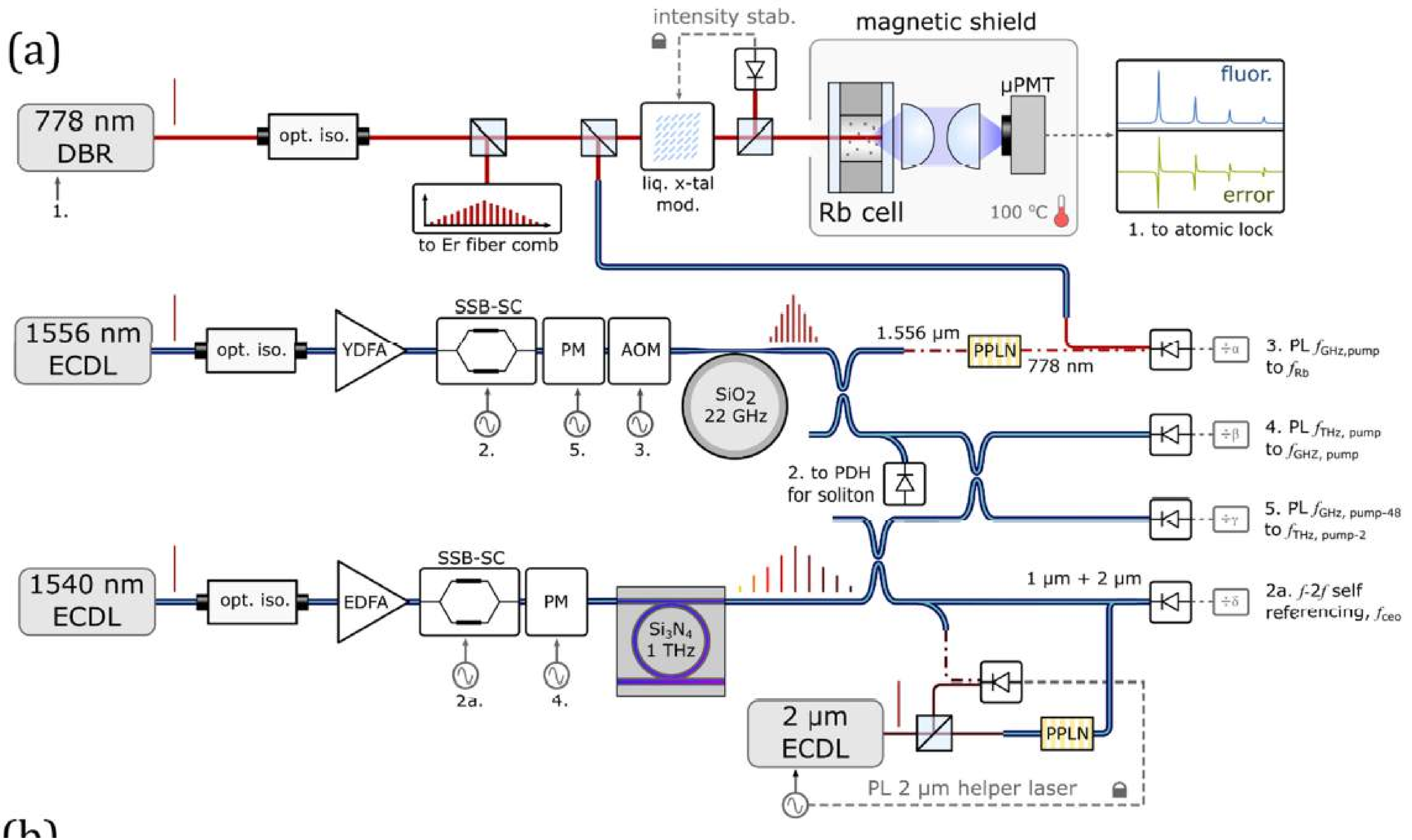

(b)

Work at UGent – imec: integrating novel laser materials

- Enabling new wavelengths and lower-noise operation through rare-earth and other solid-state laser integration on photonic chips.

- Developing low-noise, high-performance saturable absorbers for next-generation mode-locked lasers.

- Transfer-printing of novel laser crystals for compact and efficient integrated laser sources.

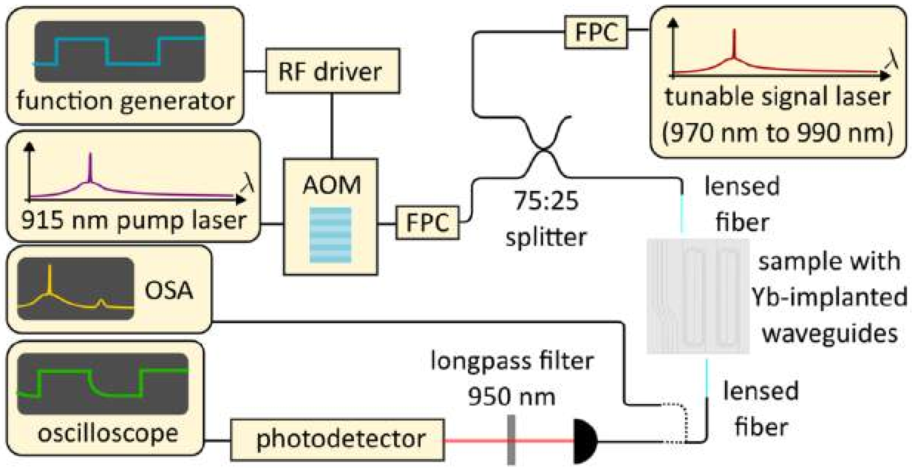

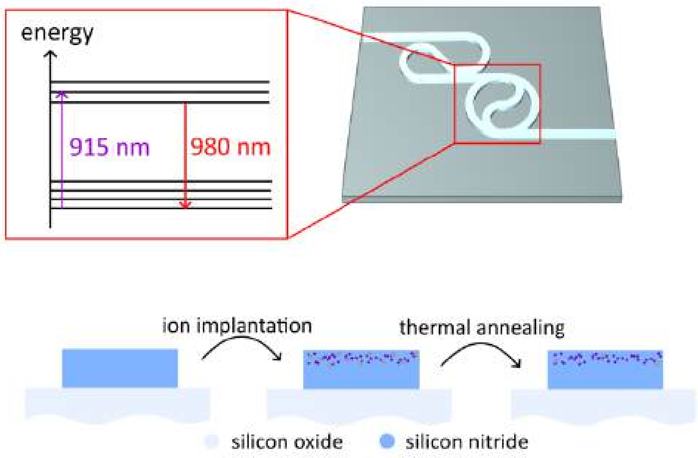

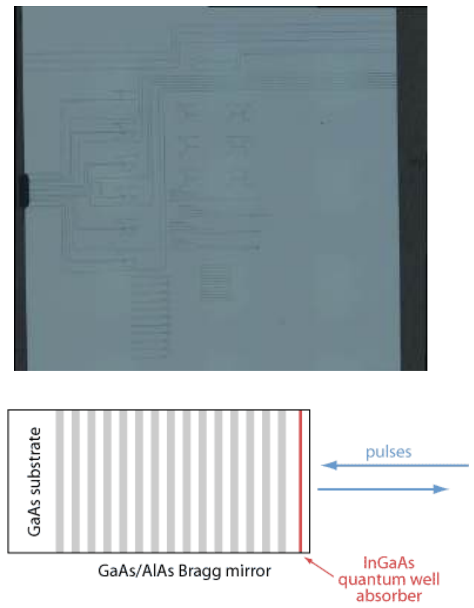

Clock evolution (2)

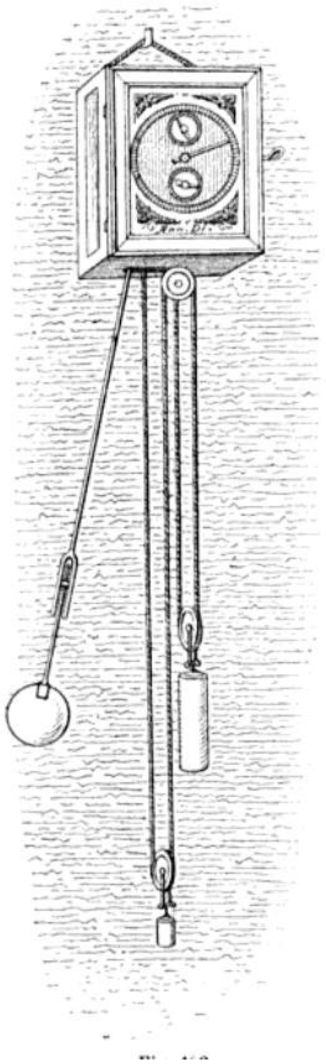

Christiaan Huygens - pendulum clock
(1656)
Accuracy: 15 seconds per day

Harrison – H4 Chronometer
(1762)
Accuracy: 0.2 seconds per day

Quartz crystal oscillator
(1927)
Accuracy: 0.004 seconds per day

NIST-F2 Cesium fountain
(2014)
Accuracy: 10 picoseconds per day

quantum simulation with cold atoms

Karel Van Acoleyen(UGent)

BeQCI quantum technology workshop at IMEC, 05/11/25

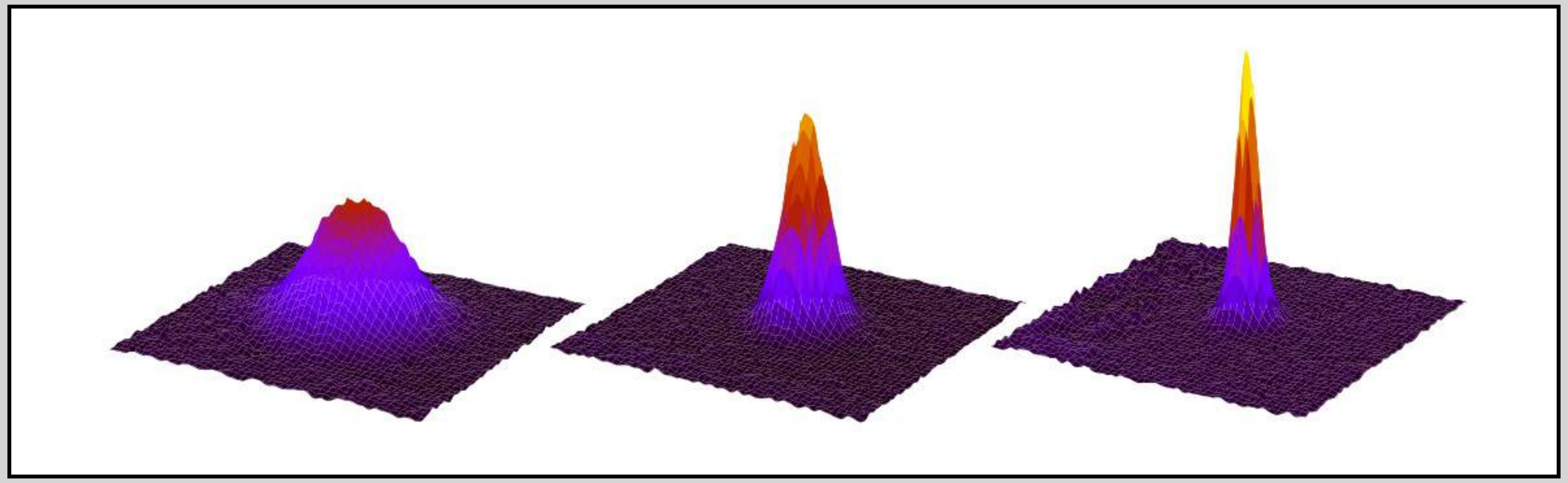

BEC@UGent 2022

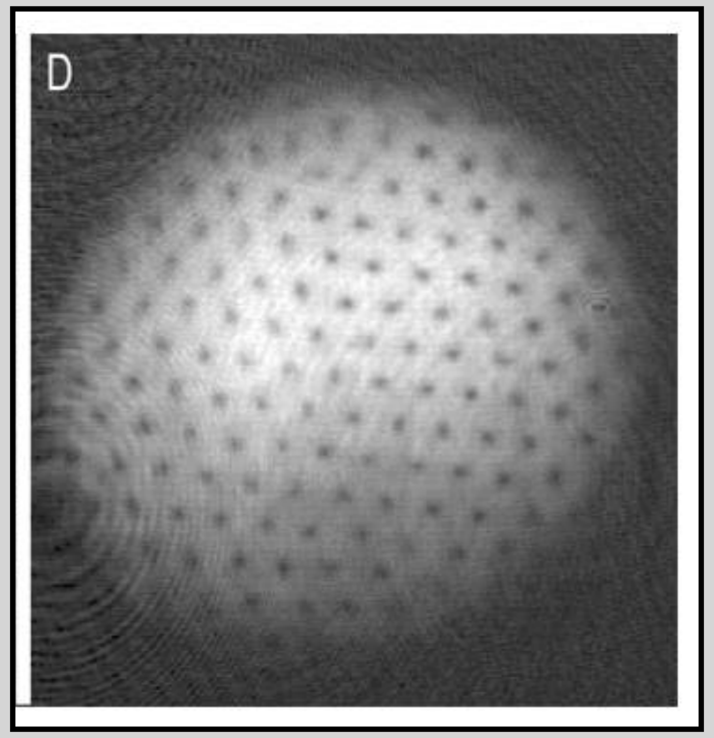

Abo-Shaeer,..,Ketterlee, 2001

Quantum gases

$N \approx 10^4 - 10^6$

$d \sim 0.1\mu m$

$T \sim 100nK$

$E \sim kHz$

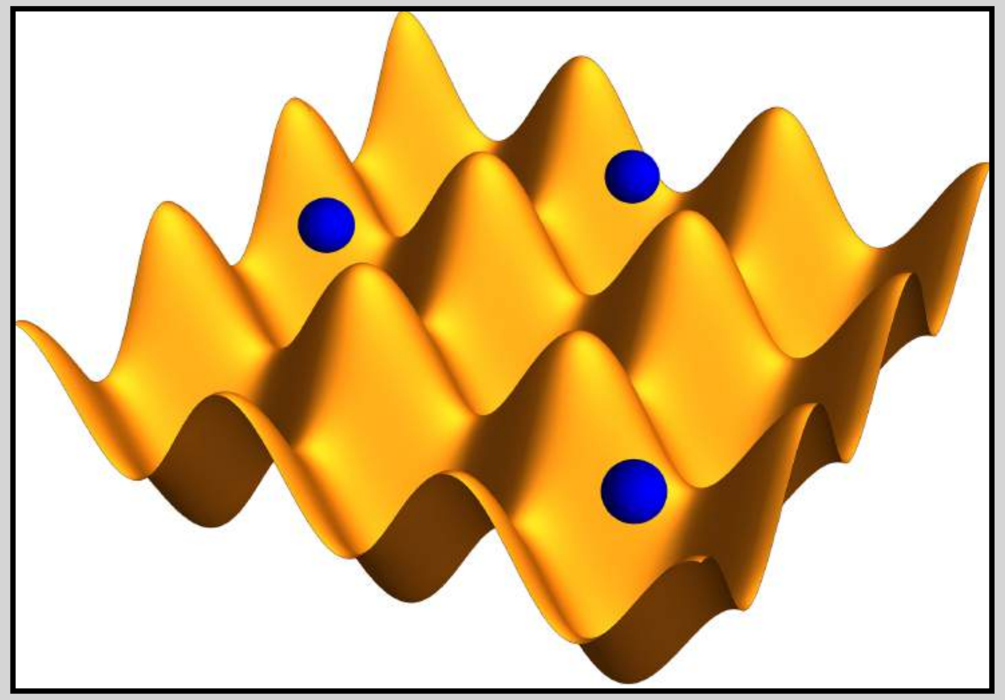

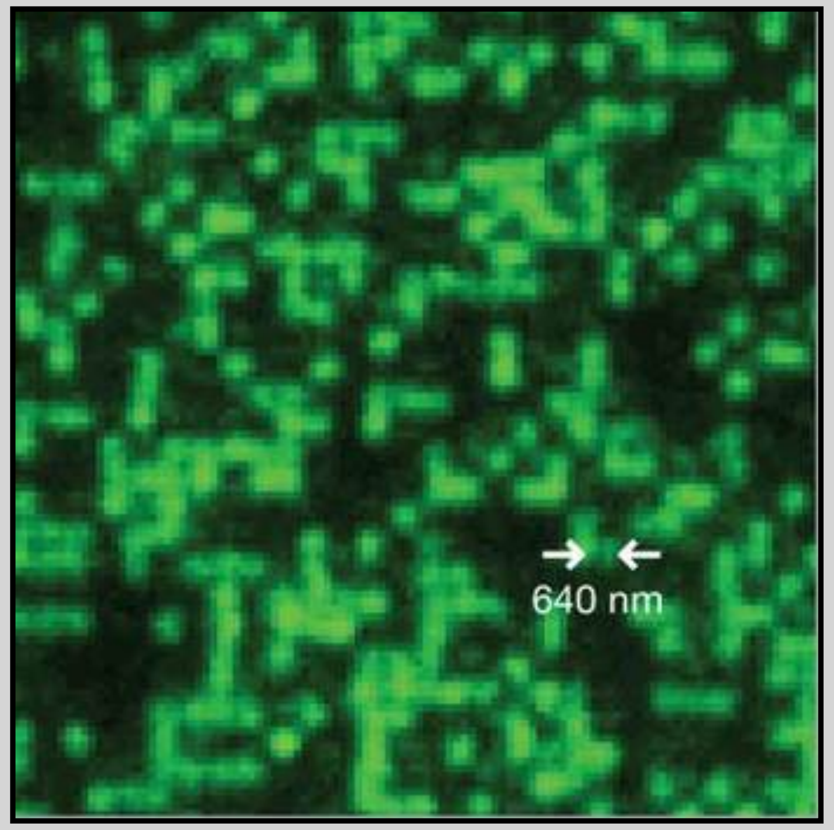

Bakr,..,Greiner 2009

Optical lattices

$N \approx 10^2 - 10^3$

$d \lesssim 1\mu m$

$E \sim kHz$

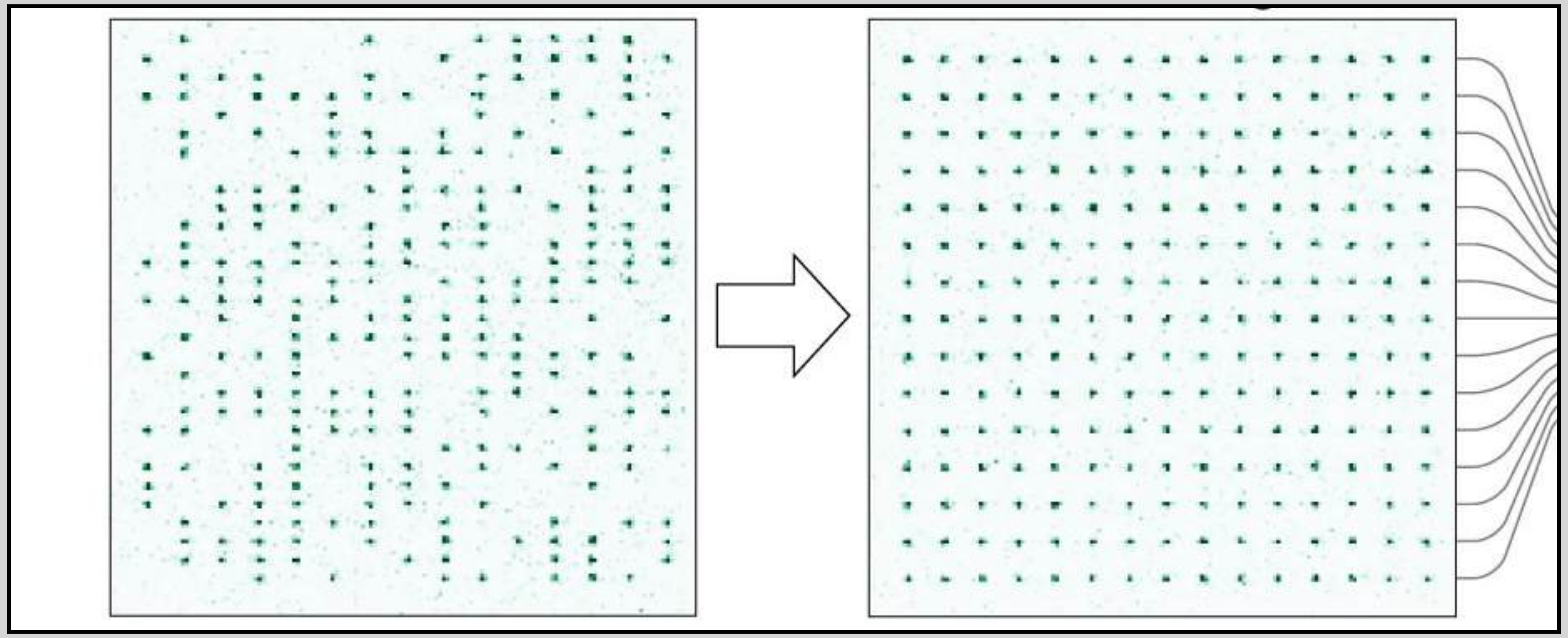

Ebadi,…,Lukin 2021

Rydberg arrays

$N \approx 10^2$

$d \sim \text{few } ums$

$E \sim MHz$

Control

"*Nature isn't classical dammit, and if you want to make a simulation of nature,* you'd better make it quantum mechanical" (Feynman, 1982)

Quantum simulation=quantum many-body experiment with a large degree of **control** (on state/Hamiltonian) and **accessibility**

$$|\psi(t)>= e^{-\frac{i}{\hbar}Ht}|\psi(0)>$$

Targets: new **phases of matter** (thermal states, groundstates) and **non-equilibrium physics**

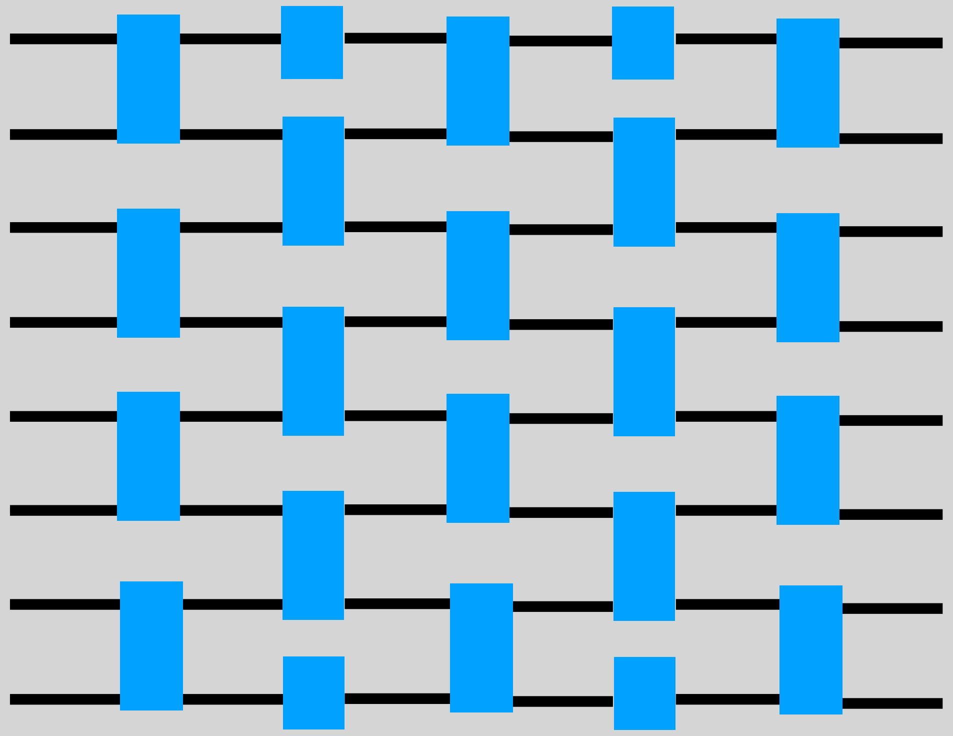

digital simulation
(universal)

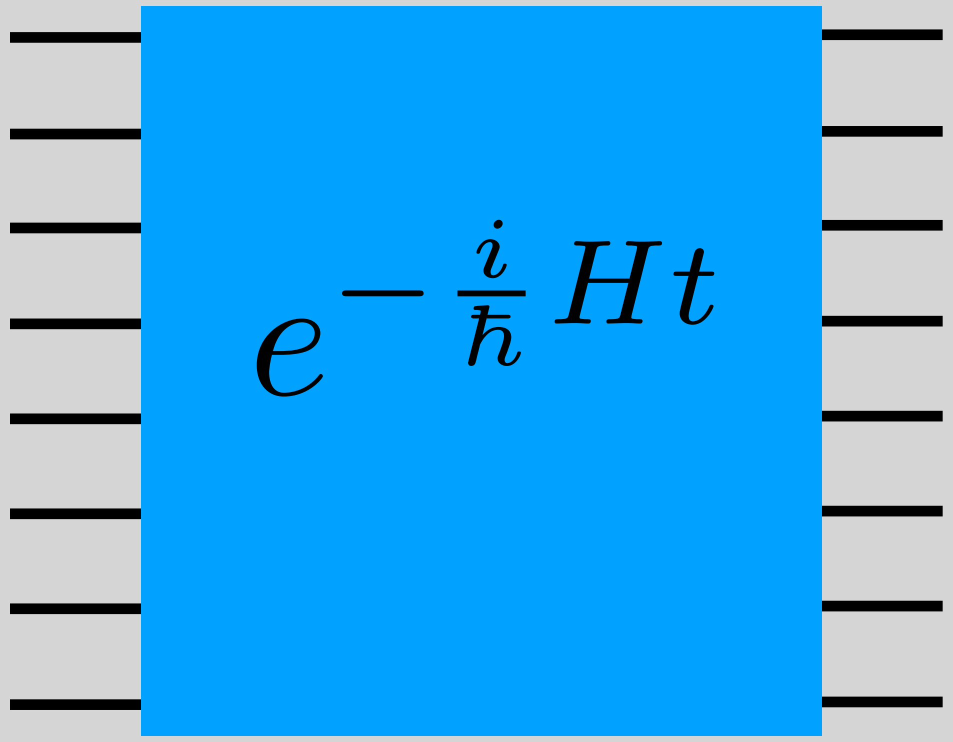

analogue simulation
(non-universal)

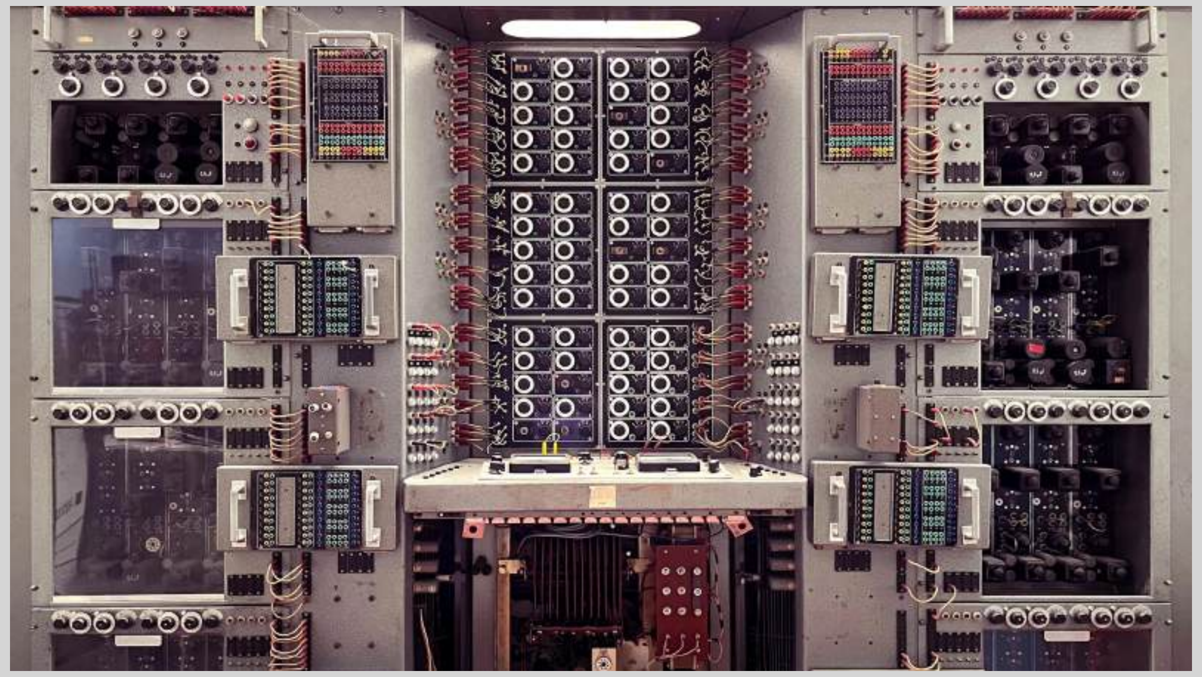

OME-P2 (1952)

Universal phenomena $(1TeV \sim 10^{23} kHz \quad \text{versus} \quad 1kHz)$

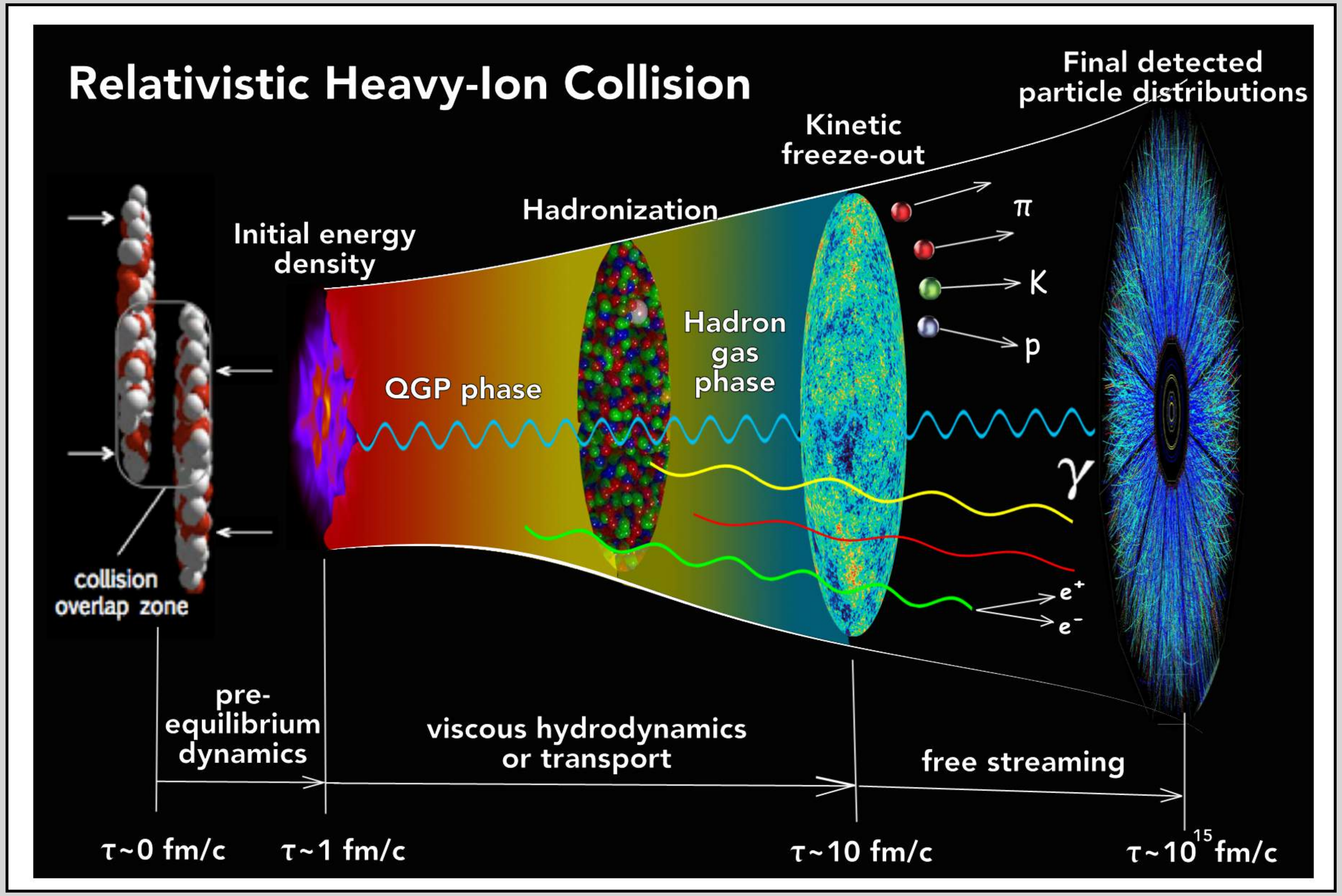

Achenbach et al, Nucl. Phys. (2024)

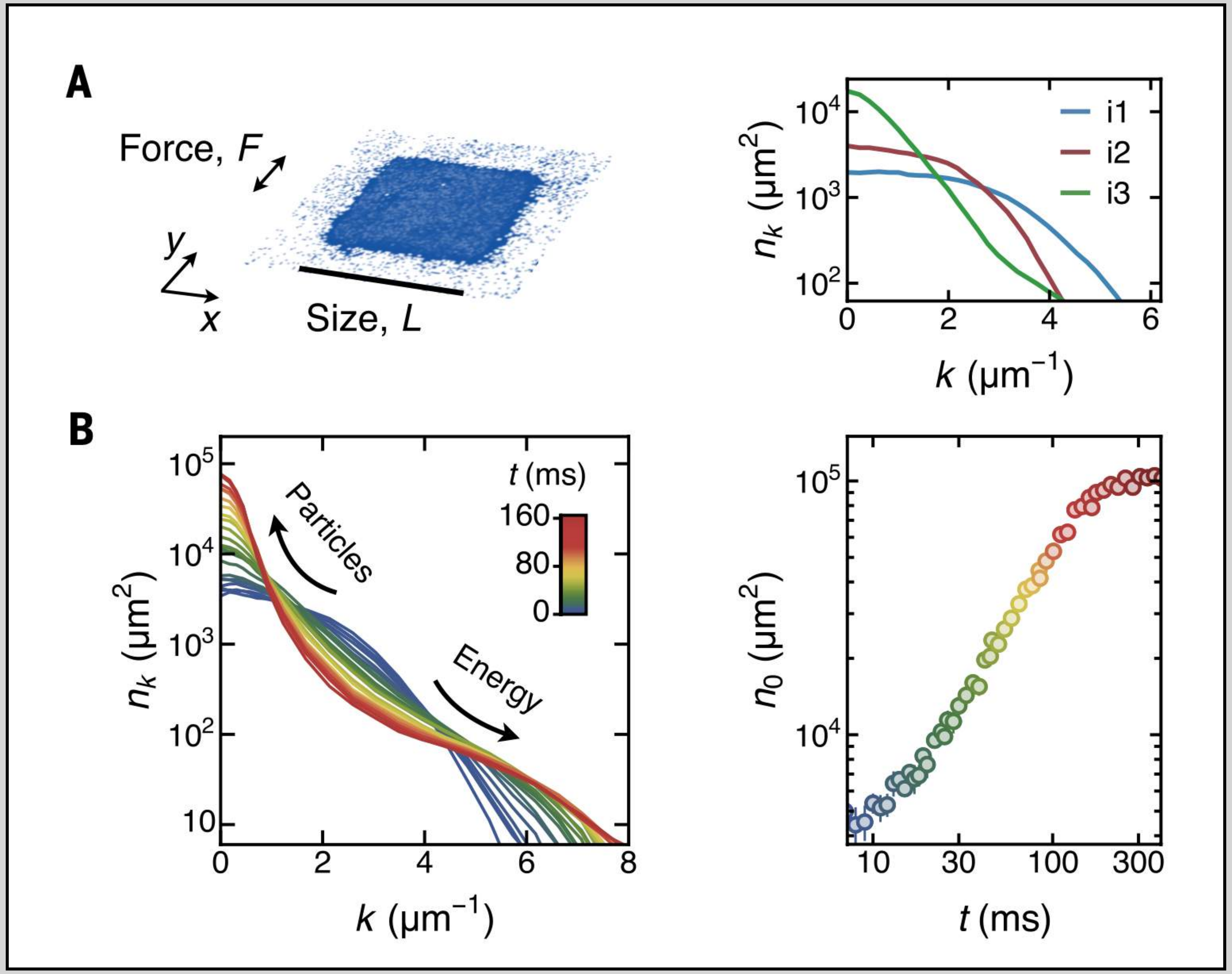

Gazo, …, Hadzibabic, Science (2025)

(pre-) initial state, BEC
control on time-dependent trap,
control on interactions,
read-out at arbitrary times

“Quantum plumbing” (Antoine Browaeys)

Playing atoms with magnetic and optical fields

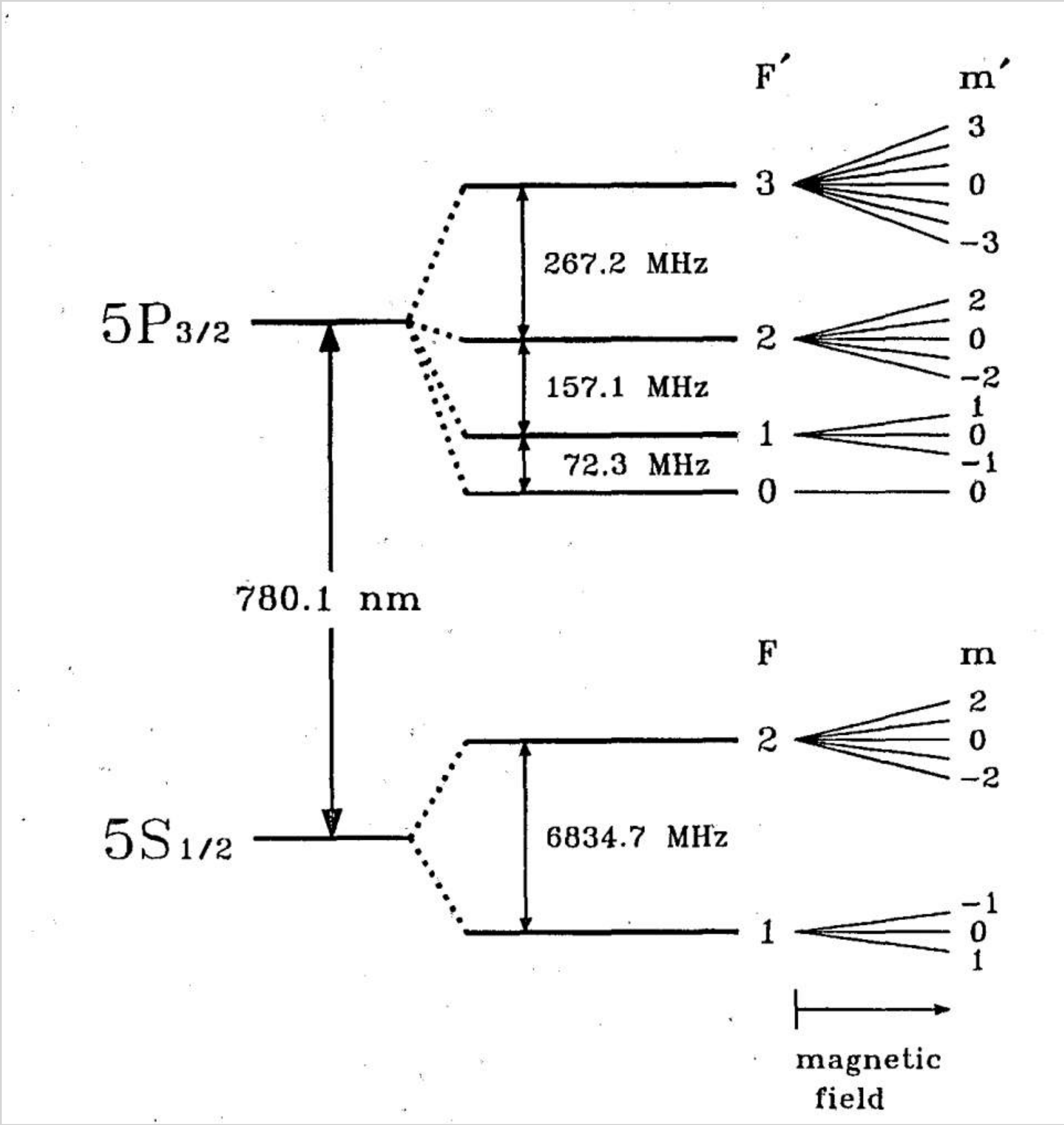

$\psi_\sigma(\vec{x})$ internal + external degrees of freedom

$H_\mu = -\vec{\hat{\mu}}.\vec{B}$ magnetic dipole interaction

$H_d = -\vec{\hat{d}}.\vec{E}$ electrical dipole interaction

$$H_\mu = -\vec{\hat{\mu}}.\vec{B} = \mu_B g_F m_F |\vec{B}|$$

Controlled with: permanent magnets, coils, atom chip

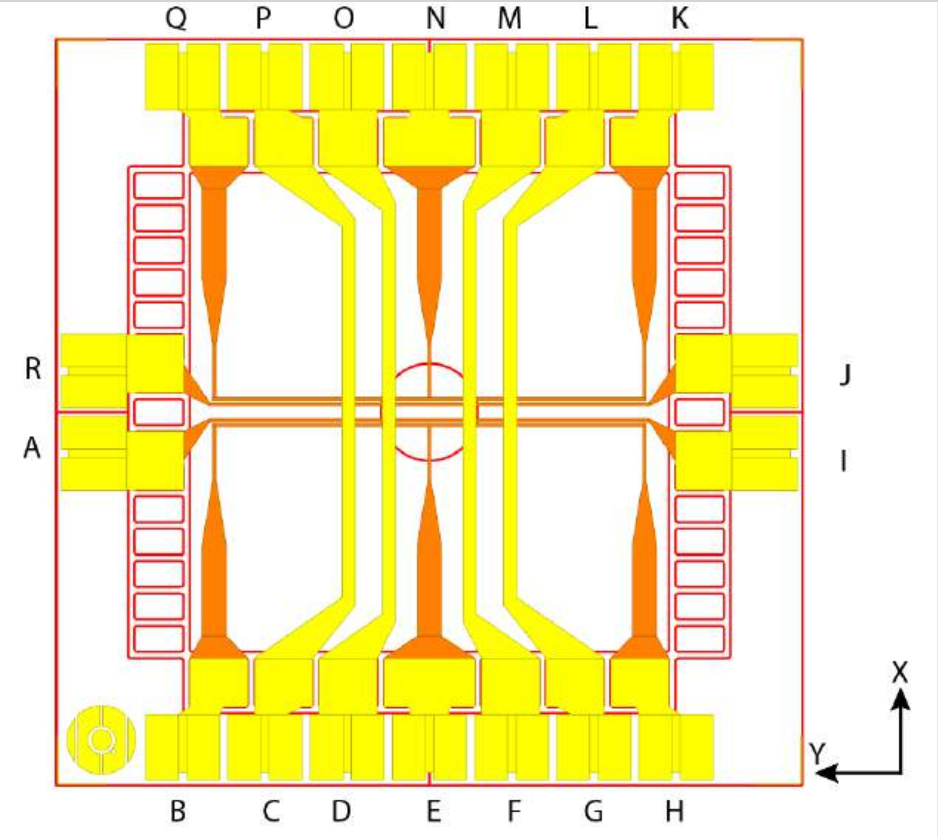

Trapping:

$$|\vec{B}|(\vec{x}) = B_0 + \frac{1}{2}(B_{xx}x^2 + B_{yy}y^2 + B_{zz}z^2)$$

Control hyperfine states:

$$B \propto e^{i\omega t}$$

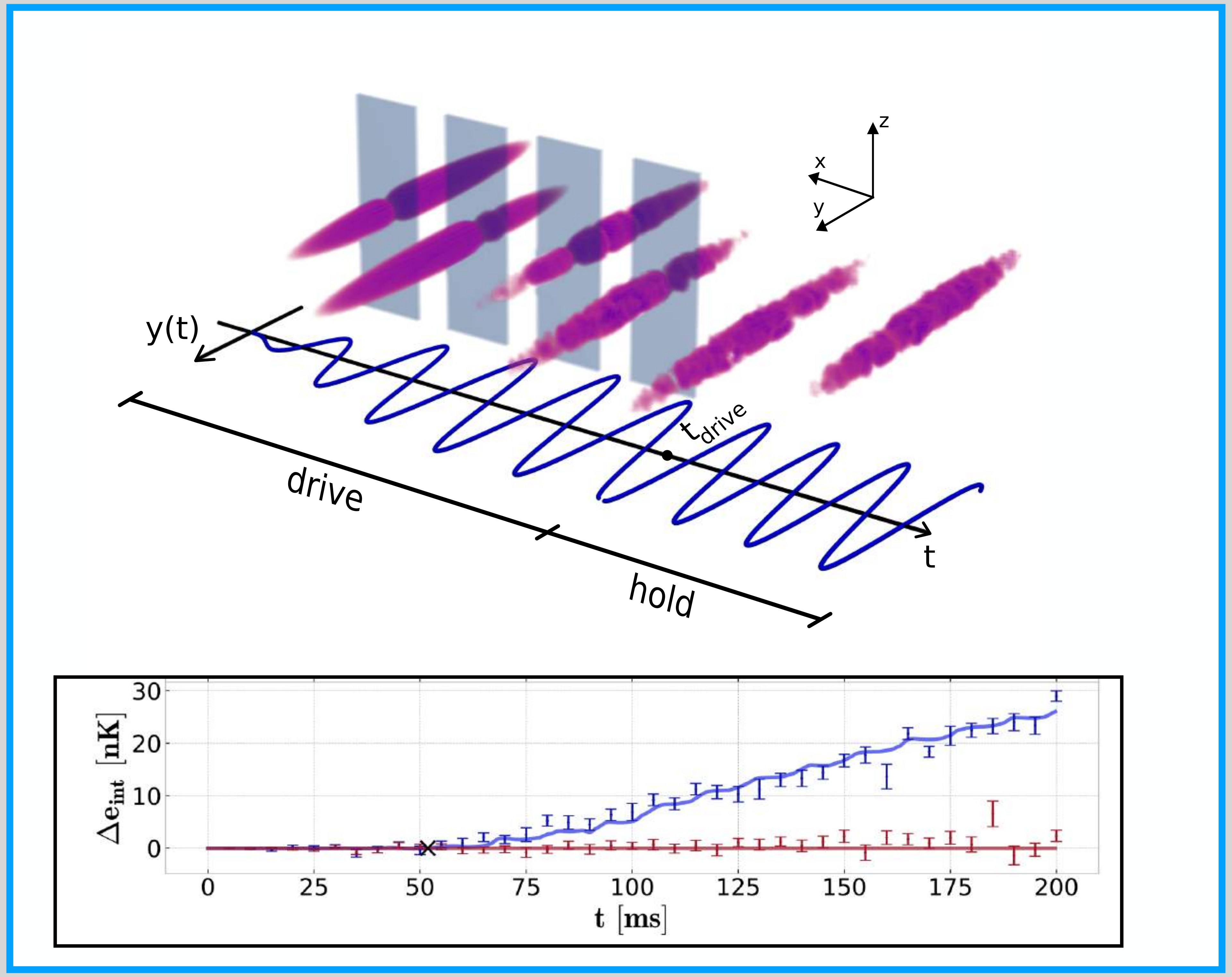

direct dissipation measurement BEC *Tanghe et al, arxiv 2025*

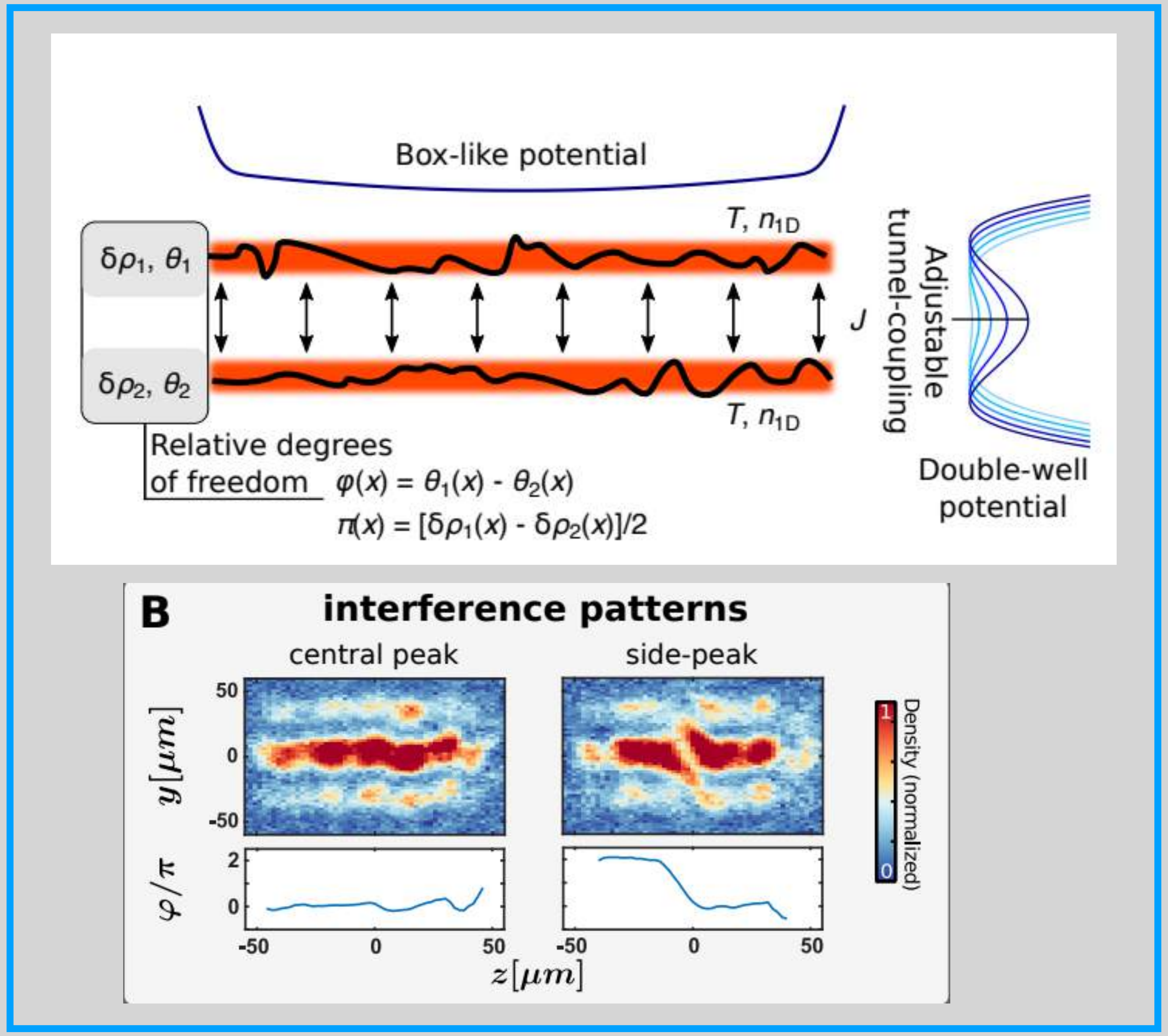

sine-Gordon model via tunneling dynamics

Schweigler,..., Schmiedmayer, Nature, (2017)

$$H_d = -\vec{\hat{d}}.\vec{E}(x)e^{-i\omega t} + h.c.$$

Control on frequency (e.g. 1 MHz / 300 THz), on polarization

Control on projected patterns, with mirrors, beam-splitters, lenses, SLMs, AODs, DMDs

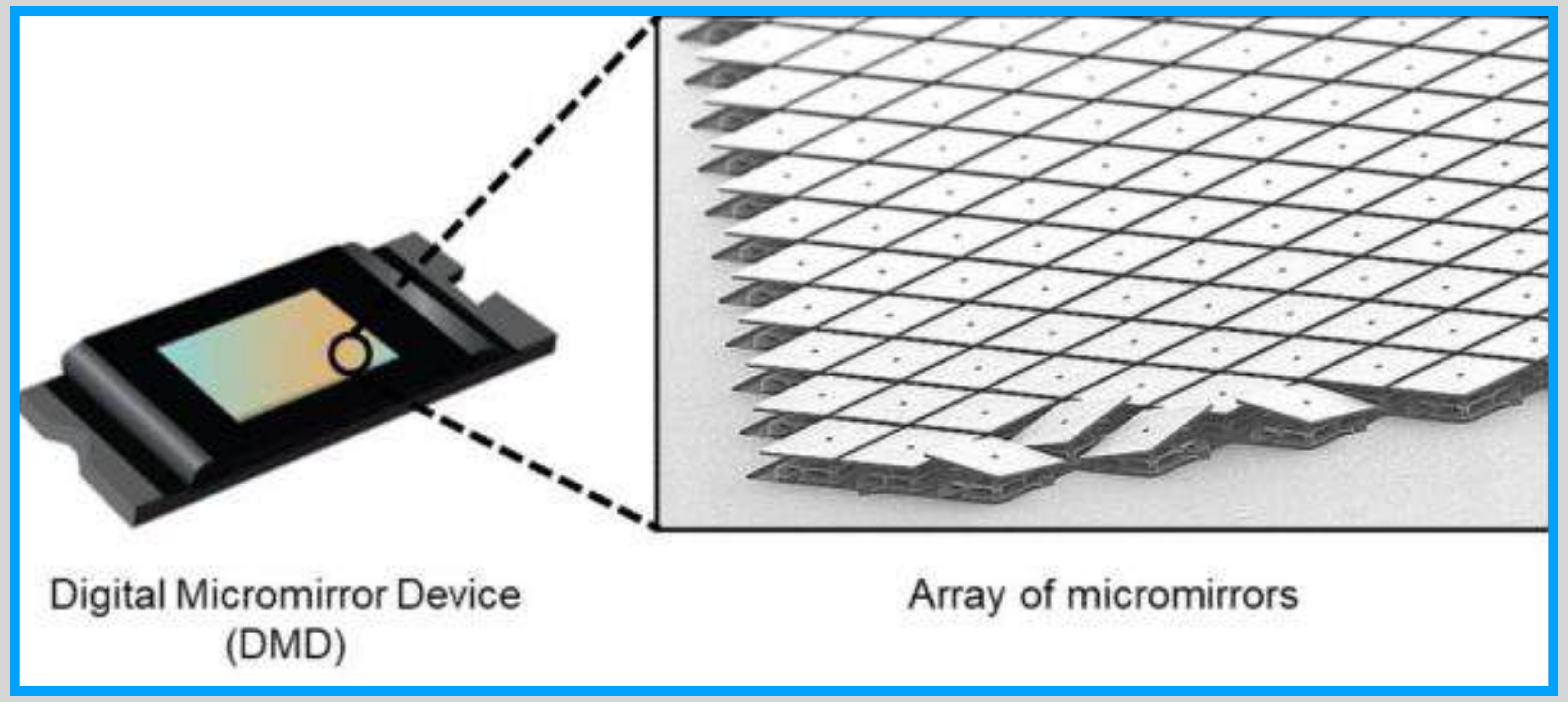

2-level case:

$$H_{RW} = -\delta|e><e| + \frac{1}{2}\left(\Omega|g><e| + \bar{\Omega}|e><g|\right)$$

$$\Omega = 2 < g|\vec{\hat{d}}.\vec{E}(\vec{x})|e > \qquad \delta = \omega - \omega_0$$

<u>Optical dipole traps (AC Stark-shift)</u>

$$E_0 \approx \frac{\hbar}{4}\frac{|\Omega|^2}{\delta}$$

$\delta > 0$ $\qquad$ $\delta < 0$

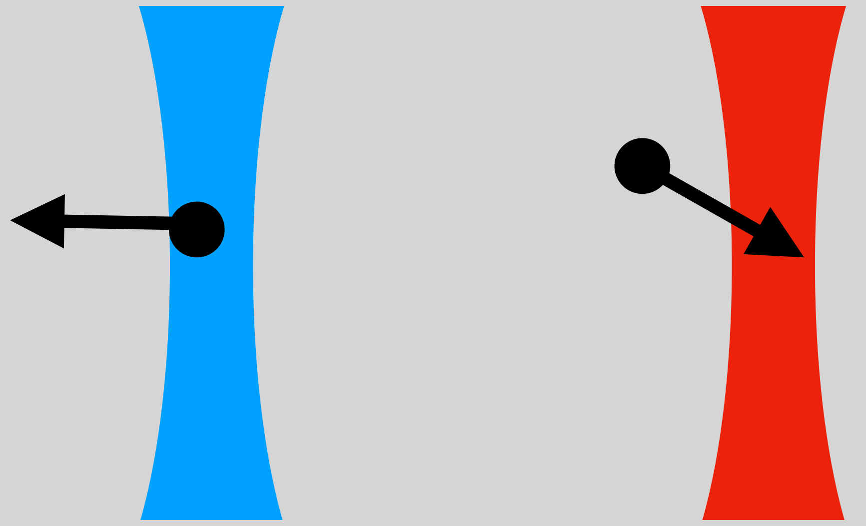

Filling up an atom array *Endres,…,Lukin, Science 2016*

Optical lattice from standing waves

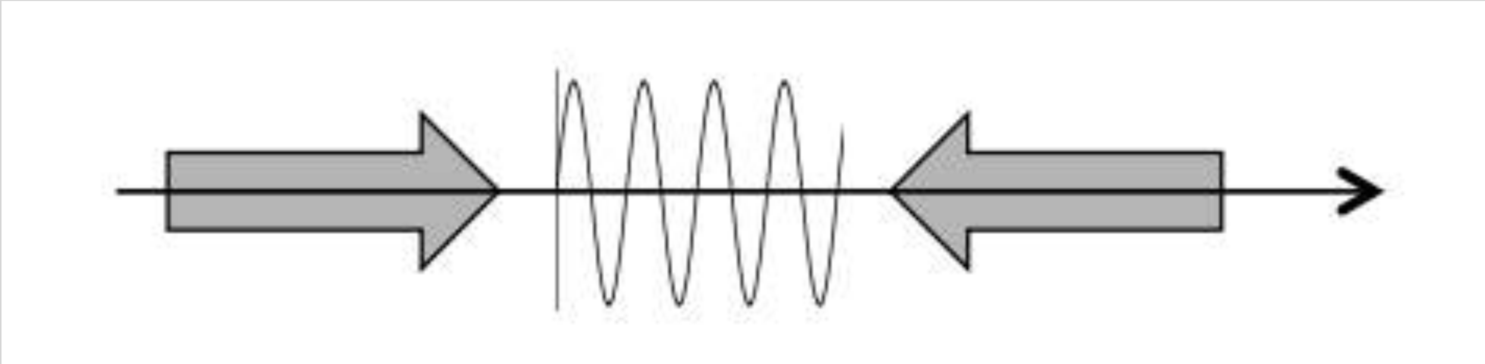

$$\vec{E}(x,t) = 2E_0\sin(kx)e^{i\omega t} + c.c.$$

$$V(x) = V_0\sin^2(kx) \qquad a = \frac{\pi}{k} = \lambda/2$$

Cooling and detecting via spontaneous emission

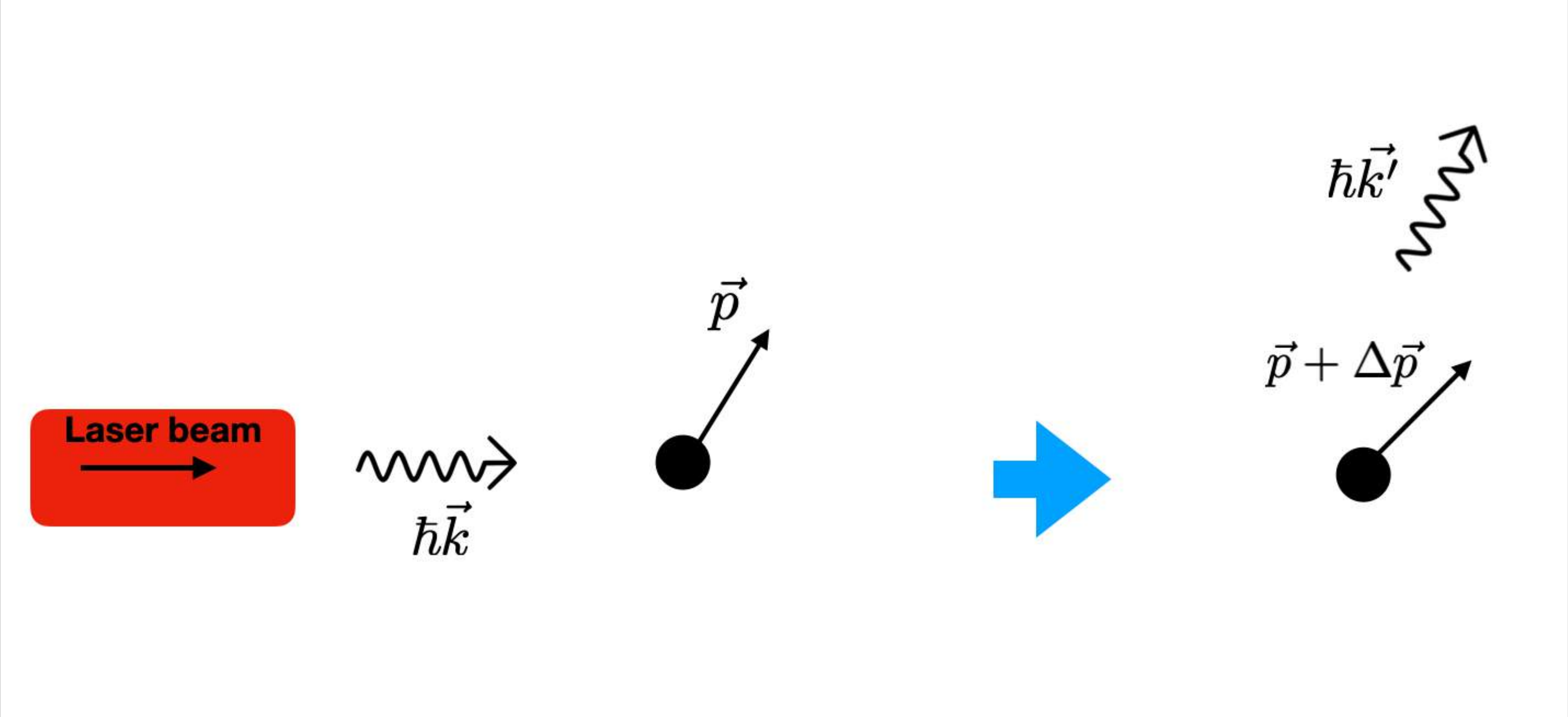

Cooling: Magneto-optical trap

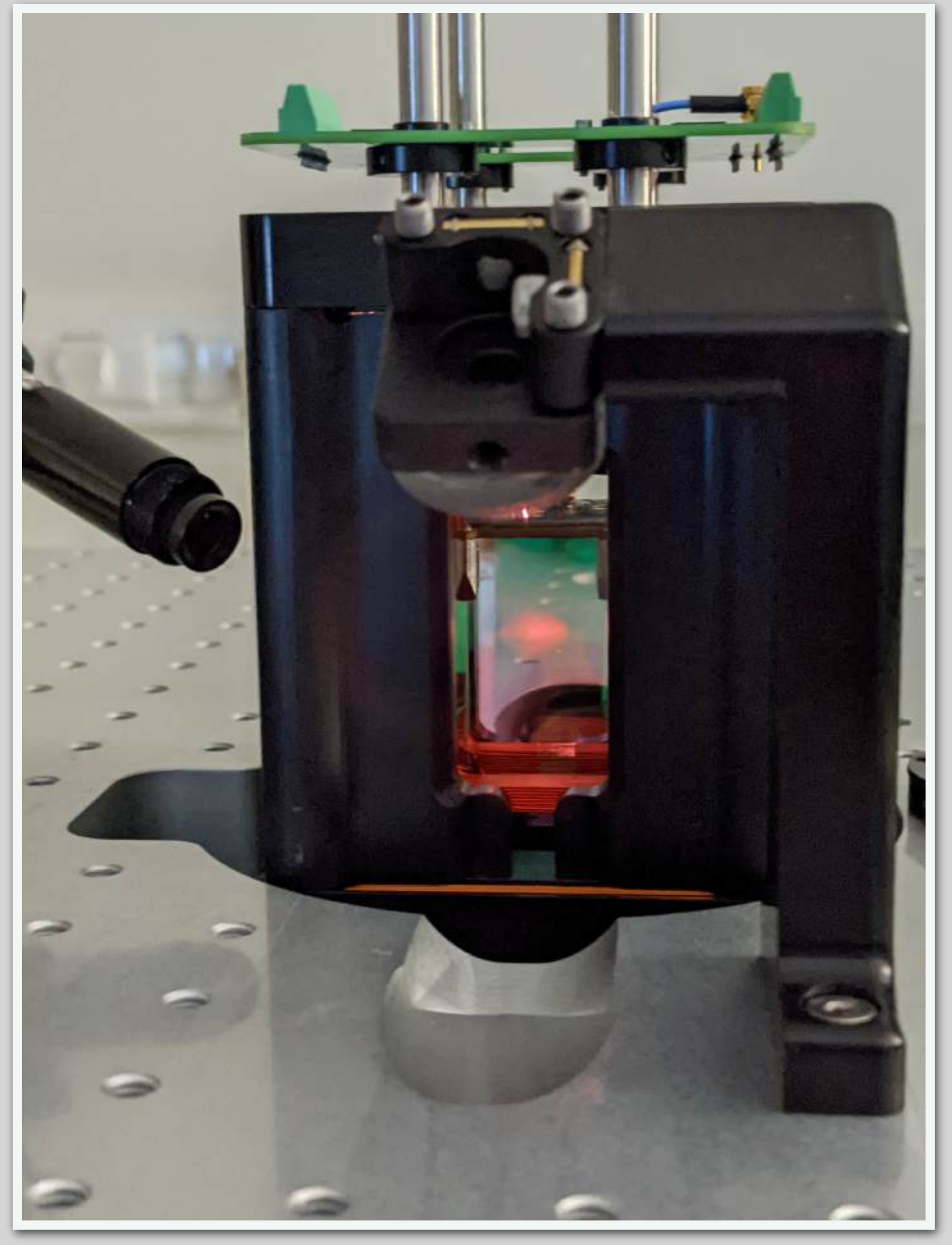

Optical molasse

$$\frac{\Gamma}{\omega_0} = \frac{6\,MHz}{300\,THz} \sim 10^{-8} = \frac{\Delta v}{c}$$

$$T \sim 100\mu K, N \sim 10^9$$

evaporative cooling

$$T \sim 100nK, N \sim 10^5$$

Detecting: Absorption imaging (destructive)

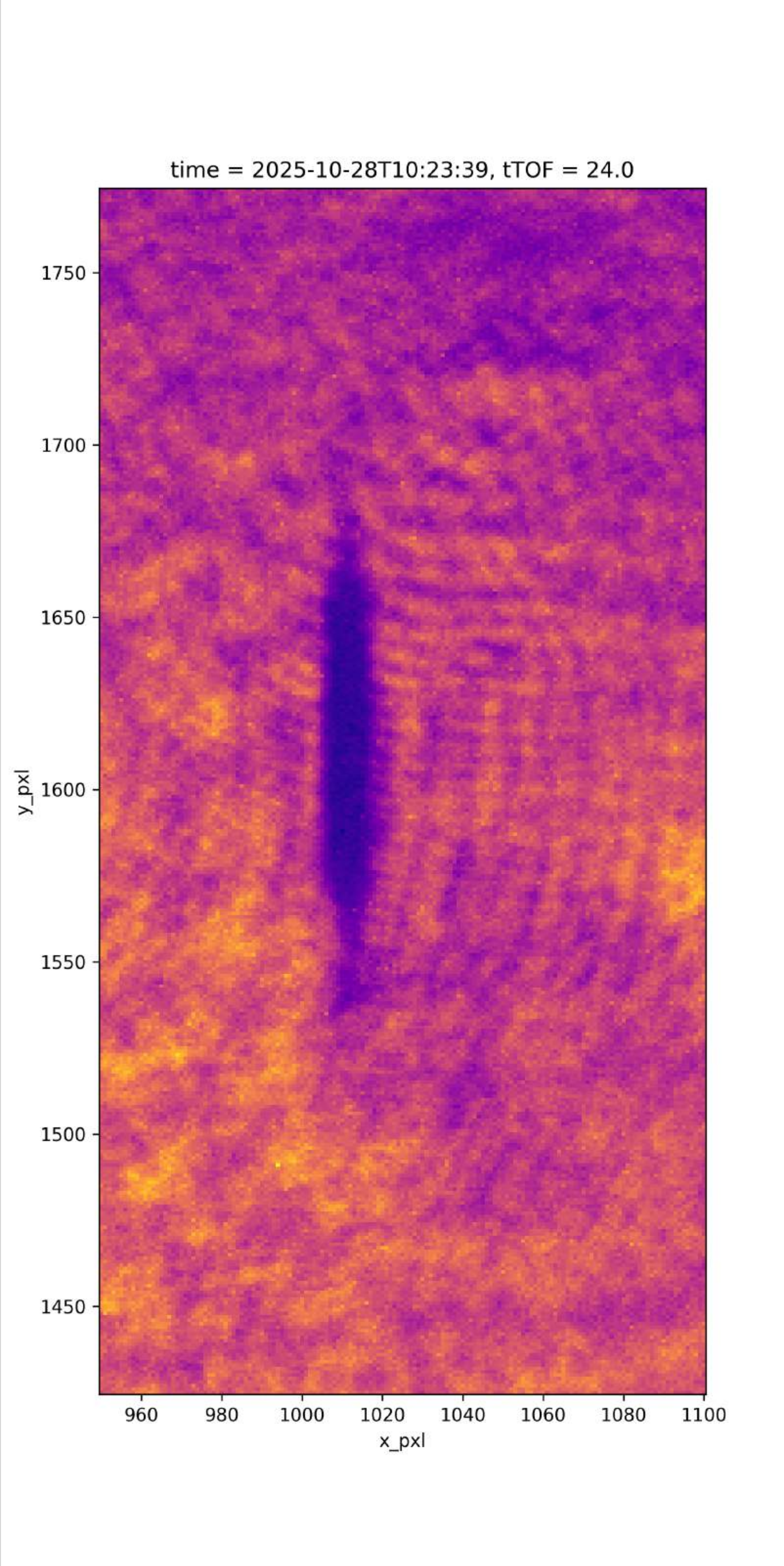

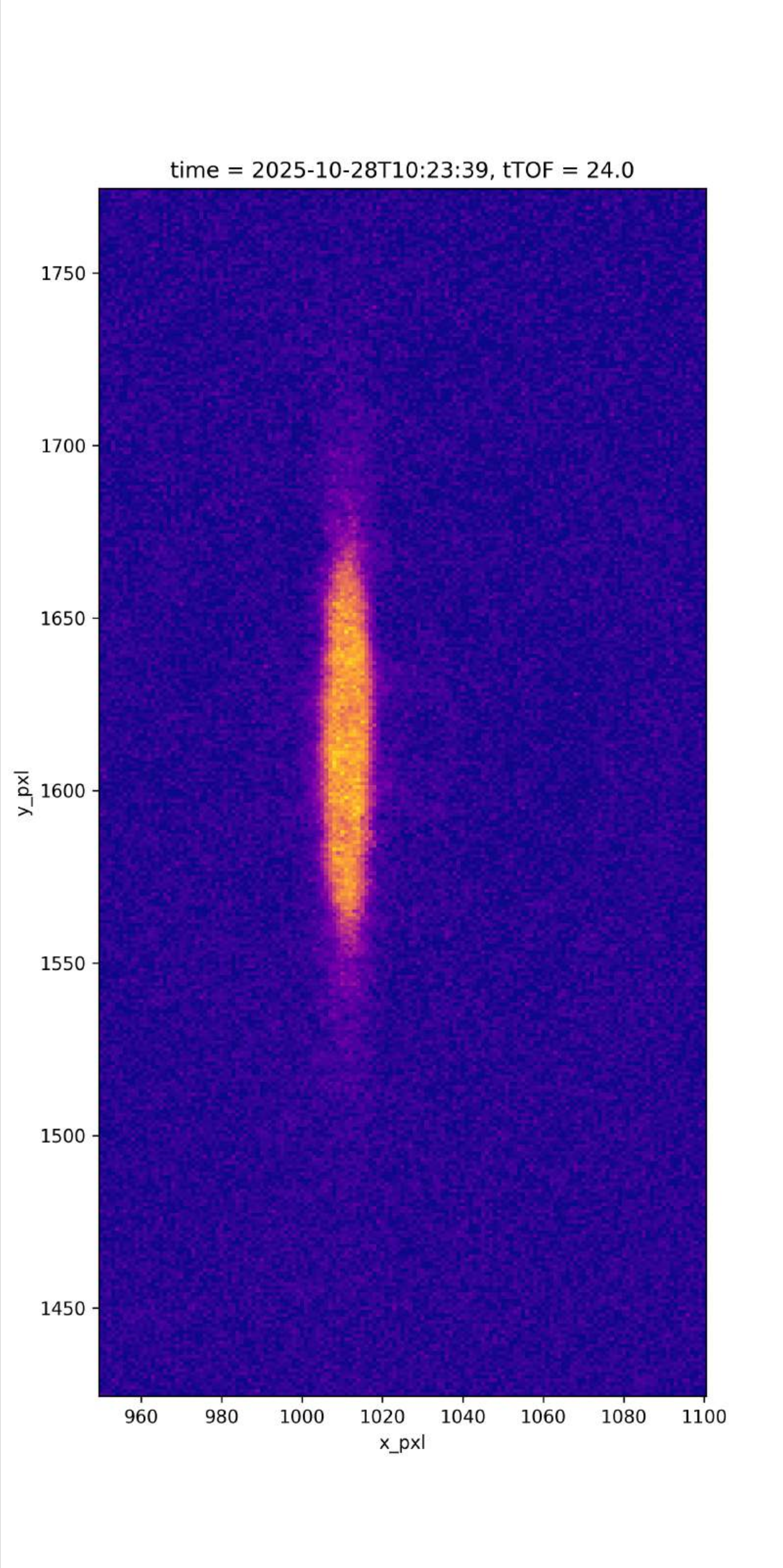

Quantum gas microscope = single-atom resolved fluorescence images (destructive) ***Sherson, et al, Nature 2010***

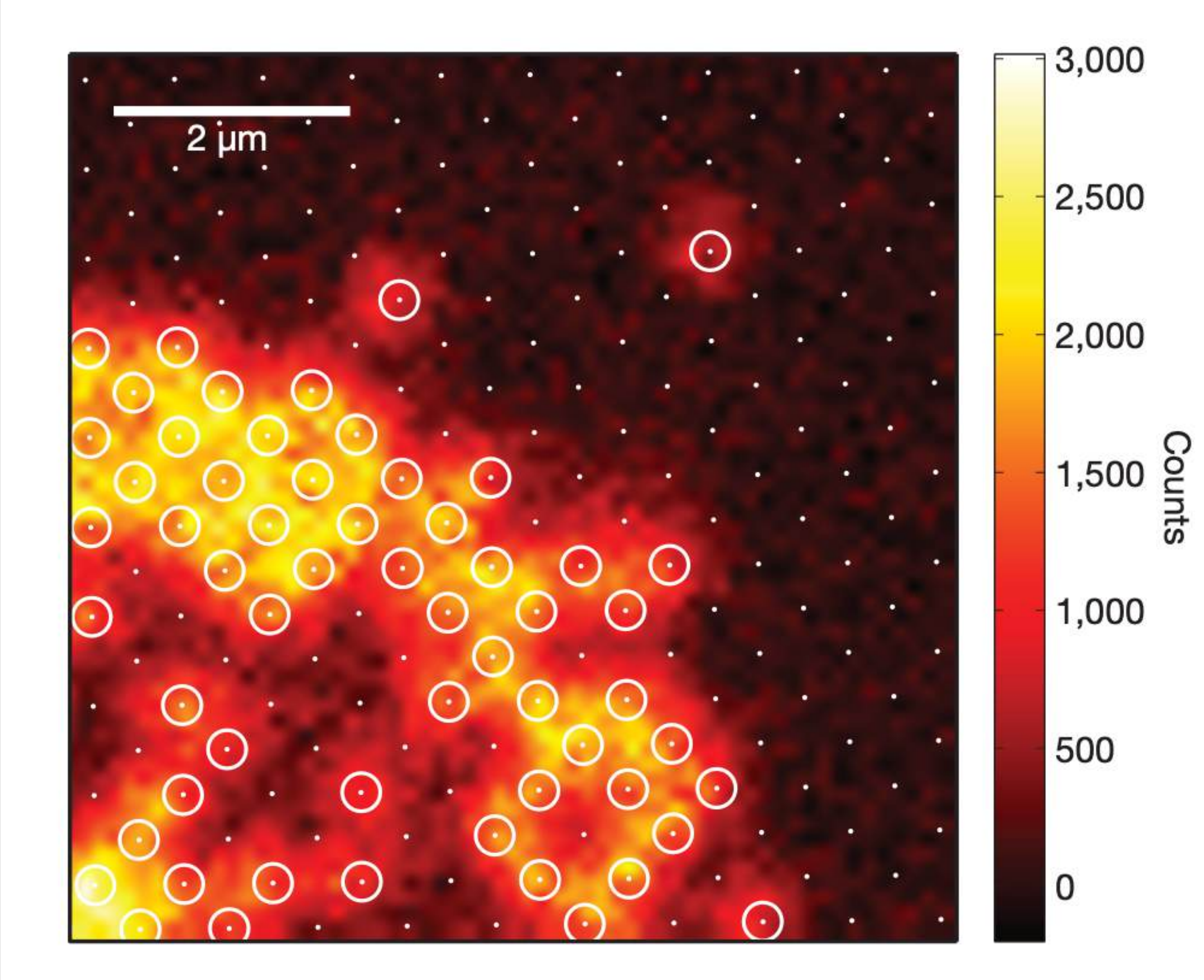

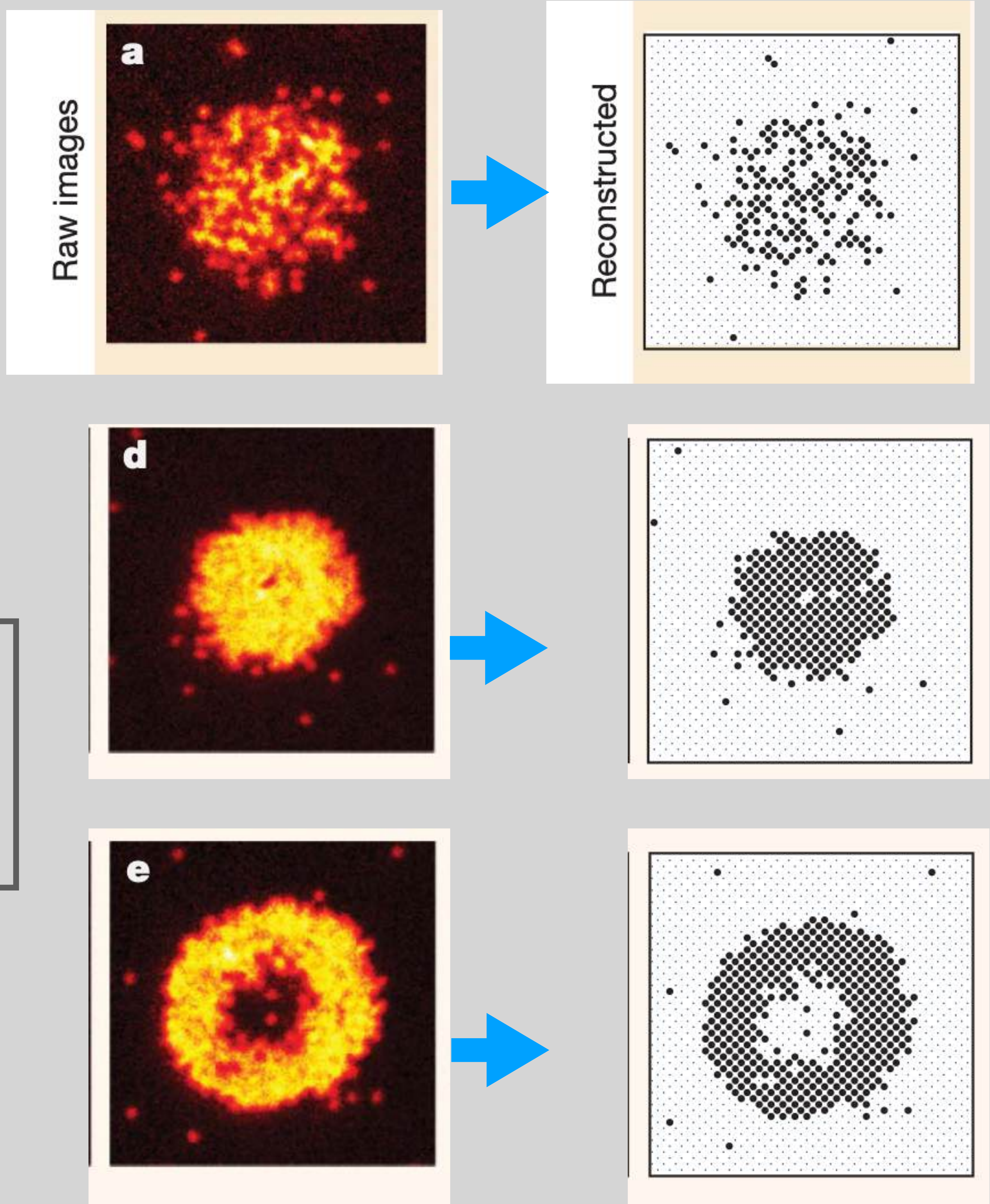

$$a = 532nm, \lambda = 780nm,$$

$$NA = 0.68, d = 700nm(FWHM)$$

Image analysis biased on lattice (needs many photons)

Deep pinning lattice

Cooling light

Recently also for continuous systems, see e.g. *Yao, …, Zwierlein, PRL 2025*

Sampling a wave-function (or a mixed state)

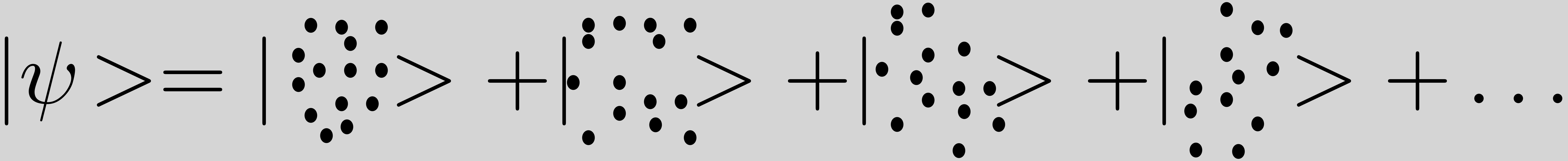

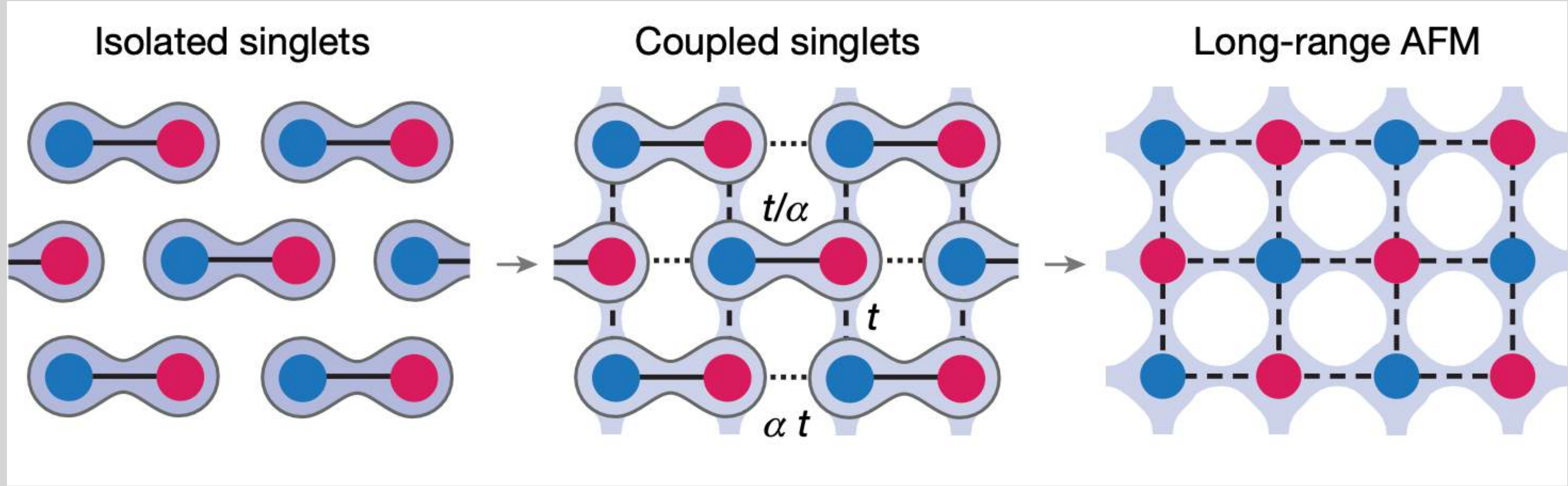

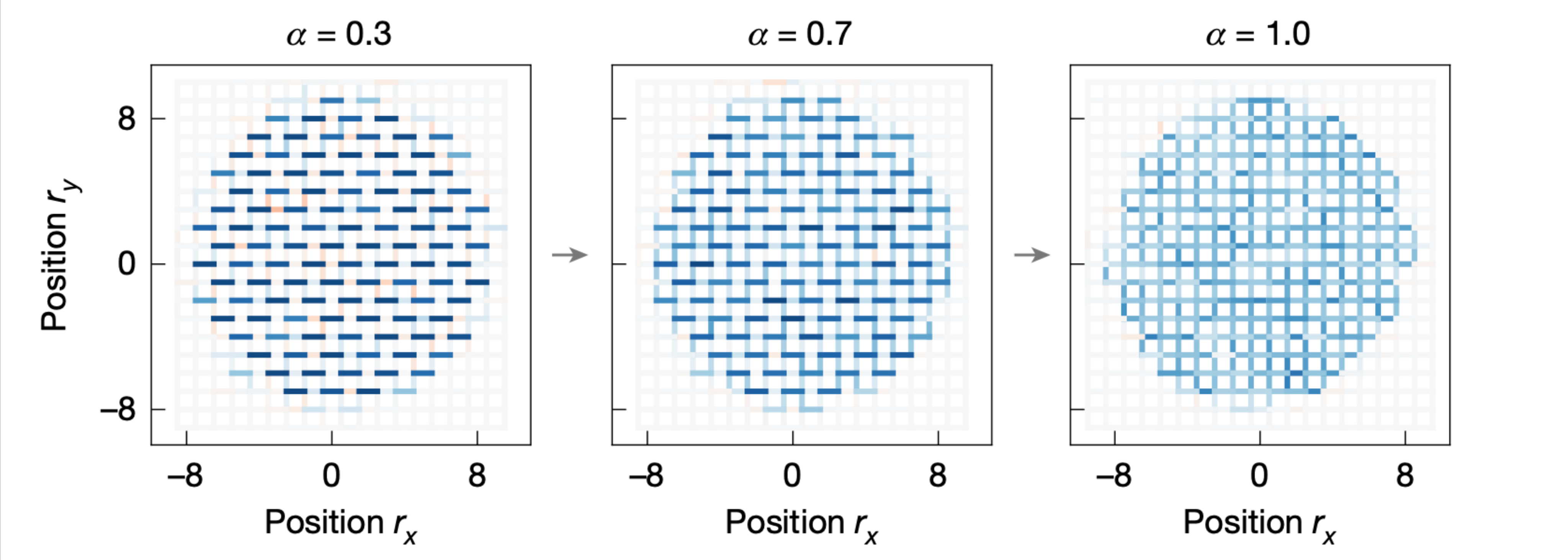

$$C^{zz}_{\vec{r},\vec{d}} \sim < S^z(\vec{r}) S^z(\vec{r}+\vec{d}) > - < S^z(\vec{r}) > < S^z(\vec{r}+\vec{d}) >$$

$$||\vec{d}|| = 1$$

A neutral-atom Hubbard quantum simulator in the cryogenic regime, Xu,..,Greiner, Nature 2025

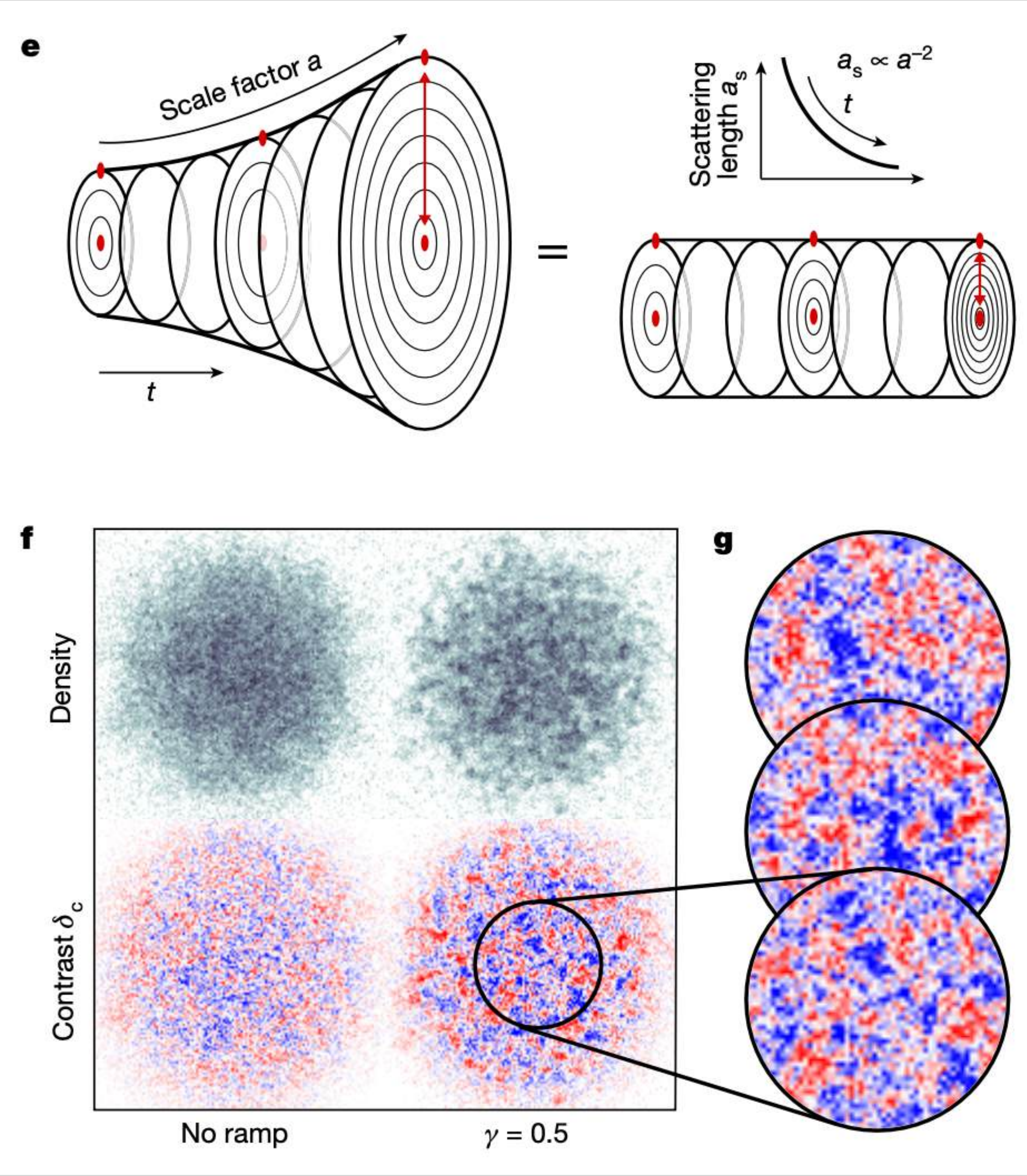

$$\delta_c(x,y) \sim n(x,y) - < n(x,y) >$$

$$< \delta_c(x_1,y_1) \delta(x_2,y_2) >$$

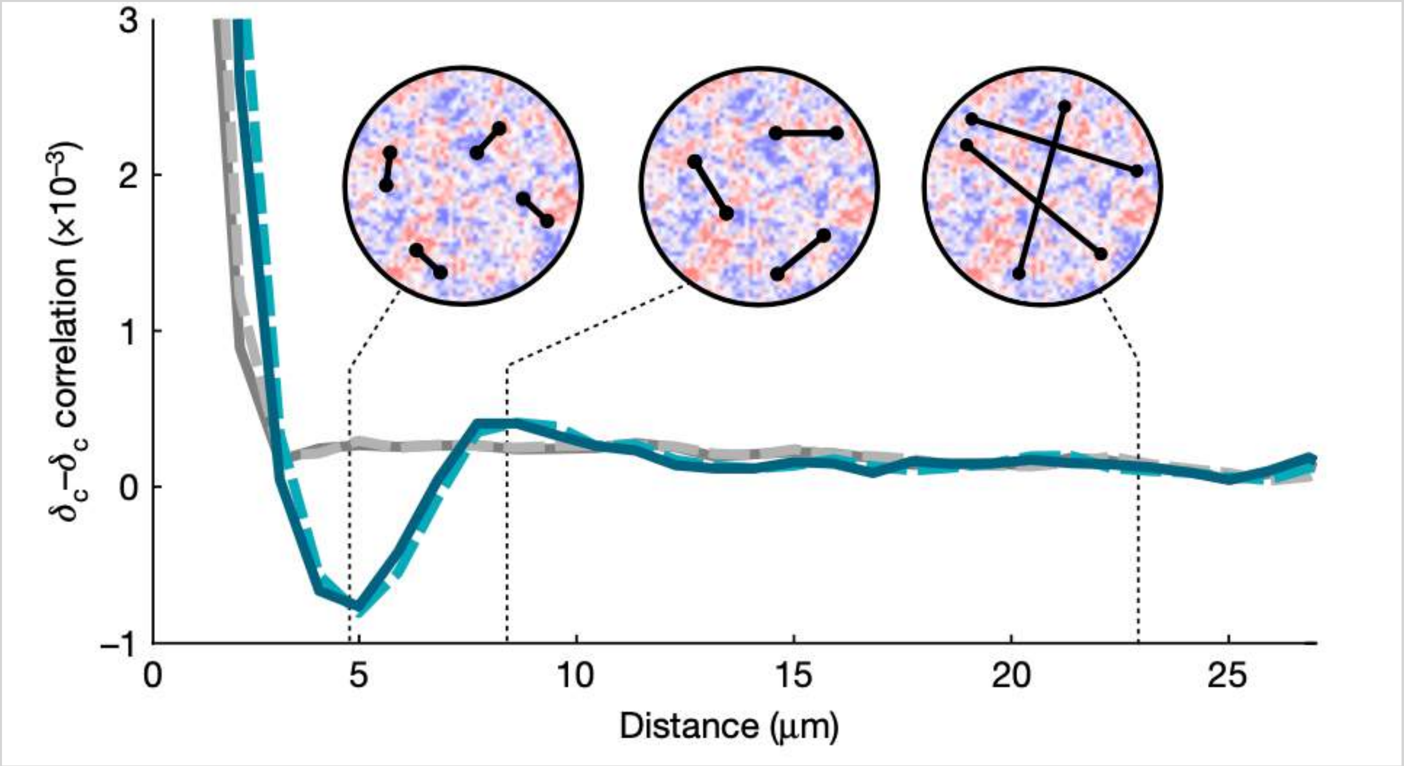

Quantum field simulator for dynamics in curved space-time, Viermann,…,Oberthaler, Nature 2022

Sculpting of a quantum many-body Hamiltonian

$$H_{free} = \int d^3x \ \frac{\hbar^2}{2m} \vec{\nabla}\psi^\dagger_\sigma . \vec{\nabla}\psi_\sigma + V_{\sigma,\sigma'}(\vec{x},t)\psi^\dagger_\sigma \psi_{\sigma'}$$

$$H_{int} = \int d^3x d^3x' U_{\sigma\sigma'}(|x-x'|)\psi^\dagger_\sigma(x)\psi^\dagger_{\sigma'}(x')\psi_\sigma(x)\psi_{\sigma'}(x')$$

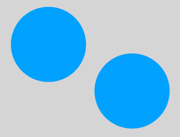

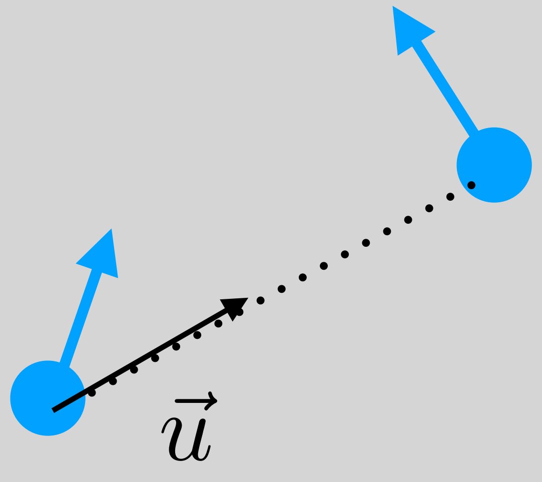

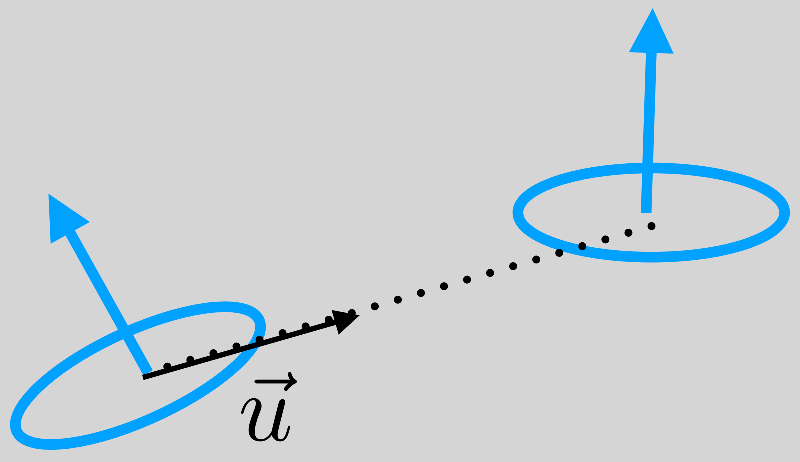

$$U_{\sigma\sigma'} = \delta^3(x-x')\frac{4\pi\hbar^2 a_{\sigma\sigma'}}{m}$$

$$\frac{1}{4\pi\epsilon_0 r^3}(\vec{d}_1.\vec{d}_2 - 3(\vec{d}_1.\vec{u})(\vec{d}_2.\vec{u}))$$

$$\frac{\mu_0}{4\pi r^3}(\vec{\mu}_1.\vec{\mu}_2 - 3(\vec{\mu}_1.\vec{u})(\vec{\mu}_2.\vec{u}))$$

tunable, via Feschbach resonance

$$a_{\sigma\sigma'} = a_{\sigma\sigma' 0}(1 - \frac{\Delta}{B-B_0})$$

VanderWaals in second order:

$$\frac{C_6}{r^6}$$

Lanthanide atoms, e.g. Dy, Yb,Er
(gave rise to supersolidity)

Optical lattice simulations of the Fermi-Hubbard model

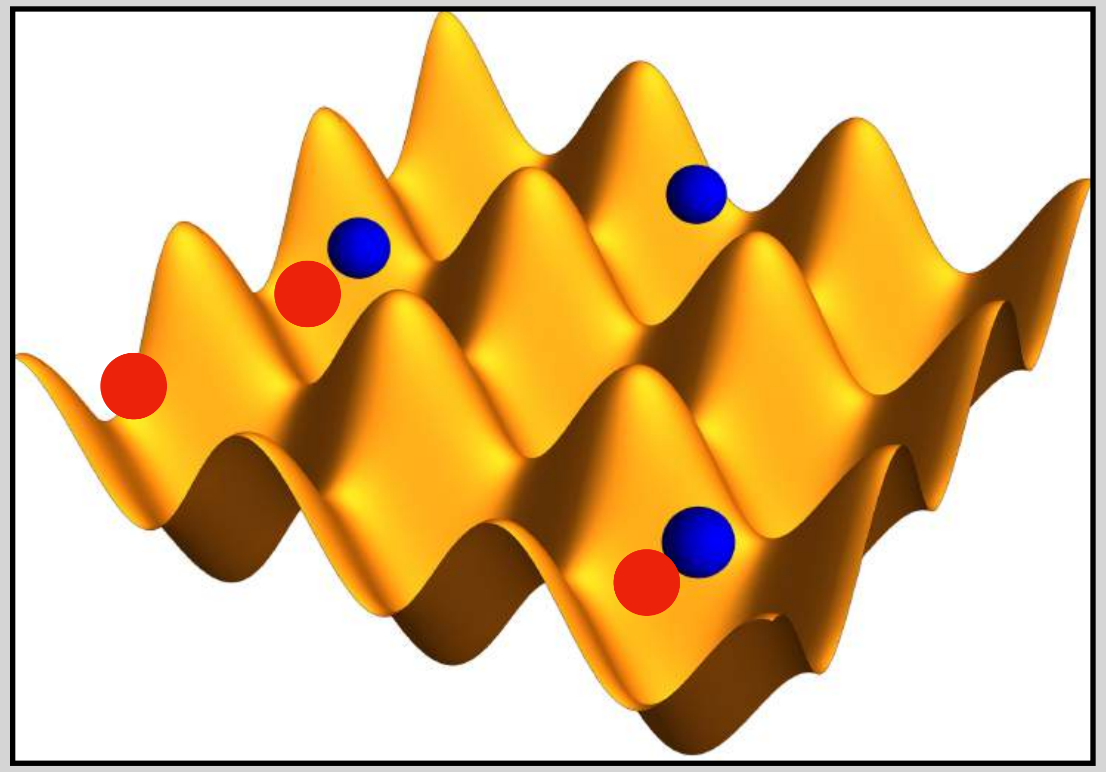

$$V_{\sigma\sigma'}(x) = \delta_{\sigma\sigma'} V_0 \sin^2(kx)$$

$$a = \frac{\pi}{k} = \lambda/2$$

$$H_{free} = \int d^3x \ \frac{\hbar^2}{2m} \vec{\nabla}\psi^\dagger_\sigma . \vec{\nabla}\psi_\sigma + V_{\sigma,\sigma'}(\vec{x},t)\psi^\dagger_\sigma \psi_{\sigma'}$$

$$H_{int} = \int d^3x \ \frac{2\pi\hbar^2 a}{m} \psi^\dagger_\uparrow(x)\psi_\uparrow(x)\psi^\dagger_\downarrow(x)\psi_\downarrow(x)$$

$$V_0 \gg \frac{\hbar^2 k^2}{2m}$$

$$H = -t \sum_{<i,j>,\sigma} c^\dagger_{i,\sigma} c_{j,\sigma} + \sum_i U n_{i\uparrow} n_{i\downarrow}$$

$$t, U \sim kHz$$

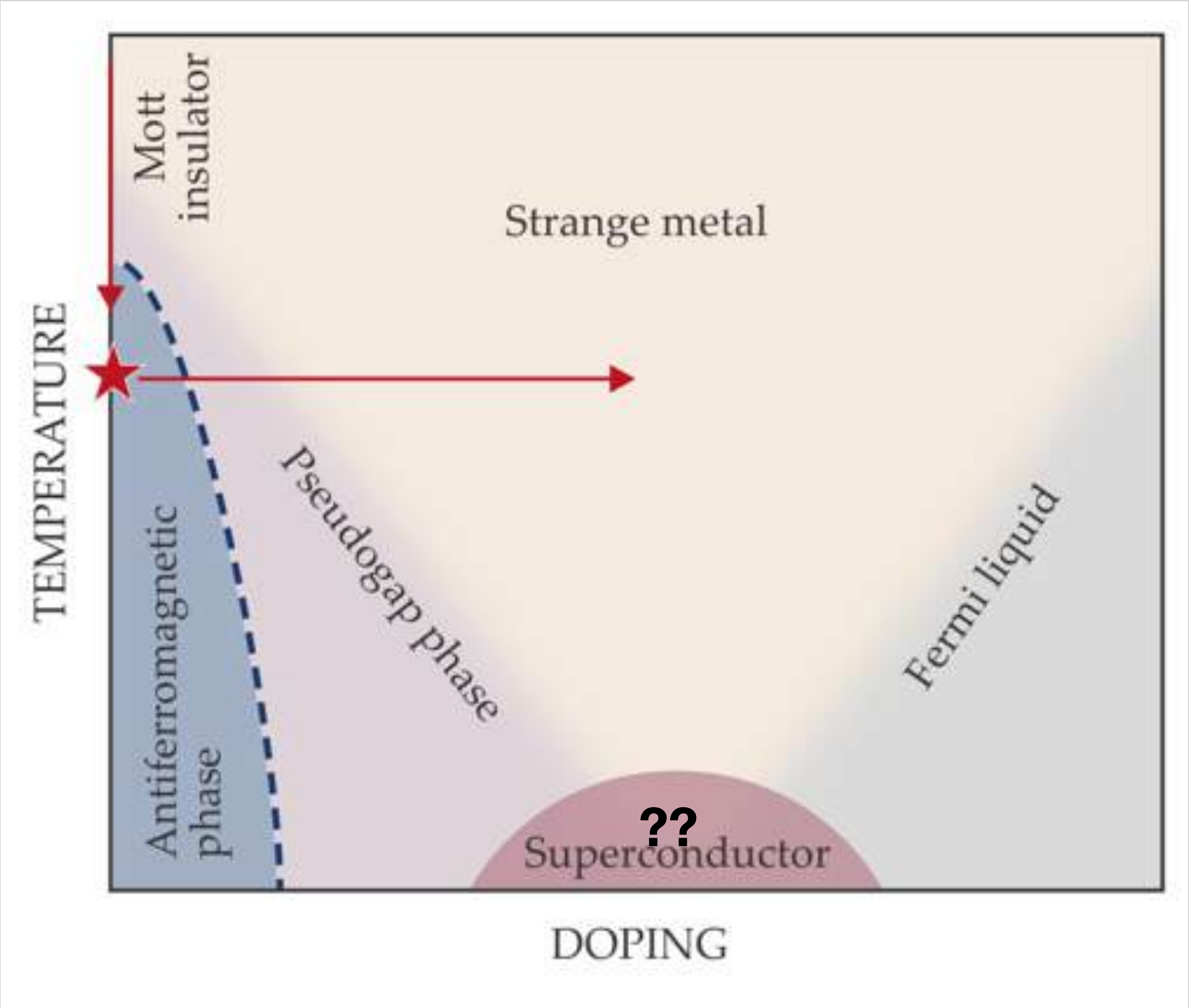

physics Today

$$T/t \approx 0.25 (T_{cuprate} \approx 700K) \rightarrow T/t \approx 0.05$$

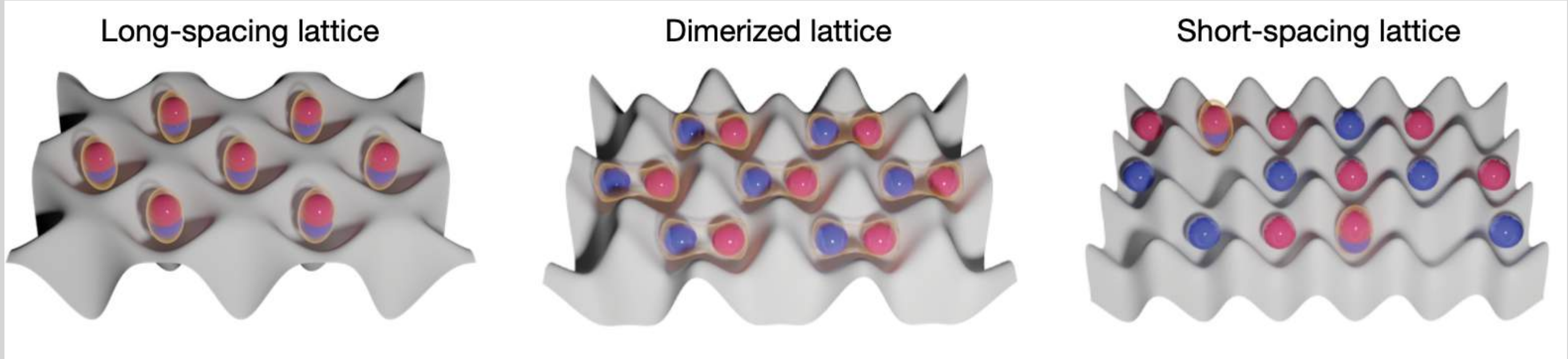

A neutral-atom Hubbard quantum simulator in the cryogenic regime, Xu,..,Greiner, Nature 2025

Rydberg arrays: positions are frozen out, internal degrees of freedom $|g_i>, |r_i>$

Rydberg excitations: atoms on steroids $C_6 \sim n^{11}, \tau \sim n^3, R \sim n^2 \quad <g|\vec{\hat{d}}|r> \sim n^{7/2}$

e.g. for $80S_{1/2}, {}^{87}Rb \quad C_6 = 4THz.\mu m^6, \tau = 200\mu s, R \sim 500nm$

$$H = \sum_i -\Delta |r_i><r_i| + \frac{\Omega}{2}(|r_i><g_i| + |g_i><r_i|) + \sum_{ij} \frac{C_6}{r_{ij}^6} n_i n_j \qquad \Delta, \Omega, \frac{C_6}{r_{ij}^6} \sim MHz(!)$$

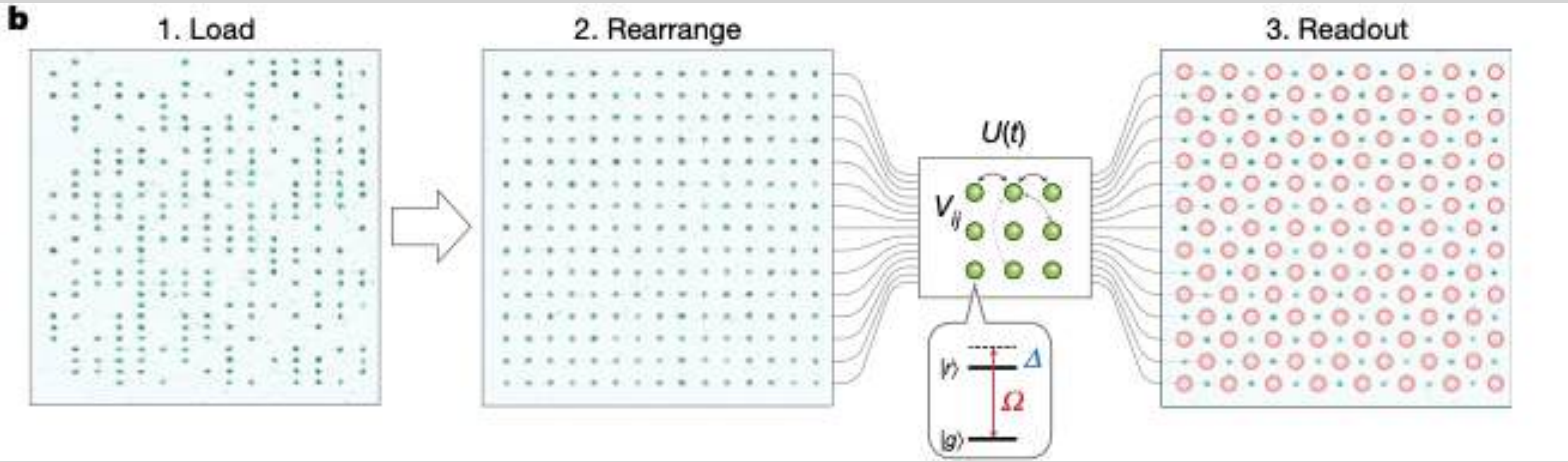

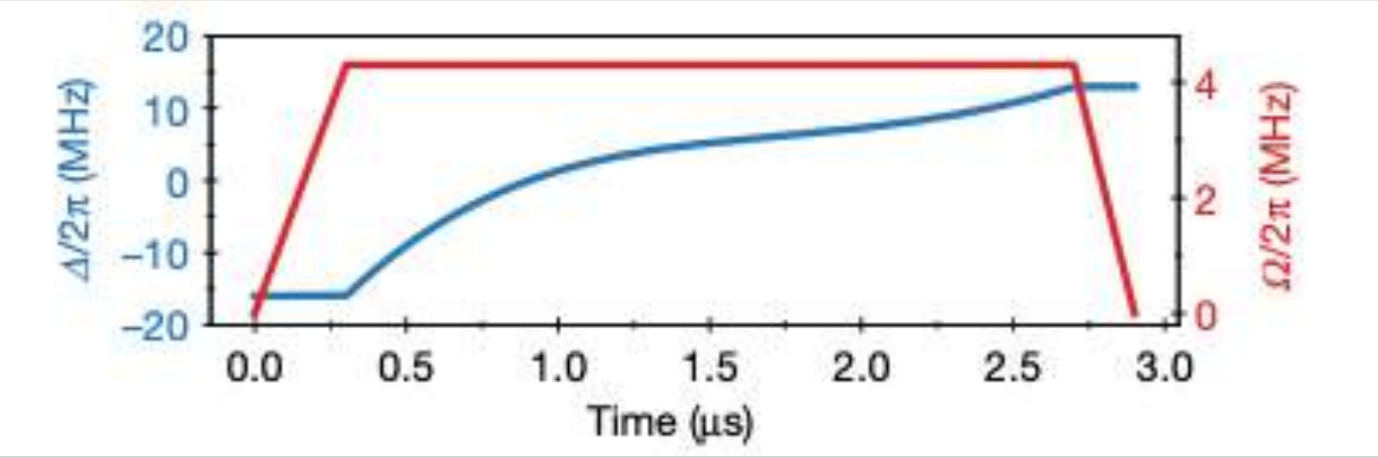

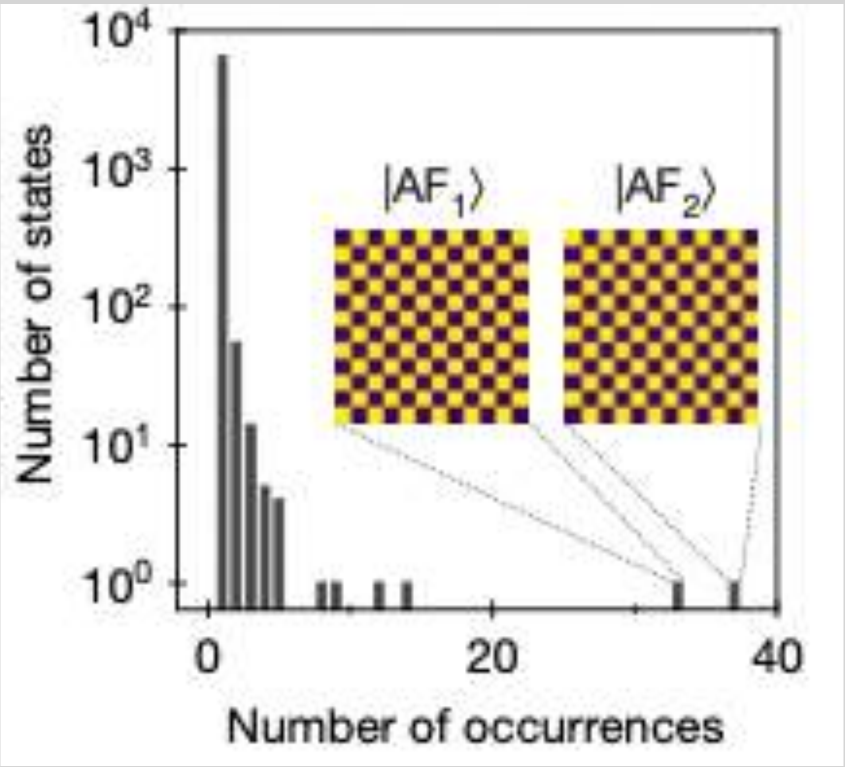

$t \sim 100ms \qquad t \sim \mu s$

Quantum phases of matter on a 256-atom programmable quantum simulator
Ebadi,…,Lukin 2021

Neutral quantum computing

Fast entangling gate via Rydberg Blockade: (Jacksch, *Cirac, Zoller, …, Lukin, PRL 2000)*

$$H = \sum_i \frac{\Omega}{2}(|r_i><g_i| + |g_i><r_i|) + \sum_{ij} \frac{C_6}{r_{ij}^6} n_i n_j \qquad C_6/r_{12}^6 \gg \Omega \quad \rightarrow \quad |g_1 g_2> \leftrightarrow \frac{1}{\sqrt{2}}(|g_1 r_2> + |r_1 g_2>)$$

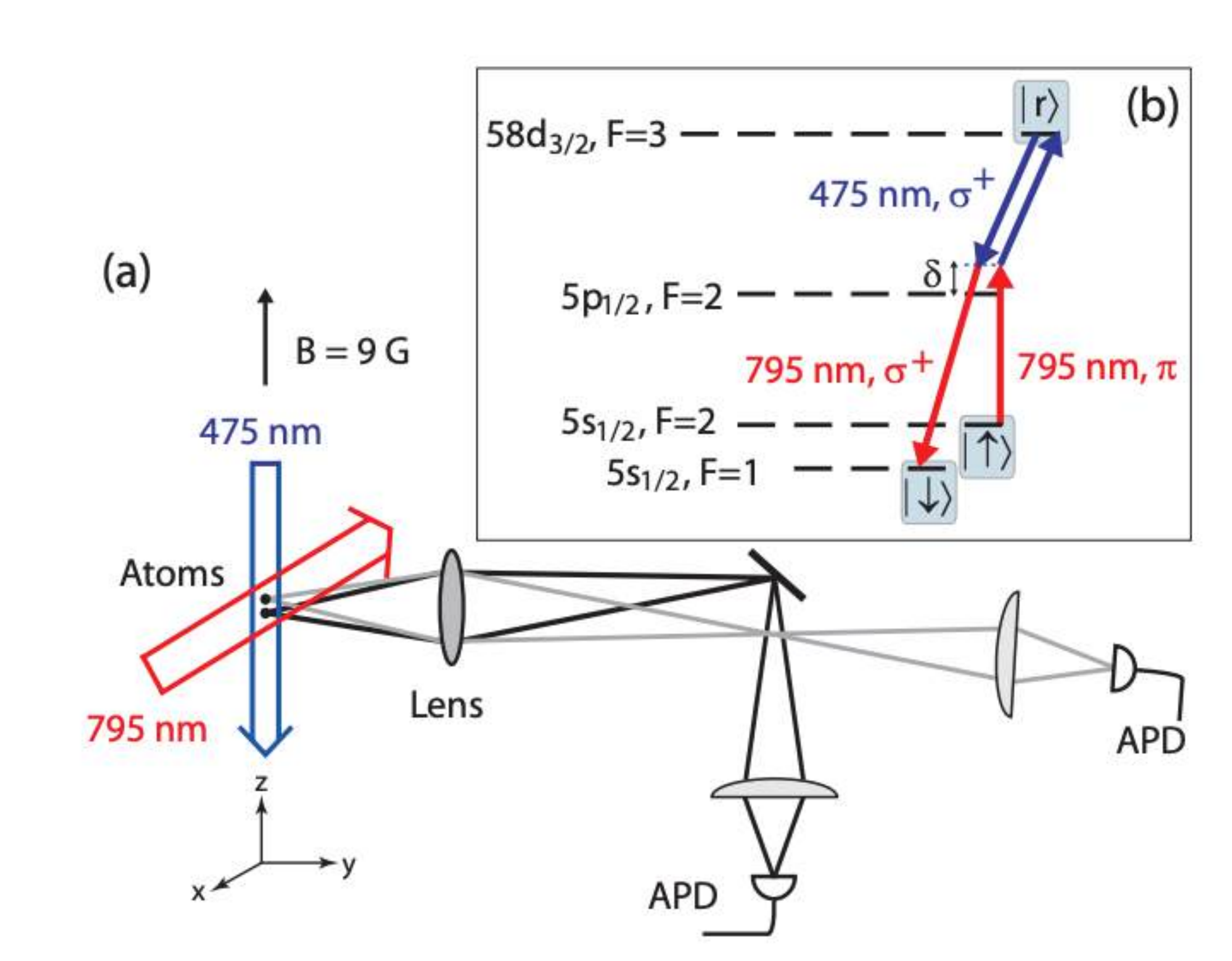

Wilk,… Browaeys, PRL 2010

Also: *Urban,…,Saffman, Nature Physics 2009*

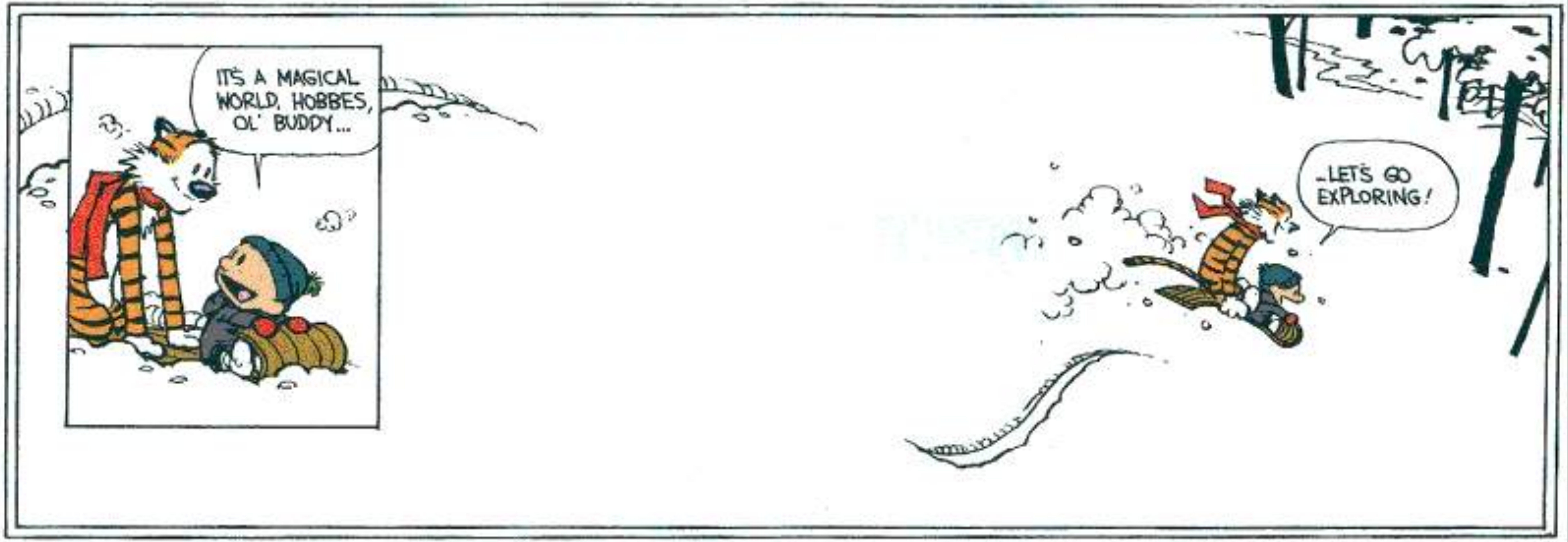
IT'S A MAGICAL WORLD, HOBBES, OL' BUDDY...
...LET'S GO EXPLORING!

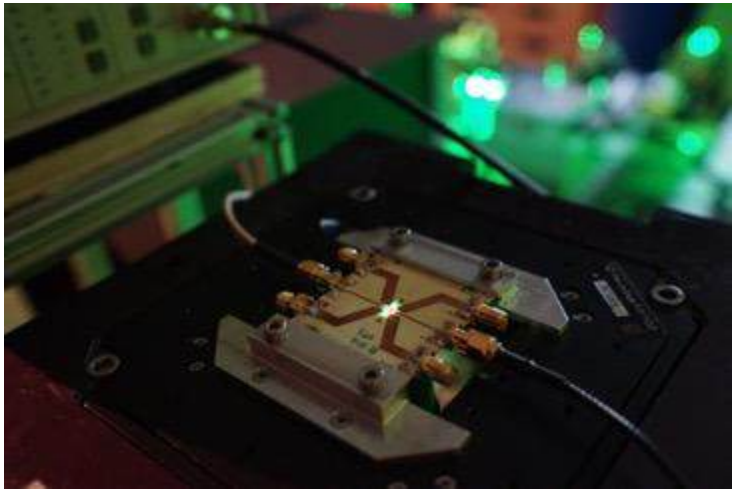

Quantum Sensing
with solid state spins

Milos Nesladek

IMO-IMOMEC

UHASSELT imec

05.11.25 Be-QCI Technology Workshop Leuven

The quantum technology at IMO-IMOMEC / UHasselt

IMEC – **Leuven** (Belgium)

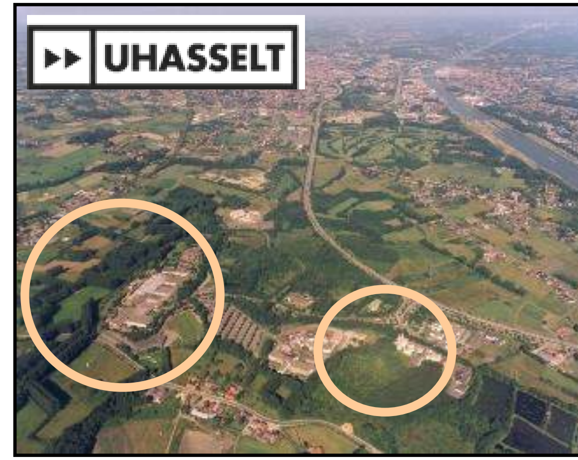

University Hasselt
(Belgium)

Diamond Qubits

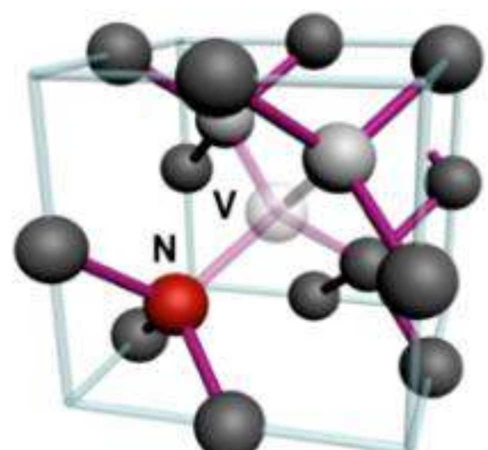

Outline

1. Introduction to quantum sensing principles

2. Solid state spins and NV centre in diamond

3. Magnetometry and QS examples

Motivation

Q. sensors enable using sensing macroscopic and microscopic fields time, temperatures

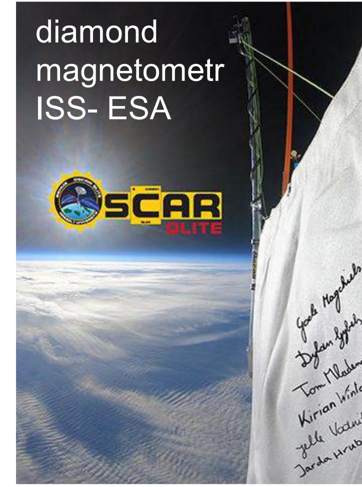

Digging information in atomistic and noisy systems:

- Macroscopic magnetic fields (earth, biomedical, industry)
- Structural analysis of single molecules probed by NMR
- Studying 2D and magnetic materials, exotic phenomena

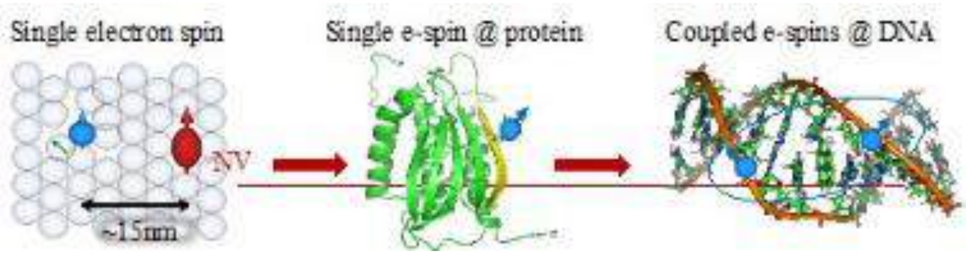

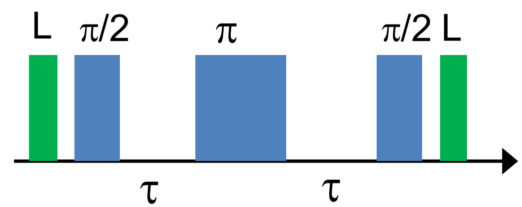

Ramsey interferometry

Electron and Nuclear spins in diamond

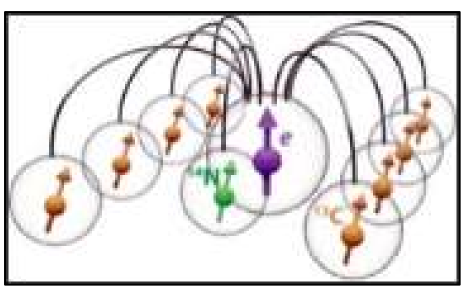

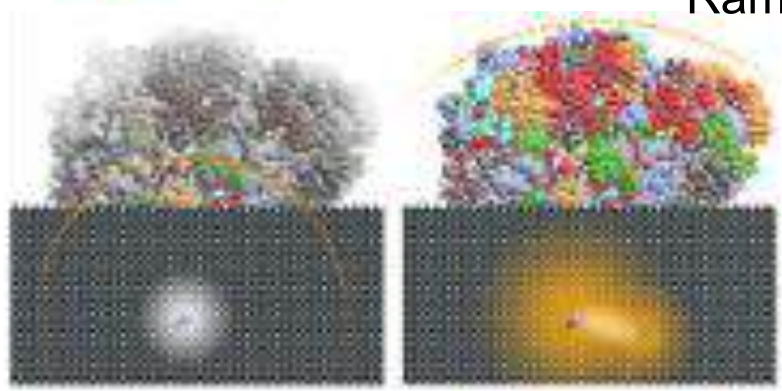

Quantum NMR

Correlated nanoscale quantum sensing

NV – solid state Quantum Sensing on ensambles

M. Huang, Nature Comm., 14, 5259 (2022), T. Staudacher , Science, 339 (2013), A.C. E. Bradley, Phys. Rev. X ***9****, 031045 (2019), F. Shi, Nat. Methods, 15, (2018), I. Lovchinsky, Science, 351, (2016)*

Classical / Quantum ?

Classical sensors rely on *classical physics* to measure quantities like time, magnetic fields, acceleration, or temperature. (e.g., changes in resistance, voltage, or displacement etc).

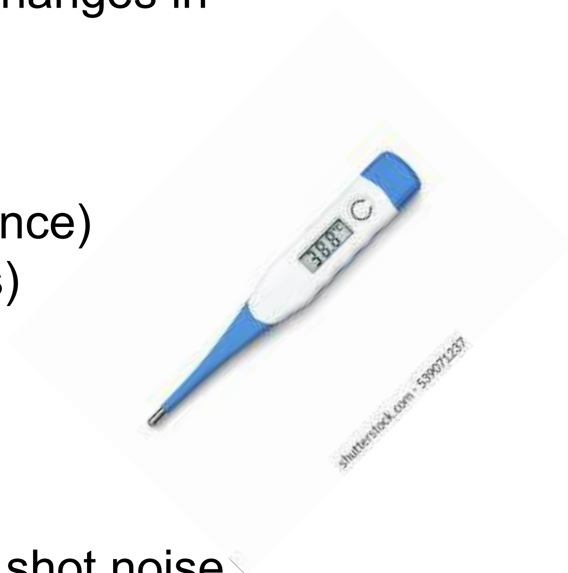

Examples:

- Thermocouples (measure temperature via voltage difference)
- Accelerometers (measure acceleration via Newton's laws)
- Photodiodes
- Optical interferometers (use classical light waves)

Characteristics:

- **Noise limited by classical sources**, e.g., thermal noise, shot noise.
- **Measurement precision** scales as **$1/N^{1/2}$, where N** is the number of measurements or particles (the **standard quantum limit**).
- **No quantum coherence or entanglement** is used — each particle (like a photon) acts independently.

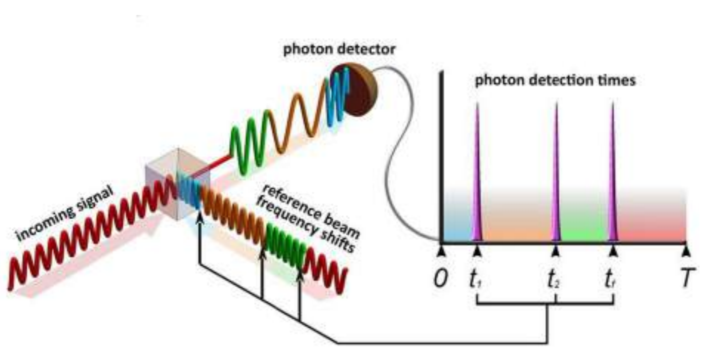

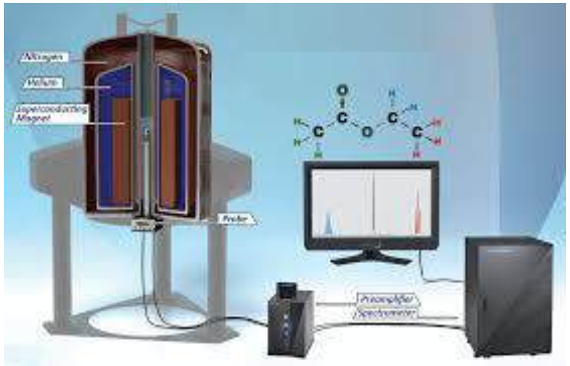

Quantum

Quantum sensors use quantum properties of matter or light — such as superposition, entanglement, or quantum squeezing — to achieve better sensitivity or new kinds of measurements that classical sensors can't.

Examples:
Atomic clocks (use quantum superposition of atomic energy levels)
NV-center diamond magnetometers (use electron spin states)
Quantum gravimeters (use atom interferometry)
Squeezed-light interferometers (used in LIGO to detect gravitational waves)

Characteristics:
Exploit quantum coherence and entanglement to enhance measurement precision.
Can surpass the standard quantum limit — approaching the Heisenberg limit (1/N scaling).
Extremely sensitive to environmental noise, requiring isolation and control.
Measurement of quantities that are classically inaccessible (single spin detection).

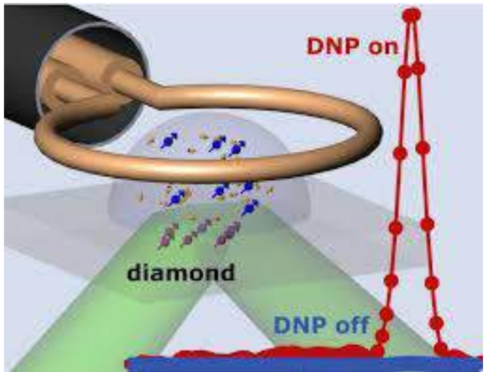

Principles

Two-level spin/photon system:

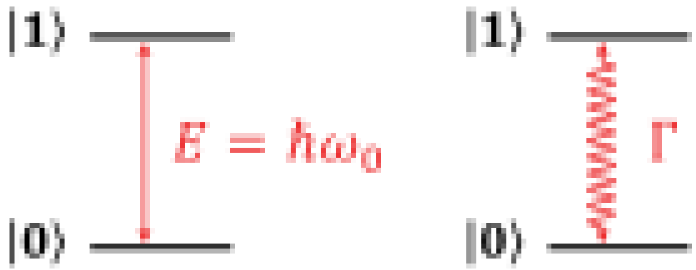

C. Degen, Rv. Mod. Phys 2017

FIG. 1. Basic features of a two-state quantum system. $|0\rangle$ is the lower energy state and $|1\rangle$ is the higher energy state. Quantum sensing exploits changes in the transition frequency ω_0 or the transition rate Γ in response to an external signal V.

in quantum system we measure difference in energy, rate and occupation

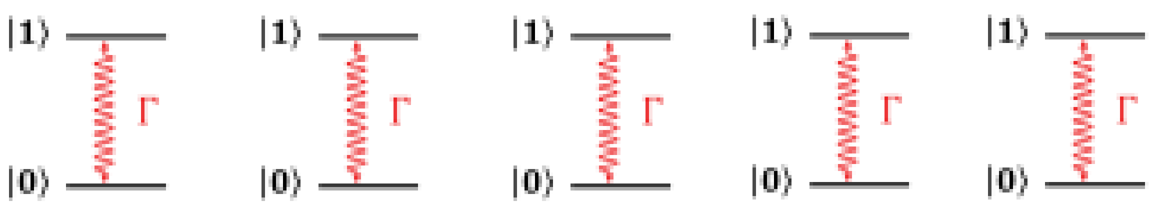

$1/\sqrt{N}$ q.limit, coherence

Sensitivity

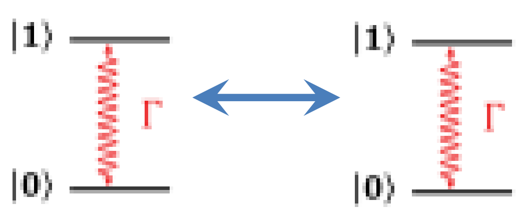

1/N Heissenberg limit Entanglement

Principles

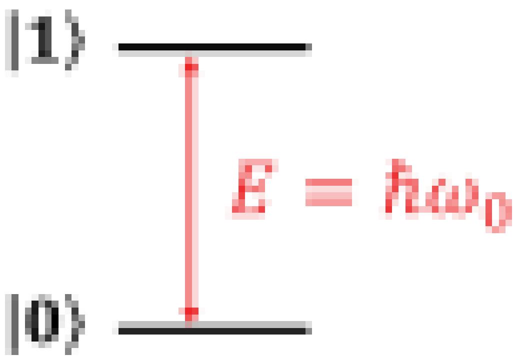

$$\hat{H}\psi(\mathbf{r}) = E\psi(\mathbf{r})$$

$$\hat{H}(t) = \hat{H}_0 + \hat{H}_V(t) + \hat{H}_{\mathrm{control}}(t), \qquad (2)$$

where $\hat{H}_0$ is the internal Hamiltonian, $\hat{H}_V(t)$ is the Hamiltonian associated with a signal $V(t)$, and $\hat{H}_{\mathrm{control}}(t)$ is the control Hamiltonian. We assume that $\hat{H}_0$ is known and that $\hat{H}_{\mathrm{control}}(t)$ can be deliberately chosen so as to manipulate or tune the sensor in a controlled way. The goal of a quantum sensing experiment is then to infer $V(t)$ from the effect it has on the qubit via its Hamiltonian $\hat{H}_V(t)$, usually by a clever choice of $\hat{H}_{\mathrm{control}}(t)$.

Quantum Sensing :

Developing Quantum Algorithm for $H_{control}$ to achieve H_V

Atomic Clocks (Alkali Metals)

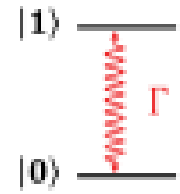

- New standarts in measurement of time and frequency. (10^{-18} second, Quartz 10^{-4})

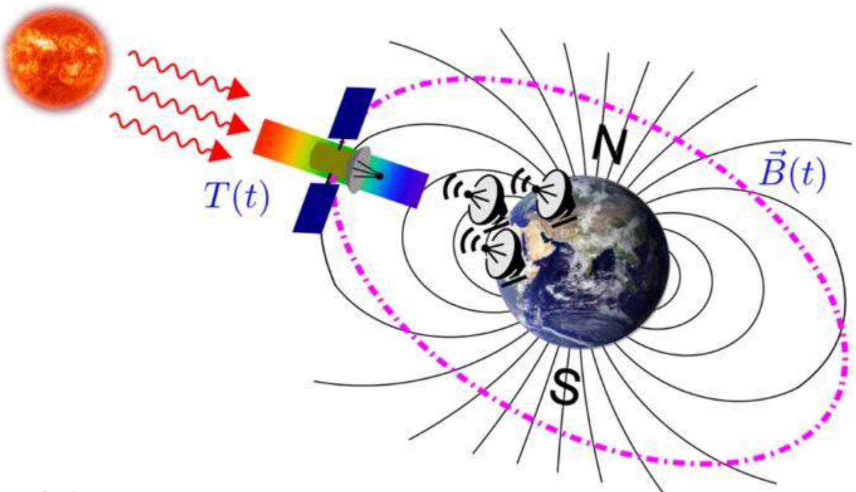

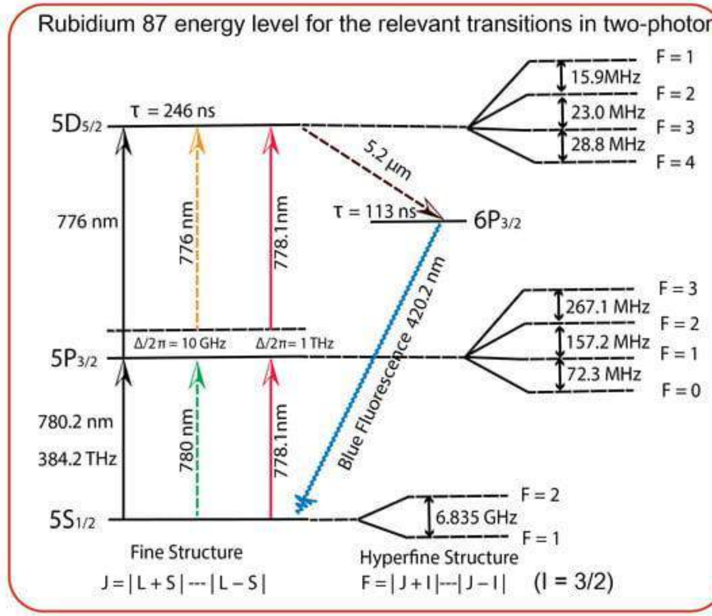

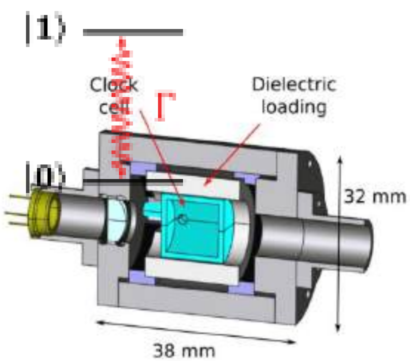

(a)

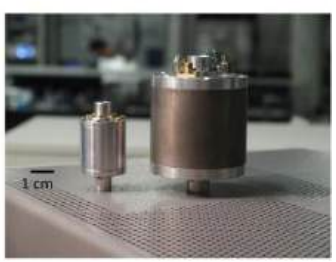

(b)

Rb atomic vapour Cell

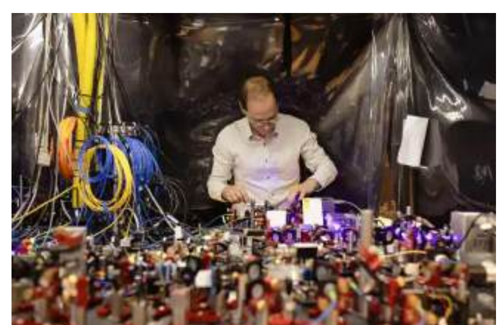

Amsterdam Uni, *AQuRA*

Limits

Coherence vs. Entanglement - enhanced sensing – N particles

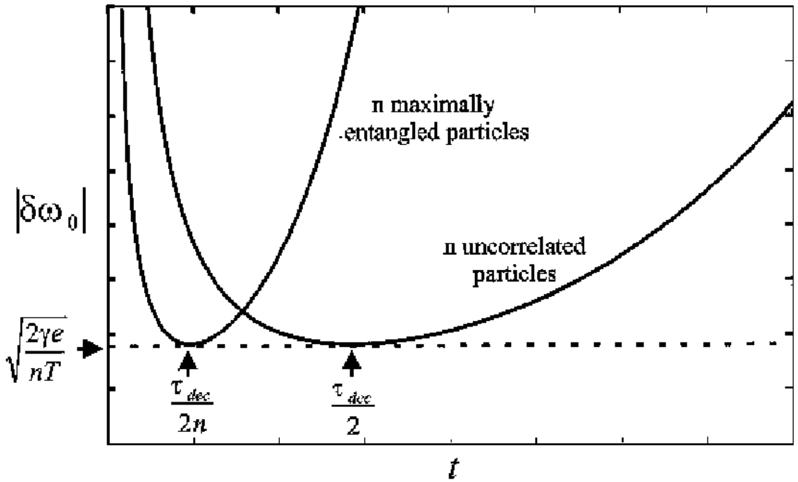

S.F. Huelga et al, PRL, 79, (1997)

S ~ $N^{1/2}$ - Heisenberg Limit ~ N

How close can we approach the Heisenberg limit in atomistic - noisy systems ?

Supressing decoherence is the key for entanglement enhanced sensitivity

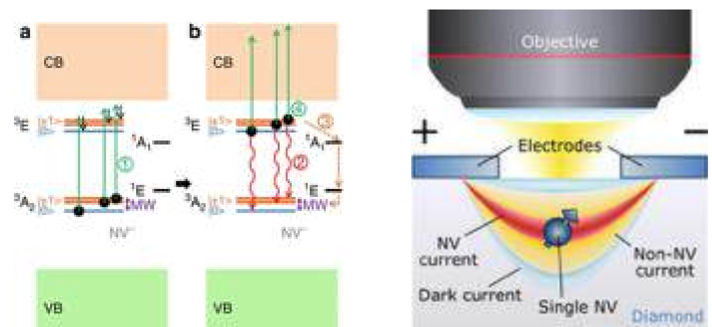

P-Siyushev et al, Science 363, 728–731 (2019)
M Gulka et al, 12, Nature Comm (2021)

imec/UHasselt
Spin Readout Techniques

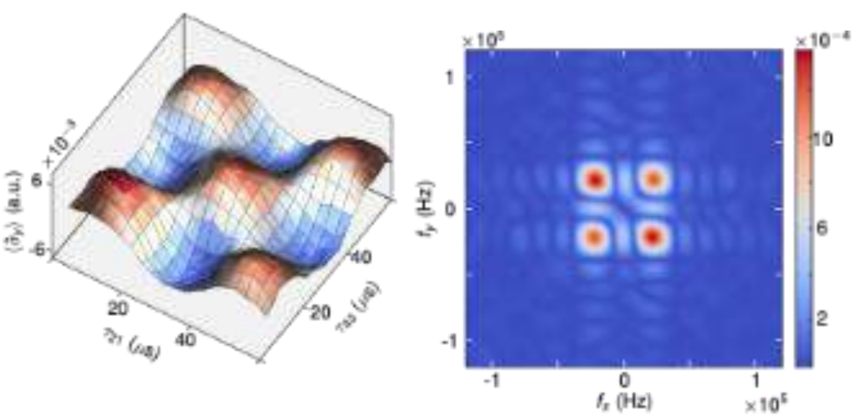

Quantum particle sensing, Wu et al , PRL, 123.050603, (2019)

Nitrogen-Vacancy (NV) center: **Quantum Probe**

- Optical Detection Magnetic Resonance (ODMR)

Readout protocol

- Optical **initialization** into m_s = 0
- MW **spin manipulation**
- Optical **readout**

C^3V

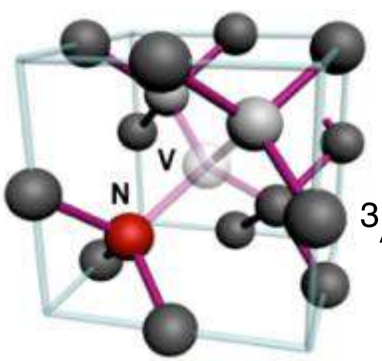

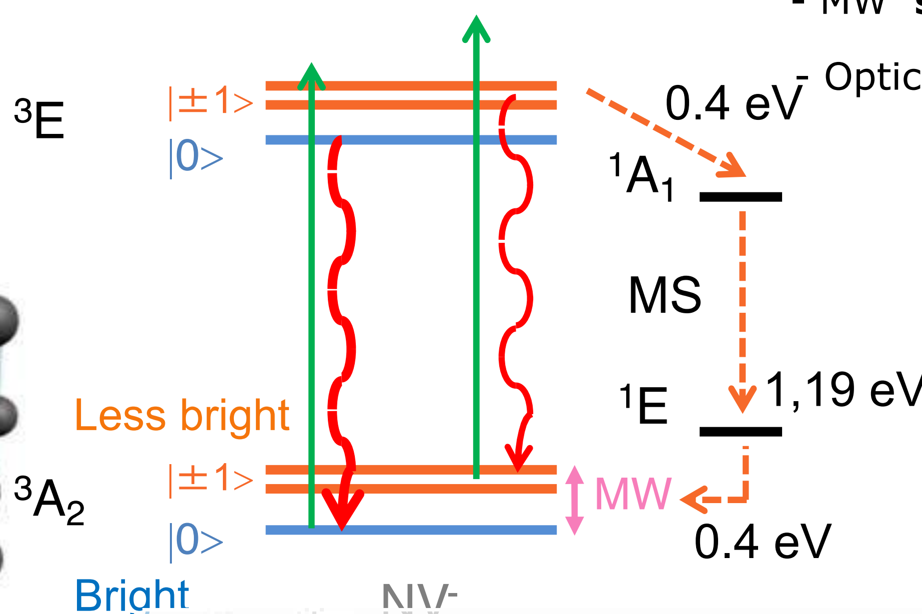

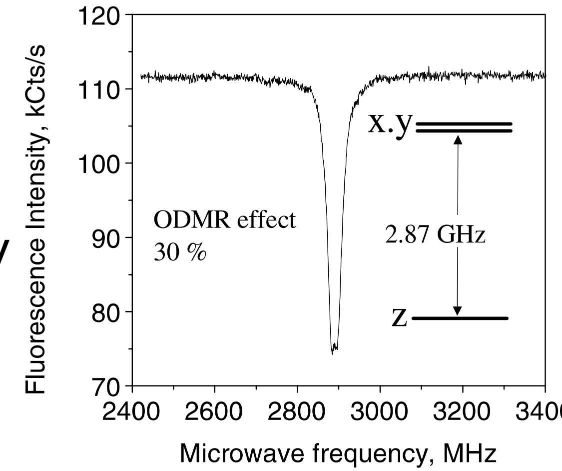

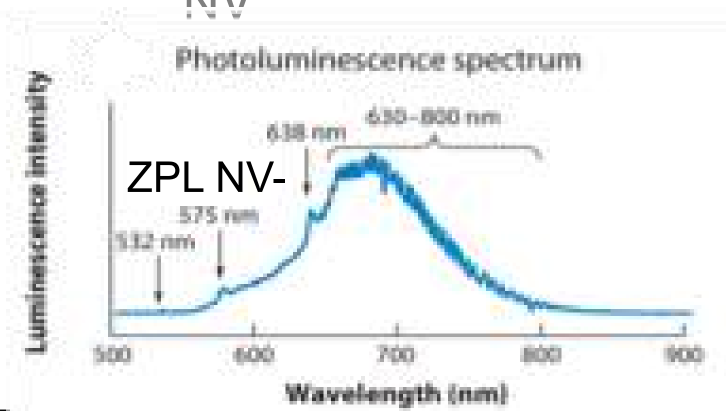

Room temperature
coherence ~2 msec

Jelezko, Wrachtrup, PSS A,2004; Nizovtsev, Optical Spectroscopy,2003,

e-NV and ^{14}N spin energy sublevels

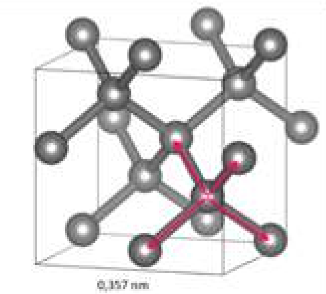

$$H = 2\pi\hbar(DS_z^2 + \gamma_e B_o S_z + PI_z^2 + \gamma_e B_o I_z + AS_z I_z)$$

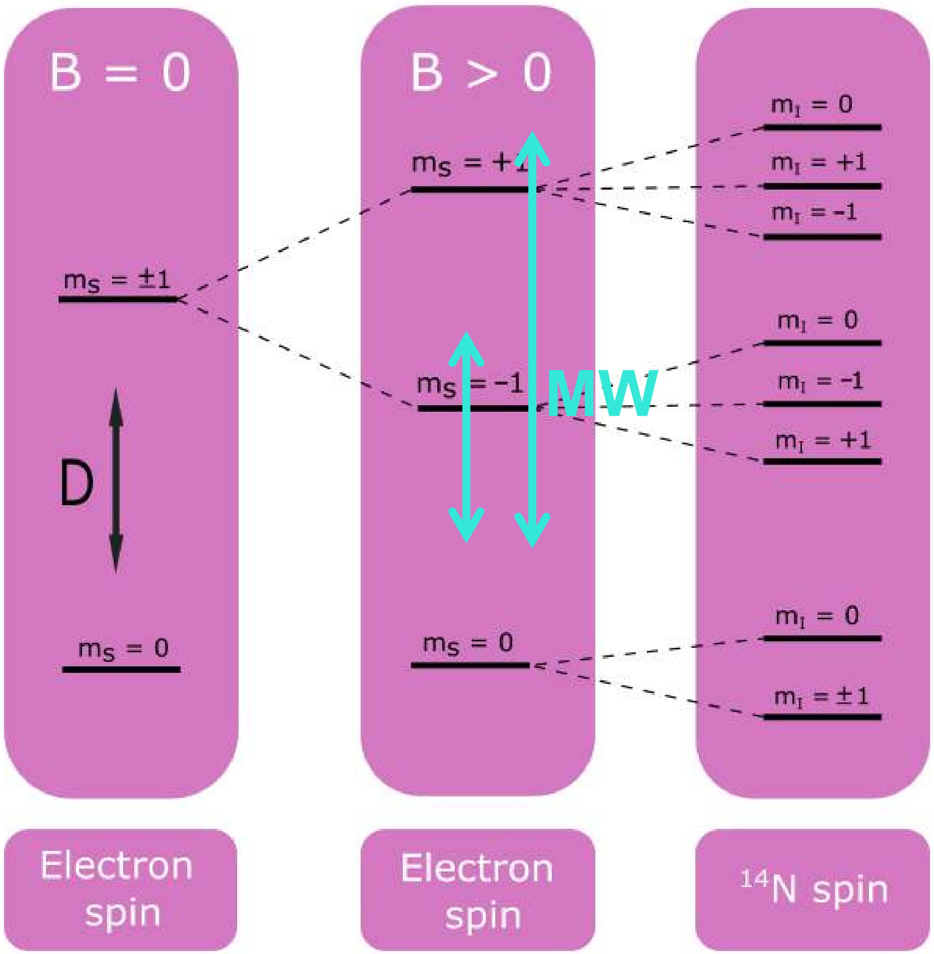

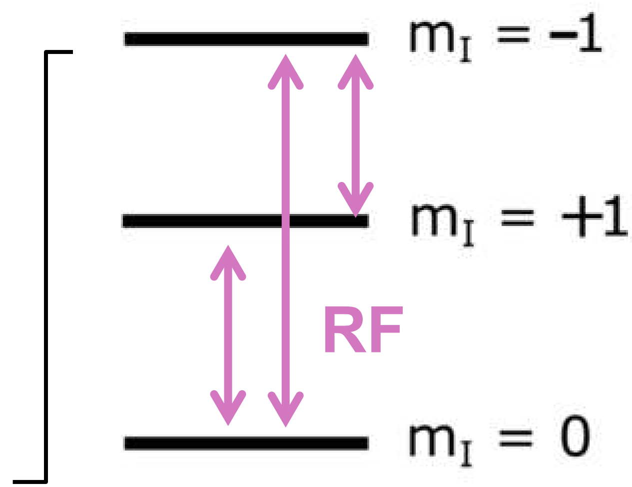

abundancy

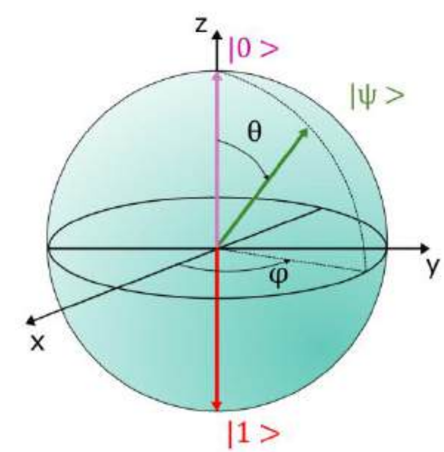

How we measure Field, Temperature..?

- quantum information science
- computing
- sensing and metrology

- *In the centre: precision and fidelity of NV electron and nuclear spin readout gates*

- Scalability and “Hot” Temperatures

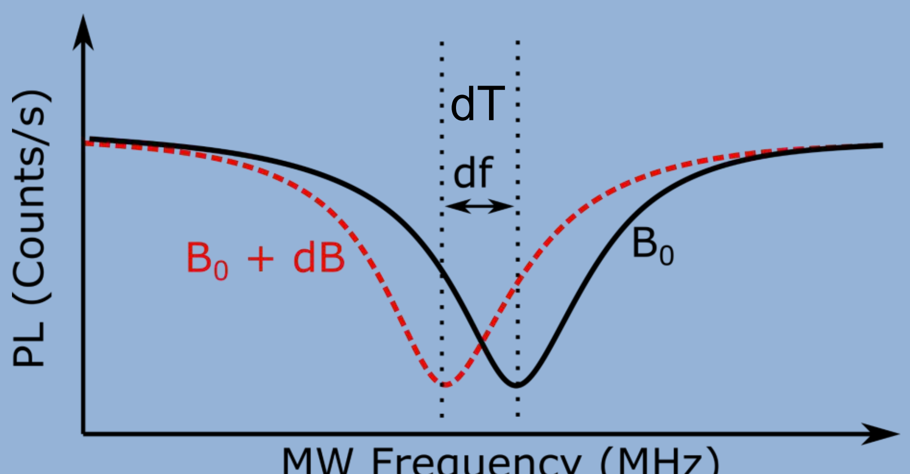

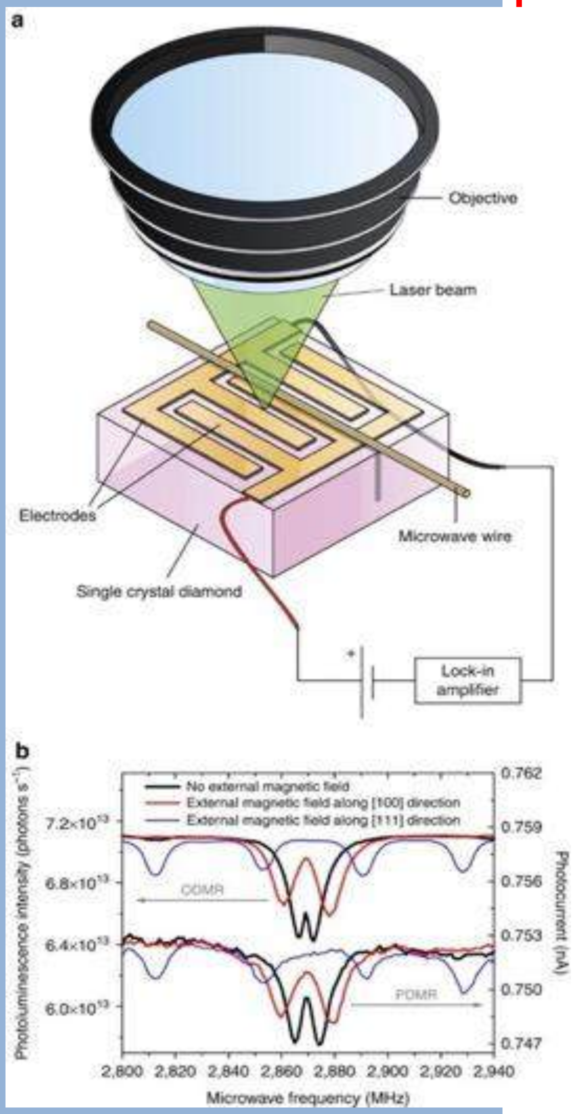

IMO-IMOMEC UHASSELT imec

E. Bourgeois et al, Nat. Comm. 6, 2015

Material Optimisation: Single NV and NV ensambles

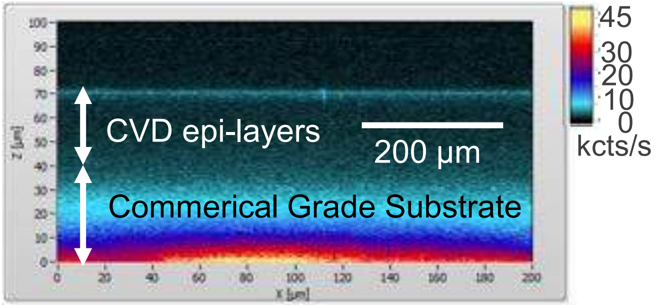

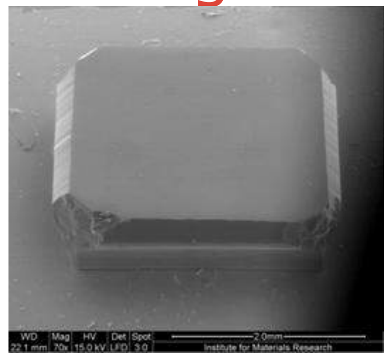

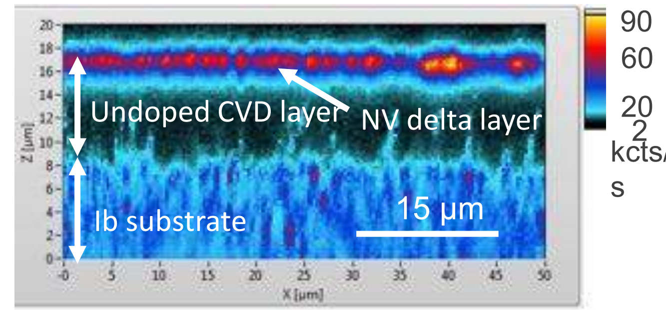

Objective NA: 0.95,
Green light power: 1 mW, Filter: LP650

Epitaxial layers with very low PL background < 500 kcts/s under 1mW

N-delta doped layer < 5nm

N- doping from 0,1 ppb – 50 ppm

Purity < 10^{13} cm^{-3}, close to ultrapure Ge

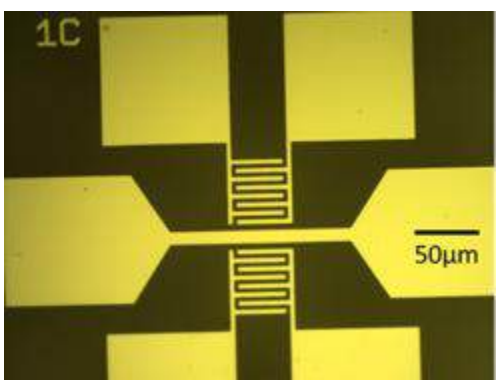

Litographic contacts

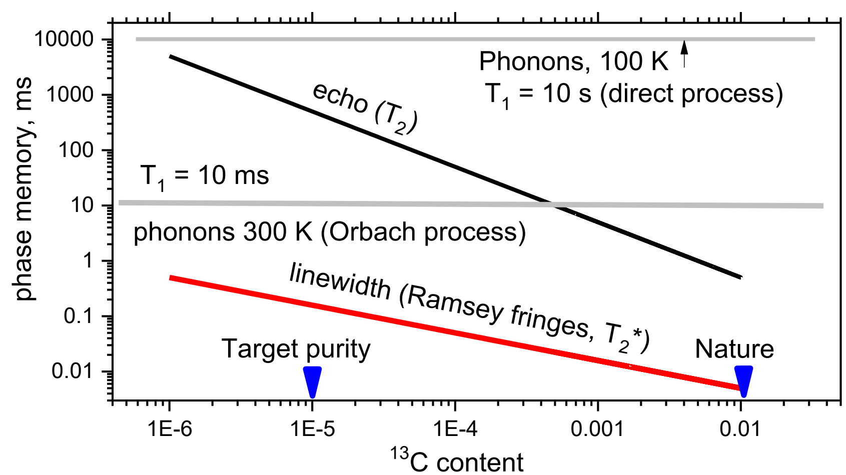

IMO-IMOMEC
UHASSELT
imec

Optimisation of NV ensembles

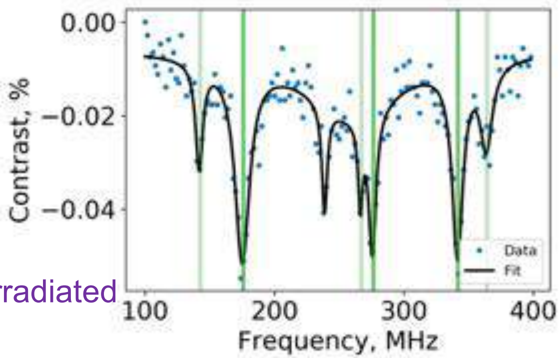

irradiated

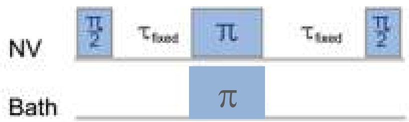

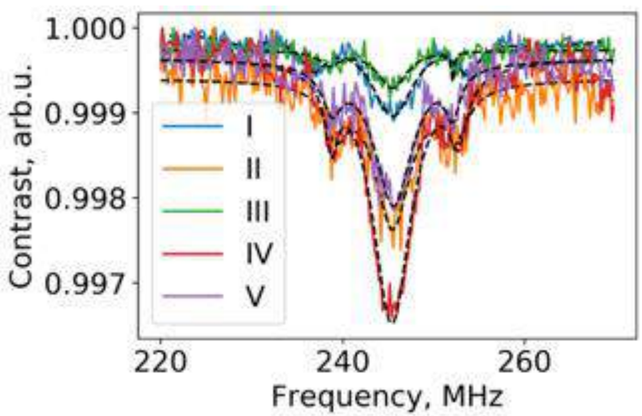

Figure 2. Zoom of the DEER spectrum at Fig.1 around extra peaks. I – V means different points on a diamond.

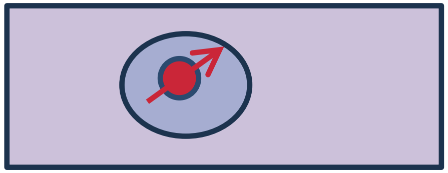

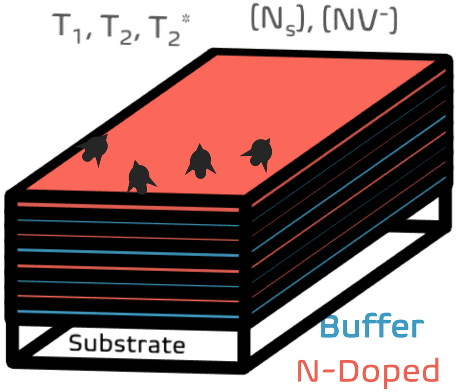

DEER
Control by Double Electron-Electron resonance

# LAYER	T1	T2	T2*	[N]	[NV]
2	4100 ms	26 us	0.6 us	6.3 ppm	35 ppb
3	4600 ms	52 us	0.9 us	3.2 ppm	22 ppb
4	4200 ms	150 us	0.5 us	1.1 ppm	7 ppb

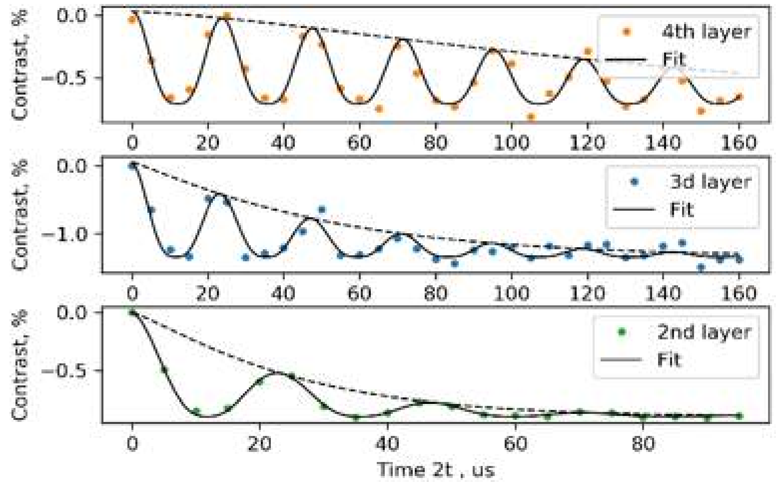

As grown

150 µs

52 µs

26 µs

NV qubit pairs – towards correlated sensing

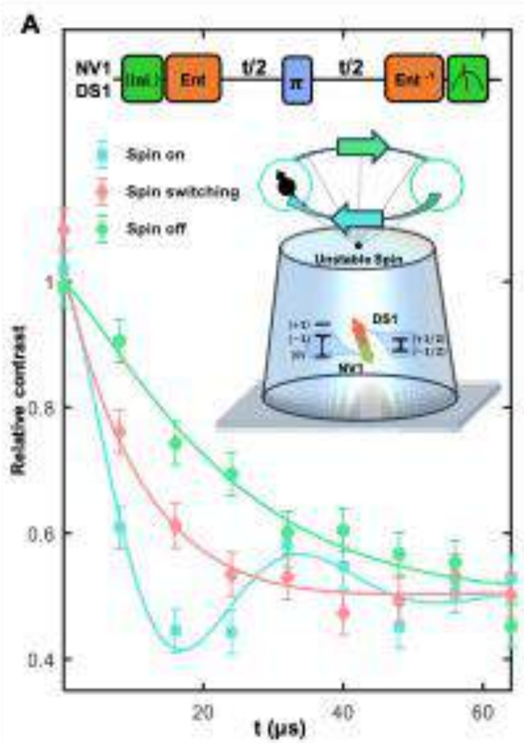

Xu Zhou, Nature 202

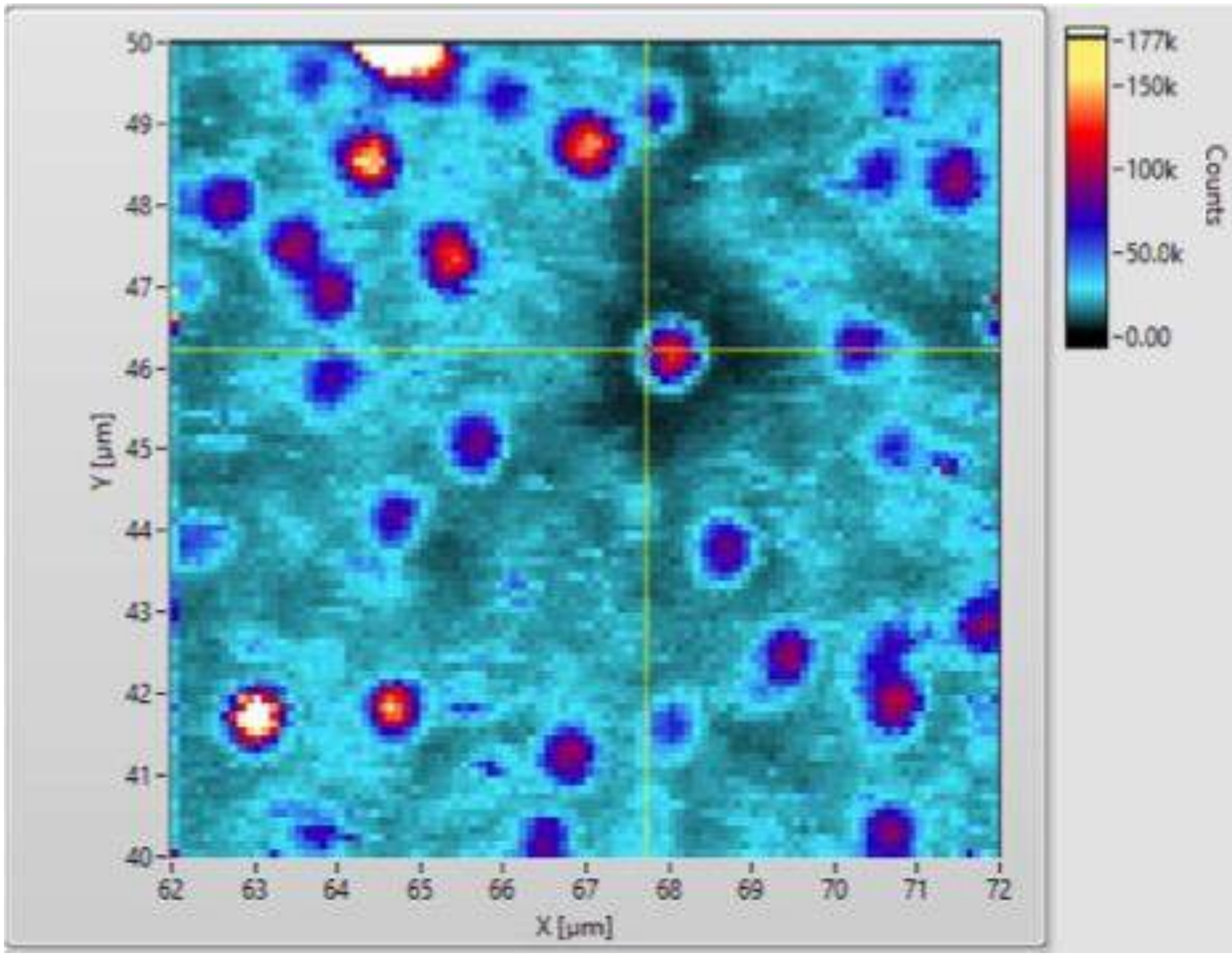

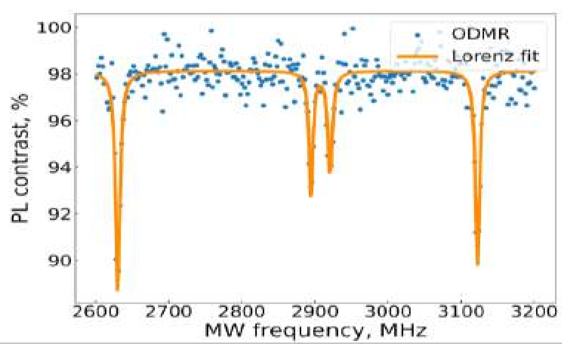

IMO-IMOMEC
UHASSELT imec

I. Petrov, under review 2025

Magnetometry

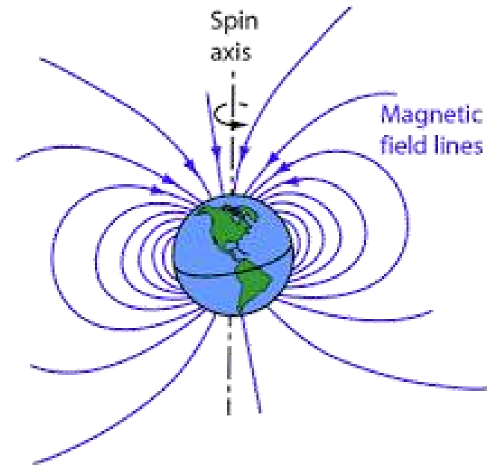

- How big is the source?
  - As big as planets and stars
  - As small as a single cell and bacteria

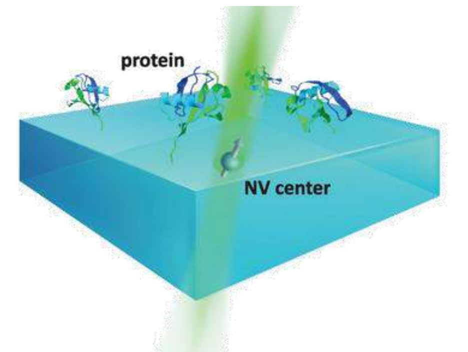

- What is “Magnetometry”?
- The field generated by a dipole moment **m**

$$\mathbf{B}_{\mathrm{dip}}(\mathbf{r}) = \frac{\mu_0 m}{4\pi r^3}\left(2\cos\theta\,\hat{r} + \sin\theta\,\hat{\theta}\right)$$

Classical definition: m = I x A

Quantum Definition:

$$\mathbf{M} = \frac{1}{V}\sum_{i=1}^{N}\boldsymbol{\mu}_i$$

$$\boldsymbol{\mu} = \gamma\mathbf{S}$$

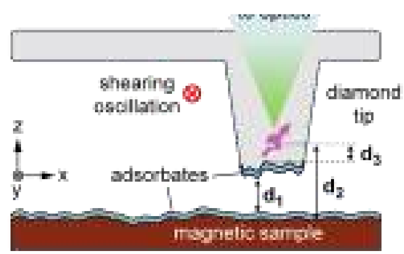

Lovchinsky et al. "Nuclear magnetic resonance detection and spectroscopy of single proteins using quantum logic." *Science* 351, no. 6275 (2016): 836-841.
Xu at all, ACS Nano (2025)

Sensing of temperature in neural cells with Nanodiamond

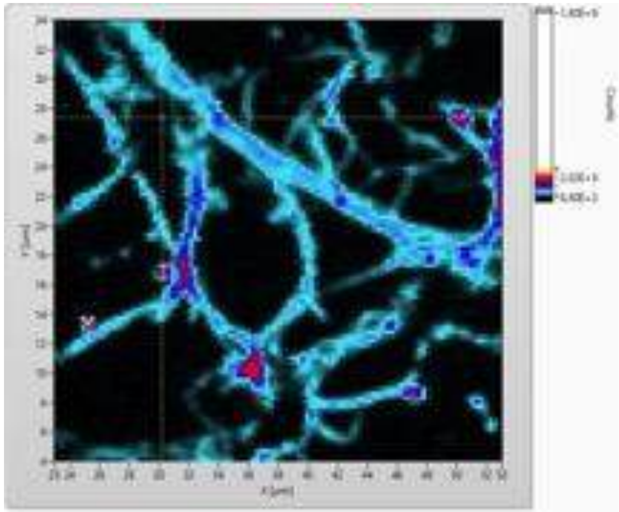

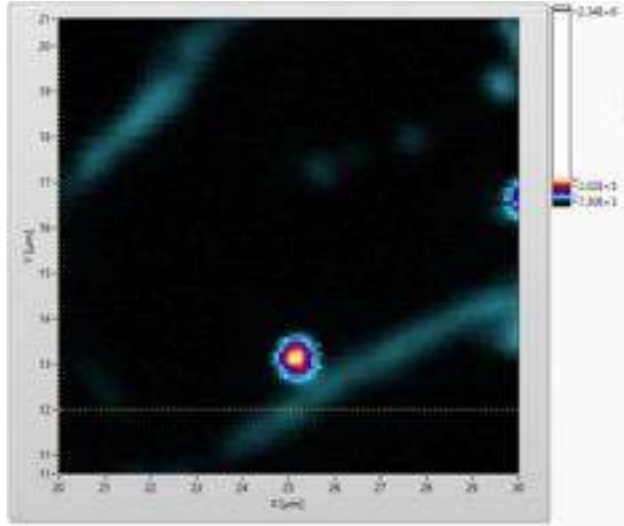

200 microK/Hz$^{1/2}$

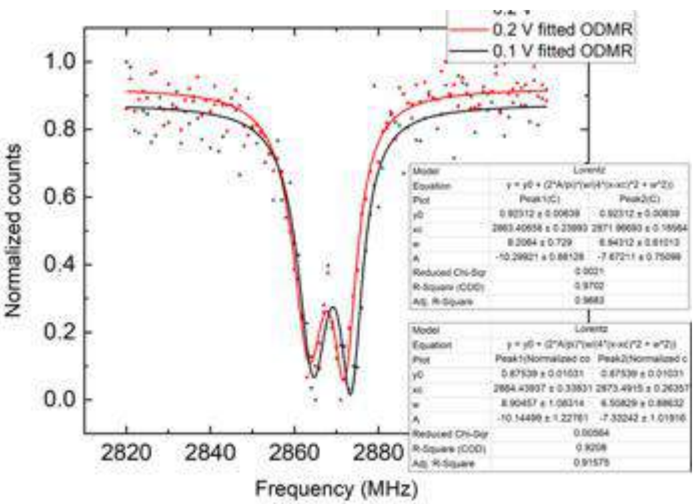

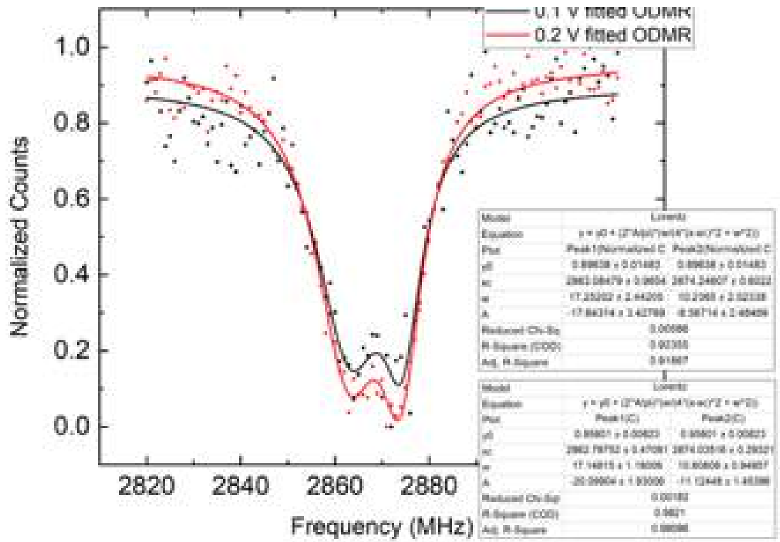

Magnetometry

- Environmental and
- Biological magnetic fields

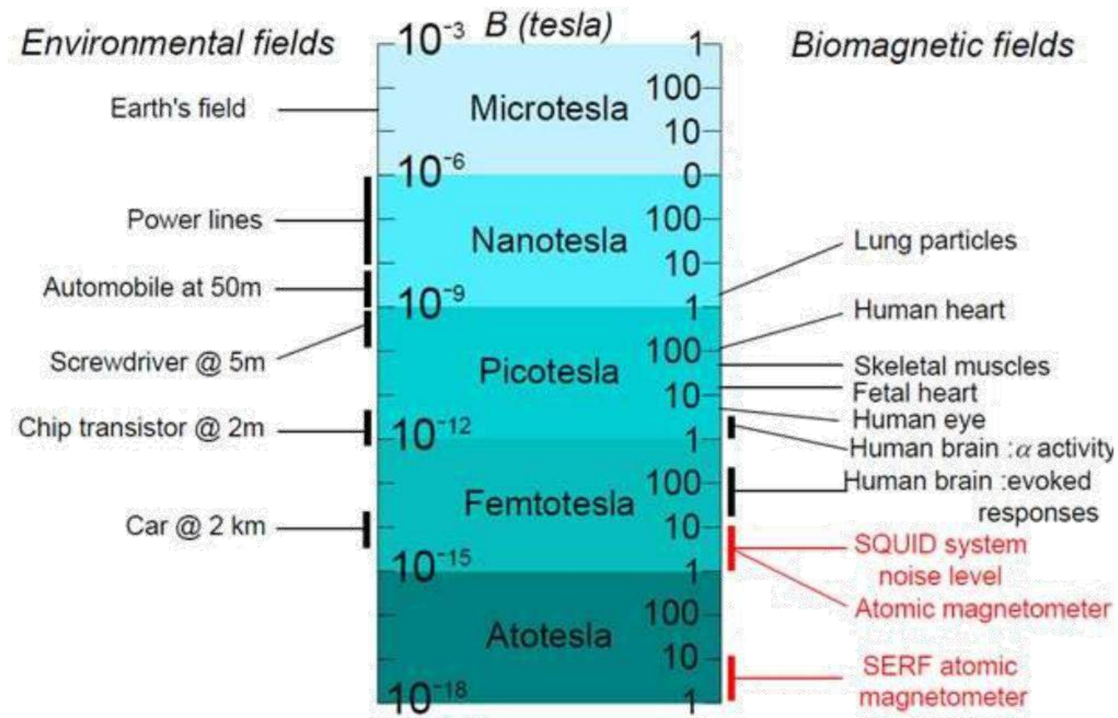

Magnetic fields generated by brain: ~100fT, <100Hz.

Features

- What features should we consider in a sensor selection?
  - Sensitivity (T/sqrt(Hz))
    - Practical sensitivity/Intrinsic sensitivity (spin projection/shot noise limited)
  - Sampling rate (bandwidth)
  - Dynamic range (linear regime)
  - Operating field (high, low, ultra-low or zero field!)
  - Operating temperature
  - Stability (drift)
  - Spatial resolution
  - Accuracy

Platforms

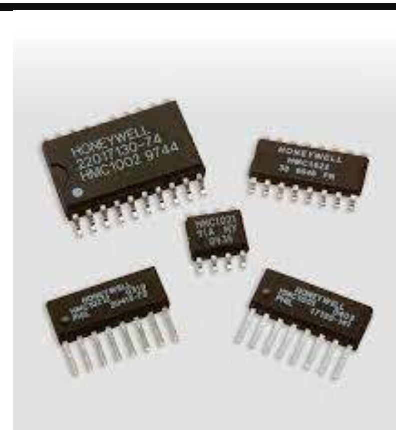

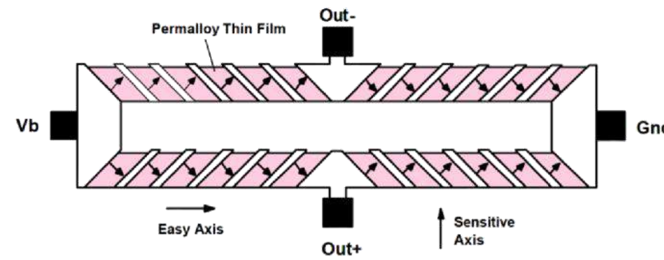

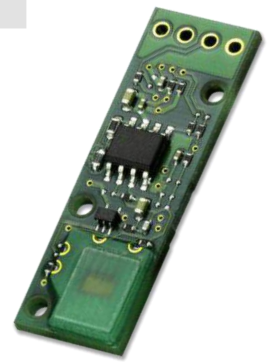

- Magneto-Impedance sensor (MI)
- Anisotropic-Magneto Resistive (AMR)
- Giant magnetoresistance (GMR)
- Extraordinary magnetoresistance (EMR)
- Magnetic Tunnel Junction (MTJ)
- Magnetoelectric Multiferroic (MEMF)
- Inductive coils
- Hall probes
- Defect centers
  - Nitrogen-Vacancy Defect Center (NVD)/RF NVD/ NVD with flux concentrator/single NV/Ensemble
  - Silicon-Vacancy in Silicon Carbide

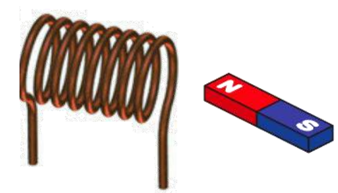

$$V = NAB\omega$$

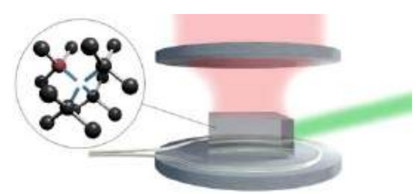

Platforms

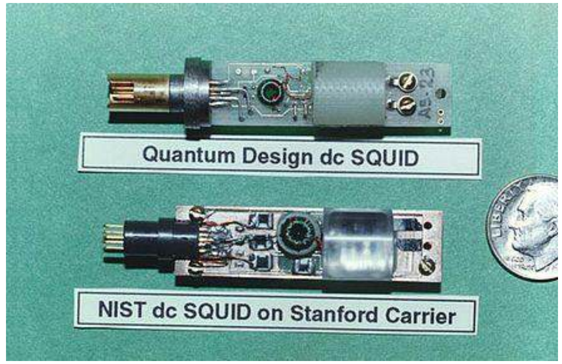

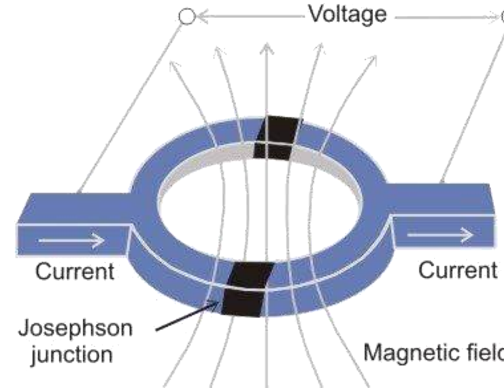

- Superconducting Quantum Interference Devices (SQUIDs)
  - Superconducting quantum interference proximity transistor (SQUIPT)
  - Superconducting kinetic impedance magnetometer (SKIM)
  - High Tc, low Tc,
- Atomic magnetometers (optically pumped magnetometer-OPM)
  - K, Rb, Cs, He, Hg
  - Flux concentrator OPM
  - Cavity-enhanced OPM
  - Cold thermal atom OPM
- Bose-Einstein Condensate (BEC)
- Rydberg Schrodinger cat (RSC)
- Fluxgates/Parallel Gating Fluxgates

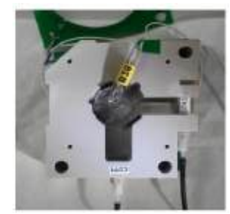

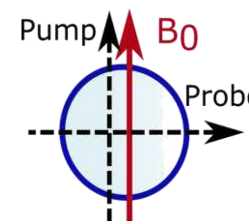

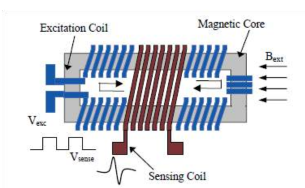

ODMR AND PDMR NV CENTRES

- A typical setup on optical table
- A compact optical part is possible using CPC lens, light guide and dichroic beam splitter

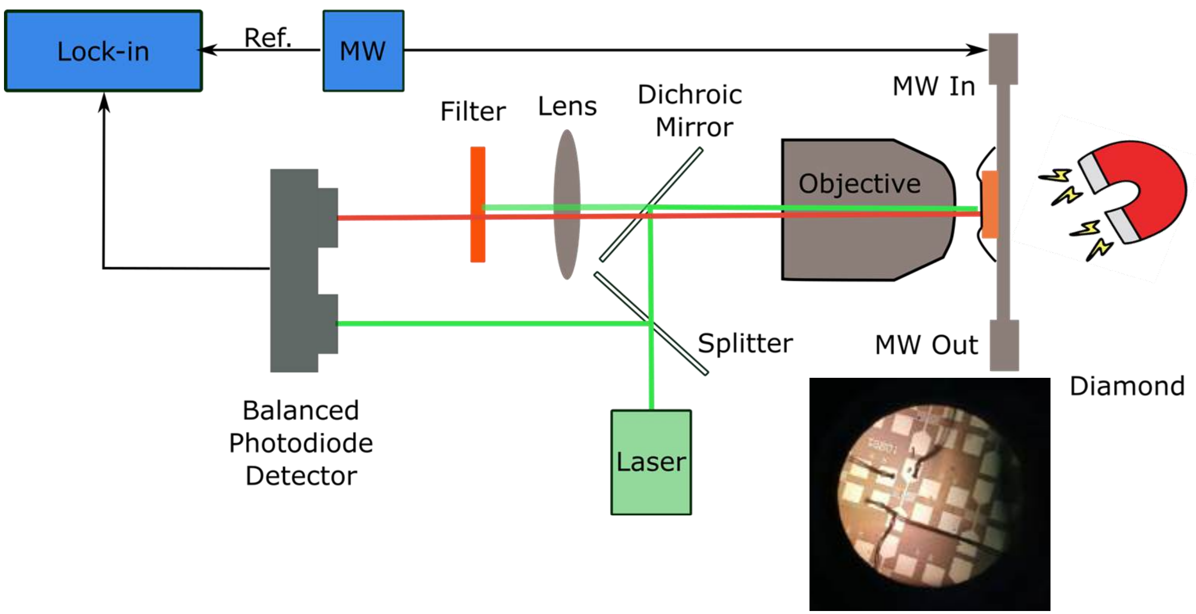

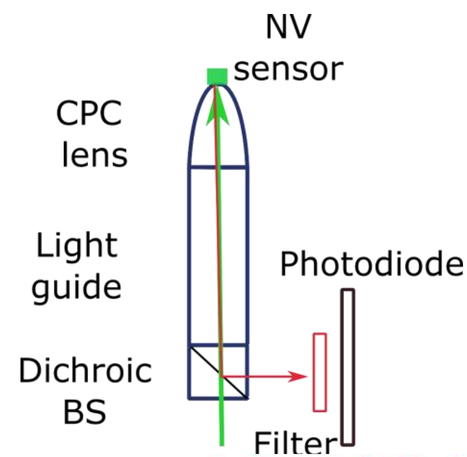

Shielding

- How can we protect our measurements?
  - Using magnetic shield (not electric shield!, skin depth!)
    - Passive shielding
    - Active shielding

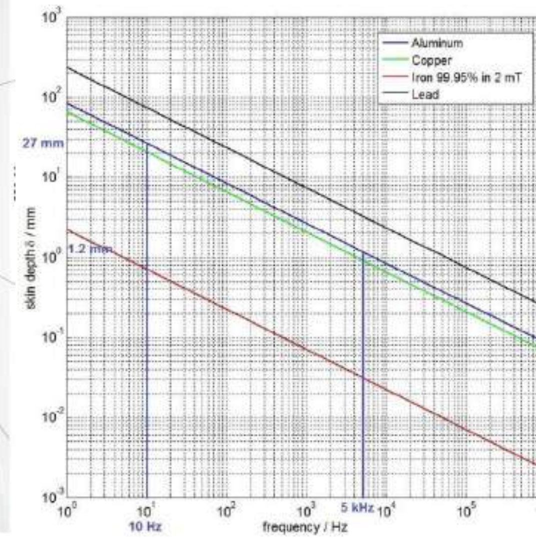

Gradiometry configuration to improve the sensitivity

- Remove common mode of noise
  - To operate in an unshielded environment
  - To achieve further noise reduction
  - One sensor close to the source, one a bit far away
  - Design complexity depends on orders of background field gradient

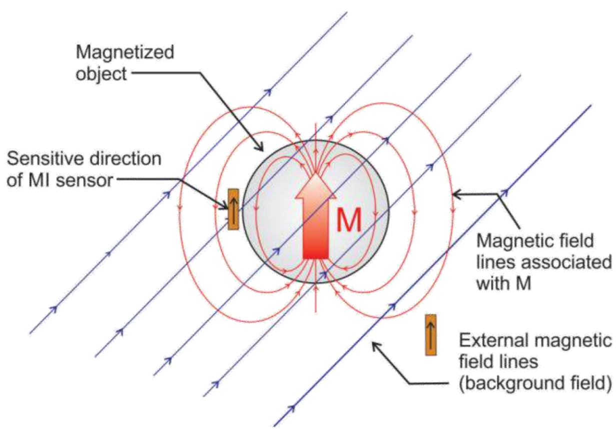

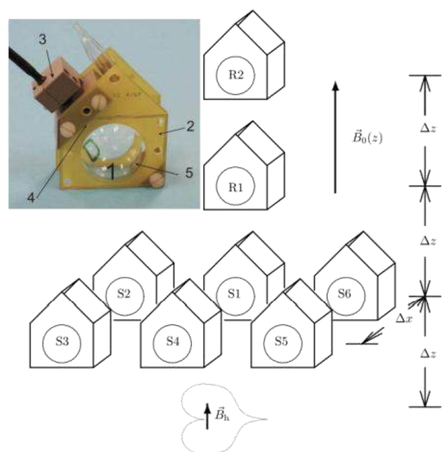

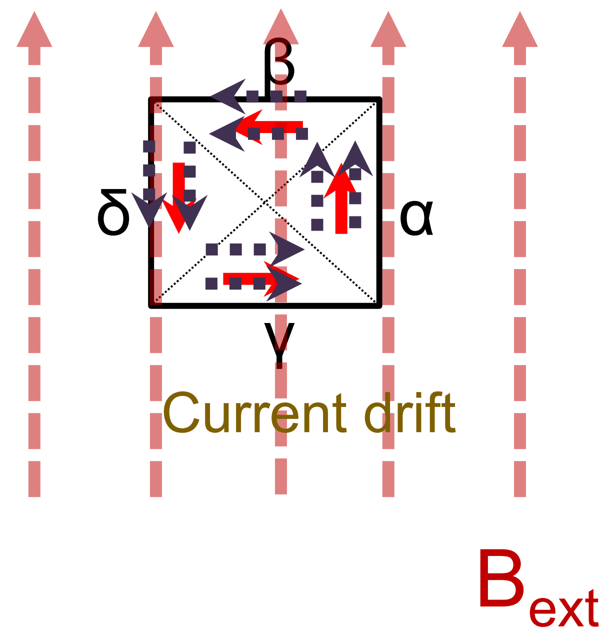

Allan Standard Deviation (ASD)

to define the measurement time

- Question: which one is better: turtle, rabbit or turbit?
- sensitive but less stable or less sensitive but stable?
  - Stability/sensitivity is matter for long/short term measurements

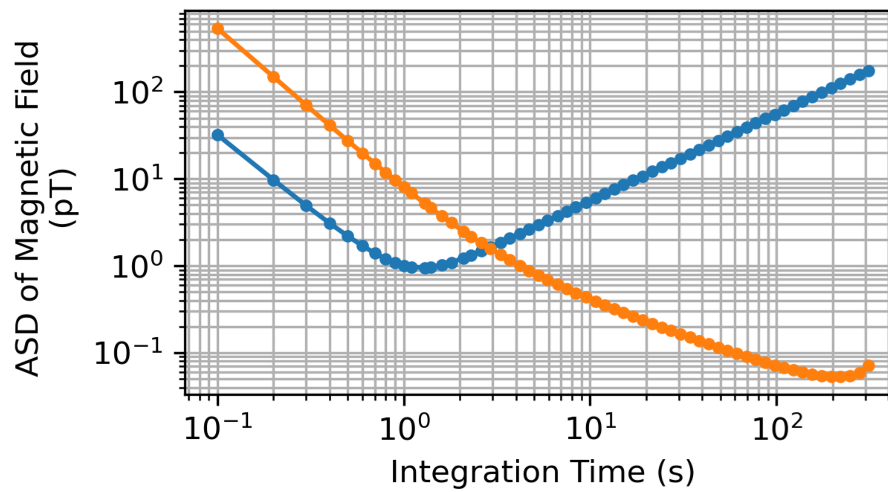

Allan Standard Deviation (ASD)

- How can we measure the stability of a system?
  - When should we stop averaging? 1 s, 1 min, 1 h, 1 d, 1 w?
- ASD shows the optimum integration time

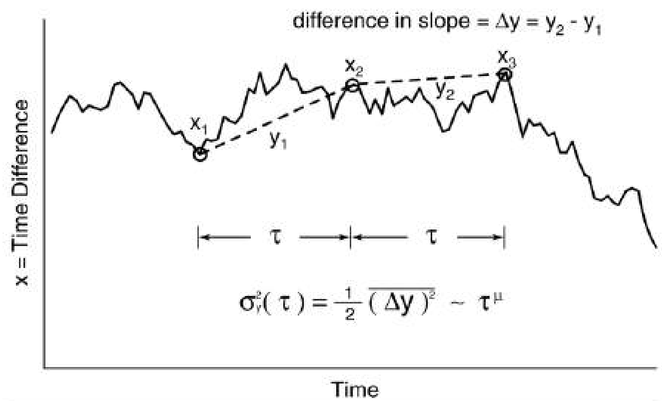

Stability : Measure of how “constant” is the slope

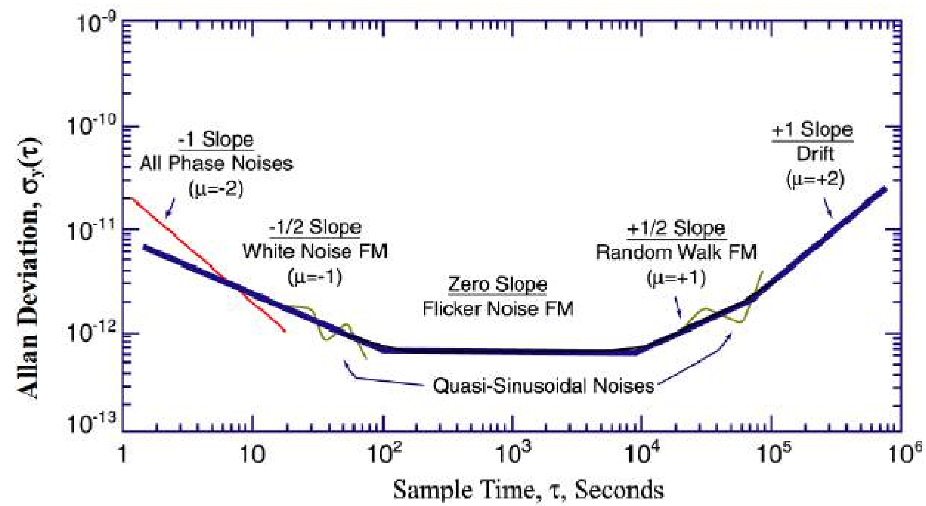

White noise
Until 20 sec

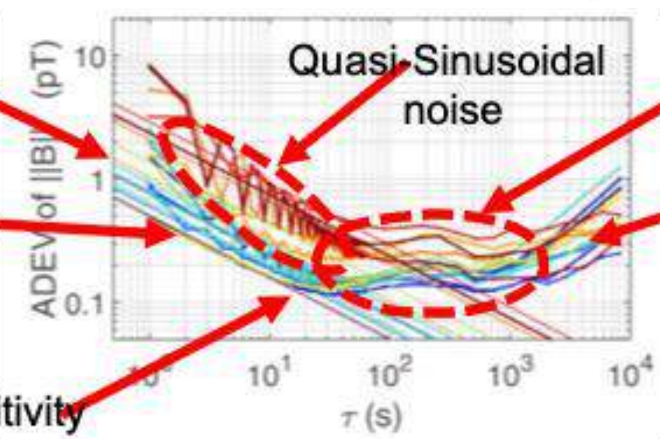

A drift appears
above 1000 sec

Best sensitivity
at 20 sec

Experimental Setup

AMADEUS

- ODMR detection scheme
- Ensemble NVs
- Sample: [NV]: 300 ppb
- Coplanar MW antenna
- Heating MW source
- Laser diode (~ 40 mW)

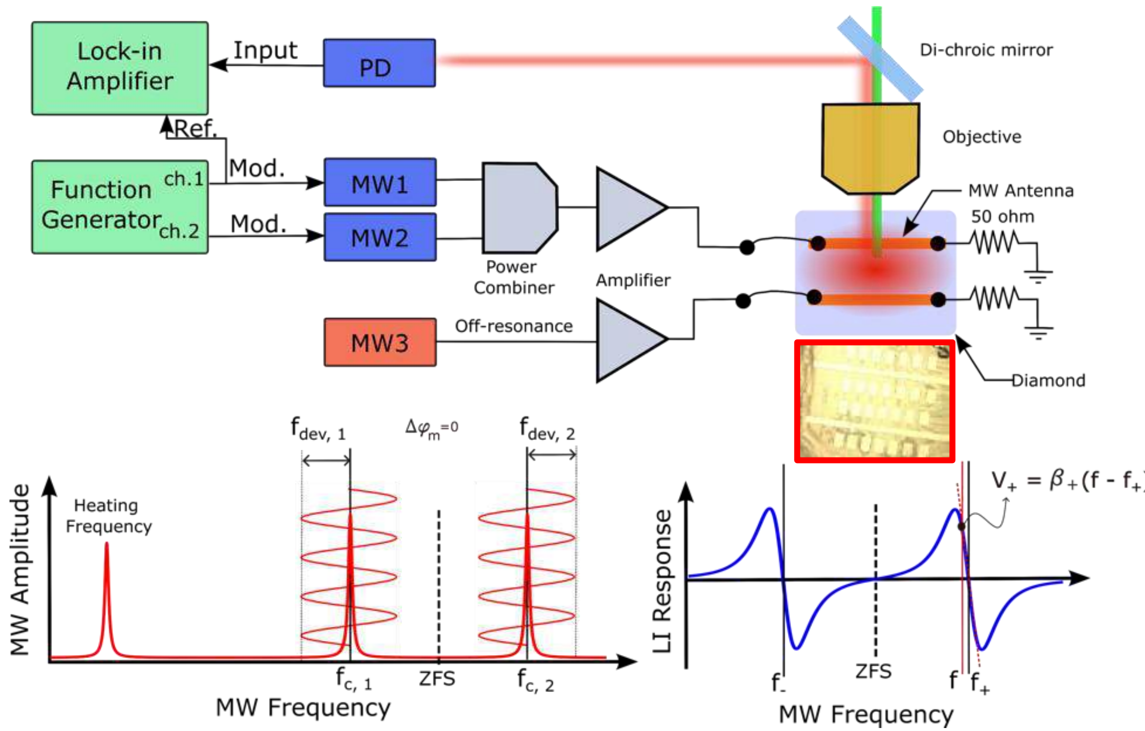

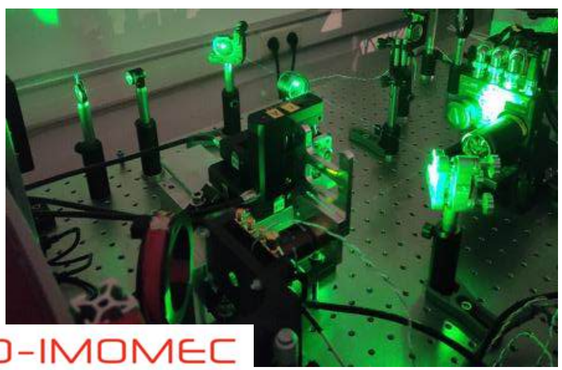

IMO-IMOMEC
UHASSELT imec

Hardware Development towards miniturisation

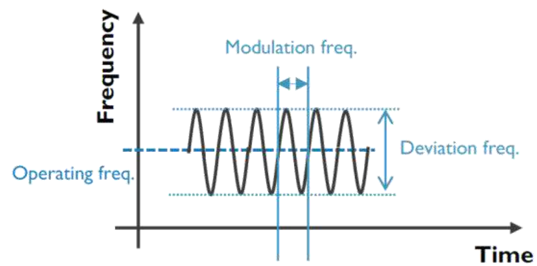

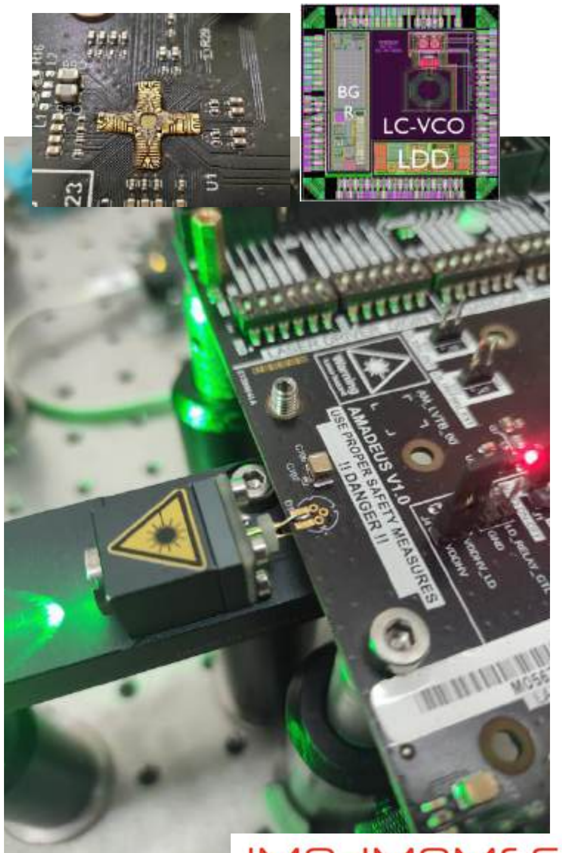

Dispersive profiles obtained while
IMEC VCO used as MW source
to drive ms=0→+/-1 transitions

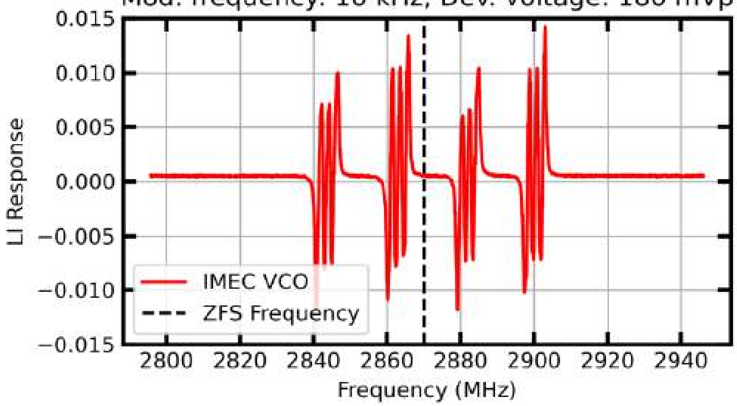

IMEC VCO vs SRS

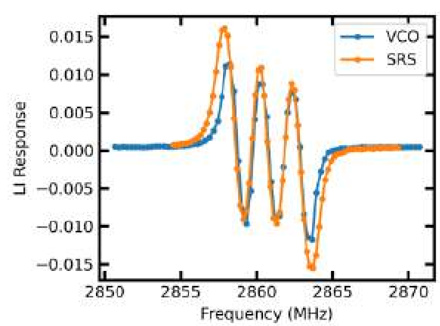

IMO-IMOMEC
UHASSELT
imec

Imaging under Ambinet conditions

Wide field
Δr~300nm

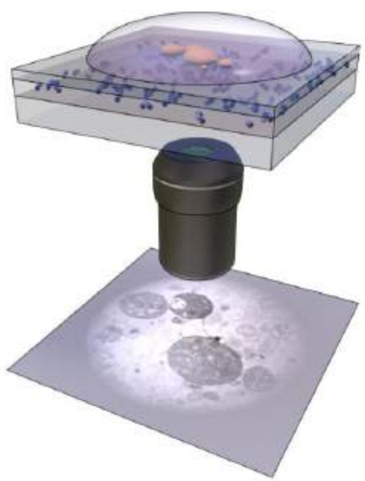

Scanning probe
Δr~30nm

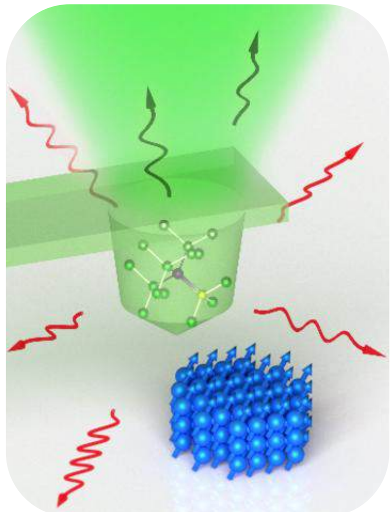

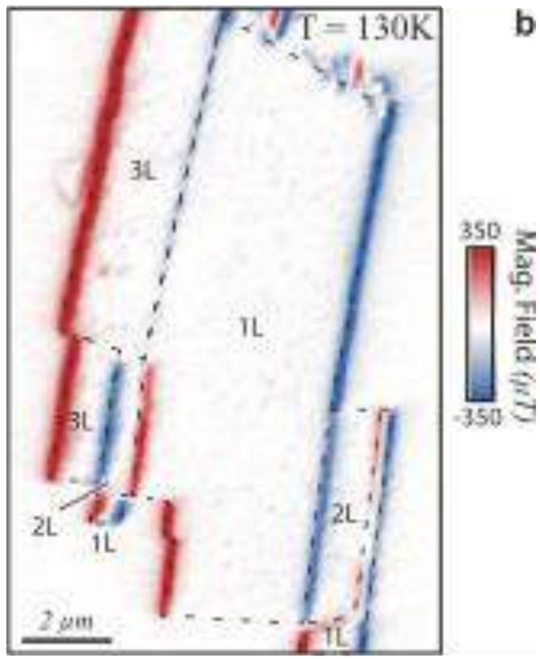

Dynamic range: 10nT-T (quenching:μT-10mT)
Band width: 0-10 GHz

Biology	Electrical Engineering
Physics	Materials Science

Altermagnets/ Spintronics
Märta A. Tschudin, P. Maletinsky et al, Nature 2024

Single NV < nT range
Ensamble: <. 1 pT range

Temperature sensing in neural cells - drug delivery

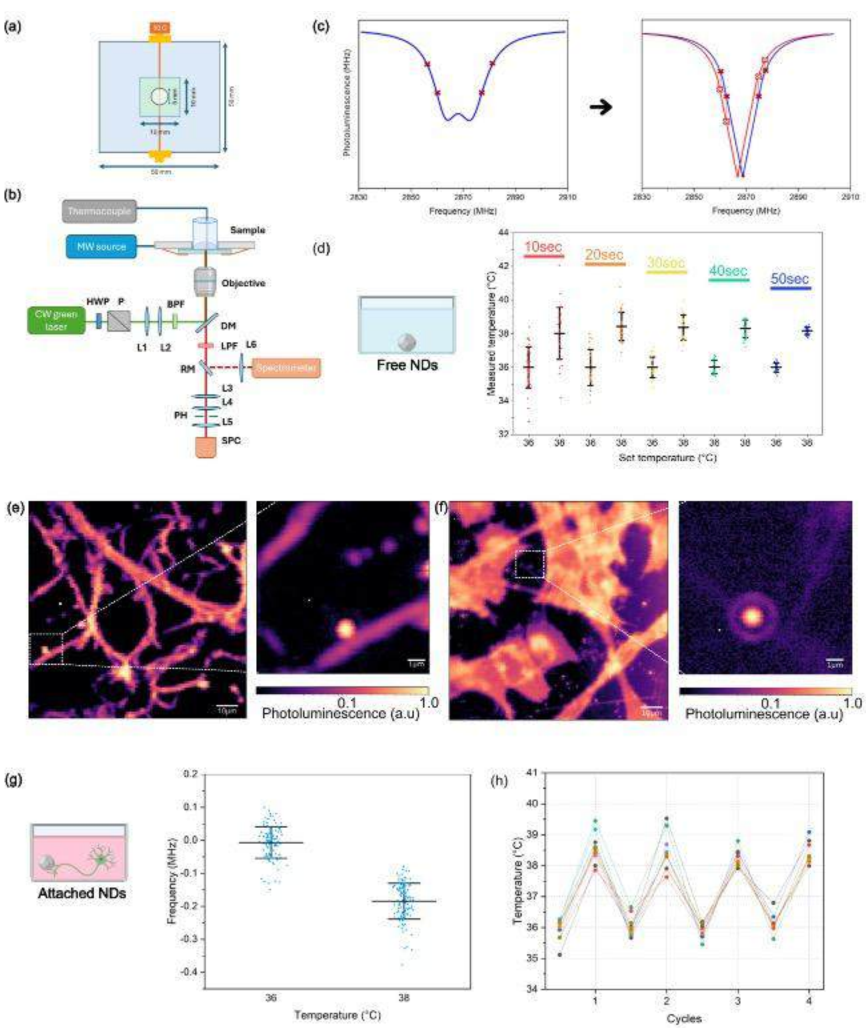

Temperature detecion in cells using
Nanodiamond. A. Shimakova, under review

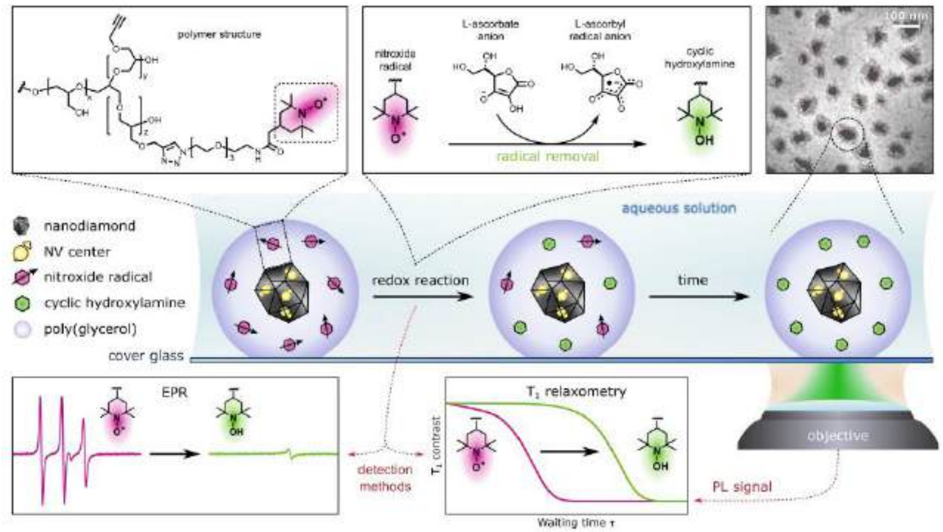

Radicals Detection (RONS)
in biological environment
Barton et al, ACS Nano, 2021

QTSense: QT Nuova

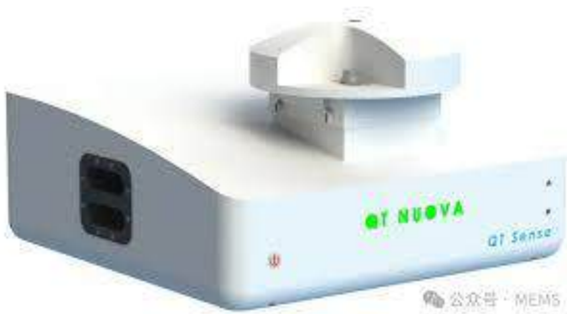

SUMMARY

- Quantum sensing principles Reviewed
- NV centre reviewed – one of the major spin qubit systm in QT: especially for quantum sensing and imaging
- Mangetometry in macroscopic and condensed matter systems
- Examples

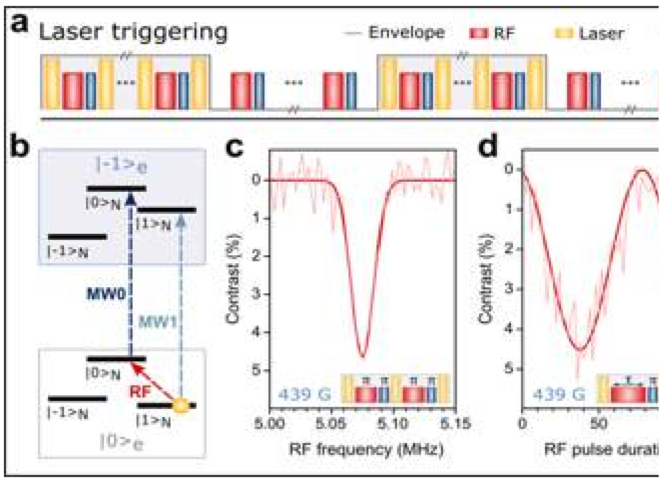

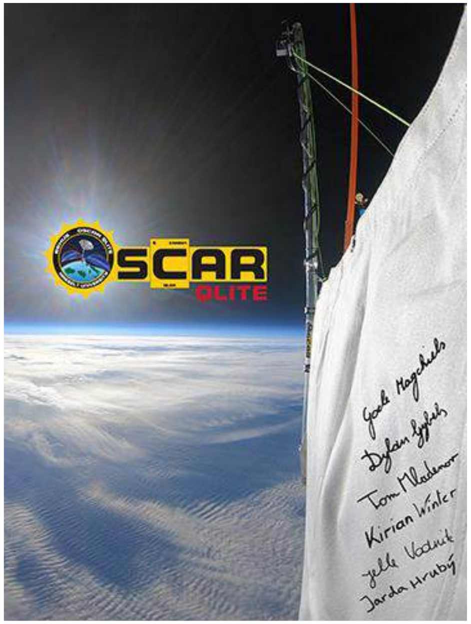

To all of u for your attention and time.

LUMI-Q

Belgian Excellence of Science Network: *CHEQs*

BeQCI

Qu-Pilot
Qu-TEst

QuMicro

AMADEUS

MAESTRO

IMO-IMOMEC
UHASSELT
imec

Collaborators

A. Shukla, B Carmans, M. Petrov, J. Soucek, D. Maniaylava, E. Bourgeois, J. Prooth, Alevtina Shimakova, UHasselt/imomec

F. Jelezko, P. Siyushev, UULM

M. Trupke D. Wirtitsch, Vienna

M. Gulka, P. Cigler, Prague

V. Ivady, A. Gali, Budapest

IMO-IMOMEC

UHASSELT imec